

THE MINOR PLANET BULLETIN

BULLETIN OF THE MINOR PLANETS SECTION OF THE
ASSOCIATION OF LUNAR AND PLANETARY OBSERVERS

VOLUME 53, NUMBER 1, A.D. 2026 JANUARY-MARCH

1.

LIGHTCURVE ANALYSIS OF MAIN-BELT ASTEROID 665 SABINE OBSERVED IN 2020 AND 2021

Ian Sherman, James Imamura, R. Scott Fisher
University of Oregon
Willamette Hall 1371 E 13th Ave #130
Eugene, OR 97403 USA
iss@uoregon.edu

Masayuki Itoh, Iku Karukome, Shunku Kataoka
Kobe University
Kobe Hyōgo, JAPAN

(Received: 2025 August 25)

We analyzed data of asteroid 665 Sabine captured in 2020 at Pine Mountain Observatory (PMO) and 2020 and 2021 at Nishi Harima Astronomical Observatory (NHAO). We find an amplitude of 0.30 ± 0.01 magnitudes and a period consistent with 4.294 ± 0.001 hours.

665 Sabine is a main-belt asteroid discovered in 1908 by W. Lorenz with an orbital inclination of 14.7° , semi-major axis of 3.1443 A.U., a diameter of 51.09 km, and eccentricity of 0.1723 (JPL, 2025b). Results from the LCDB indicate 665 Sabine has an absolute magnitude of $H = 8.93$, rotation period of 4.294 ± 0.001 h, an amplitude range of 0.27 to 0.45 mag, and an albedo of 0.3547 (Michałowski et al., 2006; Tedesco et al., 2002; Vereš et al., 2015).

Observations were conducted over three nights: 2020 Aug 16 at PMO, and 2020 Aug 24 and 2021 Nov 11 at NHAO. PMO used a 0.35 m $f/7.2$ PlaneWave CDK14 telescope paired with an Andor F9000 CCD (3056×3056 resolution, 0.96 arcsec/pix scale) using Sloan g' filters and 60 s exposures for a total of 169 image frames (PMO, 2025). NHAO employed a 0.60 m $f/12$ Cassegrain reflector with an SBIG STL-1001E CCD (1024×1024 resolution, 0.70 arcsec/pix scale) using Johnson V filters and 30 s exposures for a total of 145 image frames in 2020 and 359 frames in 2021 (NHAO, 2025). All image files were calibrated with flat, dark and bias corrections prior to analysis.

We measured the magnitude of 665 Sabine and the field's comparison stars using *AstroImageJ* (Collins et al., 2017). Candidate comparison stars were chosen using data from GAIA DR2 accessed via the *IRSA Catalog* (Gaia, 2016; Gaia, 2018; NASA/IPAC, 2025). Measurements were transformed into SDSS g' magnitudes using literature conversions from the relevant photometric systems (Jester et al., 2005; Carrasco and Bellazzini, 2023). In total, eighteen comparison stars were identified for the PMO 2020 Aug 16 data, seven for the NHAO 2020 Aug 24 data, and nine for the NHAO 2021 Nov 7 data.

Three primary sources contributed to the total magnitude uncertainty which we combined in quadrature: (1) observational counting statistics from the photometry of 665 Sabine, (2) magnitude conversions across the three employed filter sets (Carrasco and Bellazzini, 2023; Jester et al., 2005; Shevchenko et al., 2021), and (3) the one σ spread of residuals between measured and cataloged magnitudes of field comparison stars (Gaia, 2018). We find an average magnitude error of 0.083 g' mag for the 2020 PMO data, and 0.064 and 0.069 g' mag for the 2020 and 2021 NHAO data respectively.

Using Python and ephemerides from the Horizons system, we generated lightcurves for the three datasets based on the following initial conditions: Aug 16 at 00:00:00 UTC was selected as the phasing zero-point; light travel time was subtracted from each UTC timestamp; and magnitude offsets, extracted from the Horizons system using the standard IAU H-G formalism and transformed into g' , were applied relative to the PMO dataset (JPL, 2025a).

Due to the sparsity of our 2020 data and the significant time gap between our initial and final observations, extracting a reliable period from the composite lightcurve required the development of a dedicated epoch-folding routine in line with the procedures outlined by Larsson (1995). We first composited the two 2020 datasets and broadly sampled within ten σ of the literature period of 4.294 ± 0.001 h (Michałowski et al., 2006), using a step size of 0.00001 h. At each trial period, the magnitude data were binned into twenty phase intervals, weighted proportionally to counts per bin, and folded accordingly.

Number	Name	yyyy mm/dd	Phase	L_{PAB}	B_{PAB}	Period(h)	P.E.	Amp	A.E.	Grp
665	Sabine	2020 08/16-08/24	*3.8, 4.4	326	8	4.291	0.002	0.30	0.01	MB
665	Sabine	2021 11/07	5.6	40	17					

Table I. Observing circumstances and results. The phase angle is given for the first and last date. If preceded by an asterisk, the phase angle reached an extremum during the period. L_{PAB} and B_{PAB} are the approximate phase angle bisector longitude/latitude at mid-date range (see Harris et al., 1984). Grp is the asteroid family/group (Warner et al., 2009). Measurements of Period, Amp and their errors taken across both lines.

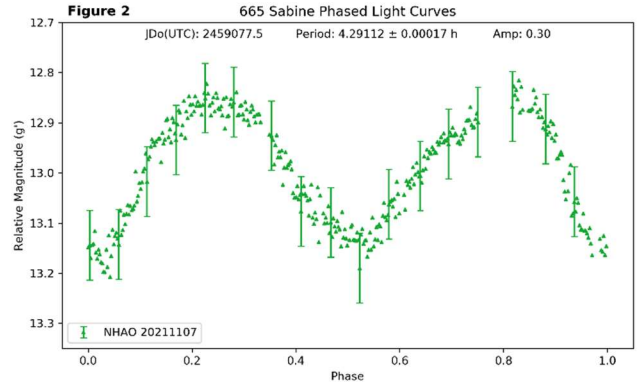
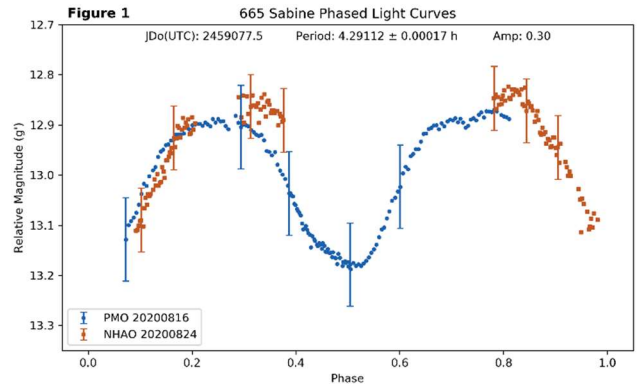
For each trial, we calculated the normalized residuals and their σ about 665 Sabine's mean magnitude. The best-fit candidate, 4.29126 h, was identified as the period that maximized the residual spread across the sampled range. Incorporating the 2021 dataset to improve phase coverage, we performed a second composite fold over a narrower period range to focus on behavior within a single rotation cycle. This allowed us to refine the period estimate to 4.29112 h and produce the lightcurves seen in Figure 1 and 2. However, the necessity of spanning all three lightcurves over a 448-day baseline introduces a cycle-count ambiguity of ± 0.002 h (Sterken, 2005). As a result, we report a synodic period for 665 Sabine of 4.291 ± 0.002 h from our observations. This period is consistent with the literature values reported by Michalowski.

To demonstrate the effect of cycle-count uncertainty over long time baselines, we also folded all three datasets across a three- σ range around the literature value. This yielded four synodic periods that modeled the data comparably well: 4.29112 ± 0.00017 h, 4.29286 ± 0.00017 h, 4.29458 ± 0.00017 h, and 4.29635 ± 0.00018 h with uncertainties derived from a Monte Carlo shuffle test permuted 5000 times per candidate. Each period corresponds to an additional complete rotation cycle over the 448-day span and cannot be uniquely distinguished without further observations. A recently published period for 665 Sabine of 4.29407 ± 0.00005 h agrees with one of these results within three σ but does not agree with our reported synodic period (Shevchenko et al., 2021).

We constructed three models – a 6th-degree polynomial, a 2nd-order Fourier fit, and a spline with a smoothing factor of 0.003 – to evaluate the amplitude of the binned, composite lightcurve. Our binning approach inherently reduced noise, and we measured amplitudes as the maximum difference between local extrema in each fit. We report an amplitude of $\Delta g' = 0.30 \pm 0.01$ magnitudes, calculated as the average of the three models as well as the amplitude given from the raw, binned data, with the uncertainty given by the standard deviation about the mean.

Acknowledgements

We thank Alton Luken, Head of Operations at PMO, for his invaluable support and stewardship of the observatory, Riley Monsrud for leading the collection of this data, and the Roundhouse and Heising-Simons Foundations for their generous support keeping PMO active. Thank you to Dr. Jun Takahashi and the University of Hyogo for their facilitation of NHAO. The codebase used in the analysis of this data is accessible on GitHub at: <https://github.com/iss-uoregon/asteroids>. This work has made use of data from the European Space Agency Gaia mission, processed by the Gaia Data Processing and Analysis Consortium. We thank the Solar System Dynamics group at the Jet Propulsion Laboratory for maintaining and providing access to the JPL Horizons On-Line Ephemeris System and the JPL Small-Body Database. Special thanks to Brian Warner and the MPB and LCDB teams. This project makes use of the python language interpreter along with several supporting packages which are made freely available: *pandas* (pandas, 2025), *Matplotlib* (Hunter, 2007), *Astropy* (Astropy, 2022), *NumPy* (Harris et al., 2020), *SciPy* (Virtanen et al., 2020), and *Astroquery* (Ginsberg et al., 2019).



References

- Astropy Collaboration (2022). “The Astropy Project: Sustaining and Growing a Community-oriented Open-source Project and the Latest Major Release (v5.0) of the Core Package.” *ApJ* **935**, 167.
- Carrasco, J.M.; Bellazzini, M. (2023). “Photometric relationships with other photometric systems.” *Gaia data release 3 documentation*, Section 5.5.1.
- Collins, K.A.; Kielkopf, J.F.; Stassun, K.G.; Hessman, F.V. (2017). “AstroImageJ: Image Processing and Photometric Extraction for Ultra-Precise Astronomical Light Curves.” *AJ* **153**, 77-89.
- Gaia Collaboration (2016). “The Gaia Mission.” *A&A* **595**, A1.
- Gaia Collaboration (2018). “Gaia Data Release 2. Summary of the contents and survey properties.” *A&A* **615**, A1.
- Ginsberg, A.; Sipőcz, B.M.; Brasseur, C.E.; Cowperthwaite, P.S. and 30 colleagues (2019). “astroquery: An Astronomical Web-querying Package in Python.” *AJ* **157**, 98-104.
- Harris, A.W.; Young, J.W.; Scaltriti, F.; Zappala, V. (1984). “Lightcurves and phase relations of the asteroids 82 Alkmene and 444 Geytis.” *Icarus* **57**, 251-258.
- Harris, C.R.; Millman, K.J.; van der Walt, S.J.; Gommers, R. and 22 colleagues (2020). “Array programming with NumPy.” *Nature* **585**, 357-362.
- Hunter, J.D. (2007). “Matplotlib: A 2D Graphics Environment.” *Computing in Science & Engineering* **9**, 90-95.

Jester, S; Schneider, D.P.; Richards, G.T.; Green, R.F.; Schmidt, M.; Hall, P.B.; Strauss, M.A.; Vanden Berk, D.E.; Stoughton, C.; Gunn, J.E.; Brinkmann, J.; Kent, S.M.; Smith, J.A.; Tucker, D.L.; Yanny, B. (2005). "The Sloan Digital Sky Survey View of the Palomar-Green Bright Quasar Survey." *ApJ* **130**, 873-895.

JPL (2025a). "Horizons System."
<https://ssd.jpl.nasa.gov/horizons/app.html>

JPL (2025b). "Small-body Database."
https://ssd.jpl.nasa.gov/tools/sbdb_lookup.html

Larsson, S. (1995). "Parameter estimation in epoch folding analysis." *A&A Suppl. Ser.* **117**, 197-201.

Michałowski, T.; Kaasalainen, M.; Polińska, M.; Marciniak, A.; Kwiatkowski, T.; Kryszczyńska, A.; Velichko, F.P. (2006). "Photometry and models of selected main belt asteroids." *A&A* **459**, 663-668.

NASA/IPAC (2025). "Infrared Science Archive."
<https://irsa.ipac.caltech.edu/frontpage/>

NHAO (2025). "Nishi-Harima Astronomical Observatory."
http://www.nhao.jp/en_pub/

pandas Development Team (2025). "pandas-dev/pandas: Pandas (v2.3.0)." *Zenodo*. <https://doi.org/10.5281/zenodo.15597513>

PMO (2025). "Pine Mountain Observatory."
<https://pmo.uoregon.edu/>

Shevchenko, V.G.; Mikhalechenko, O.I.; Belskaya, I.N.; Slyusarev, I.G. and 16 colleagues. (2021). "Photometry of selected outer main belt asteroids." *Planetary and Space Science* **202**, id.105248.

Sterken, C. (2005). "The O - C Diagram: Basic Procedures." *ASP Conference Series* **335**, 3.

Tedesco, E.F.; Noah, P.V.; Noah, M.; Price, S.D. (2002). "The Supplemental IRAS Minor Planet Survey." *AJ* **123**, 1056-1085.

Vereš, P.; Jedicke, R.; Fitzsimmons, A.; Denneau, L. and 13 colleagues (2015). "Absolute magnitudes and slope parameters for 250,000 asteroids observed by Pan-STARRS PS1 - Preliminary results." *Icarus* **261**, 34-47.

Virtanen, P; Gommers, R.; Oliphant, T.E.; Haberland, M. and 30 colleagues. (2020). "SciPy 1.0: Fundamental Algorithms for Scientific Computing in Python." *Nature Methods* **17**, 261-272.

Warner, B.D.; Harris, A.W.; Pravec, P. (2009). "The Asteroid Lightcurve Database." *Icarus* **202**, 134-146. Updated 2025 June.
<http://www.minorplanet.info/lightcurvedatabase.html>

LIGHTCURVES AND ROTATION PERIODS FOR (259) ALETHEIA, (1146) BIARMIA AND (1714) SY

Timothy C. Brothers

Massachusetts Institute of Technology (MIT)
Department of Earth, Atmospheric and Planetary Sciences
Wallace Astrophysical Observatory (810)
50 Groton Rd., Westford, MA 01886, USA
bro@mit.edu

McKenzie Coleman

MIT Department of Mechanical Engineering
Cambridge, MA 02139, USA

Nina Cranor

MIT Department of Mechanical Engineering
Cambridge, MA 02139, USA

Victoria Sconce

MIT Department of Chemistry
Cambridge, MA 02139, USA

Stephen M. Slivan

Massachusetts Institute of Technology
Department of Earth, Atmospheric and Planetary Sciences
Cambridge, MA 02139, USA

Katherine Panebianco, Layna Oberg

MIT Department of Physics
Cambridge, MA 02139, USA

Erez Fass

MIT Department of Mechanical Engineering
Cambridge, MA 02139, USA

Alex Chen

MIT Department of Aeronautics and Aeronautics
Cambridge, MA 02139, USA

Aiden Stoltz

MIT Department of Chemistry
Cambridge, MA 02139, USA

Artem Burdanov

MIT Department of Earth, Atmospheric and Planetary Sciences
Cambridge, MA 02139, USA

Jayna Ekelmann

MIT Department of Earth, Atmospheric and Planetary Sciences
Cambridge, MA 02139, USA

Michael J. Person

MIT Department of Earth, Atmospheric and Planetary Sciences
Cambridge, MA 02139, USA

(Received: 2025 October 15)

During 2025 summer research program at MIT Wallace Observatory, we conducted an observation campaign focused on main-belt asteroids, (259) Aletheia, (1146) Biarmia, (5386) Bajaja and (1714) Sy, all of which had favorable apparitions during this effort.

The observation campaign we describe here was a continued response to the notice in *MPB* Issue 51-1 of minor planets with favorable apparitions in 2025 (Pilcher, 2025) as our team prepares to help characterize an anticipated onslaught of newly discovered near-Earth objects (NEOs) by the Vera C. Rubin Observatory (Kurlander et al., 2025). All observations were made in 2025 by MIT astronomers and undergraduate researchers at Wallace Astrophysical Observatory (WAO), Westford, MA, USA (810) and Teide Observatory on the island of Tenerife, Spain. In the following text we present period and amplitude solutions for (259) Aletheia, (1146) Biarmia and (1714) Sy. Data over several nights were collected for (5386) Bajaja, but this target proved elusive due to weather interruptions and will be followed up on a future apparition or collaboration.

(259) Aletheia is an X-type asteroid with an albedo of 0.043 (JPL Horizons, 2025) and a diameter of 185 km (Kleshchonok et al., 2021). In Jun, Aletheia presented us with a favorable apparition as it passed within 1.7156 AU of Earth. As recorded in the Light Curve Database (Warner et al., 2009), previous period and amplitude measurements have been reported as, 15 h with amplitude of 0.19 magnitude (Weidenschilling, 1990), 12.23 h with amplitude of 0.1 (Robinson, 2011web) and ~8.14 h with amplitude ranging from 0.09 to 0.12 (Koff, 2006; Behrend and Antonini, 2007web, 2019web). While the large asteroid's period solution is classified as a U3, it was decided that this presented an excellent instructional opportunity for our undergraduate students.

All five nights of Aletheia observations were made by the Elliot 24-inch telescope (Planewave CDK24 f/6.5), an FLI 16803 CCD, and a Sloan r' filter. Observations were scripted with Voyager software (Orazi, 2025), where the object was prioritized in a queue for 14 nights, of which 5 nights were successful, collecting 15 hours of data. Images were reduced with dark, bias and flat frames in *Maxim D/L v6* (Diffraction Limited, 2025). Photometry was generated and the resulting light curve was analyzed in *Tycho Tracker* (Parrott, 2020). Standards were sourced from ATLAS2 r' comparison stars within a color index range of $0.5 < B-V < 0.9$. No manual offsets to the magnitudes were made. On 2025 Jun 6 at 6:58 UT, we measured the maximum brightness during our campaign to be 11.173 ± 0.021 magnitude in the Sloan r' band.

Utilizing 565 observations of Aletheia, we were able to determine a period of 8.14 ± 0.001 hours with a 0.1 ± 0.01 magnitude amplitude (Figure 1). Given the 4 minima and 4 maxima, fitting was started at 4th order, though, we found 6th order made significant reductions in error while making obvious improvements to the correlation between data peaks and that of the fit (Figure 2). Comparing our results to previously published values, we have high confidence that the 15 and 12.23 h periods can be regarded as highly unlikely. Our measured amplitude is well within the range of recently reported values, 0.09 to 0.12 magnitude.

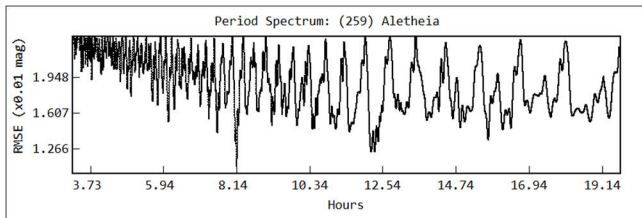


Figure 1. Periodogram in linear scale of (259) Aletheia, showing a strong preference for an 8.140 h period.

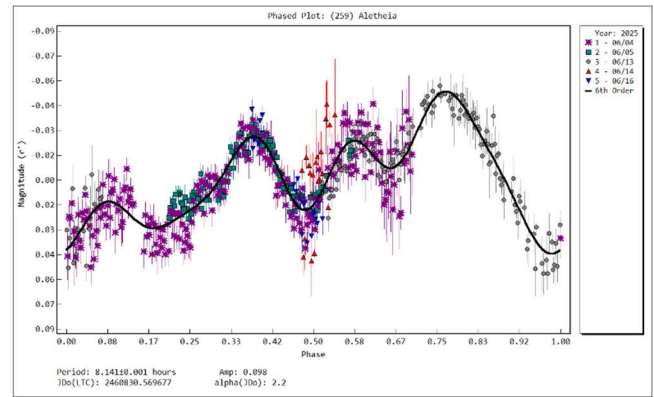


Figure 2. Phased plot of (259) Aletheia, centered around 0.0 magnitude. Here we plot all data utilized in the final fitted solution.

(1146) Biarmia is an X-type asteroid with an albedo of 0.196 and a diameter estimate ranging from 21.59 to 32.93 km (Mainzer et al., 2019). Previous periods have ranged from 5.33 to 11.514 h, while 5.47 h has been reported several times. With a U=3 rating (Warner et al., 2009) at 5.47 hours, we hoped to confirm this value again during an ideal apparition where the object was only 1.313 AU from the observer. The amplitude, on the other hand, has varied significantly in previous publications, ranging from 0.07 to 0.32.

All three nights of Biarmia data were recorded locally by undergraduate researchers using robotic 14-inch telescopes (Celestron C14 f/11) fitted with a QHY268M CMOS detector and a Sloan r' filter. A total of 283 images, comprising 17 hours of observation time, were used in analysis. Reduction and analysis methods are identical to that of Aletheia and no manual offsets were made to the photometry. On 2025 Jun 13 at 3:23 UT, we measured the maximum brightness during our campaign to be 12.346 ± 0.011 magnitude.

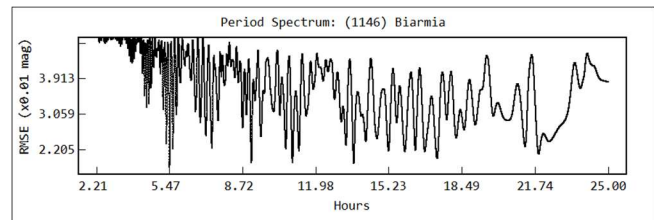


Figure 3. Periodogram, linear scale, of (1146) Biarmia showing a strong preference for a 5.471 h period.

Given the previously reported range of period values, we searched 1 hour to 50 hours with a simple 2nd order fit. The dominant period was by far 5.47 h (Figure 3). Though, the obvious 0.02 magnitude increase near the 0.3 phase position and higher-order features were not adequately fit. Increasing the fit order to the 4th and running a new search resulted again with a preferred solution of 5.47 ± 0.01 h and an amplitude of 0.15 ± 0.02 magnitude (Figure 4).

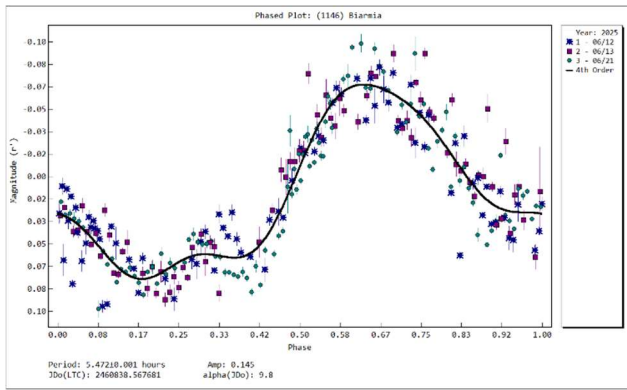


Figure 4. Phased plot of (1146) Biarmia, centered around 0.0 magnitude. Here we plot all data utilized in the final fitted solution.

(1714) Sy is an asteroid with a reported albedo of 0.157 and a diameter of 13.998 km. On the first night of this campaign, Jul 4 UT, we observed Sy at 13.837 ± 0.017 r' magnitude while it was at a distance of 1.17 AU from Earth. An additional motivation for focusing on this object was our conclusion that Sy's period had not been previously determined, an exciting prospect for our team as we begin to approach newly discovered NEOs. This was surprising given this low designation-number asteroid was discovered almost 75 years ago and its rather large physical dimensions, yet our best attempts to locate previous efforts in the Light Curve Database or online searches yielded nothing. As we learned after our analysis was complete from Slivan and Brothers (2026; this issue), this understanding was in error.

20 nights of usable data were collected in the Sloan r' filter. The first 17 nights (Jul 4 to Aug 10 UT) were observed at Wallace Observatory, collecting 54 hours of data. Of those nights, 16 were recorded on various 14-inch telescopes run locally by students and 1 night from the Elliot 24-inch telescope in its automated mode. The 3 latter nights (Sep 25 to Sep 27) UT were observed at Teide Observatory on the ACP-scripted 1m SPECULOOS-North/Artemis (Z25) (Burdanov et al., 2022) telescope by Artem Burdanov, collecting an additional 6 hours of data. Early on in the analysis phase, it was noticed that data from Aug 4 was a significant outlier and due to report of haze in the 'End of Night Report' from student observers, we omitted this night going forward.

Our first step in analysis was to plot the usable 19 nights of unfolded data in order to get a sense of the amplitude's scale in magnitude. In Figure 5 we saw a relatively consistent range of nearly 0.4 magnitude values. To further investigate, we plotted three sets of three consecutive nights in hopes that we would see at least one triplet indicating a similar change in magnitude: (a) Jul 21 to Jul 23, (b) Aug 8 to Aug 10 and (c) Sep 25 to Sep 27. Of these, the first two progressions further support an amplitude of at least 0.4: (a) 0.34 magnitude over 46.7 hours, (b) -0.49 magnitude over 48.44 hours and (c) -0.12 magnitude over 48 hours. We hypothesize (a) and (b) indicate a transition from peaks and that (c) is possibly near a maxima given its peak magnitude compared to that of the first three triplets. It also seemed reasonable that this was a possible slow rotator given that there were no obvious extremum or significant

slope in any given night's worth of data. Therefore, we bound Tycho's 2nd order period search to only include solutions with 0.35 to 0.5 magnitude amplitudes, while also limiting the search range from 1 to 1000 hours at 20000 steps.

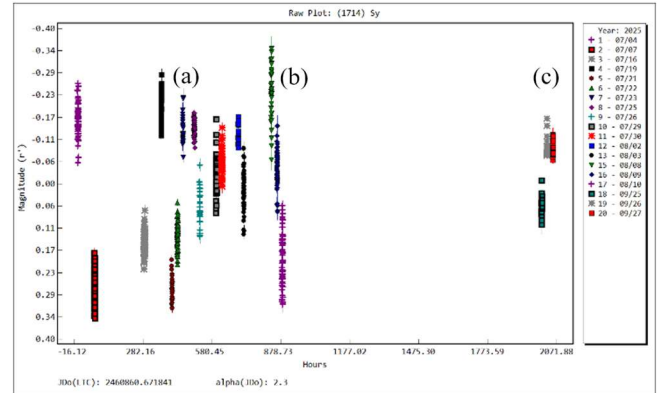


Figure 5. 19 nights of data used for our initial period calculation. Comparing 3 sets of 3 consecutive nights, (a) Jul 21 to Jul 23, (b) Aug 8 to Aug 10 and (c) Sep 26 to Sep 27, we see (a) and (b) showing a nearly 0.4 magnitude range of values over ~48 consecutive hours. The three nights at Tenerife (c), show a much shorter range in values, possibly indicating at maxima.

To further narrow down period candidates we interpret a magnitude of greater than 0.4 to indicate an elongated body and therefore requiring a doubly periodic solution. The final set of 10 "best" candidates, ranked in Tycho by root mean square error or RMSE, had a mean amplitude of 0.43 ± 0.04 magnitude. This first group of doubly periodic solutions include 59.9 h, 39.8h, 237.9 h, 329.7 h and 56.1 h (see Figure 6). The 39.8, 56.1, and 59.9 h solutions make little sense when plotted as each night is very flat compared to the fit or the slope was misaligned to the fit, indicating a much longer period. We also note that the ~60 and the ~237 h solutions have self-consistency issues, in that, nights overlapping in time do not overlap in magnitude by as much as 0.1-0.2 magnitude. 237.9 hours has too small of an amplitude at 0.39 to be considered a top choice. 329.7 h has less of the consistency issue, though it does have an interesting feature magnitude around 0.15 and 0.85 in phase where magnitude seems to increase. If real, this may indicate a brighter orientation since those two points mirror each other in phase space. Considering Wallace data only, we see 329.7 h as the most likely period.

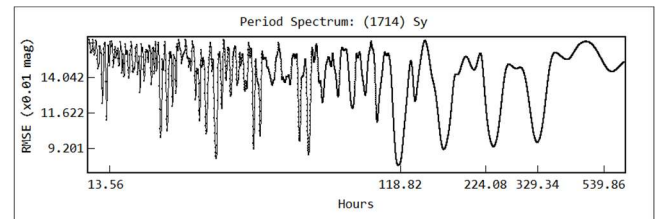


Figure 6. Log scale periodogram using all Wallace-collected data, except for the problematic #14 (Aug 4), with doubly periodic candidates of 59.9 h, 39.8h, 237.9 h, 329.7 h and 56.1 h as contenders.

Number	Name	yyyy mm/dd	Phase	L _{PAB}	B _{PAB}	Period(h)	P.E.	Amp	A.E.
259	Aletheia	2025 06/04-06/16	*2.2, 6.6	250	4	8.14	0.01	0.1	0.01
1146	Biarmia	2025 06/12-06/21	*9.8, 11.0	262	18	5.47	0.01	0.15	0.02
1714	Sy	2025 07/04-09/27	*2.0, 16.8	285	-1	320.5	0.1	0.39	0.09

Table I. Observing circumstances and results. The phase angle is given for the first and last dates. If preceded by an asterisk, the phase angle reached an extremum during the period. L_{PAB} and B_{PAB} are the approximate phase angle bisector longitude/latitude at mid-date range.

Our final period search included the Artemis data, while further binding the solution range to between 70 and 400 hours. In Figure 7 we see our final period candidates. It is worth noting the bifurcation of the minima, or double minima, in the periodogram is due to the 46-day gap in observations between the Wallace data and the Artemis data (Figure 5), which introduces an ambiguity in how many rotations elapsed during the gap. Regardless, it is reassuring that the Wallace-only and the Wallace-plus-Artemis sets have relative overlap in possible solutions. Again the 239.5 and 220 h solutions have self-consistency issues and we removed them from consideration. This left us with either: 320.5 h with $A=0.42$ or 343.6 h with $A=0.4$. Comparing the RMSE of those two period solutions, 320.5 is the preferred solution.

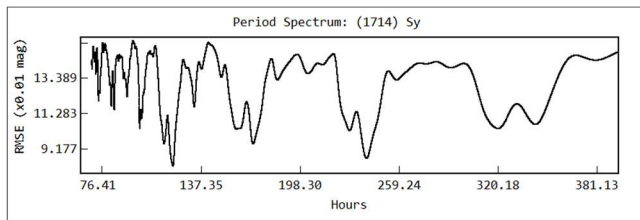


Figure 7. Linear scale periodogram using data from both Wallace and Artemis, with candidates of 239.5 h, 229.0 h, 320.5 h and 343.6 h as the most-favored, doubly periodic solutions.

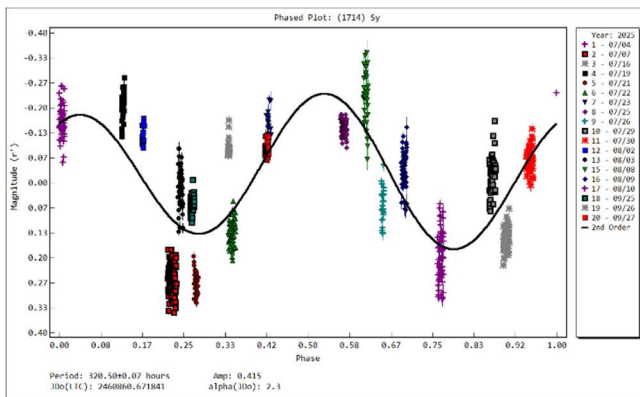


Figure 8. Our preferred solution of 320.5 h and amplitude of 0.42 magnitude.

While we cannot be absolutely confident without more data, our analysis points towards 320.5 ± 0.1 h and an amplitude of 0.42 ± 0.1 magnitude.

Acknowledgements

We would like to acknowledge the continued support for WAO by the MIT Department of Earth, Atmospheric and Planetary Sciences. Partial support for student observers was provided by the MIT Undergraduate Research Opportunities Program. Artem Burdanov and MIT gratefully acknowledge financial support from the Heising-Simons Foundation, Dr. and Mrs. Colin Masson and Dr. Peter A. Gilman for Artemis, the first telescope of the SPECULOOS network situated in Tenerife, Spain.

References

- Behrend, R., Antonini, P. (2007web, 2019web). Résultats CdR&CdL. Observatoire de Geneve web site. <https://www.astro.unige.ch/~behrend/page1cou.html#000259>
- Burdanov, A.Y.; de Wit, J.; Gillon, M.; Rebolo, R.; Sebastian, D.; Alonso, R.; Sohy, S.; Niraula, P.; Garcia, L.; Barkaoui, K.; Chinchilla, P.; Ducrot, E.; Murray, C.A.; Pedersen, P.P.; Jehin, E.; McCormac, J.; Zúñiga-Fernández, S. (2022). "SPECULOOS Northern Observatory: Searching for Red Worlds in the Northern Skies." *Publications of the Astronomical Society of the Pacific* **134**(1040), 105001. doi:10.1088/1538-3873/ac92a6
- Diffraction Limited (2025). Maxim D/L v6. [Online]. Available: <https://diffractionlimited.com/product/maxim-dl/>
- Kleshchonok, V.V.; Karbovsky, V.L.; Buromsky, M.I.; Lashko, M.V. (2021). "Observation of Stellar Occultations by Asteroid (259) Alethea and Comet 21P/Jacobini-Zinner. Kinemat." *Phys. Celest. Bodies* **37**, 41-51. <https://doi.org/10.3103/S0884591321010025>
- Koff, R.A. (2006). "Lightcurves of asteroids 141 Lumen, 259 Alatheia, 363 Padua, 455 Bruchsalia, 514 Armida, 524 Fidelio, and 1139 Atami." *The Minor Planet Bulletin* **33**(2), 31-33.
- Kurlander, J.A.; Bernardinelli, P.H.; Schwamb, M.E.; Jurić, M.; Murtagh, J.; Chandler, C.O.; Merritt, R.; Nesvorný, D.; Vokrouhlický, D.; Jones, R.L.; Fedorets, G.; Cornwall, S.; Holman, M.J.; Eggl, S.; West, M.; Kubica, J.; Yoachim, P.; Moeyens, J.; Kiker, K.; Buchanan, L.E. (2025). "Predictions of the LSST Solar System Yield: Near-Earth Objects, Main Belt Asteroids, Jupiter Trojans, and Trans-Neptunian Objects." *The Astronomical Journal* **170**(2), 99. doi:10.3847/1538-3881/add685.
- Mainzer, A.; Bauer, J.; Cutri, R.; Grav, T.; Kramer, E.; Masiero, J.; Sonnett, S.; Wright, E. Eds. (2019). "NEOWISE Diameters and Albedos V2.0." NASA Planetary Data System. <https://doi.org/10.26033/18S3-2Z54>
- NASA/JPL-Caltech. (2025) JPL Horizons System. <https://ssd.jpl.nasa.gov/horizons/>. Accessed October 8, 2025.
- Orazi, L. (2025). Voyager Advanced. [Online]. Available: <https://software.starkeeper.it/>
- Parrott, D. (2020). "Tycho Tracker: A New Tool to Facilitate the Discovery and Recovery of Asteroids using Synthetic Tracking and Modern GPU Hardware." *Journal of the American Association of Variable Star Observers (JAAVSO)* **48**, 262.
- Pilcher, F. (2025). "Minor Planets at Unusually Favorable Elongations in 2025." *Minor Planet Bulletin* **52-1**, 1.
- Robinson, L. (2011web). Asteroid Lightcurves from Sunflower Observatory 739. <https://btboar.tripod.com/lightcurves/id32.html>
- Slivan, S.M.; Brothers, T.C. (2026). "Spin Properties of Slow Rotator (1714) Sy Determined from Sky Survey Photometry." *Minor Planet Bull.* **53**, 7-10.
- Warner, B.D.; Harris, A.W.; Pravec, P. (2009). "The Asteroid Lightcurve Database." *Icarus* **202**, 134-146. Updated 2016 Sep. <http://www.minorplanet.info/lightcurvedatabase.html>
- Weidenschilling, S.J.; Chapman, C.R.; Davis, D.R.; Greenberg, R.; Levy, D.H. (1990). "Photometric geodesy of main-belt asteroids: III. Additional lightcurves." *Icarus* **86**(2), 402-447.

SPIN PROPERTIES OF SLOW ROTATOR (1714) SY DETERMINED FROM SKY SURVEY PHOTOMETRY

Stephen M. Slivan, Timothy C. Brothers
Massachusetts Institute of Technology
Dept. of Earth, Atmospheric, and Planetary Sciences
77 Mass. Ave. Rm. 54-424, Cambridge, MA 02139
slivan@mit.edu

(Received: 2025 October 14)

Lightcurves of (1714) Sy assembled from archival sky survey data are analyzed for synodic and sidereal rotation periods, spin vector orientation, and a preliminary convex model shape.

Inner main-belt asteroid (1714) Sy was the target of an observational campaign in 2025 by Brothers et al. (2026; this issue) to investigate its rotation period. After their database searches and literature search had not found any prior period information, they carried out a zero-based study that concluded that Sy is a slowly rotating elongated object. Their data allow several possible periods, initially identifying candidates as short as about 40 h as well as the ultimately favored result near 320 h.

The present study was motivated directly by the 2025 campaign, and also found in the literature a sidereal period determination from ASAS-SN survey data of 317.8 h (Hanuš et al., 2021) which validates the alias resolution result favored by Brothers et al. (2026; this issue). Here we present an independent determination of the synodic rotation period based on archived sky survey observations from multiple apparitions, followed by combined analyses of the data for sidereal rotation period, spin vector orientation and convex model shape.

The Minor Planet Center Orbits/Observations Database was checked for photometry of Sy suitable for investigating its spin properties. Such a data set was found from the ATLAS sky survey (Tonry et al., 2018) *o*-band observations made at four telescopes during the six consecutive apparitions between 2018 and 2025 (Table I). Each apparition of photometry was composited separately by correcting the time tags for light time, reducing the brightnesses to unit Sun-asteroid and Earth-asteroid distances, and also approximately adjusting them to the solar phase angle on the composite date using an initial estimate of 0.15 for the solar phase slope parameter G .

Synodic rotation period: A noise spectrum approach fitting a Fourier series model including through the second harmonic was used to identify candidate rotation periods in the range 20 h to 2000 h, which were then individually checked for credible doubly periodic composite lightcurves. The data from 2023–2024 and 2025 were selected for this analysis because they include observations at three substantially different longitudes, which helps suppress alias periods. Only one of the two clearly favored RMS local minima corresponds to a doubly-periodic composite, yielding an initial period estimate near 317 h (Fig. 1).

This first period estimate was used in identifying statistically unlikely “outlier” measurements to exclude from the data by fitting to each apparition a Fourier series model lightcurve and applying Chauvenet’s criterion to the residuals. Next, an empirical slope parameter value of $G = 0.255$ was derived by fitting the Lumme-Bowell model (Bowell et al., 1989) to the data from the two apparitions for period determination, using the iterative approach

described by Slivan et al. (2008). Finally, those data were re-reduced using the empirical G value for improved solar phase corrections, and a new noise spectrum was calculated, this time including through the fourth harmonic in the model. The derived synodic period 316.5 ± 0.8 h was used to fold all six composite lightcurves for Fig. 2, and the period error was estimated using self-consistency of the 2023–2024 composite.

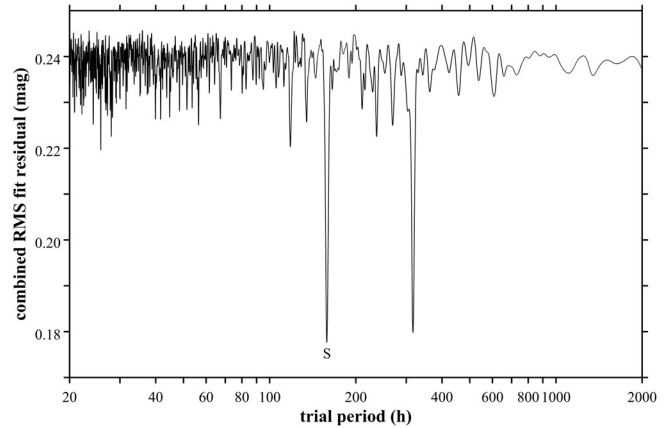


Figure 1. Noise spectrum for Fourier series model fitting with the favored local minimum near 317 h. The adjacent minimum marked “S” corresponds to a rejected singly periodic composite.

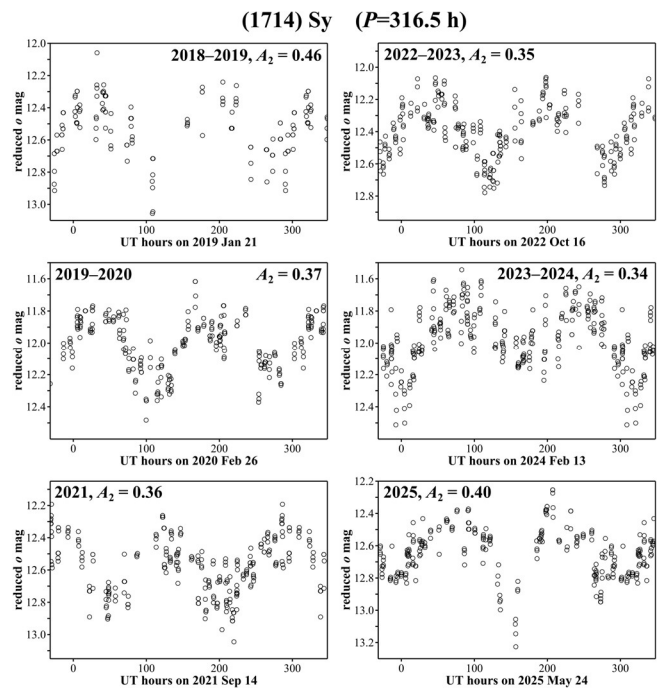


Figure 2. Folded composite lightcurves used to determine epochs. Data are composited by apparition to the median date of the observations, using the derived slope parameter $G = 0.255$ to reduce for changing solar phase angle. Each composite is folded using the same indicated period, with the earliest and latest 10% of rotation repeated. A_2 on each graph is the amplitude in magnitudes of the second harmonic of a fitted fourth order Fourier series model.

Sidereal rotation period and direction of spin: The sieve algorithm described by Slivan (2013) was applied to the set of lightcurve epochs measured from the six apparitions of data (Tables II and III) yielding the results shown in Fig. 3. Both the largest range and the small one just below it on the graph represent the same set of rotation counts but for opposite spin directions; together they

comprise the solution corresponding to 175.0 sidereal rotations over the maximum interval for a sidereal period initial estimate of 317.78 ± 0.13 h. An additional small range that appears on the graph above the actual solution is a spurious overlap in the tails that is sensitive to the epoch uncertainties.

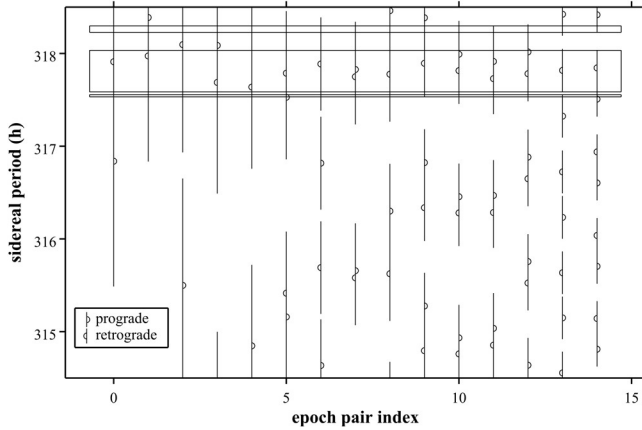


Figure 3. Sieve algorithm output showing ranges of sidereal rotation periods (thin horizontal rectangles) allowed by the intervals in Table III. The largest range together with the small one below it comprise the actual solution which spans from 317.53 h to 318.03 h. Candidate ranges of periods for each epoch interval were calculated using epoch range half-widths of 2.0 times the epoch errors, and the epoch uncertainties were added in quadrature.

Analysis of the epochs using sidereal photometric astrometry (SPA) (Slivan, 2014; Drummond et al., 1988) indicates retrograde rotation (Fig. 4). Epochs analysis constrains pole latitude but is not reliable for pole longitude, which could explain the peculiar shape of this SPA pole region whose two local minima are not symmetric with respect to the “photometric great circle” (Slivan et al., 2023; Appendix A).

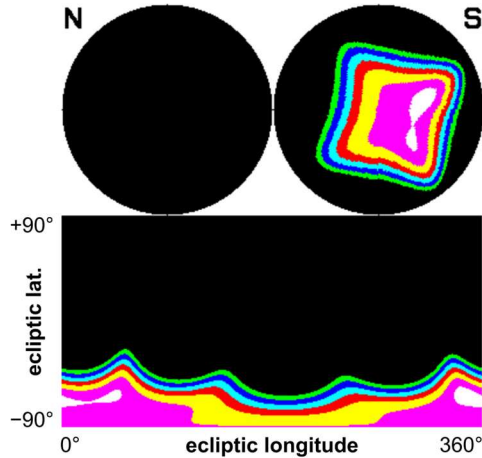


Figure 4. Contour graphs of RMS error of trial poles for the SPA analyses of the epochs in Table II. The lower half of the figure represents the celestial sphere as a rectangular grid; in the upper half the north and south hemispheres are plotted separately in a polar format. The best-fit areas (white) in the south hemisphere indicate retrograde rotation, and suggest a pole latitude near -63° .

Spin vector and convex model shape: Finally, the data were analyzed for spin vector and model shape as described by Slivan et al. (2023) using convex inversion (CI) (Kaasalainen et al., 2001). Per the constraints from the epochs analyses the sieve result provided the initial sidereal period, and the grid search of candidate poles was limited to the south ecliptic hemisphere. The search identifies a pair of retrograde pole regions with the expected symmetry (Fig. 5), but the 8° inclination of Sy’s orbit is too small to resolve which region corresponds to the true pole. The CI analysis results are summarized in Table IV, model lightcurve fits for all six apparitions are shown in Fig. 6, and renderings of the model shape are shown in Fig. 7. Our sidereal period is consistent with the Hanuš et al. (2021) result.

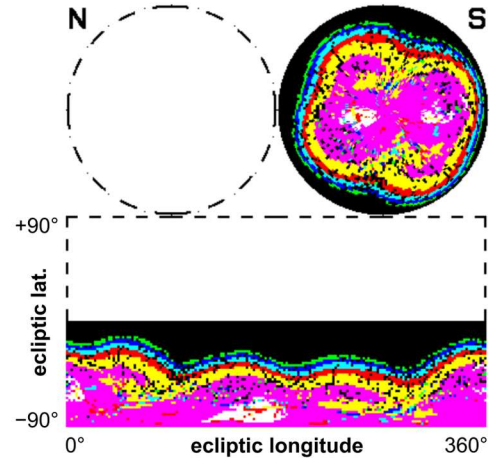


Figure 5. Similar to Fig. 4 but for the CI analysis which locates a pair of retrograde pole regions having the expected symmetry.

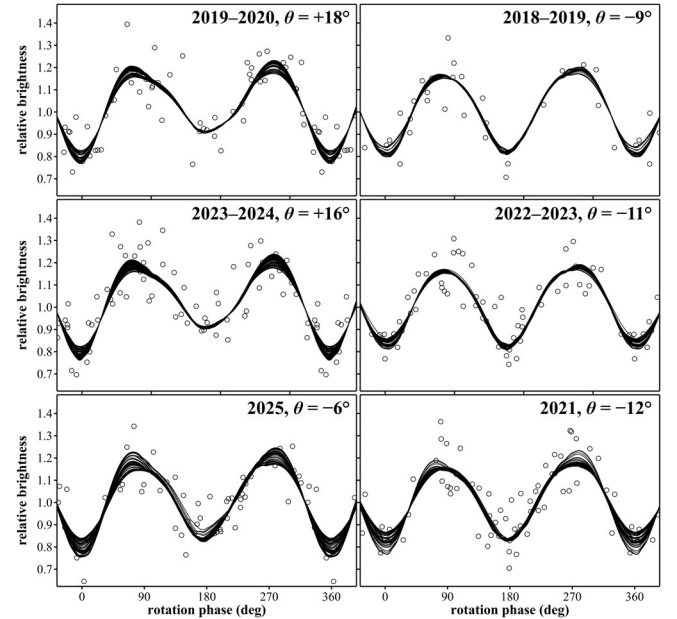


Figure 6: CI model lightcurves for pole P_3 as brightness vs. sidereal rotation phase, presented in order of decreasing sub-PAB latitude θ . Changes in lightcurve shape during the spans of the observations appear as dispersion of overlapping model curves. The RMS error of the fit to the combined data set corresponds to 0.086 mag.

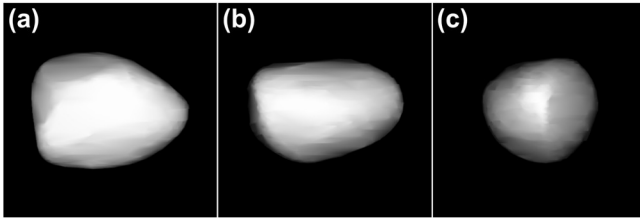


Figure 7. Renderings of convex model for pole P_3 . (a) Polar aspect. (b) Equatorial aspect for lightcurve maximum at rotation phase 90° in Fig. 6. (c) Equatorial aspect for minimum at rotation phase 0° . The model for the symmetric pole P_4 is essentially a mirror image.

Apparition	Number of nights	Span of nights (d)	Telescopes
2018-2019	28	200	a, b
2019-2020	58	275	a, b
2021	60	271	a, b
2022-2023	55	259	a, b, c
2023-2024	64	223	a, b, c, d
2025*	51	239	a, b, c, d

Table I: Summary of ATLAS α -band observations of Sy analyzed in this paper. Telescopes are: a, ATLAS-MLO; b, ATLAS-HKO; c, ATLAS-Chile; d, ATLAS-South Africa. *The 2025 photometry includes observations only through Sep 10 because the data were retrieved while the apparition was still in progress.

UT date	Epoch (UT h)	PAB λ, β ($^\circ$)
2019 Jan 21	33 ± 12	$67.0, +6.4$
2020 Feb 26	34 ± 12	$149.9, -5.3$
2021 Sep 14	127 ± 14	$308.6, +3.2$
2022 Oct 16	41 ± 14	$56.7, +9.1$
2024 Feb 13	84 ± 17	$138.4, -3.4$
2025 May 24	67 ± 11	$280.4, -5.3$

Table II: Summary of lightcurve epochs, each determined using a Fourier series model fit to the lightcurves as described by Slivan et al. (2024). PAB λ, β are the J2000.0 ecliptic longitude and latitude of the phase angle bisector.

Epoch pair index	Interval (d)	Interval (app.)	Epochs source apparitions
0	393.4	1	2021, 2022
1	401.0	1	2019, 2020
2	465.3	1	2024, 2025
3	486.8	1	2022, 2024
4	569.9	1	2020, 2021
5	880.2	2	2021, 2024
6	952.0	2	2022, 2025
7	963.3	2	2020, 2022
8	970.9	2	2019, 2021
9	1345.5	3	2021, 2025
10	1364.3	3	2019, 2022
11	1450.1	3	2020, 2024
12	1851.1	4	2019, 2024
13	1915.3	4	2020, 2025
14	2316.4	5	2019, 2025

Table III: Time intervals between lightcurve epochs analyzed using the sieve algorithm (Table II). Columns are: epoch pair index label, interval length rounded to 0.1 d, the corresponding integer count of elapsed apparitions, and the apparitions from which the defining epochs were measured.

Synodic period: 316.5 ± 0.8 h

Pole solution P_3

Sidereal period: 317.79 ± 0.02 h

Spin pole: $\frac{\lambda_0}{7^\circ} \frac{\sigma(\lambda_0)}{5} \frac{\beta_0}{-60^\circ} \frac{\sigma(\beta_0)}{5} \frac{\varepsilon}{157^\circ}$

Model axial ratios: $a/b: 1.4 \quad b/c: 1.1$

Pole solution P_4

Sidereal period: 317.78 ± 0.02 h

Spin pole: $\frac{\lambda_0}{161^\circ} \frac{\sigma(\lambda_0)}{5} \frac{\beta_0}{-78^\circ} \frac{\sigma(\beta_0)}{5} \frac{\varepsilon}{162^\circ}$

Model axial ratios: $a/b: 1.4 \quad b/c: 1.2$

Table IV: Spin properties results. λ_0 and β_0 are the pole solutions' ecliptic longitudes and latitudes, respectively; σ are the estimated pole errors in degrees of arc; ε are the spin obliquities. The axial ratios are very coarse estimates with uncertainties of at least ± 0.1 .

Acknowledgments

This work made use of data and services from the International Astronomical Union's Minor Planet Center; specifically, the brightnesses accompanying astrometry from the Asteroid Terrestrial-impact Last Alert System (ATLAS) survey observing program.

References

- Bowell, E.; Hapke, B.; Domingue, D.; Lumme, K.; Peltoniemi, J.; Harris, A.W. (1989). "Application of Photometric Models to Asteroids." In *Asteroids II* (R.P. Binzel; T. Gehrels; M.S. Matthews, eds.) pp. 524-556. Appendix: The IAU Two-Parameter Magnitude System for Asteroids. U. of Arizona Press, Tucson, AZ.
- Brothers, T.C.; Coleman, M.A.; Cranor, N.; Sconce, V.B.; Slivan, S.M.; Panbianco, K.M.; Oberg, L.J.; Fass, E.R.; Chen, A.Y.; Stoltz, A.O.; Burdanov, A.Y.; Ekelmann, J.R.; Person, M.J. (2026). "Lightcurves and Rotation Periods for (259) Aletheia, (1146) Biarmia, and (1714) Sy." *Minor Planet Bull.* **53**, 3-6.
- Drummond, J.D.; Weidenschilling, S.J.; Chapman, C.R.; Davis, D.R. (1988). "Photometric geodesy of main-belt asteroids. II. Analysis of lightcurves for poles, periods, and shapes." *Icarus* **76**, 19-77.
- Hanuš, J.; Pejcha, O.; Shappee, B.J.; Kochanek, C.S.; Stanek, K.Z.; Holien, T.W-S. (2021). "V-band photometry of asteroids from ASAS-SN. Finding asteroids with slow spin." *A&A* **654**, A48.
- Kaasalainen, M.; Torppa, J.; Muinonen, K. (2001). "Optimization methods for asteroid lightcurve inversion. II. The complete inverse problem." *Icarus* **153**, 37-51.
- Slivan, S.M.; Binzel, R.P.; Boroumand, S.C.; Pan, M.W.; Simpson, C.M.; Tanabe, J.T.; Villastrigo, R.M.; Yen, L.L.; Ditteon, R.P.; Pray, D.P.; Stephens, R.D. (2008). "Rotation Rates in the Koronis Family, Complete to $H \approx 11.2$." *Icarus* **195**, 226-276.

Slivan, S.M. (2013). "Epoch Data in Sidereal Period Determination. II. Combining Epochs from Different Apparitions." *Minor Planet Bull.* **40**, 45-48.

Slivan, S.M. (2014). “Sidereal Photometric Astrometry as Efficient Initial Search for Spin Vector.” *Minor Planet Bull.* **41**, 282-284.

Slivan, S.M.; Hosek Jr., M.; Kurzner, M.; Sokol, A.; Maynard, S.; Payne, A.V.; Radford, A.; Springmann, A.; Binzel, R.P.; Wilkin, F.P.; Mailhot, E.A.; Midkiff, A.H.; Russell, A.; Stephens, R.D.; Gardiner, V.; and 5 colleagues (2023). “Spin vectors in the Koronis family: IV. Completing the sample of its largest members after 35 years of study.” *Icarus* **394**, A115397.

Slivan, S.M.; Barrera, K.; Colclasure, A.M.; Cusson, E.M.; Larsen, S.S.; McLellan-Cassivi, C.J.; Moulder, S.A.; Nair, P.R.; Namphy, P.D.; Neto, O.S.; Noto, M.I.; Redden, M.S.; Rhodes, S.J.; Youssef, S.A. (2024). “Lightcurves and Derived Results for Koronis Family Member (5139) Rumoi, Including a Discussion of Measurements for Epochs Analysis.” *Minor Planet Bull.* **51**, 6-10.

Tonry, J.L.; Denneau, L.; Heinze, A.N.; Stalder, B.; Smith, K.W.; Smartt, S.J.; Stubbs, C.W.; Weiland, H.J.; Rest, A. (2018). “ATLAS: A High-cadence All-sky Survey System.” *PASP* **130**, 064505.

LIGHTCURVE ANALYSIS OF NEA 2025 OW

Gonzalo Fornas, Alvaro Fornas, AVA - J57, CAAT
Centro Astronómico del Alto Turia, Aras de los Olmos, SPAIN
gon@iicv.es

Enrique Arce, AVA, J67
Vallbona Observatory, Puebla de Vallbona, SPAIN

(Received: 2025 September 5)

We report rotation lightcurves of 2025 OW observed during its apparition in 2025. We have analyzed our data to calculate the synodic period with the *MPO Canopus* software. Our conclusion with the available data is that the synodic rotation period is 0.02696 h.

In the present study we report on data obtained during the observation campaign of the asteroid 2025 OW carried out during the apparition of 2025. This work has been done from Astronomical Center Alto Turia (CAAT), with the MPC code J57, located in Aras de los Olmos, Valencia, operated by members of the Valencian Astronomy Association (AVA) (<http://www.astroava.org>).

Observatory	Telescope (meters)	CCD	Observations
C.A.A.T. J57	43 cm DK	QHY 600	07/26 07/27 07/28

Table I. List of instruments and observations

The asteroid 2025 OW was recently discovered, on July 4th, by Pan-STARRS 2. From our observatory, we tracked it over three nights to calculate its astrometry and later analyzed its photometry.

Work Methods

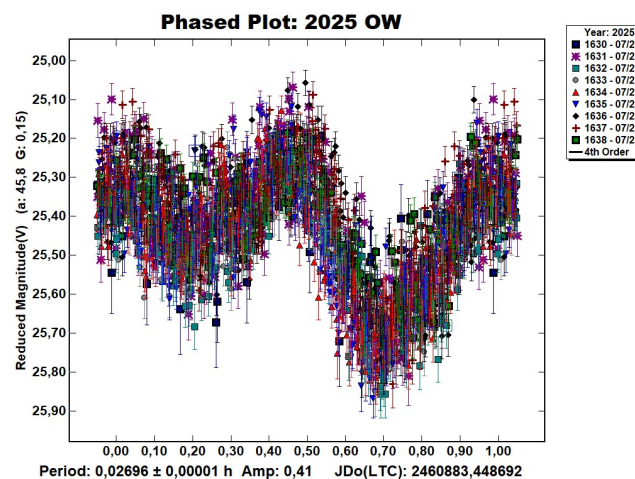
Images were measured using *MPO Canopus* (Bdw. Publishing) with a differential photometry technique. The comparison stars were restricted to near solar color to minimize color dependencies, especially at larger air masses. The lightcurves show the synodic rotation period. The amplitude (peak-to-peak) that is shown is that for the Fourier model curve and not necessarily the true amplitude.

Number	Name	yyyy mm/dd	Phase	L _{PAB}	B _{PAB}	Period(h)	P.E.	Amp	A.E.	Grp
2025 OW		2025/07/26-28	45.8, 54.4	310.7	24.7	0.02696	0.00001	0.41	0.05	NEA

Table I. Observing circumstances and results. The phase angle is given for the first and last date. L_{PAB} and B_{PAB} are the approximate phase angle bisector longitude/latitude at mid-date range. Grp is the asteroid family/group (Warner et al., 2009).

Results

Our observations were made on 4 nights in 2025 Jul 26-28. Our analysis with Canopus shows a synodic rotation period of 0.02696 ± 0.00001 h which is shown in the figure. There are no other studies available to us on the rotation period of this asteroid, as it has just been discovered and we received no reports at the time of this writing.



Acknowledgements

We would like to express our gratitude to Vicente Mas for his incredible work in setting up and improving the J57 observatory over the last few years.

References

Warner, B.D.; Harris, A.W.; Pravec, P. (2009). “The Asteroid Lightcurve Database.” *Icarus* **202**, 134-146. Updated 2016 Sep. <http://www.minorplanet.info/lightcurvedatabase.html>

LIGHTCURVE AND ROTATION PERIOD ANALYSIS OF 6690 MESSICK

Wayne Hawley
Old Orchard Observatory (Z09)
Fiddington, UK
hawley.wayne@gmail.com

James D. Armstrong
University of Hawaii Institute for Astronomy
(L09) (Q58) (Q59) (V38) (T04) (W89) (Z21)
34 Ohia Ku Street
Pukalani, HI 96768 USA

(Received: 2025 July 4)

Photometric observations of asteroid 6690 Messick were obtained during 2025 August. For 6690 Messick, we found $P = 2.995 \pm 0.001$ h, $A = 0.227 \pm 0.15$ magnitudes.

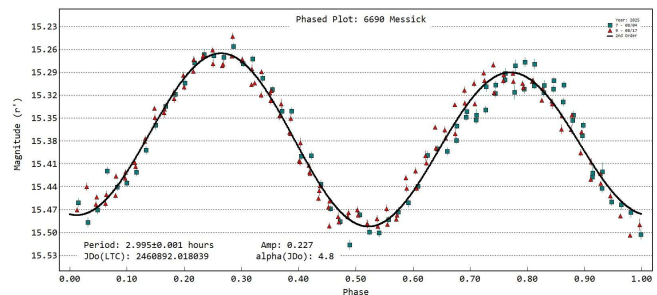
Minor planet 6690 Messick is a member of the Flora family that was discovered on 1981 Sep 25 by B.A. Skiff at the Anderson Mesa Station of the Lowell Observatory. Our CCD photometric observations of 6690 Messick were made on 2025-08-04 from Siding Spring and 2025-08-17 from Cerro Tololo. Photometry and period determination were carried out with *TychoTracker Pro* Version 12.5.7. (TT). The photometric analysis was performed using standard differential techniques on images with the comparison stars employed selected by TT to be within the colour range of $+0.50 < (B-V) < +0.90$.

The Asteroid Terrestrial-impact Last Alert System (ATLAS) catalog (Tonry et al, 2015; Kostov and Bonev, 2017) was used as the source of reference stars. TT's period determination operates by finding model lightcurves based on a user-defined number of Fourier components which best fit the asteroid photometric data. The program lists the candidate periods found within a user-defined period range and sampling frequency, based on minimizing Root Mean Square Errors (RMSE), between the modelled and photometric magnitudes. The candidate periods are listed in increasing RMSE value and the entire suite of RMSE values is plotted as a "periodogram" for quality control. In these periodograms the object yielded a clear 'best-fit' period solution having well defined minima as shown in the following figures. Periodograms often exhibit several possible candidate periods, in which case an examination of the rotational phase plot for each of these is then conducted looking for a credible lightcurve. Where the

object shape is the dominant factor in producing the observed magnitude changes, (typically having lightcurve amplitudes of >0.2 mag), the rotational phase plot often has two peaks and two troughs (bimodal) and this is usually chosen as the most likely for such asteroids.

In this paper no attempt is made to find an absolute magnitude and a value of $G = 0.15$ has been used throughout the calculations. Time-series magnitude estimates from different nights and observing locations using a variety of imaging equipment were offset in magnitude to bring them into alignment when producing the raw and rotational-phase plots. The same offset was used for each instance of an individual imaging setup. When this paper is accepted for publication all the observations will be loaded into the Asteroid Lightcurve Data Exchange Format (ALCDEF) database.

The lightcurve period and amplitude results reported here are based on a total of 195 exposures obtained during 2025 August. Our analysis found a synodic rotation period of 2.995 ± 0.001 h and peak-to-peak amplitude of 0.227 ± 0.15 mag. These results are summarized in Table 1 below. Column 3 gives the span of dates over which the observations were made. Column 4 is the range of phase angles for each date range, if this is preceded by an asterisk this means the asteroid passed through minimum phase angle during the observing period. Columns 5 and 6 give the range of values for the Phase Angle Bisector (PAB) longitude and latitude respectively, for the mid date of the observation set. Column 7 gives the period and Column 8 the minimum possible formal error in hours given by TT. Columns 9 and 10 give the amplitude and its associated uncertainty in magnitude. Dips in the results from the period analysis have been checked to see if they are monomodal or bimodal and a bimodal period has been chosen for the best-fit result. Information given for the object is taken from the NASA Jet Propulsion Laboratory (JPL) Small-Body Database Lookup webpage (2023).

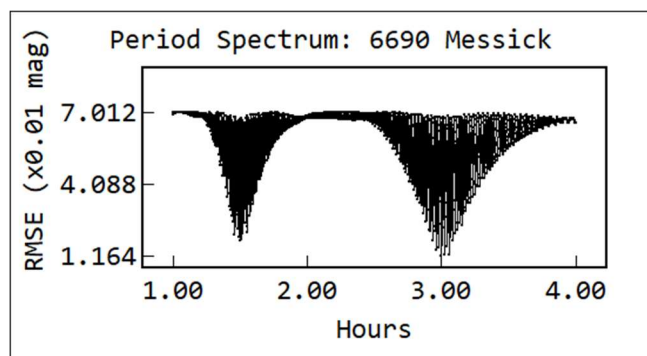


Number	Name	yyyy mm/dd	Phase	L_{PAB}	B_{PAB}	Period (h)	P.E.	Amp	A.E.	Grp
6690	Messick	2025 08/04-08/17	*3.0, 4.8	319	0	2.995	0.001	0.227	0.15	402

Table I. Observing circumstances and results. The phase angle is given for the first and last date. If preceded by an asterisk, the phase angle reached a minimum during the period. L_{PAB} and B_{PAB} are the approximate phase angle bisector longitude/latitude at mid-date range (see Harris et al., 1984). Grp is the asteroid family/group (Warner et al., 2009).

Observatory	Telescope (m)	Camera	Filter	Object (sessions)
Siding Spring LCO Clamshell #2 (Q59), Armstrong	0.35 f/3	QHY 600 CMOS (1×1)	SR	6690 (1)
Cerro Tololo LCO Aqawan B #1 (W79), Armstrong	0.35 f/3	QHY 600 CMOS (1×1)	SR	6690 (1)

Table II. List of observers and equipment. The number in parentheses in the last column is the number of sessions for the given object.



Acknowledgements

Our thanks are extended to Daniel Parrott, author of *Tycho Tracker Pro*. This work has made use of data from the Asteroid Terrestrial-impact Last Alert System (ATLAS) project. ATLAS is primarily funded to search for near earth asteroids through NASA grants NN12AR55G, 80NSSC18K0284, and 80NSSC18K1575; byproducts of the NEO search include images and catalogs from the survey area. The ATLAS science products have been made possible through the contributions of the University of Hawaii Institute for Astronomy, the Queen's University Belfast, the Space Telescope Science Institute, and the South African Astronomical Observatory. The ATLAS Catalog makes use of the formulae to convert Pan-STARRS gri to BVRI (Kostov and Bonev, 2017). This paper is based on observations made with the Las Cumbres Observatory's education network telescopes that were upgraded through generous support from the Gordon and Betty Moore Foundation.

This work makes use of observations from the Las Cumbres Observatory global telescope network.

References

- Harris, A.W.; Young, J.W.; Scaltriti, F.; Zappala, V. (1984). "Lightcurves and phase relations of the asteroids 82 Alkmene and 444 Gytis." *Icarus* **57**, 251-258.
- JPL (2023). Small-Body Database Lookup. https://ssd.jpl.nasa.gov/tools/sbdb_lookup.html
- Kostov, A.; Bonev, T. (2017). "Transformation of Pan-STARRS1 gri to Stetson BVRI magnitudes. Photometry of small bodies observations." *Bulgarian Astron. J.* **28**, 3 (*ArXiv:1706.06147v2*).
- Tonry, J.L.; Denneau, L.; Flewelling, H.; Heinze, A.N.; Onken, C.A.; Smartt, S.J.; Stadler, B.; Weiland, H.J.; Wolf, C. (2018). "The ATLAS All-Sky Stellar Reference Catalog." *Ap. J.* **867**, A105.
- Warner, B.D.; Harris, A.W.; Pravec, P. (2009). "The Asteroid Lightcurve Database." *Icarus* **202**, 134-146. Updated 2023 Oct 1. <https://minplanobs.org/mpinfo/php/lcdb.php>

LIGHTCURVE ANALYSIS OF 5066 GARRADD

Kelly Le, Melissa Hayes-Gehrke, Elizabeth Warner
Department of Astronomy
University of Maryland, College Park, MD 20742 USA
kle12314@terpmail.umd.edu

(Received: 2025 August 14)

Lightcurve measurements for the asteroid 5066 Garradd were analyzed using *MPO Canopus*. The analysis of the measurements indicated the absence of a detectable lightcurve amplitude greater than ~ 0.1 magnitude, suggesting a somewhat spherical geometry, or a near pole-on aspect, or a long period.

5066 Garradd is a Mars-crossing asteroid that was discovered on 1954 01/03. This asteroid has an absolute magnitude of 14.21 and a diameter of 4.937 km. It has a semi-major axis of 1.937 AU, an eccentricity of 0.1542, an inclination of 41.44° , and an orbital period of 2.69 years (JPL, 2024). Its apparent magnitude is approximately 15.9.

Observations of 5066 Garradd were conducted using a 7-inch Astro-Physics refracting telescope with a focal length of 1600 mm, located at the UMD Observatory in College Park, MD, part of the University of Maryland's Department of Astronomy. Imaging was performed with an ST-10XME CCD camera featuring an array of 2184×1472 pixels, 6.8×6.8 -micron pixel size, and a plate scale of 0.9 arcseconds/pixel. All data were collected using a clear filter.

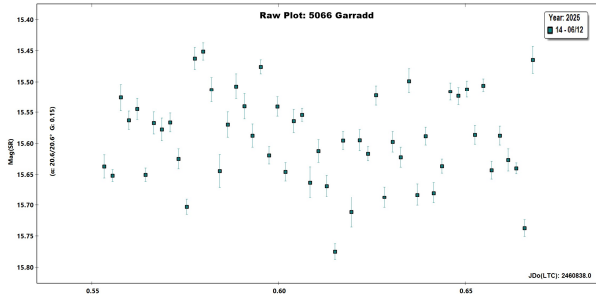
Observations were collected over four nights by Le (2025 06/20, 06/22, 06/24, and 06/25), averaging approximately 40 usable frames per night. Additional data were contributed on dates (2025 06/04, 06/12) by Warner. Weather conditions during the observations ranged from average to above-average transparency, with seeing rated around 3/5. Temperatures were hot, between 77°F to 95°F , accompanied by moderate humidity and frequent hazy skies throughout the nights. Visibility remained decent despite mild atmospheric distortion. The dataset from 06/22 was excluded following initial photometric reduction, as it did not meet quality standards.

Images were first processed with plate solving using *ASTAP* (Kleijn, n.d.). The Data Processor module in *AstroImageJ* (Collins et al., 2017) software enabled the effective application of calibration frames including bias, dark, and flat fields. The frames were collected each night of observation and later applied to the science images, helping reduce instrumental noise and correct sky illumination patterns. As a result, the accuracy of photometric measurements was significantly improved.

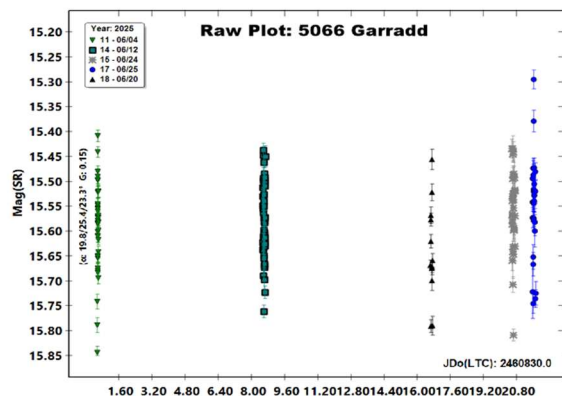
Using *SAOImage DS9* (Smithsonian Astrophysics Observatory, 2023), all calibrated images were visually inspected, labeling any frames affected by tracking issues and noise that could impede the identification of 5066 Garradd's lightcurve. The selected, calibrated images were processed using *MPO Canopus* (Warner, 2025), which performed aperture photometry and identified a minimum of five comparison stars to generate differential magnitude measurements of the target asteroid. Further photometric analysis and an attempted Fourier analysis were applied to the combined dataset, including trials with various Fourier orders.

Number	Name	yyyy mm/dd	Phase	L _{PAB}	B _{PAB}	Period(h)	P.E.	Amp	A.E.	Grp
5066	Garradd	2025 06/03-06/25	19.8, 23.2	243	16					MCA

Table I. Observing circumstances and results. The phase angle is given for the first and last date. If preceded by an asterisk, the phase angle reached an extrema during the period. L_{PAB} and B_{PAB} are the approximate phase angle bisector longitude/latitude at mid-date range (see Harris et al., 1984). Grp is the asteroid family/group (Warner et al., 2009).



The lightcurve shows significant amounts of scatter, suggesting noise rather than clear periodic features like defined peaks and troughs, as seen in the first figure of data which represents solely the night of 2025 06/12. The second figure, which includes data from all nights, displays a consistent cluster of magnitudes around 15.55-15.60 SR mag, similar to the random scatter observed in the first figure. This pattern suggests that the observed variability is not primarily due to rotation, but rather results from observational noise or other external factors, indicating that 5066 Garradd's brightness remains relatively steady without the strong variations typically expected from an asteroid's rotation. A flat lightcurve is typically caused by one of three factors: the asteroid could have a shape considered nearly spherical meaning it reflects light consistently as it rotates; it might be viewed as pole-on so the rotation doesn't produce noticeable brightness changes from our perspective at UMD Observatory; or it could be a slow rotator, meaning the full range of brightness variation wasn't captured. We consider the nearly spherical shape to be the most plausible explanation, as the pole-on orientation represents an improbable coincidence, and a slow rotator would likely exhibit detectable brightness variations where it failed to during the 23 days of observations. The absence of any recorded period for 5066 Garradd in the *Asteroid Lightcurve Database* (Warner et al., 2021) combined with current observations further supports the conclusion that its rotation period remains unidentified.



Acknowledgements

This research was made possible from funding by the S-STEM Chesapeake Scholars program, a multi-disciplinary scholarship within the College of Computer, Mathematical, and Natural Sciences at the University of Maryland, College Park, supported by the National Science Foundation.

References

- Collins, K.A.; Kielkopf, J.F.; Stassun, K.G.; Hessman, F.V. (2017). "AstroImageJ: Image Processing and Photometric Extraction for Ultra-precise Astronomical Light Curves." *Astron. J.* **153**, 77-89.
- Harris, A.W.; Young, J.W.; Scaltriti, F.; Zappala, V. (1984). "Lightcurves and phase relations of the asteroids 82 Alkmene and 444 Gryptis." *Icarus* **57**, 251-258.
- JPL (2024). Small Body Database Lookup. https://ssd.jpl.nasa.gov/tools/sbdb_lookup.html#/
- Kleijn, H. (n.d.). ASTAP Astrometric Stacking Program. <https://www.hnsky.org/astap.htm>
- Smithsonian Astrophysics Observatory (2023). "SAOImage DS9: A utility for displaying astronomical images in the X11 window environment." *Astrophysics Source Code Library*, ascl: 0003.002.
- Warner, B.D.; Harris, A.W.; Pravec, P. (2009). "The Asteroid Lightcurve Database." *Icarus* **202**, 134-146. Updated 2016 Sep. <http://www.minorplanet.info/lightcurvedatabase.html>
- Warner, B.D.; Harris, A.W.; Pravec, P. (2021). Asteroid Lightcurve Data Base (LCDB) Bundle V4.0. urn:nasa:pds:ast-lightcurve-database::4.0. NASA Planetary Data System. doi: 10.26033/j3xc-3359.
- Warner, B.D. (2025). MPO Software, *MPO Canopus* version 12.0.6.6. BdwPublishing. <http://www.bdwpublishing.com/>

LIGHTCURVE AND ROTATION PERIOD OF (2977) CHIVILIKHIN

Arushi Nath

MonitorMyPlanet Observatory (R60), Nerpio, SPAIN
Arushi@MonitorMyPlanet.com

(Received: 2025 September 14)

Photometric observations of the main-belt asteroid (2977) Chivilikhin obtained in August 2025 over five nights yielded a synodic rotation period of 6.257 ± 0.001 h with a peak-to-peak amplitude of 0.98 mag. These results agree with the 2016 apparition (6.2574 ± 0.0007 h; amplitude 1.00 mag), confirming the stability of the rotation period across multiple apparitions.

Asteroid (2977) Chivilikhin is a main-belt object. Its 2025 apparition provided favorable viewing conditions which motivated new photometric observations to refine its rotational parameters and compare them with prior results.

Our observations were conducted on five nights in 2025: 8, 23, 29-31 August 2025 (UT). Standard calibration (bias, dark, and flat-field corrections) and differential photometry were applied. Observations were made at Monitor My Planet Observatory (MPC code R60), Nerpio, Spain. A 12-inch Ritchey-Chrétien telescope on a Sky-Watcher EQ8-R mount with an ASI2600 mono camera, Cousins Red filter, and 0.75× focal reducer was used. Images were binned 2×2, providing a pixel scale of 0.848 arcsec/pixel. Reduction and calibration were performed with Tycho Tracker using ATLAS catalog stars.

The dataset was phased using a fourth-order Fourier series fit. The derived synodic rotation period is 6.257 ± 0.001 h, with a peak-to-peak amplitude of 0.98 mag. Amplitude Error (A.E.) was estimated as 0.06 mag from $\sqrt{2}$ times the RMS residual of the lightcurve. The period spectrum (Figure 1) shows a well-defined solution of 6.257 ± 0.001 h. The phased lightcurve, combining all five nights of data (Figure 2) shows an amplitude of 0.98 mag. These results are consistent with the 2016 apparition reported by Washburn and Ditteon (2017).

Source	Period (h)	Amplitude (mag)
Washburn & Ditteon (2017)	6.2574 ± 0.0007	1.00
This work (2025)	6.257 ± 0.001	0.98

Table I. Rotation period comparison for (2977) Chivilikhin.

Observations of (2977) Chivilikhin in 2025 yield a synodic rotation period of 6.257 ± 0.001 h and an amplitude of 0.98 mag. This work confirms the rotational stability of (2977) Chivilikhin across nearly a decade of observations.

Acknowledgements

The author thanks the Masason Foundation for providing funding for the telescope and AstroCamp for hosting my observatory in Nerpio, Spain.

References

- Harris, A.W.; Young, J.W.; Scaltriti, F.; Zappala, V. (1984). "Lightcurves and phase relations of the asteroids 82 Alkmene and 444 Gyptis." *Icarus* **57**, 251-258.
- Parrott, D. (2020-2024). Tycho Tracker: Photometry and astrometry software. <https://www.tycho-tracker.com>
- Washburn, K.; Ditteon, R. (2017). "Lightcurve analysis of asteroids observed at the Oakley Southern Sky Observatory: 2016 October." *Minor Planet Bulletin* **44**, 184-185.
- Warner, B.D.; Harris, A.W.; Pravec, P. (2009). "The Asteroid Lightcurve Database." *Icarus* **202**, 134-146. Updated 2023 Oct. <http://www.minorplanet.info/lightcurvedatabase.html>

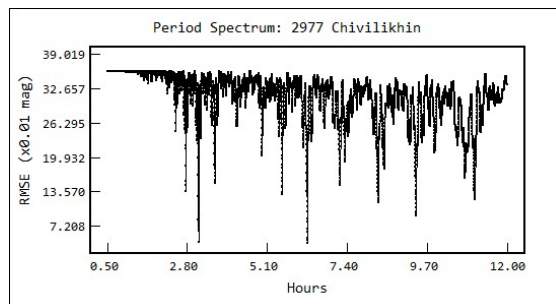


Figure 1. Periodogram (0.5–12 h) computed with a 4th-order Fourier fit showing the preferred solution at 6.257 h.

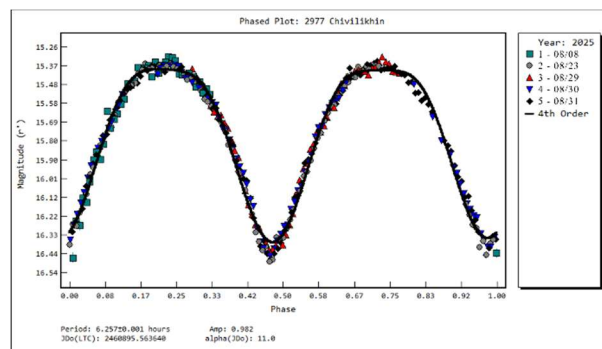


Figure 2. Lightcurve of (2977) Chivilikhin combining all five nights (2025 Aug 8–31) phased to a period of 6.257 hours.

Number	Name	yyyy mm/dd	Phase	L _{PAB}	B _{PAB}	Period(h)	P.E.	Amp	A.E.	Grp
2977	Chivilikhin	2025 08/08-08/31	*11.0, 1.8	336	4	6.257	0.001	0.98	0.06	MB-M

Table II. Observing circumstances and results. The phase angle is given for the first and last date. If preceded by an asterisk, the phase angle reached an extrema during the period. L_{PAB} and B_{PAB} are the approximate phase angle bisector longitude/latitude at mid-date range (see Harris et al., 1984). Grp is the asteroid family/group (Warner et al., 2009).

LIGHTCURVES AND DERIVED RESULTS FOR KORONIS FAMILY MEMBER (1913) SEKANINA

Stephen M. Slivan, Alex Y. Chen, McKenzie A. Coleman,
Nina Cranor, Jayna R. Ekelmann, Erez R. Fass, Layna J. Oberg,
Katherine M. Panebianco, Victoria B. Sconce, Aiden O. Stoltz
Massachusetts Institute of Technology
Dept. of Earth, Atmospheric, and Planetary Sciences
77 Mass. Ave. Rm. 54-424, Cambridge, MA 02139
slivan@mit.edu

(Received: 2025 October 3)

Lightcurves of (1913) Sekanina recorded during three apparitions are presented with an independent determination of the synodic rotation period, which is used to constrain a reanalysis of data from a prior apparition for a final result of 14.0311 ± 0.0007 h. A comprehensive analysis of data from six apparitions is then presented to determine the sidereal rotation period, spin vector orientation, and a preliminary model shape.

Koronis family member (1913) Sekanina was observed as part of a program to extend the study sample of rotation properties of the family's brightest objects (Slivan et al., 2023) to smaller sizes. Observations of Sekanina in 2021–22 by Dose (2022) were reported with a derived rotation period of 14.035 ± 0.003 h, which currently stands in the Asteroid Lightcurve Database (Warner et al., 2009, updated 2023 Oct.) as the accepted “best result” with a period quality code indicating that it is likely correct but not entirely secure. It is corroborated by two analyses of photometric survey data (Chang et al., 2014; Erasmus et al., 2020) but differs from the result of a third (Waszczak et al., 2015). Additional lightcurves are reported here from three apparitions, including data from two aspects lacking previous densely-sampled observations. In this paper we begin by presenting an independent determination of the synodic rotation period based on new observations, followed by a combined analysis of these new lightcurves with archived low-noise sky survey data spanning four lunations for a more precise period. That result is then used in comprehensive analyses of data from a total of six apparitions to determine the sidereal rotation period, spin vector orientation, and a convex model shape.

The lightcurves of Sekanina reported here were recorded during three apparitions, for which the instrumentation is detailed in Table I and the nightly observing information is summarized in Table II. Image processing and measurement procedures were as described by Slivan et al. (2008) using synthetic aperture sizes informed by Howell (1989). The lightcurves were corrected for light-time prior to compositing. Brightnesses that also had been calibrated to a common zero point were reduced to unit distances and corrected to the solar phase angle on the composite date using the slope parameter $G = 0.23$ for S-type objects (Lagerkvist and Magnusson, 1990), while uncalibrated relative photometry was shifted in brightness as needed for a self-consistent composite.

2014 apparition. Fig. 1(a): These observations from the Whitt Observatory (WhO) in Wellesley, MA record about a half of a rotation showing an amplitude of about 0.13 mag, near the reflex of the aspect observed by Dose (2022). Three of the four individual lightcurves were calibrated to standard R magnitudes using observations of the comparison stars and a Landolt (1983) standard star during photometric sky conditions.

2016 apparition. Fig. 1(b): These observations also from WhO were made using a secondary camera and its colorless “Luminance” (L) filter while the primary camera was out for service. The data were recorded at an aspect similar to that observed by Dose (2022) and show a comparable amplitude of about 0.14 mag. All three individual lightcurves were calibrated to a common brightness zero point using observations of the comparison stars during photometric sky conditions.

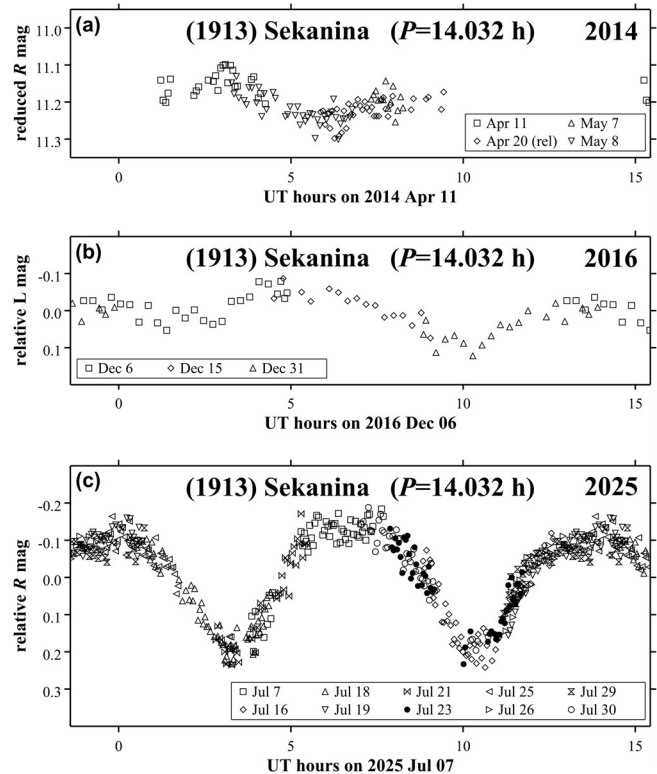


Figure 1. Composite lightcurves of Sekanina during the apparitions in (a) 2014, (b) 2016, and (c) 2025. Each composite is folded using the same 14.032 h period derived from the 2025 data, with the earliest and latest 10% of rotation repeated. Legends give the UT dates of observations.

2025 apparition. Fig. 1(c): These lightcurves were recorded at the Wallace Astrophysical Observatory (WAO) in Westford, MA, at an aspect near the reflex of the 2012–13 aspect from which survey observations were analyzed by Waszczak et al. (2015). The lightcurve amplitude of about 0.33 mag is more than twice as large as was observed in 2014 and 2016, making the 2025 lightcurves best suited for period determination.

In 2025 the nightly availability for observing was limited by Sekanina’s southern declination during northern hemisphere summer; most of the individual lightcurves span from 3.6 to 4.0 hours. These lightcurves show clear brightness changes, and most of them include either a maximum or a minimum, but no single span is long enough to show two extrema. Assuming that spans of this length are recording about a quarter-rotation of a doubly periodic lightcurve, and including a generous allowance for possible lightcurve asymmetry, the full period is estimated to be within the range of about 10.8 h to 24 h. For periods in this range, the data sampling rate is sufficient to average the brightness measurements in groups of four to reduce the errors by a factor of about two

without loss of lightcurve shape information. A period noise spectrum calculated for a Fourier series model including through the second harmonic was used to identify candidate periods in the range 8 h to 32 h, that were then individually checked for credible doubly-periodic composites (Fig. 2). Only one period yields an entirely self-consistent composite for a derived synodic period of 14.032 ± 0.005 h, a result that is consistent with that of Dose (2022). It is also corroborated by the survey data analyses of Chang et al. (2014) and Erasmus et al. (2020) but differs from the Waszczak et al. (2015) analysis; the explanation for that difference is discussed two paragraphs hence.

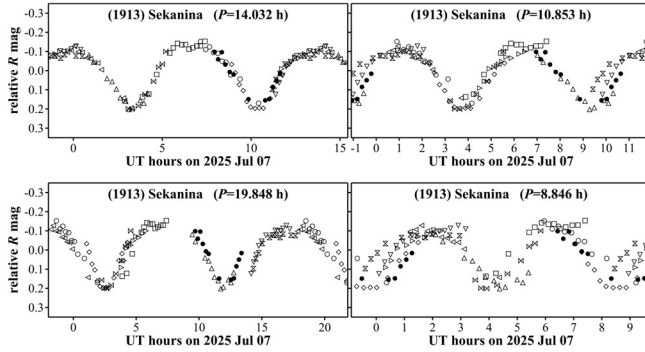


Figure 2. The lightcurves from 2025 folded using the best-fitting four candidate periods in order of increasing RMS fit error, showing that only the composite for 14.032 h (upper left panel) is entirely self-consistent. Graph symbols are identified in the legend of Fig. 1(c), and the original data there were averaged here in groups of four points to more clearly show inconsistencies in the composites.

To investigate whether the 2025 data might make possible a determination of the sidereal rotation period, Eqs. 3-5 from Slivan (2012) are used to test whether the synodic period and precision are sufficient to unambiguously count rotations between epochs not in the same apparition. For the synodic period determined from the 23-day span of 2025 data the calculation yields $N_{\text{per}} = 3$ possible sidereal rotation periods, indicating that the count would be ambiguous and thus a more precise synodic period constraint would be helpful.

The only other larger-amplitude aspect apparition during which densely-sampled observations were made is 2012-13, which was observed by the Palomar Transient Factory (PTF) survey as analyzed by Waszczak et al. (2015). We retrieved these data from the ALCDEF database and found both densely-sampled and sparse-in-time observations. Analysis of the four-night span of dense data by itself yields an unambiguous period, albeit with an uncertainty about 12 times larger than our 2025 result. Combining the sparse data with the dense data for a much longer data span of 102 days substantially reduces the error in the derived period, but also includes the long gap of more than two months that elapsed between the sparse and dense data, which introduces ambiguity in the rotation count and thus unresolved alias period solutions. Applying the constraint of the 2025 period to the solutions resolves the ambiguity by isolating the correct period as 14.0311 ± 0.0007 h (Fig. 3(a)), for which the same test calculation as before now yields $N_{\text{per}} = 1$. The 13.985 h synodic period result reported by Waszczak et al. (2015) from analysis of the same 2012-13 data appears to be an alias based on counting an incorrect extra 0.5 rotation during the long gap.

Having satisfied the first prerequisite toward sidereal rotation counting, we next checked how well available data could constrain the sidereal period. Past experience with the sidereal rotation period sieve algorithm described by Slivan (2013) is that a suitable set of five epochs typically has been sufficient to unambiguously count sidereal rotations. Table III summarizes the epochs from five apparitions of lightcurve data: the three newly reported in this work, plus the 2012-13 PTF data already discussed, plus the 2021-22 observations by Dose (2022) which were retrieved from the ALCDEF database. The full set of corresponding epoch intervals is given in Table IV. Applying the sieve algorithm to all ten available intervals identifies an unambiguous integer count of sidereal half-rotations across the entire set of epochs as shown in Fig. 4. It is apparent from the graph that the sidereal period proposed by Durech et al. (2020) 14.0313 h does not satisfy the rotation counting constraints, which also implies that its accompanying reported pole latitude constraint is spurious.

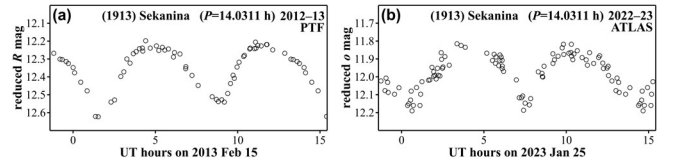


Figure 3. Folded composite lightcurves used to locate epochs from sky survey photometry. Data are composited to the median date of the observations, using the slope parameter $G = 0.23$ for S-type objects (Lagerkvist and Magnusson, 1990) to reduce for changing solar phase angle. (a) 2012–13 apparition from the Palomar Transient Factory survey (Law et al., 2009). (b) 2022–23 apparition from the ATLAS survey (Tonry et al., 2018) for the observations made when Sekanina was between its stationary points.

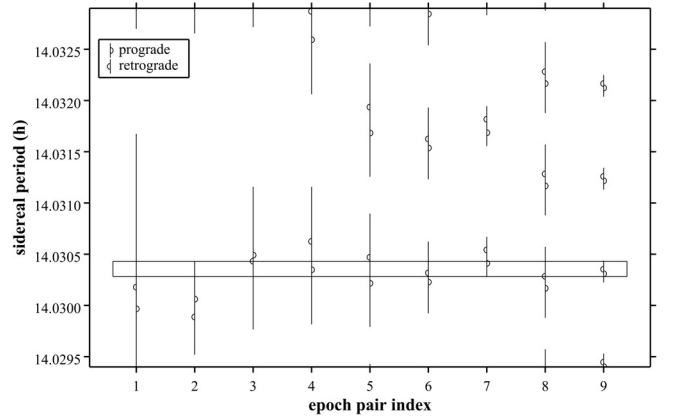


Figure 4. Sieve algorithm output showing that only the single range of sidereal rotation periods 14.03028 h to 14.03043 h (thin horizontal rectangle) is allowed by the epoch intervals in Table IV, corresponding to 7740.5 sidereal rotations for the maximum interval. Candidate period ranges for each interval were calculated using epoch range half-widths of 2.5 times the epoch errors.

Although the period constraint from the sieve algorithm does not distinguish Sekanina's direction of spin, analyzing a suitable set of epochs using sidereal photometric astrometry (SPA) (Slivan, 2014; Drummond et al., 1988) should be able to distinguish spin direction. The polar graph of phase angle bisector (PAB) longitudes in Fig. 5 shows that the longitudes of the five densely-sampled lightcurves' data sets lie close to 90° apart in a nearly symmetric pattern, a

consequence of Sekanina's orbit period being close to 5:1 commensurate with Earth's orbit period. By themselves, these five epochs yield unsatisfactory SPA analyses because they lack the observations from intermediate longitudes needed to break the symmetry and distinguish the direction of spin. To address this issue, photometry of Sekanina during the 2022-23 apparition by the ATLAS sky survey (Tonry et al., 2018) was retrieved from the Minor Planet Center Orbits/Observations Database, to assemble a composite lightcurve (Fig. 3(b)) from a large-amplitude aspect that maximizes the difference in PAB longitude from the nearest densely-sampled apparition. After adding the epoch measured from these data to the analysis input data set, SPA indicates that the pole lies at a mid-latitude in the north ecliptic hemisphere for prograde rotation (Fig. 6).

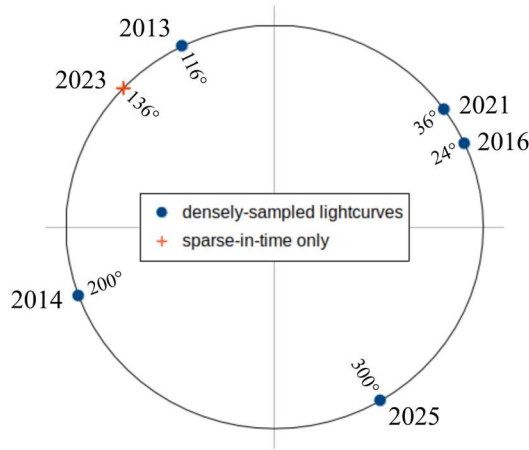


Figure 5. Angular distribution of ecliptic longitudes of phase angle bisectors for the lightcurve data used in this paper. Each apparition of sparse-in-time data is represented by a single longitude calculated for the median date of the UT dates of observations. The larger-amplitude lightcurve aspects lie near 120° and 300°; smaller-amplitude aspects are near 30° and 210°.

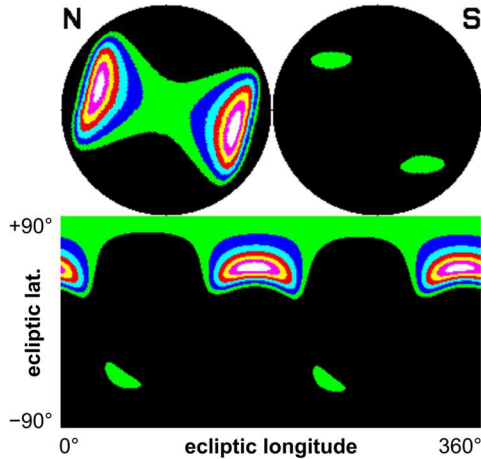


Figure 6. Contour graphs of RMS error of trial poles for the SPA analyses of the six epochs in Table III. The lower half of the figure represents the celestial sphere as a rectangular grid of ecliptic longitude and latitude; the same data in a polar format undistorted near the ecliptic poles appear in the upper half of the graph, where north and south hemispheres are plotted separately. The best-fit areas in white locate a symmetric pair of prograde pole regions at mid-northern ecliptic latitudes.

Finally, the six apparitions' lightcurves were analyzed for spin vector and model shape using convex inversion (CI) (Kaasalainen et al., 2001) as described by Slivan et al. (2023). Per the constraints from the epochs analyses, the midpoint of the allowed range from the sieve provided the initial sidereal period, and the grid search of trial poles was limited to the north ecliptic hemisphere. The search identified a symmetric pair of prograde pole regions (Fig. 7) whose ambiguity is a consequence of the small 2° orbit inclination of Sekanina. The CI analysis results are summarized in Table V, model lightcurve fits for all six apparitions are shown in Fig. 8, and model shape renderings are shown in Fig. 9.

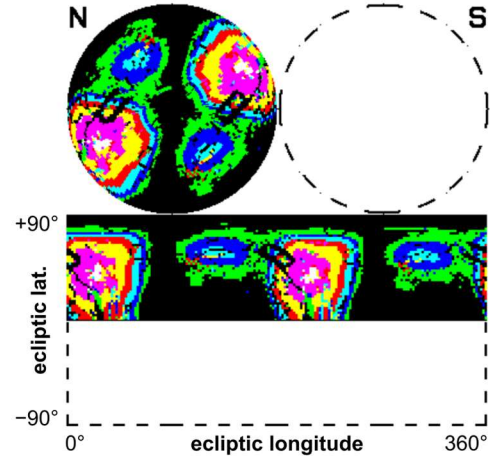


Figure 7. Similar to Fig. 6 but for the CI analysis of the six apparitions of lightcurve data, locating a pair of prograde pole regions having the expected symmetry.

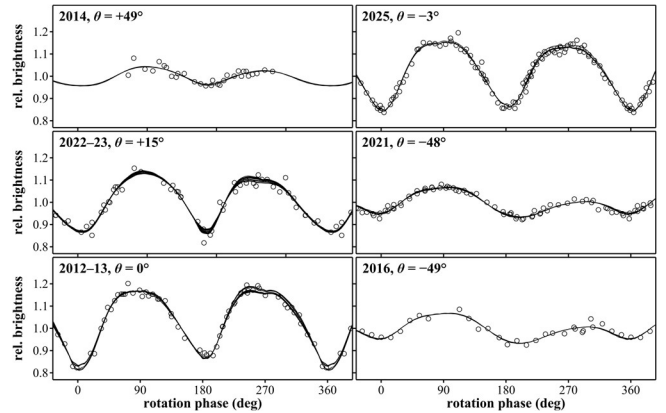


Figure 8. CI model lightcurve fits for pole P_1 as brightness vs. sidereal rotation phase, presented in order of decreasing sub-PAB latitude θ . Changes in lightcurve shape during the apparition appear as dispersions of the overlapping model curves. The RMS error of the fit to the combined data set corresponds to 0.016 mag.

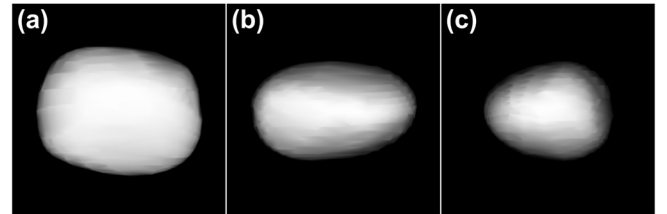


Figure 9. Renderings of convex model for pole P_1 . (a) Polar aspect. (b) Equatorial aspect for lightcurve maximum. (c) Equatorial aspect for lightcurve minimum. The convex model for the symmetric pole P_2 is essentially a mirror image.

Tel. ID	Dia. (m)	Camera	FOV (')	Bin	Blk. avg.	Scale (" / px)
WhO+AP	0.61	CCD Apogee 2k	20×20	2×2		1.16
WhO+SBIG	0.61	CCD SBIG STL-1001	16×16	1×1		0.96
WAO-2	0.36	CMOS QHY268M	20×13	1×1	5×5	0.94

Table I: Telescopes and cameras information. Columns are: telescope ID (WhO, Sawyer Boller & Chivens 24-in, WAO-2, shed pier #2 Celestron C14), telescope diameter, camera, detector field of view, binning for camera readout, block averaging when used to rebin images after processing, and image scale for photometry.

UT date	α (°)	Tel. ID	Filter	Int. (s)	Span (h)
2014 Apr 11.1	0.5	WhO+AP	R	240	3.0
2014 Apr 20.1	3.8	WhO+AP	R	240	3.6
2014 May 07.1	9.7	WhO+AP	R	240	0.9
2014 May 08.1	10.1	WhO+AP	R	240	3.5
2016 Dec 06.1	18.6	WhO+SBIG	L	240	5.9
2016 Dec 15.1	20.0	WhO+SBIG	L	240	4.5
2016 Dec 31.0	21.5	WhO+SBIG	L	240	5.1
2025 Jul 07.3	6.5	WAO-2	R	180	3.9
2025 Jul 16.2	3.1	WAO-2	R	180	3.8
2025 Jul 18.2	2.3	WAO-2	R	180	3.6
2025 Jul 19.2	1.9	WAO-2	R	180	3.3
2025 Jul 21.2	1.2	WAO-2	R	180	2.6
2025 Jul 23.2	0.7	WAO-2	R	180	3.8
2025 Jul 25.2	1.0	WAO-2	R	180	3.7
2025 Jul 26.2	1.3	WAO-2	R	180	2.1
2025 Jul 29.2	2.4	WAO-2	R	180	3.6
2025 Jul 30.2	2.8	WAO-2	R	180	3.7

Table II: Nightly observing information, with rows grouped by apparition. Columns are: UT date at lightcurve mid-time, solar phase angle α , telescope ID (Table I), filter used (R, Cousins R; L, colorless), image integration time, and lightcurve duration.

UT date	Epoch (UT h)	PAB λ, β (°)	Data ref.
---------	--------------	--------------------------	-----------

Part A: Densely-sampled lightcurves

2013 Feb 15	5.01 ± 0.14	116.3, +1.6	a
2014 Apr 11	3.04 ± 0.78	200.0, -0.7	b
2016 Dec 06	5.94 ± 0.62	24.4, +1.1	b
2021 Dec 07	3.22 ± 0.25	35.6, +1.3	c
2025 Jul 07	6.79 ± 0.22	300.5, -1.7	b

Part B: Sparse-in-time photometry only

2023 Jan 25	3.89 ± 0.28	136.5, +1.4	d, e, f, g
-------------	-------------	-------------	------------

Table III: Summary of lightcurve epochs, in each case determined using a Fourier series model fit to the lightcurves as described by Slivan (2024). The 2014 epoch is estimated from a composite lightcurve that is too incomplete to use a doubly-periodic model; instead, a singly-periodic model at half the rotation period was fit and then filtered for the fundamental. PAB λ, β are the J2000.0 ecliptic longitude and latitude of the phase angle bisector. Data references are: a, Waszczak et al. (2015); b, this work; c, Dose (2022); d, ATLAS-MLO o-band; e, ATLAS-HKO o-band; f, ATLAS-Chile o-band; g, ATLAS-South Africa o-band.

Epoch pair index	Interval (d)	Interval (app.)	Epochs source apparitions
0	419.9	1	2013, 2014
1	970.1	2	2014, 2016
2	1308.1	3	2021, 2025
3	1390.0	3	2013, 2016
4	1826.9	4	2016, 2021
5	2797.0	6	2014, 2021
6	3135.0	7	2016, 2025
7	3216.9	7	2013, 2021
8	4105.2	9	2014, 2025
9	4525.1	10	2013, 2025

Table IV: Time intervals between lightcurve epochs analyzed using the sieve algorithm (Table III, Part A). Columns are: epoch pair index label on Fig. 4, interval length rounded to 0.1 d, the corresponding integer count of elapsed apparitions, and the apparitions from which the defining epochs were measured.

Sidereal period: 14.03031 ± 0.00004 h

Spin poles	λ_0	$\sigma(\lambda_0)$	β_0	$\sigma(\beta_0)$	ε
P1:	25°	5	+42°	5	49°
P2:	208°	5	+39°	5	50°

Model axial ratios: a/b: 1.3 b/c: 1.3

Table V: Spin vector results. λ_0 and β_0 are the pole solutions' ecliptic longitudes and latitudes, respectively; σ are the estimated pole errors in degrees of arc; ε are the spin obliquities. The axial ratios are very coarse estimates with uncertainties of at least ± 0.1.

Number	Name	yyyy mm/dd	Phase	L _{PAB}	B _{PAB}	Period(h)	P.E.	Amp	A.E.
1913	Sekanina	2014 04/11-05/08	0.5, 10.1	200	-1			0.13	0.06
1913	Sekanina	2016 12/06-12/31	18.6, 21.5	26	1			0.14	0.03
1913	Sekanina	2025 07/07-07/30	*6.5, 2.8	301	-2	14.032	0.005	0.33	0.04
1913	Sekanina	(caption Note)				14.0311	0.0007		

Table VI: Observing circumstances and results. Solar phase angle is given for the first and last dates; the asterisk indicates that the phase angle reached a minimum during the period. L_{PAB} and B_{PAB} are the approximate phase angle bisector longitude/latitude at mid-date range. Note: Synodic period from constraint of this work's 2025 data applied to reanalysis of 2012-13 PTF data as described in the text.

Acknowledgments

We thank Dr. Michael Person and Timothy Brothers at Wallace Observatory for allocation of telescope time, and for observer instruction and support. The student observers at Wallace were supported by a grant from MIT's Undergraduate Research Opportunities Program. At Whittin Observatory we thank student observers Kirsten Blancato, Michaela Fendrock, and Carolyn Thayer, who were supported in part by grants from the Massachusetts Space Grant Consortium. This work uses data obtained from the Asteroid Lightcurve Data Exchange Format (ALCDEF) database, which is supported by funding from NASA grant 80NSSC18K0851. This work also has made use of data and services provided by the International Astronomical Union's Minor Planet Center; specifically, the brightnesses accompanying astrometry from the Asteroid Terrestrial-impact Last Alert System (ATLAS) survey observing program.

References

- Chang, C.; Ip, W.; Lin, H.; Cheng, Y.; Ngeow, C.; Yang, T.; Waszczak, A.; Kulkarni, S.; Levitan, D.; Sesar, B.; Laher, R.; Surace, J.; Prince, T.A. (2014). "313 New Asteroid Rotation Periods from Palomar Transient Factory Observations." *Astrophys. J.* **788**, A17.
- Dose, E.V. (2022). "Lightcurves of Seventeen Asteroids." *Minor Planet Bull.* **49**, 141-148.
- Drummond, J.D.; Weidenschilling, S.J.; Chapman, C.R.; Davis, D.R. (1988). "Photometric geodesy of main-belt asteroids. II. Analysis of lightcurves for poles, periods, and shapes." *Icarus* **76**, 19-77.
- Đurech, J.; Tonry, J.; Erasmus, N.; Denneau, L.; Heinze, A.N.; Flewelling, H.; Vančo, R. (2020). "Asteroid models reconstructed from ATLAS photometry." *Astron. Astrophys.* **643**, A59.
- Erasmus, N.; Navarro-Meza, S.; McNeill, A.; Trilling, D.E.; Sickafoose, A.A.; Denneau, L.; Flewelling, H.; Heinze, A.; Tonry, J.L. (2020). "Investigating Taxonomic Diversity within Asteroid Families through ATLAS Dual-band Photometry." *Astrophys. J. Suppl. Ser.* **247**, A13.
- Howell, S.B. (1989). "Two-dimensional Aperture Photometry: Signal-to-noise Ratio of Point-source Observations and Optimal Data-extraction Techniques." *PASP* **101**, 616-622.
- Kaasalainen, M.; Torppa, J.; Muinonen, K. (2001). "Optimization methods for asteroid lightcurve inversion. II. The complete inverse problem." *Icarus* **153**, 37-51.
- Lagerkvist, C.I.; Magnusson, P. (1990). "Analysis of asteroid lightcurves. II. Phase curves in a Generalized HG-system." *Astron. Astrophys. Suppl. Ser.* **86**, 119-165.
- Landolt, A.U. (1983). "UBVRI Photometric Standard Stars Around the Celestial Equator." *Astron. J.* **88**, 439-460.
- Law, N.M.; Kulkarni, S.R.; Dekany, R.G.; Ofek, E.O.; Quimby, R.M.; Nugent, P.E.; Surace, J.; Grillmair, C.C.; Bloom, J.S.; Kasliwal, M.M.; Bildsten, L.; Brown, T.; Cenko, S.B.; Ciardi, D.; Croner, E.; and 26 colleagues (2009). "The Palomar Transient Factory: System Overview, Performance, and First Results." *PASP* **121**, 1395-1406.
- Slivan, S.M.; Binzel, R.P.; Boroumand, S.C.; Pan, M.W.; Simpson, C.M.; Tanabe, J.T.; Villastrigo, R.M.; Yen, L.L.; Ditteon, R.P.; Pray, D.P.; Stephens, R.D. (2008). "Rotation Rates in the Koronis Family, Complete to $H \approx 11.2$." *Icarus* **195**, 226-276.
- Slivan, S.M. (2012). "Epoch Data in Sidereal Period Determination. I. Initial Constraint from Closest Epochs." *Minor Planet Bull.* **39**, 204-206.
- Slivan, S.M. (2013). "Epoch Data in Sidereal Period Determination. II. Combining Epochs from Different Apparitions." *Minor Planet Bull.* **40**, 45-48.
- Slivan, S.M. (2014). "Sidereal Photometric Astrometry as Efficient Initial Search for Spin Vector." *Minor Planet Bull.* **41**, 282-284.
- Slivan, S.M.; Hosek Jr., M.; Kurzner, M.; Sokol, A.; Maynard, S.; Payne, A.V.; Radford, A.; Springmann, A.; Binzel, R.P.; Wilkin, F.P.; Mailhot, E.A.; Midkiff, A.H.; Russell, A.; Stephens, R.D.; Gardiner, V.; and 5 colleagues (2023). "Spin vectors in the Koronis family: IV. Completing the sample of its largest members after 35 years of study." *Icarus* **394**, A115397.
- Slivan, S.M.; Barrera, K.; Colclasure, A.M.; Cusson, E.M.; Larsen, S.S.; McLellan-Cassivi, C.J.; Moulder, S.A.; Nair, P.R.; Namphy, P.D.; Neto, O.S.; Noto, M.I.; Redden, M.S.; Rhodes, S.J.; Youssef, S.A. (2024). "Lightcurves and Derived Results for Koronis Family Member (5139) Rumoi, Including a Discussion of Measurements for Epochs Analysis." *Minor Planet Bull.* **51**, 6-10.
- Tonry, J.L.; Denneau, L.; Heinze, A.N.; Stalder, B.; Smith, K.W.; Smartt, S.J.; Stubbs, C.W.; Weiland, H.J.; Rest, A. (2018). "ATLAS: A High-cadence All-sky Survey System." *PASP* **130**, 064505.
- Warner, B.D.; Harris, A.W.; Pravec, P. (2009). "The Asteroid Lightcurve Database." *Icarus* **202**, 134-146. Updated 2023 Oct. <http://www.minorplanet.info/php/lcdb.php>
- Waszczak, A.; Chang, C.; Ofek, E.O.; Laher, R.; Masci, F.; Levitan, D.; Surace, J.; Cheng, Y.; Ip, W.; Kinoshita, D.; Helou, G.; Prince, T.A.; Kulkarni, S. (2015). "Asteroid Light Curves from the Palomar Transient Factory Survey: Rotation Periods and Phase Functions from Sparse Photometry." *Astron. J.* **150**, A75.

LIGHTCURVE AND ROTATION PERIOD OF THE NEAR-EARTH ASTEROID 2025 QB21

Heiko Duin
Olbers-Gesellschaft e. V. Bremen
Bredenkamp Observatory (L65)
Am Bredenkamp 6, 28203 Bremen, GERMANY
heiko.duin@web.de

(Received: 2025 September 9)

Photometric observations of the near-Earth asteroid 2025 QB21 were conducted to determine its synodic rotation period. It was found that $P=0.1695\pm0.0003$ hours with $A=1.677\pm0.376$ mag. The data have been submitted to the ALCDEF database (Warner et al., 2009).

Photometric observations of the near-Earth Asteroid 2025 QB21 were carried out at the Bredenkamp Observatory (L65) on 2025 September 6 using a 0.23-m Schmidt-Cassegrain telescope mounted on an EQ6-Pro mount and a monochrome ZWO ASI533MM Pro CMOS camera operated at a chip temperature of -10°C . The observations were made with a clear filter and with the telescope operating with a focal reducer at $f/6.3$. The planning of observations had been done with *NeoPlanner* (Haeusler, 2025), image acquisition software was *NINA* (Berg, 2025).

All images were calibrated with dark and flat frames and were software-binned 3×3 resulting in an image scale of 1.50 arcsec/pix. Data reduction and period analysis were performed with *Tycho Tracker Pro v12* (Parrott, 2025). The asteroid and five comparison stars were measured for differential photometry. The comparison stars were selected from the ATLAS catalogue (Tonry et al., 2018) using V magnitudes with color indices in the range of $0.5 < B-V < 0.95$ covering the typical color range of asteroids. Some observations with inference from nearby stars have been discarded.

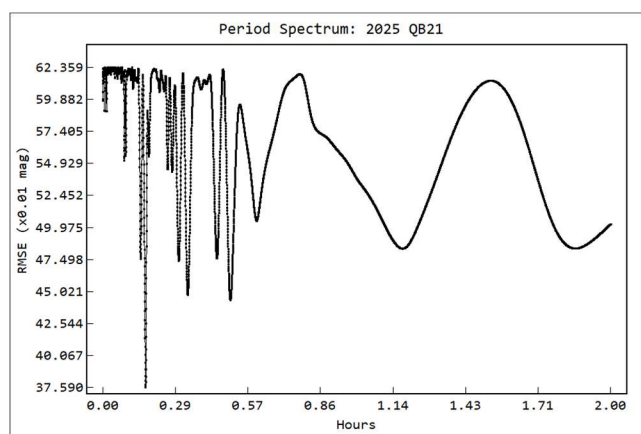
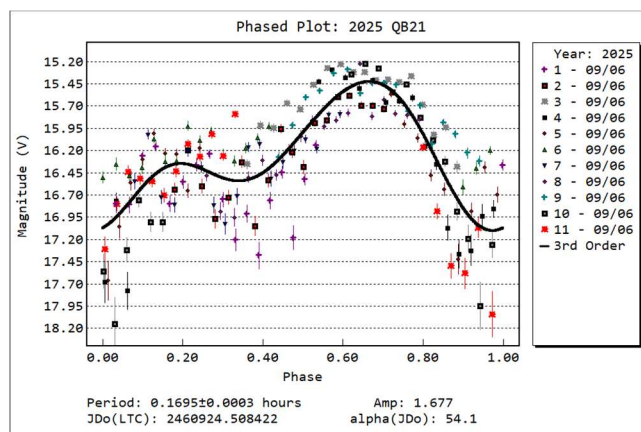
2025 QB21 is an Apollo-type near-Earth asteroid discovered on 2025 August 31 by Pan-STARRS 2, Haleakala ($H = 26.6$, $D \sim 22$ m) (ESA NEOCC, 2025). The object made an approach to 1.63 LD on 2025 Sep 6.002 UTC. It was observed for 2.2 h starting on 2025 Sep 6.008 UTC. Exposure times were 1.6 s due to the high sky motion of around 110 arcsec/minute. Eleven fields were necessary for observing the object resulting in eleven sets of measurements with a time difference of 12 minutes between the beginning of each set. Each set consisted of 114-118 single images. Groups of 5-6 images were stacked to increase signal-to-noise ratio. Data was light time corrected, and phase-angle corrections were made by applying a H-G model. Searching the ALCDEF database and other Internet resources did not reveal any previously published results. The measured synodic period is 0.1695 h (10.17 min) with an amplitude of 1.677 mag.

Acknowledgements

Acknowledgements go to Bernhard Haeusler (*NeoPlanner*), Stefan Berg (*NINA*), and Daniel Parrot (*Tycho Tracker Pro*).

References

- Berg, S. (2025). “Nighttime Imaging ‘N’ Astronomy (NINA)” <https://nighttime-imaging.eu/>
- ESA NEOCC (2025). Search for Asteroids. <https://neo.ssa.esa.int/search-for-asteroids>
- Haeusler, B. (2025). “NEO Planner.” <https://www.k87dettelbach.vineyardobservatory.bayern/NeoPlanner.htm>
- Harris, A.W.; Young, J.W.; Scaltriti, F.; Zappala, V. (1984). “Lightcurves and phase relations of the asteroids 82 Alkmene and 444 Gyptis.” *Icarus* **57**, 251-258.
- Parrot, D. (2025). Tycho software. <https://www.tycho-tracker.com>
- Tonry, J.L.; Denneau, L.; Flewelling, H.; Heinze, A.N.; Onken, C.A.; Smartt, S.J.; Stalder, B.; Weiland, H.J.; Wolf, C. (2018). “The ATLAS All-Sky Stellar Reference Catalog.” *Astrophys. J.* **867**, A105.
- Warner, B.D.; Harris, A.W.; Pravec, P. (2009). “The Asteroid Lightcurve Database.” *Icarus* **202**, 134-146. 2023 October Release #2. <https://minplanobs.org/mpinfo/php/lcdb.php>



Number	Name	yyyy mm/dd	Phase	L _{PAB}	B _{PAB}	Period(h)	P.E.	Amp	A.E.	Grp
2025	QB21	2025 09/06	54.1, 57.1	10	8	0.170	0.0003	1.68	0.38	NEA

Table I. Observing circumstances and results. The phase angle is given for the first and last date. If preceded by an asterisk, the phase angle reached an extrema during the period. L_{PAB} and B_{PAB} are the approximate phase angle bisector longitude/latitude at mid-date range (see Harris et al., 1984). Grp is the asteroid family/group (Warner et al., 2009).

LIGHTCURVE OF NEAR-EARTH ASTEROID 2025 RL2

Daniel P. Bamberger
Northolt Branch Observatories
Alfred-Wegener-Straße 34
35039 Marburg, GERMANY
danielpeter1204@aol.com

Guy Wells
Northolt Branch Observatories
Northolt, ENGLAND

(Received: 2025 September 20)

Unfiltered CMOS photometric observations of 2025 RL2 show that it is a fast rotator with a large lightcurve amplitude. The asteroid is either tumbling with a main period of 0.0725 h and an amplitude of 0.62 mag, or it has an irregular shape, resulting in a lightcurve with four peaks of different heights, with a period of 0.1452 h and amplitude 0.76 mag.

2025 RL2 is an Aten-type near-Earth asteroid. Its absolute magnitude of $H=26.0$ indicates a diameter within a factor of two of 25 meters. It was first observed at Kitt Peak-Bok on 13 September 2025, and made a close approach to Earth on 19 September 2025 at a distance of 0.0014 au (270,000 km). At the time of writing, the LCDB listed no period for 2025 RL2.

We observed this asteroid with the 0.25-m Ritchey-Chrétien telescope at Northolt Branch Observatory (Z80). Our data consist of 3-seconds exposures in three batches of 15 minutes, recorded between 21:25 and 22:17 UTC on 18 September 2025. While it is possible to fit a simple double-peaked lightcurve with a period of 0.0725 h to the data, that fit is not very satisfying, and the large residuals could indicate a secondary rotation period; that is, a non-principal axis rotation (tumbling). A better fit is a lightcurve with four peaks of different heights, at a period of 0.1452 h. For the latter solution, *MPO Canopus* finds an amplitude of 0.76 mag. A visual inspection of the data indicates that the true amplitude is probably larger, up to 1.0 mag. Such a lightcurve would indicate that the asteroid has an elongated and irregular shape.

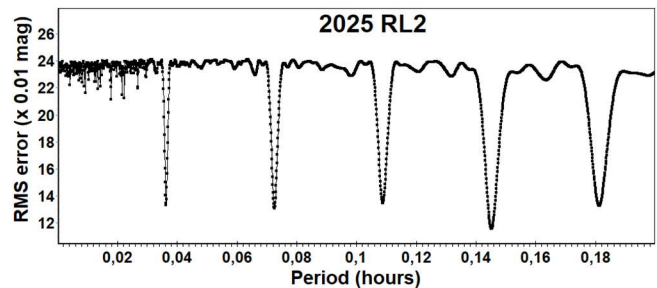
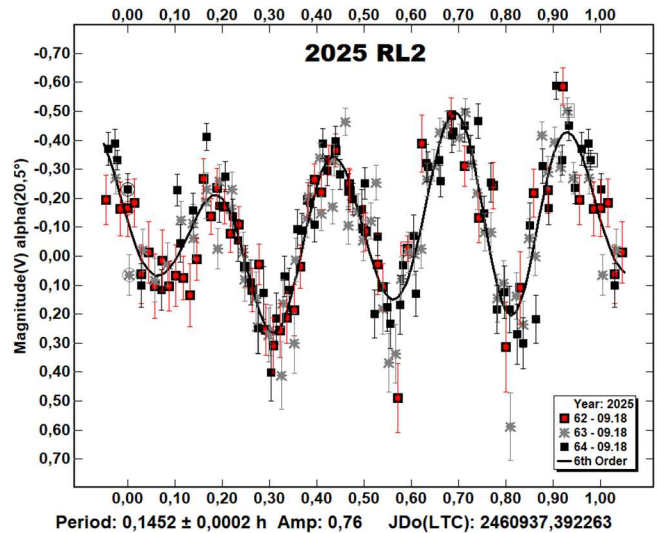
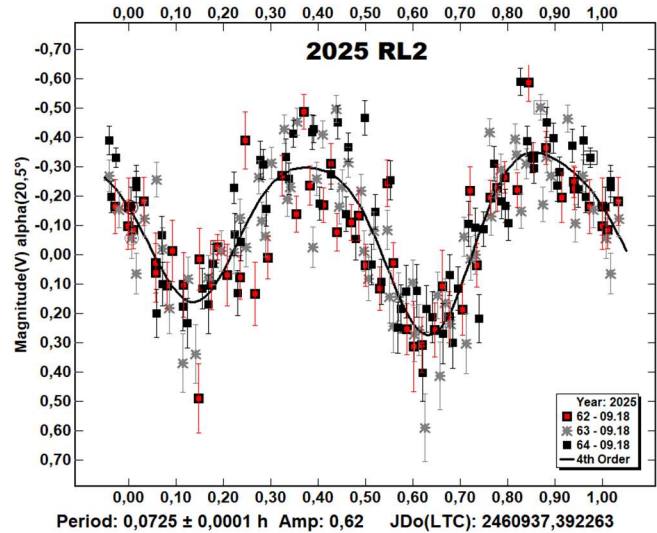
Our data is available in the Asteroid Lightcurve Photometry Database (ALCDEF).

References

Harris, A.W.; Young, J.W.; Scaltriti, F.; Zappala, V. (1984). "Lightcurves and phase relations of the asteroids 82 Alkmene and 444 Gytis." *Icarus* **57**, 251-258.

JPL (2025). Small-Body Database Lookup.
https://ssd.jpl.nasa.gov/tools/sbdb_lookup.html#/?sstr=2025%20RL2

Warner, B.D.; Harris, A.W.; Pravec, P. (2009). "The Asteroid Lightcurve Database." *Icarus* **202**, 134-146. Updated 2023 Oct. 1.
<https://www.minorplanet.info/php/lcdb.php>



Number	Name	yyyy/mm/dd	Phase	L_{PAB}	B_{PAB}	Period(h)	P.E.	Amp	A.E.	Grp
2025	RL2	2025/09/18	20.5	358	10	0.1452	0.0002	0.76	0.05	9101 NEA

Table I. Observing circumstances and results. The phase angle is given for the first and last date. If preceded by an asterisk, the phase angle reached an extrema during the period. L_{PAB} and B_{PAB} are the approximate phase angle bisector longitude/latitude at mid-date range (see Harris et al., 1984). Grp is the asteroid family/group (Warner et al., 2009).

LIGHTCURVE ANALYSIS OF NEO 2025 MY89

Peter Birtwhistle
Great Shefford Observatory (J95)
Phlox Cottage, Wantage Road
Great Shefford, Berkshire, RG17 7DA
UNITED KINGDOM
peter@birtwhistle.org.uk

James D. Armstrong
University of Hawaii Institute for Astronomy (V37, V39)
34 Ohia Ku Street
Pukalani, HI 96768, USA

Matthieu Conjat
Boulevard de l'Observatoire, Nice (020)
FRANCE

Jiashuo Zhang, Binyu Wang
HuanYu Observatory (41.8696° N, 114.6885° E)
Dingjiaying Village, Kangbao Town,
Kangbao County, Zhangjiakou City,
Hebei Province, CHINA

Joan Genebriera
Astropriorat Observatory (M02)
Catalonia, SPAIN

Mohammad Shawkat Odeh
Al-Khatim Observatory (M44)
Abu Dhabi, UAE

Wayne Hawley
Old Orchard Observatory (Z09)
Fiddington, UK

(Received: 2025 October 2)

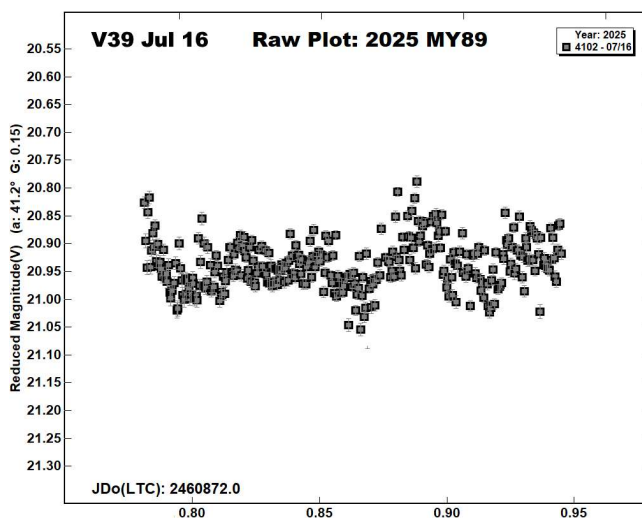
The analysis of photometric observations of the NEO 2025 MY89 obtained by a collaboration of eight people during July 2025 indicates that Apollo 2025 MY89 has a low amplitude lightcurve with a likely synodic period of 2.623 ± 0.005 h.

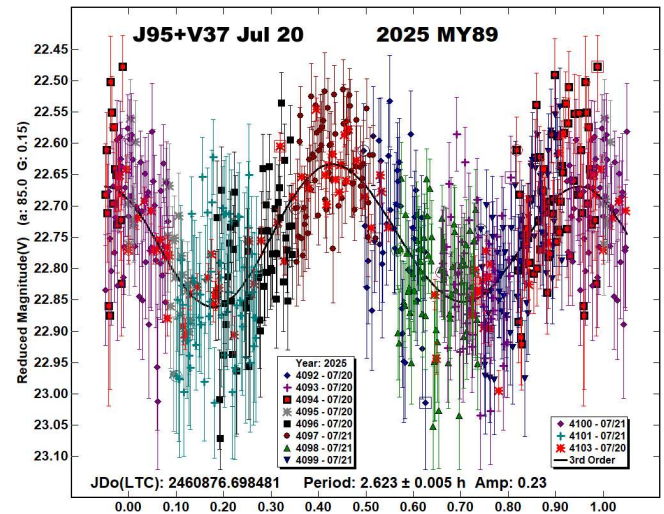
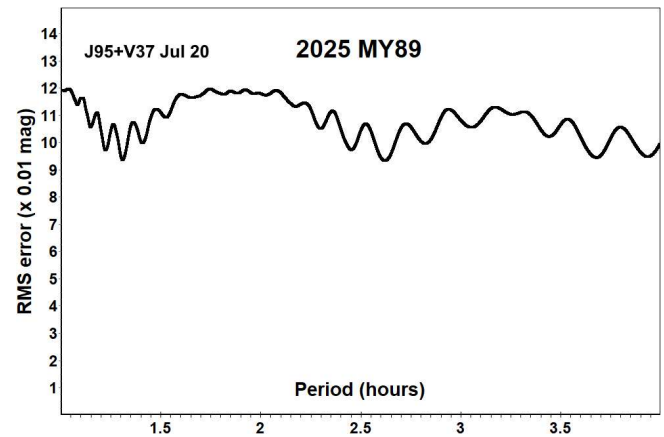
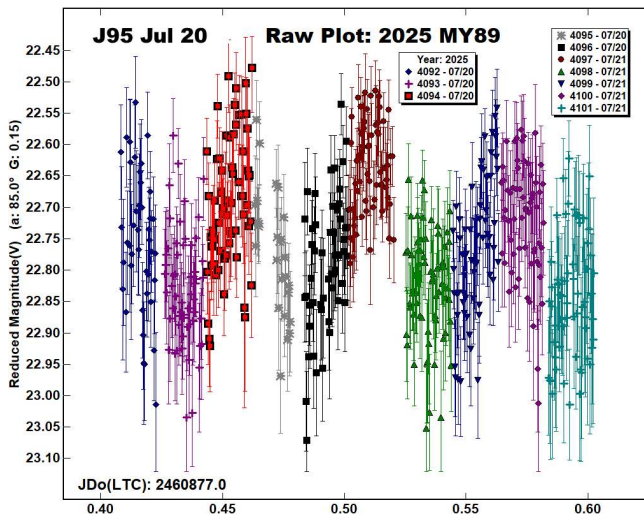
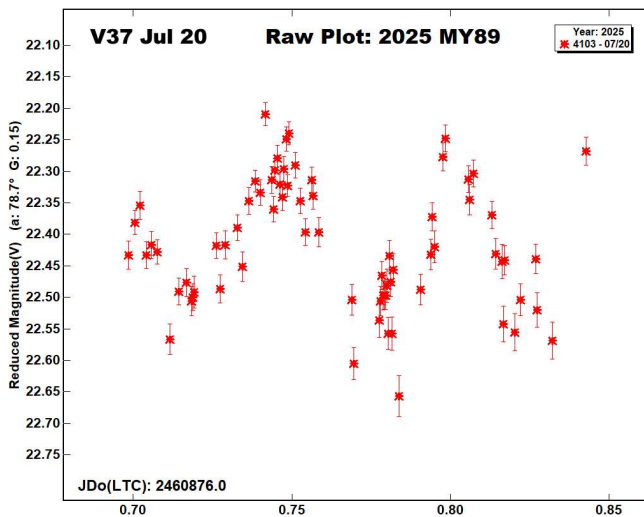
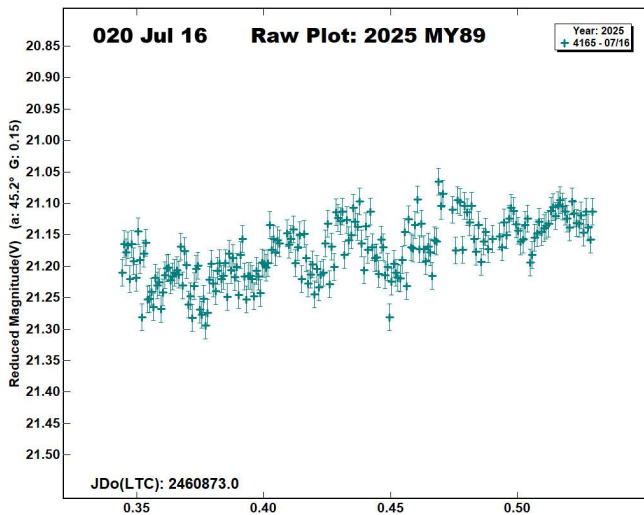
Following an alert on a forum of the British Astronomical Association's Asteroid and Remote Planets (ARPS) section, observers from six countries attempted observations of the relatively large newly discovered Apollo 2025 MY89 ($H = 19.6$, $D \sim 351$ m, albedo $p_V = 0.2$ assumed) as it approached Earth to within 30 Lunar Distances (0.08 AU) on 2025 July 18.9 UTC (Bosch et al., 2025). For three days around that date, the object passed through dense regions of the Milky Way in central Cygnus. Observations were made both before this passage, from July 15.8 to 17.0, when it reached its peak apparent brightness of approximately magnitude 16.2, then after, from July 20.2 to 21.1 UTC, by which time it had faded by about one magnitude. During the apparition phase angle reached a minimum of 30° on 2025 July 11 and increased from $38 - 46^\circ$ during the earlier set of observations and from $78 - 86^\circ$ in the later set. Photometry was measured by Birtwhistle for J95, V37 and V39 using *Astrometrica* (Raab, 2025), by Hawley for M02 and 247 using *Tycho* (Parrott, 2025), by Conjat

for 020 using *IRIS* (Buil, 2010) and by Odeh for M44 using *Tycho*. Photometry reference data was obtained from the Gaia DR3, ATLAS (Tonry et al., 2018) and Tycho-2 star catalogues and further details including a summary of the equipment used are listed in Table III. Birtwhistle used 637 photometric measurements from the later set of observations for the phased lightcurve analysis using *MPO Canopus* (Warner, 2023) which incorporates the Fourier algorithm developed by Harris (Harris et al., 1989). No previously reported results for 2025 MY89 have been found in the Asteroid Lightcurve Database (LCDB) (Warner et al., 2009), from searches via the Astrophysics Data System (ADS, 2025) or from wider searches.

An examination of the raw lightcurves from the first observing interval (July 15.8-17.0) shows that only the two datasets with the highest signal-to-noise ratios – from V39 and 020 – display even marginal evidence of periodic variation. Their data are presented here; however, due to changes in viewing geometry between this and the second observing interval three days later, the earlier datasets are not suitable for combining with those from the second interval. Unfortunately, the measurements from M02, M44, and HuanYu Observatory show too much scatter to detect any potential rotational variation. As a consequence of both issues, none of the data from this first observing interval were used in the period analysis.

In contrast, the two datasets from the second observing interval (July 20.2-21.1), when the phase angle had nearly doubled, reaching 86° , both show clear – though low-amplitude – periodic variations. Assuming a bimodal lightcurve, the raw lightcurve labelled 'V37 Jul 20' appears to cover just over one full rotation in 3.5 hours, while 'J95 Jul 20', obtained 14 h later, covers just under two rotations in 4.7 hours. A period spectrum derived from the combined datasets suggests a best-fit rotation period of approximately 2.6 hours. To minimize the overall RMS scatter of the lightcurve, a zero-point adjustment of 0.11 magnitudes was applied to the V37 dataset. The resulting phased lightcurve, with a period of $P = 2.623 \pm 0.005$ hours and an amplitude of 0.23 ± 0.12 magnitudes, is shown below. However, because neither dataset covers significantly more than a single rotation cycle, this period determination is not considered reliable.





Number	Name	Integration times	Max intg/Pd	Min a/b	Pts	Flds
2025 MY89		10, 20	0.002	1.1*	627	11

Table I. Ancillary information, listing the integration times used (seconds), the fraction of the period represented by the longest integration time (Pravec et al., 2000), the calculated minimum elongation of the asteroid (Zappala et al., 1990), the number of data points used in the analysis and the number of times the telescope was repositioned to different fields. Note: * = Value uncertain, based on phase angle $> 40^\circ$.

Acknowledgements

The first author wishes to express his thanks to the co-authors for expending their time and resources after answering the call to observe 2025 MY89. This work makes use of observations from the Las Cumbres Observatory global telescope network. This work has made use of data from the European Space Agency (ESA) mission Gaia (<https://www.cosmos.esa.int/gaia>), processed by the Gaia Data Processing and Analysis Consortium (DPAC, <https://www.cosmos.esa.int/web/gaia/dpac/consortium>). Funding for the DPAC has been provided by national institutions, in particular the institutions participating in the Gaia Multilateral Agreement.

Number	Name	yyyy mm/dd	Phase	L _{PAB}	B _{PAB}	Period(h)	P.E.	Amp	A.E	H
2025 MY89	2025 07/20–07/21	78.0, 86.7	302	46	2.623	0.005	0.23	0.12	19.6	

Table II. Observing circumstances and results. The phase angle is given for the first and last date. If preceded by an asterisk, the phase angle reached an extrema during the period. L_{PAB} and B_{PAB} are the approximate phase angle bisector longitude/latitude at mid-date range (see Harris et al., 1984). Amplitude error (A.E.) is calculated as $\sqrt{2} \times$ (lightcurve RMS residual) and H is the absolute magnitude at 1 au from Sun and Earth taken from the Small-Body Database Lookup (JPL, 2025).

Observer, Observatory (MPC code)	Telescope	Detector	Filter/ mag band	Star Catalogue	Photometry software	Obs span 2025 July UTC	Data points (not used)
Birtwhistle, Great Shefford Observatory, UK (J95)	0.41-m f/6.3 SCT	CCD	None / G	Gaia DR3	Astrometrica	20.91-21.10	565
Armstrong, McDonald Observatory LCO ELP A & B, USA (V37, V39)	1.0-m f/8 Ritchey-Chretien	CCD	clear / G	Gaia DR3	Astrometrica	16.28-16.45, 20.20-20.34	(326) 72
Conjat, Observatoire de la Cote d'Azur, FRANCE (020)	0.4-m f/5 Cassegrain	CMOS	None / V	Tycho-2	Iris	16.84-17.03	(214)
Zhang, HuanYu Observatory, Hebei Province, CHINA (41.8696° N, 114.6885° E)	0.13-m f/7.7 reflector	CMOS	Optolong L-band / SR	ATLAS	Tycho	16.65-16.73	(75)
Genebriera, Astropriorat Observatory, SPAIN (M02)	0.41m f/8 Ritchey-Chretien	CMOS	V / SR	ATLAS	Tycho	16.03-16.04	(50)
Odeh, Al-Khatim Observatory, Abu Dhabi, UAE (M44)	0.36-m f/7.7 SCT	CMOS	None / SR	ATLAS	Tycho	15.75-15.79	(10)

Table III. Equipment list.

References

ADS (2025). Astrophysics Data System.
<https://ui.adsabs.harvard.edu/>

Bosch, J.M.; Hidas, A.; Lowe, T.; Minguéz, P.; Schultz, A.; Smith, I.; Chambers, K.; de Boer, T.; Fairlamb, J.; Gao, H.; Huber, M.; Lin, C.-C.; Magnier, E.; Paek, G.; Ramanjooloo, Y. and 15 colleagues (2025). “2025 MY89.” MPEC 2025-M143.
<https://www.minorplanetcenter.net/mpec/K25/K25ME3.html>

Buil, C. (2010). “IRIS image processing software.”
<https://buil.astrosurf.com/iris-software.html>

Harris, A.W.; Young, J.W.; Scaltriti, F.; Zappala, V. (1984). “Lightcurves and phase relations of the asteroids 82 Alkmene and 444 Gyptis.” *Icarus* **57**, 251-258.

Harris, A.W.; Young, J.W.; Bowell, E.; Martin, L.J.; Millis, R.L.; Poutanen, M.; Scaltriti, F.; Zappala, V.; Schober, H.J.; Debehogne, H.; Zeigler, K. (1989). “Photoelectric Observations of Asteroids 3, 24, 60, 261, and 863.” *Icarus* **77**, 171-186.

JPL (2025). Small-Body Database Lookup.
https://ssd.jpl.nasa.gov/tools/sbdb_lookup.html

Parrott, D. (2025). Tycho Software.
<https://www.tycho-tracker.com>

Pravec, P.; Hergenrother, C.; Whiteley, R.; Sarounova, L.; Kusnirak, P.; Wolf, M. (2000). “Fast Rotating Asteroids 1999 TY2, 1999 SF10, and 1998 WB2.” *Icarus* **147**, 477-486.

Raab, H. (2025). Astrometrica software, version 4.16.4.468.
<http://www.astrometrica.at/>

Warner, B.D.; Harris, A.W.; Pravec, P. (2009). “The Asteroid Lightcurve Database.” *Icarus* **202**, 134-146. Updated 2023 Oct.
<https://www.minorplanet.info/php/lcdb.php>

Warner, B.D. (2023). MPO Software, Canopus version 10.8.6.20.
<https://minplanobs.org/BdwPub/>

Zappala, V.; Cellini, A.; Barucci, A.M.; Fulchignoni, M.; Lupishko, D.E. (1990). “An analysis of the amplitude-phase relationship among asteroids.” *Astron. Astrophys.* **231**, 548-560.

LIGHTCURVE ANALYSIS OF NEO 2025 RL2

Peter Birtwhistle
Great Shefford Observatory (J95)
Phlox Cottage, Wantage Road
Great Shefford, Berkshire, RG17 7DA
UNITED KINGDOM
peter@birtwhistle.org.uk

Jakub Koukal
Valašské Meziříčí Observatory
Vsetínská 78 757 01 Valašské Meziříčí
CZECH REPUBLIC

(Received: 2025 October 1)

The newly discovered Aten-type NEO 2025 RL2 had a very favourable close-approach to Earth in September 2025 and photometry obtained from two observatories show that this small asteroid has tumbling rotation with periods of 4.4 and 18.6 minutes.

Photometric observations of near-Earth object (NEO) 2025 RL2 during a close approach to Earth in September 2025 were made from Great Shefford Observatory in the UK and from Valašské Meziříčí Observatory in the Czech Republic. At Great Shefford Observatory a 0.41-m Schmidt-Cassegrain and Apogee Alta U47+ CCD camera were used, exposures were unfiltered and, with the telescope operating with a focal reducer at $f/6$ and with the $1K \times 1K$, 13-micron CCD binned 2×2 the image scale was 2.16 arcsec/pix. *Astrometrica* (Raab, 2025) was used to measure photometry using G band data from the Gaia DR3 catalogue. At Valašské Meziříčí Observatory unfiltered exposures were obtained with a 0.50-m $f/4$ reflector and a Moravian instruments CMOS detector. *AstroImageJ* (Collins and Collins, 2017) which incorporates *ImageJ* (Schneider et al., 2012) was used to measure photometry, again using G band data from the Gaia DR3 catalogue. Further details including a summary of the equipment used are listed in Table III. Birtwhistle used *MPO Canopus* (Warner, 2023), incorporating the Fourier algorithm developed by Harris (Harris et al., 1989) for lightcurve analysis.

No previously reported results have been found in the Asteroid Lightcurve Database (LCDB) (Warner et al., 2009), from searches via the Astrophysics Data System (ADS, 2025) or from wider searches. The size estimate is calculated using the H value from the Small-Body Database Lookup (JPL, 2025), using an assumed albedo for NEAs of 0.2 (LCDB readme.pdf file) and is therefore uncertain and offered for relative comparison only.

2025 RL2. This Aten ($H = 26.0$, $D \sim 19$ m) was a Kitt Peak-Bok 2.25-m reflector discovery from 2025 Sep 13.5 UTC (Bacci et al., 2025) and made an approach to within 0.6 Lunar Distances (LD) of Earth on Sep 19.4 UTC and in the preceding 12 hours it brightened to an apparent mag of +14. Koukal obtained 19 min of photometry starting at 2025 Sep. 18.87 UTC and within 5 minutes of the end of that session a further 1 h of photometry was started by Birtwhistle. In all 495 measurements were obtained over an 83-minute span. Initial analysis revealed very obvious 1 mag amplitude brightness variations with a period $P1 = 0.0727$ h (~ 4.4 min), but small trends in the resulting lightcurve suggested that some low-level tumbling (non-principal axis rotation, or NPAR) was also probably present. A period spectrum labelled “no subtraction” was generated in the

normal way in *MPO Canopus* and revealed a set of small but well-defined minima starting at 0.03 h, spaced in between the deep minima resulting from the dominant period, together with some broader shallow minima above 0.2 h. The Dual Period Search function in *MPO Canopus* was then used to subtract the dominant $P1$ variations from the data and generate a new period spectrum. This is labelled ‘ $P1$ subtracted’ and reveals at least two independent sets of regularly spaced minima at integer multiples of 0.029 hours and 0.153 hours. Further analysis using the Dual Period Search function found potential NPAR secondary period solutions as follows:

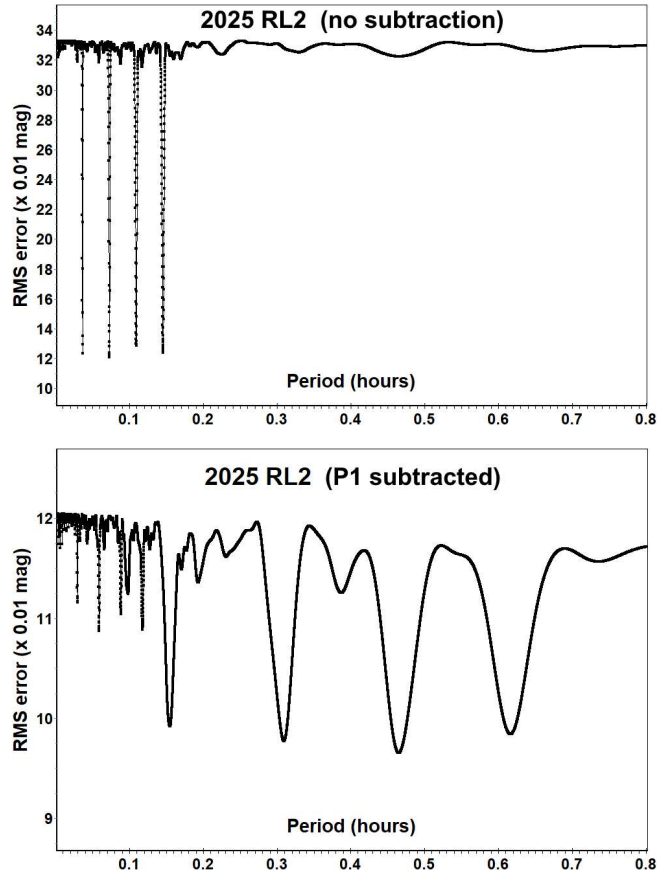
$$P2 = 0.309 \pm 0.001 \text{ h } (\sim 18.6 \text{ min})$$

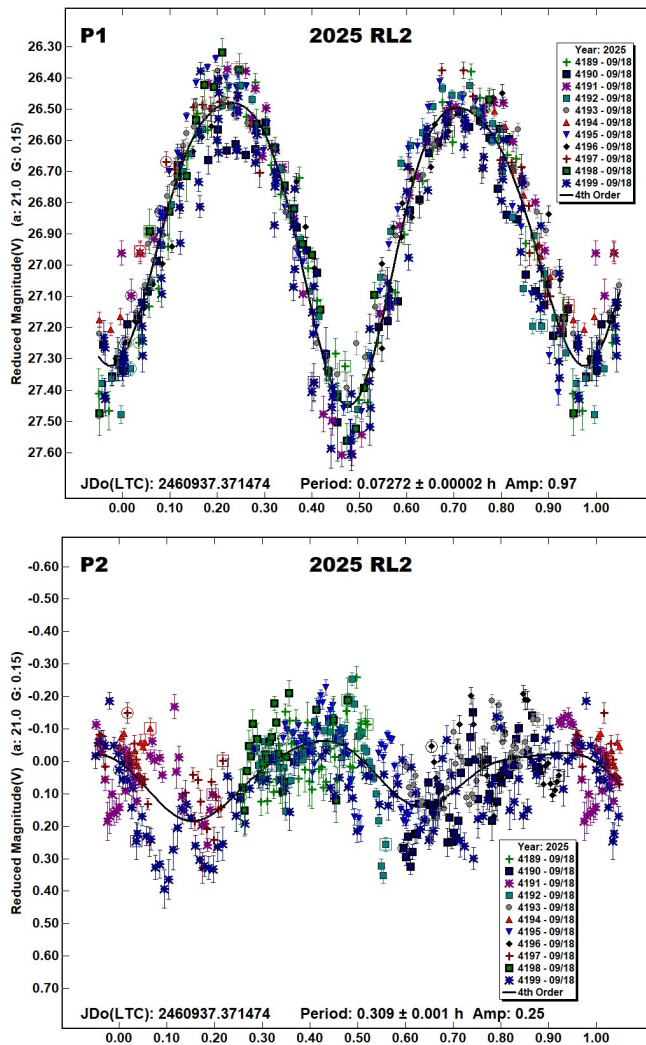
$$P3 = 0.0587 \pm 0.0001 \text{ h } (\sim 3.5 \text{ min})$$

The best-fit is obtained using the $P1$ and $P2$ combination and it is likely that the $P3$ period is just an alias of the two main periods $P1$ and $P2$, being a linear combination of their respective frequencies, i.e.:

$$1/P1 + 1/P2 = 1/P3$$

Lightcurves are given for the best-fit periods, labelled $P1$ and $P2$ and it is expected that 2025 RL2 may be assigned a rating of $PAR = -3$ (NPA rotation reliably detected with the two periods resolved. An ambiguity of the periods solution may be tolerated provided the resulting spectrum of frequencies with significant signal is the same for the different solutions) on the PAR scale defined in Pravec et al. (2005). The full amplitude implied by the NPAR lightcurves is 1.2 mag and during the time 2025 RL2 was being observed it completed 19 rotations of the $P1$ period and 4 of the $P2$ period.





Number	Name	Integration times	Max intg/Pd	Min a/b	Pts	Flds
2025	RL2	3.5–10	0.038 ¹	2.0	495	11

Table I. Ancillary information, listing the integration times used (seconds), the fraction of the period represented by the longest integration time (Pravec et al., 2000), the calculated minimum elongation of the asteroid (Zappala et al., 1990), the number of data points used in the analysis and the number of times the telescope was repositioned to different fields. Note: 1 = Calculated using the shorter of the NPAR periods.

Acknowledgements

The authors would like to thank Dr. Petr Pravec, Astronomical Institute, Czech Republic for his help in reviewing this NPAR analysis. The first author also gratefully acknowledges a Gene Shoemaker NEO Grant from the Planetary Society (2005) and a Ridley Grant from the British Astronomical Association (2005), both of which facilitated upgrades to observatory equipment at Great Shefford used in this study. Installation of a new robotic telescope in the western dome of the Valašské Meziříčí Observatory is part of the Cultural and Creative Centre project, co-financed by the European Union and the National Recovery Plan, under Call No. 0231/2022 - Development of Regional Cultural and Creative Centres (Project Reg. No. 0231000014), administered by the Ministry of Culture of the Czech Republic. The installation costs were covered by a co-financing contribution provided by the Zlín Region. This work has made use of data from the European Space Agency (ESA) mission Gaia (<https://www.cosmos.esa.int/gaia>), processed by the Gaia Data Processing and Analysis Consortium (DPAC, <https://www.cosmos.esa.int/web/gaia/dpac/consortium>). Funding for the DPAC has been provided by national institutions, in particular the institutions participating in the Gaia Multilateral Agreement.

Number	Name	yyyy mm/dd	Phase	L _{PAB}	B _{PAB}	Period(h)	P.E.	Amp	A.E	PAR	H
2025	RL2	2025 09/18–09/18	*20.6,20.6	358	10	0.07272	0.00002	0.97	0.14	–3	26.0
						0.309	0.001	0.25	0.14		

Table II. Observing circumstances and results. The phase angle is given for the first and last date. If preceded by an asterisk, the phase angle reached an extrema during the period. L_{PAB} and B_{PAB} are the approximate phase angle bisector longitude/latitude at mid-date range (see Harris et al., 1984). Amplitude error (A.E.) is calculated as $\sqrt{2} \times$ (lightcurve RMS residual). PAR is the expected Principal Axis Rotation quality detection code (Pravec et al., 2005) and H is the absolute magnitude at 1 au from Sun and Earth taken from the Small-Body Database Lookup (JPL, 2025).

Observer, Observatory (MPC code)	Telescope	Detector	Filter/mag band	Star Catalogue	Photometry software	Obs span 2025 September 18 UTC	Data points
Birtwhistle, Great Shefford Observatory, UK (J95)	0.41-m f/6.3 Schmidt-Cassegrain	CCD	None / G	Gaia DR3	Astrometrica	21:19 – 22:18	386
Koukal, Valašské Meziříčí Observatory, Czech Republic	0.5-m f/4 Newtonian	CMOS	None / G	Gaia DR3	AstroImageJ	20:55 – 21:14	109

Table III. Equipment list

References

- ADS (2025). Astrophysics Data System.
<https://ui.adsabs.harvard.edu/>
- Bacci, P.; Maestripieri, M.; Dupouy, P.; Bosch, J.M.; Holmes, R.; Linder, T.; Hutton, L.; Beuden, T.; Carvajal, V.F.; Fay, D.; Fazekas, J.B.; Fuls, D.C.; Gibbs, A.R.; Grauer, A.D.; Groeller, H. and 16 colleagues (2025). “2025 RL2.” MPEC 2025-R93.
<https://www.minorplanetcenter.net/mpec/K25/K25R93.html>
- Collins, B.; Collins, A.L. (2017). “ASTROIMAGEJ: Image processing and photometric extraction in astronomy.” *The Astronomical Journal* **153**(2), 77.
- Harris, A.W.; Young, J.W.; Scaltriti, F.; Zappala, V. (1984). “Lightcurves and phase relations of the asteroids 82 Alkmene and 444 Gytis.” *Icarus* **57**, 251-258.
- Harris, A.W.; Young, J.W.; Bowell, E.; Martin, L.J.; Millis, R.L.; Poutanen, M.; Scaltriti, F.; Zappala, V.; Schober, H.J.; Debehogne, H.; Zeigler, K. (1989). “Photoelectric Observations of Asteroids 3, 24, 60, 261, and 863.” *Icarus* **77**, 171-186.
- JPL (2025). Small-Body Database Lookup.
https://ssd.jpl.nasa.gov/tools/sbdb_lookup.html
- Pravec, P.; Hergenrother, C.; Whiteley, R.; Sarounova, L.; Kusnirak, P.; Wolf, M. (2000). “Fast Rotating Asteroids 1999 TY2, 1999 SF10, and 1998 WB2.” *Icarus* **147**, 477-486.
- Pravec, P.; Harris, A.W.; Scheirich, P.; Kušnirák, P.; Šarounová, L.; Hergenrother, C.W.; Mottola, S.; Hicks, M.D.; Masi, G.; Krugly, Yu. N.; Shevchenko, V.G.; Nolan, M.C.; Howell, E.S.; Kaasalainen, M.; Galád, A. and 5 colleagues. (2005). “Tumbling Asteroids.” *Icarus* **173**, 108-131.
- Raab, H. (2025). Astrometrica software, version 4.16.4.468.
<http://www.astrometrica.at/>
- Schneider, C.A.; Rasband, W.S.; Eliceiri, K. W. (2012). “NIH Image to ImageJ: 25 years of image analysis.” *Nature Methods* **9**(7), 671-675.
- Warner, B.D.; Harris, A.W.; Pravec, P. (2009). “The Asteroid Lightcurve Database.” *Icarus* **202**, 134-146. Updated 2023 Oct.
<https://www.minorplanet.info/php/lcdb.php>
- Warner, B.D. (2023). MPO Software, Canopus version 10.8.6.20. Bdw Publishing, Colorado Springs, CO.
<https://minplanobs.org/BdwPub/>
- Zappala, V.; Cellini, A.; Barucci, A.M.; Fulchignoni, M.; Lupishko, D.E. (1990). “An analysis of the amplitude-phase relationship among asteroids.” *Astron. Astrophys.* **231**, 548-560.
- PHOTOMETRIC ANALYSIS OF 5806 ARCHIEROY AND (49667) 1999 OM2: ROTATION PERIODS AND PRELIMINARY SPIN-SHAPE MODELS**
- Jonatan Michimani, Eduardo Rondón, Plácida Arcoverde, Wesley Pereira, Rodolpho Degen, Eddie Andrews, Teresinha Rodrigues, Daniela Lazzaro
Observatório Nacional, COAST, Rua Gal. José Cristino 77, 20921-400, Rio de Janeiro, BRASIL.
jonatangarcia@on.br
- (Received: 2025 Aug 20 - Revised: 2025 Nov 24)
- Photometric observations of Main-belt asteroids 5806 Archieroy and (49667) 1999 OM2 conducted at the Observatório Astronômico do Sertão de Itaparica (OASI) during 2025 enabled the determination of rotation periods of 12.16 ± 0.01 hours and 3.480 ± 0.001 hours, respectively. Combining these new observations with archival lightcurve data from the Asteroid Lightcurve Database allowed for preliminary spin-shape modeling with resulting spin axis orientations of $(\lambda, \beta) = (216.0^\circ, 65.8^\circ)$ and $(34.9^\circ, -64.0^\circ)$.
- Inner Main-belt objects 5806 Archieroy and (49667) 1999 OM2 have been observed at multiple previous apparitions, with lightcurves available in the Asteroid Lightcurve Database (Warner et al., 2009). While both objects have well-constrained rotation periods, their spin-pole orientations remain undetermined. To increase aspect angle coverage and enable spin-shape modeling, we conducted additional observations at the Observatório Astronômico do Sertão de Itaparica (OASI) (MPC code Y28, Nova Itacuruba), a dedicated facility of the IMPACTON project for small solar system body studies. We merged our 2025 photometric data with existing Asteroid Lightcurve Database (LCDB; Warner et al., 2009) observations to perform lightcurve inversion analysis and derive preliminary spin-shape models for both objects.
- CCD photometric observations were carried out at OASI between February and May 2025. We used the 1.0-m f/8 telescope equipped with an ATIK TE-42 CCD camera with a 2048×2048-pixel array and an R-Cousins filter. More details on available instrumentation at OASI are given in Rondón et al. (2020). The data reduction process included calibration of raw images with dark and flat frames via IRAF. *MPO Canopus* (Warner, 2017a) was used for photometric measurements, and Fourier analysis (Harris et al. 1989) was applied for calculating rotation periods and producing the final lightcurves. After photometric measurements, the resulting data from each observing night were exported into a suitable format for analysis. For a comprehensive description of the photometry and file export process, see the MPO Users Guide (Warner, 2012).
- We merged the data from the Asteroid Lightcurve Database available at the ALCDEF (2021) web site with our own observations to proceed with the lightcurve inversion process. For the sidereal period search, we used the *period_scan* routine, which incorporates algorithms written in Fortran by Mikko Kaasalainen (Kaasalainen & Torppa, 2010; Kaasalainen et al., 2010) and converted to C by Josef Ďurech (Ďurech et al., 2010). The period

Number	Name	2025/mm/dd	Phase	L_{PAB}	B_{PAB}	Period(h)	P.E.	Amp
5806	Archieroy	04/27-05/31	19.05, 23.03	216.3	-29.7	12.16	0.01	0.74
49667	1999 OM2	02/21-04/05	15.10, 29.50	139.8	-18.7	3.480	0.001	0.44

Table I. Observing circumstances and results. The phase angle is given for the first and last date. L_{PAB} and B_{PAB} are the approximate phase angle bisector longitude/latitude at mid-date range (see Harris et al., 1984).

search evaluates how well different trial periods fit the observational data using chi-squared (χ^2) statistics, where lower χ^2 values indicate better fits. However, for reliable lightcurve inversion, the solution must be unique—that is, one period should clearly provide the best fit to distinguish it from potential aliases or local minima. To ensure solution uniqueness, we identify periods with χ^2 values within 10% of the lowest value; ideally, only the true period should fall within this threshold, while all other trial periods should have significantly higher χ^2 values. We then use these candidate periods to proceed to the spin-pole search using *MPO LCInvert*, a Windows-based software (Warner, 2017b). This software allows us to examine fits to models with discrete longitude-latitude poles using coarse, medium, or fine search grids with varying pole position densities and longitude-latitude steps.

The resulting spin axis parameters are then used to generate final shape and spin axis models using *MPO LCInvert*'s convex hull approach with facet normal coordinates. For comprehensive details on the modeling methodology, consult the *MPO LCInvert* Manual and Tutorials (Warner, 2018) and references therein. We present rotation periods determined using OASI data and preliminary spin-shape models derived from lightcurve inversion analysis that combines our new photometric data with archival lightcurve measurements. Table I summarizes the OASI observation circumstances for each object along with the derived rotation periods and lightcurve amplitudes.

5806 Archieroy. This inner Main-belt object was observed at OASI in April and May 2025. Our photometric analysis allowed us to derive a rotational period of 12.16 ± 0.01 h (Fig. 1). The lightcurve shows a maximum amplitude of 0.74 mag (Fig 2).

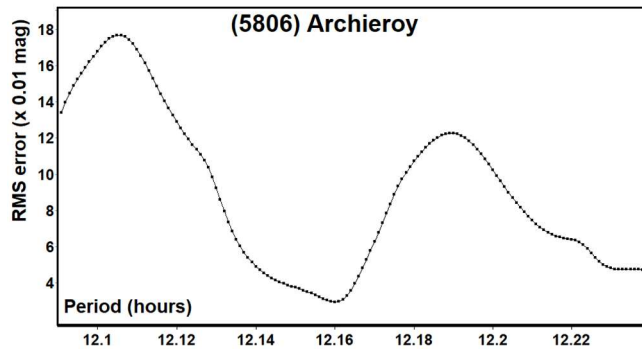


Figure 1. Periodogram of object 5806 Archieroy.

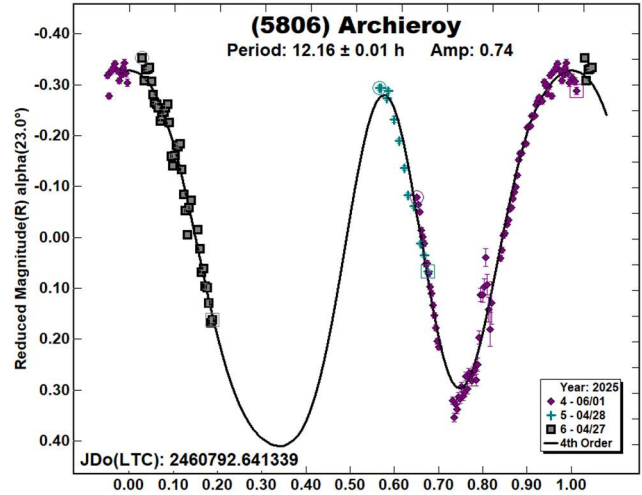


Figure 2. Lightcurve and Fourier fit of 5806 Archieroy.

The period of rotation of 5806 Archieroy has been reported as approximately 12.16 hours, which is in agreement with our results. Photometric observational data from four previous apparitions are available at ALCDEF (2019) as described in Table II. These data were merged with the OASI data for the inversion process. Figure 3 shows the distribution of L_{PAB} and B_{PAB} of all merged data used.

Reference	Mid date	# LC	L_{PAB}°	B_{PAB}°
Warner (2005)	2004/12/11	4	69.7	23.4
Warner (2008)	2008/01/31	5	120.2	-1.5
Warner (2013)	2012/10/12	7	7.5	29.2
Stephens (2016)	2015/11/28	4	68.8	25.3

Table II. Observational details for the data used in the lightcurve inversion process for 5806 Archieroy. The table shows reference sources, mid-observation dates, number of lightcurves (# LC), and Phase Angle Bisector longitude (L_{PAB}) and latitude (B_{PAB}) values.

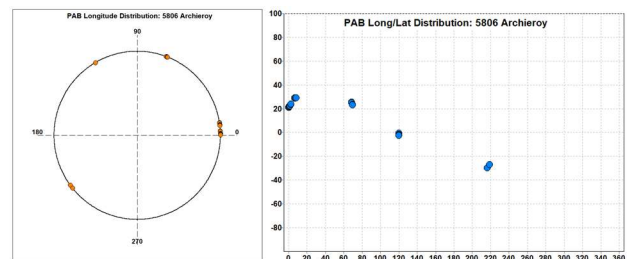


Figure 3. Phase Angle Bisector Longitude (L_{PAB}) and Latitude (B_{PAB}) distribution of the data used for the lightcurve inversion model of 5806 Archieroy, showing the observational geometry coverage.

We performed a period search around 12.16 h, looking for the sidereal period with the minimum χ^2 . This search can find local minima; hence, it is necessary to cover a sufficient period range centered on the suspected value. In this case, we used a range around the published values. The period search spectrum is shown in Figure 4. The period with the lowest χ^2 value was 12.158521 hours ($\chi^2 = 1.138201$), which lies exactly on the green horizontal line in the spectrum (10% threshold).

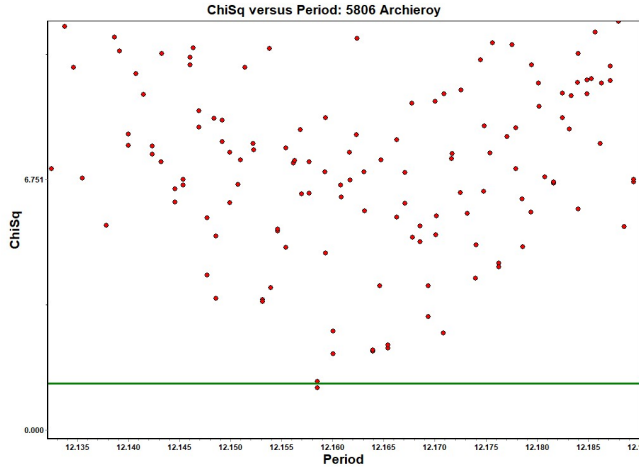


Figure 4. The period search spectrum for 5806 Archieroy. The plot was generated using *MPO LCInvert* and shows the rotation period versus χ^2 values, with the minimum indicating the best-fit period.

The period with the lowest χ^2 value was then used as input for the pole search (λ, β), i.e., the ecliptic longitude and latitude coordinates of the object's spin axis (J2000.0). We performed a medium pole search (Figure 5) where we found a region of low χ^2 values (shown in blue), but the solution was somewhat dispersed, which is not ideal for a unique pole determination. The pole solutions found showed possible ambiguity in λ . Hence, a fine search was performed at around $\lambda=225^\circ$ and $\beta=75^\circ$. Finally, λ, β values with the lowest χ^2 in the latter search were used to generate the shape model (Figure 6).

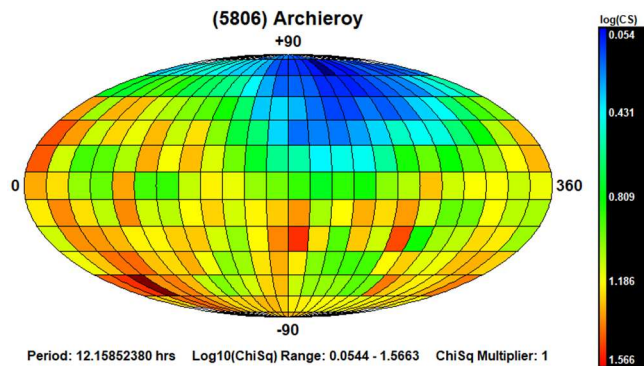


Figure 5. Pole search distribution for 5806 Archieroy (medium search). The dark blue region indicates the smallest χ^2 value while the dark red region indicates the largest.

λ°	β°	Sidereal Period (hours)	χ^2	RMS
216.0	65.8	12.15852381	1.018	0.020

Table III. Spin axis solutions (fine search) for 5806 Archieroy (ecliptic coordinates).

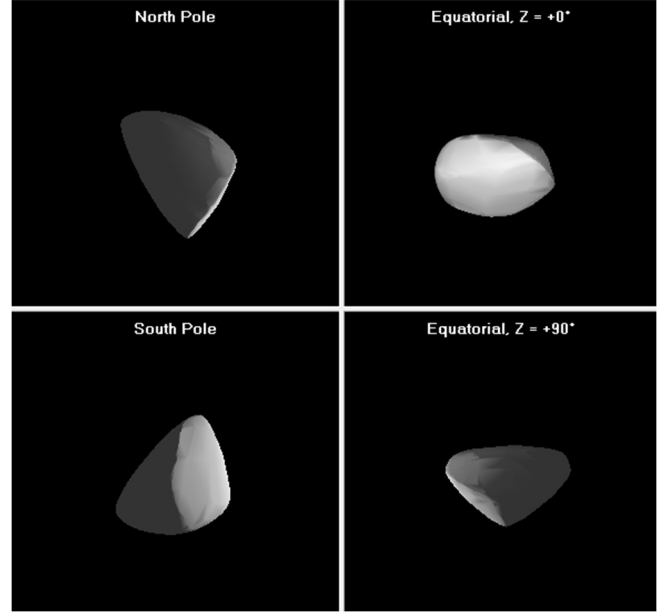


Figure 6. Shape model for 5806 Archieroy ($\lambda = 216.0^\circ$, $\beta = 65.8^\circ$).

(49667) 1999 OM2. This inner Main-belt object, a member of the Hungaria family, was observed at OASI in February and April 2025. Our photometric analysis allowed us to derive a rotational period of 3.480 ± 0.001 h (Fig. 7). The calculated amplitude was 0.44 mag (Fig. 8).

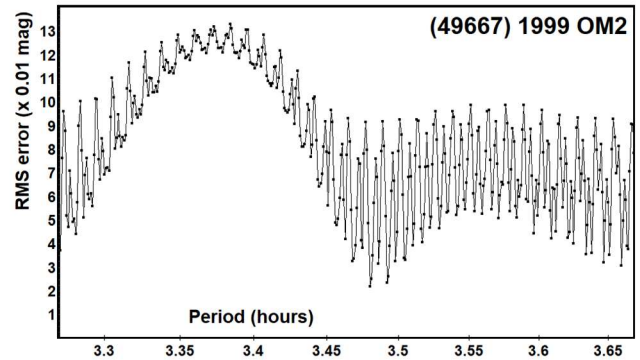


Figure 7. Periodogram of object 49667 1999 OM2.

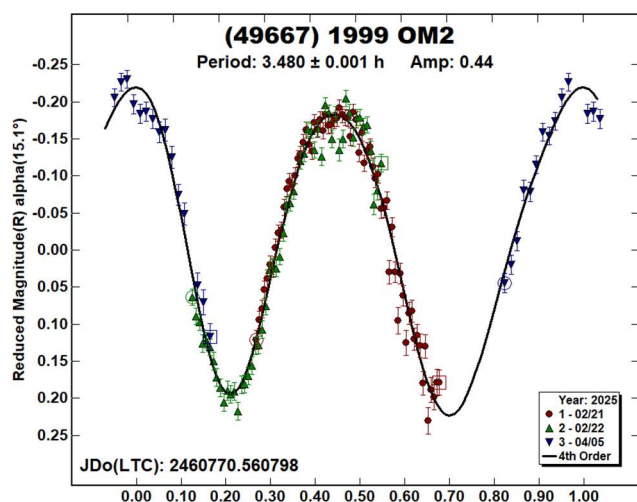


Figure 8. Lightcurve and Fourier fit of 49667 1999 OM2.

In accordance with our results, the period of rotation of (49667) 1999 OM2 has been reported as approximately 3.48 hours. Observational data from previous apparitions are available at ALCDEF (2019) as described in Table IV. As with the previous object, we merged the OASI and ALCDEF data for the inversion process. Figure 9 shows the distribution of L_{PAB} and B_{PAB} of all merged data used.

Reference	Mid date	# LC	L_{PAB}°	B_{PAB}°
Warner et al. (2011)	2010/11/18	14	52.8	19.6
Warner (2014a)	2013/12/14	2	104.2	2.1
Warner (2014b)	2014/03/07	3	111.0	-9.4
Warner (2016)	2015/07/02	3	331.5	16.0

Table IV. Observational details for the data used in the lightcurve inversion process for (49667) 1999 OM2. The table shows reference sources, mid-observation dates, number of lightcurves (# LC), and Phase Angle Bisector longitude (L_{PAB}) and latitude (B_{PAB}) values.

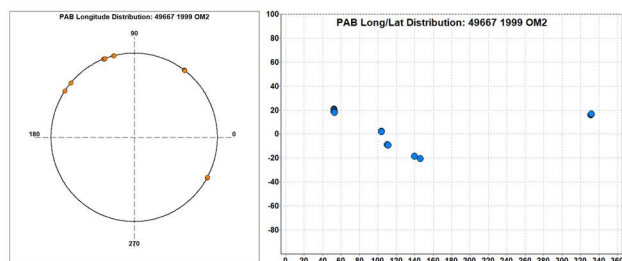


Figure 9. Phase Angle Bisector Longitude (L_{PAB}) and Latitude (B_{PAB}) distribution of the data used for the lightcurve inversion model of (49667) 1999 OM2, showing the observational geometry coverage.

The period search performed covered the range around the published values. In this case, the period search spectrum (Figure 10) shows several local minima. Unfortunately, instead of a unique minimum, we found a group of period values with similarly low χ^2 values that lay around 3.4864 hours, so we proceeded to work with this group of solutions in the next step of the inversion process.

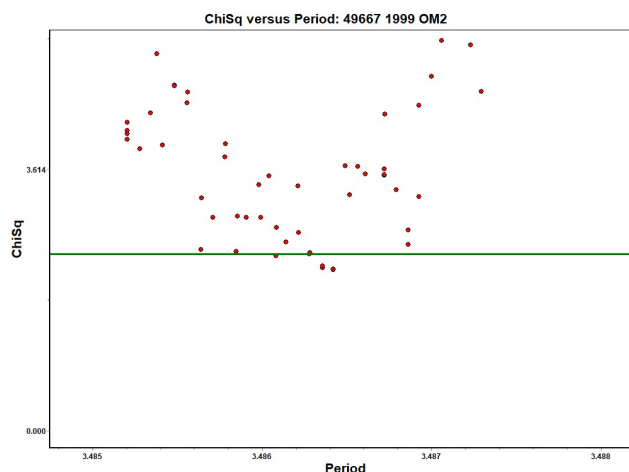


Figure 10. The period search spectrum for (49667) 1999 OM2. The plot was generated using *MPO LCinvert* and shows the rotation period versus χ^2 values.

The pole search for this object was a bit complex and also computational time consuming. We first ran medium pole searches with the four lowest χ^2 values found in the previous step. We then compare the pole solutions for each of the four period searches looking for the minimum values in χ^2 pole solutions. We found that the period of 3.486421 hours (the one with lower χ^2) also provided the pole solutions with lowest χ^2 . From the medium pole searches with the referred period we ran a fine search around the region of low χ^2 values (shown in dark blue in Figure 11). Finally, λ, β values with the lowest χ^2 were used to generate the shape model (Figure 12).

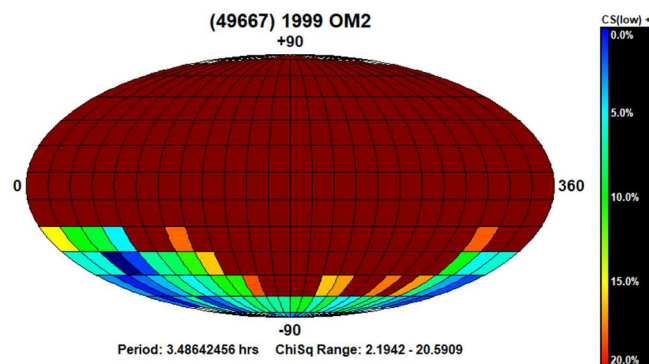


Figure 11. Pole search distribution for (49667) 1999 OM2 (medium search). The dark blue region indicates the smallest χ^2 value while the dark red region indicates the largest.

λ°	β°	Sidereal Period (hours)	χ^2	RMS
34.9	-64.0	3.48642467	2.178	0.037

Table V. Spin axis solutions (fine search) for (49667) 1999 OM2 (ecliptic coordinates).

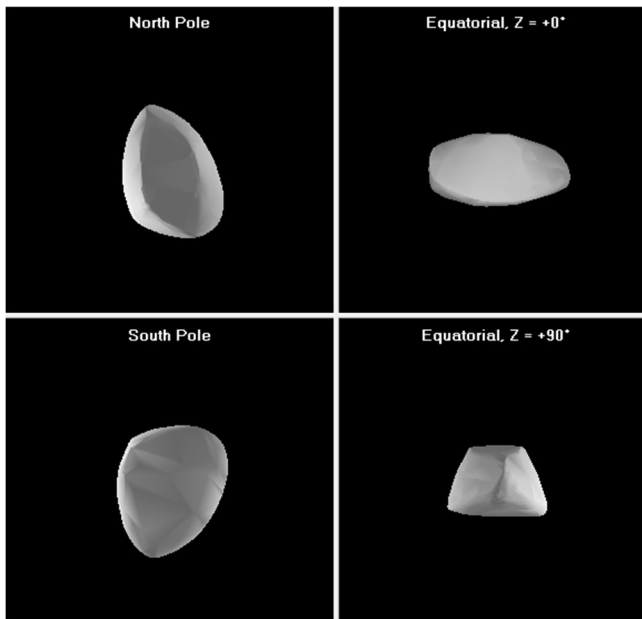


Figure 12. Shape model for (49667) 1999 OM2 ($\lambda = 34.9^\circ$, $\beta = -64.0^\circ$).

The preliminary pole solutions presented here demonstrate both the potential and challenges of lightcurve inversion techniques. While these results could be refined through future apparition observations, this work illustrates the critical value of combining archival data with new observations from dedicated facilities like OASI to address the characterization deficit among small solar system bodies. The analyzed data did not distinguish a single sidereal period that fits significantly better than other alternatives. It should be kept in mind that minor deviations in the sidereal period can lead to considerably erroneous rotation vectors.

Acknowledgements

The authors acknowledge CNPq, CAPES and FAPERJ for supporting this work through diverse fellowships and grants. Support by CNPq (proc. 310964/2020-2) and FAPERJ (proc. E-26/204.276/2024) is acknowledged by D.L. ER would like to acknowledge FAPERJ for their support (proc. E-26/204.602/2021). Technical support at OASI is also recognized, in particular, R. Souza, A. Santiago and A. Santos.

References

ALCDEF (2021). Asteroid Lightcurve Data Exchange Format web site. <http://www.alcdef.org/>

Đurech, J.; Sidorin, V.; Kaasalainen, M. (2010). "DAMIT: a database of asteroid models." *Astronomy and Astrophysics* **513**, A46.

Harris, A.W.; Young, J.W.; Scaltriti, F.; Zappala, V. (1984). "Lightcurves and phase relations of the asteroids 82 alkmene and 444 Gytis." *Icarus* **57**, 251-258.

Harris, A.W.; Young, J.W.; Bowell, E.; Martin, L.J.; Millis, R.L.; Poutanen, M.; Scaltriti, F.; Zappala, V.; Schober, H.J.; Debehogne, H.; Zeigler, K. (1989). "Photoelectric Observations of Asteroids 3, 24, 60, 261, and 863." *Icarus* **77**, 171-186.

JPL (2025). Small-Body Database Lookup. https://ssd.jpl.nasa.gov/tools/sbdb_lookup.html#/

Kaasalainen, M.; Torppa, J. (2001). "Optimization Methods for Asteroid Lightcurve Inversion. I. Shape Determination." *Icarus* **153**, 24-36.

Kaasalainen, M.; Torppa, J.; Muinonen, K. (2001). "Optimization Methods for Asteroid Lightcurve Inversion. II. The Complete Inverse Problem." *Icarus* **153**, 37-51.

MPInfo (2025). One Asteroid Info. <https://minorplanet.info/php/oneasteroidinfo.php>

Rondón, E.; Lazzaro, D.; Rodrigues, T.; Carvano, J.M.; Roig, F.; Monteiro, F.; Arcoverde, P.; Medeiros, H.; Silva, J.; Jasmin, F.; de Prá, M.; Hasselmann, P.; Ribeiro, A.; Dávalos, J.; Souza, R. (2020). "OASI: A Brazilian Observatory Dedicated to the Study of Small Solar System Bodies-Some Results of NEOs Physical Properties." *PASP* **132**, 065001.

Stephens, R.D. (2016). "Asteroids Observed from CS3: 2015 October - December." *Minor Planet Bulletin* **43**, 158-159.

Warner, B.D. (2005). "Asteroid lightcurve analysis at the Palmer Divide Observatory - Fall 2004." *Minor Planet Bulletin* **32**, 29-32.

Warner, B. D. (2008). "Asteroid Lightcurve Analysis at the Palmer Divide Observatory: December 2007 - March 2008." *Minor Planet Bulletin* **35**, 95-98.

Warner, B.D.; Harris, A.W.; Pravec, P. (2009). "The Asteroid Lightcurve Database." *Icarus* **202**, 134-146. Updated 2016 Sep. <http://www.minorplanet.info/lightcurvedatabase.html>

Warner, B.D.; Galad, A.; Veres, P.; Pravec, P.; Kusnirak, P. (2011). "Lightcurve Analysis of Hungaria Asteroid (49667) 1999 OM2." *Minor Planet Bulletin* **38**, 103.

Warner, B.D. (2012). The MPO Users Guide: A Companion Guide to the MPO Canopus/PhotoRed Reference Manuals. BDW Publishing, Eaton, CO.

Warner, B.D. (2013). "Asteroid Lightcurve Analysis at the Palmer Divide Observatory: 2012 September - 2013 January." *Minor Planet Bulletin* **40**, 71-80.

Warner, B.D. (2014a). "Asteroid Lightcurve Analysis at CS3-Palmer Divide Station: 2013 September-December." *Minor Planet Bulletin* **41**, 102-112.

Warner, B.D. (2014b). "Asteroid Lightcurve Analysis at CS3-Palmer Divide Station: 2014 January-March." *Minor Planet Bulletin* **41**, 144-155.

Warner, B.D. (2016). "Asteroid Lightcurve Analysis at CS3-Palmer Divide Station: 2015 June-September." *Minor Planet Bulletin* **42**, 57-65.

Warner, B.D. (2017a). MPO Canopus software. Version 10.7.11.1. <http://www.bdwpublishing.com>

Warner, B.D. (2017b). MPO LCInvert software. Version 11.7.8.0. <http://www.bdwpublishing.com>

Warner, B.D. (2018). The MPO LCInvert Users Guide. BDW Publishing, Eaton, CO. <https://bdwpublishing.com/php/mpolcinvert.php>

PHOTOMETRIC OBSERVATIONS OF ASTEROIDS 1967 MENZEL, 2949 KAVERZNEV AND 3024 HAINAN

Alessandro Marchini, Riccardo Papini
Astronomical Observatory, University of Siena (K54)
Via Roma 56, 53100 - Siena, ITALY
marchini@unisi.it

Lorenzo Franco
Balzaretto Observatory (A81), Rome, ITALY

(Received: 2025 October 15)

Photometric observations of three main-belt asteroids were conducted to verify or determine their synodic rotation periods. For 1967 Menzel, we found $P = 2.835 \pm 0.001$ h with $A = 0.25 \pm 0.01$ mag. For 2949 Kaverznev, a very slow rotator, we present an attempt at a bimodal solution of $P = 84.1 \pm 0.2$ h with $A = 1.4 \pm 0.1$ mag. For 3024 Hainan, we found $P = 11.743 \pm 0.001$ h with $A = 0.10 \pm 0.02$ mag.

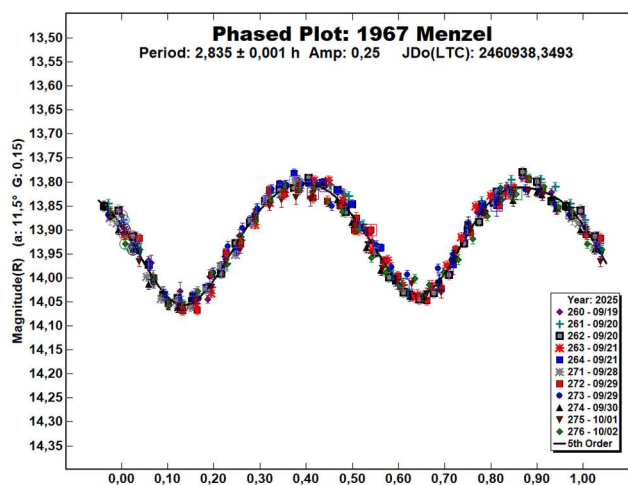
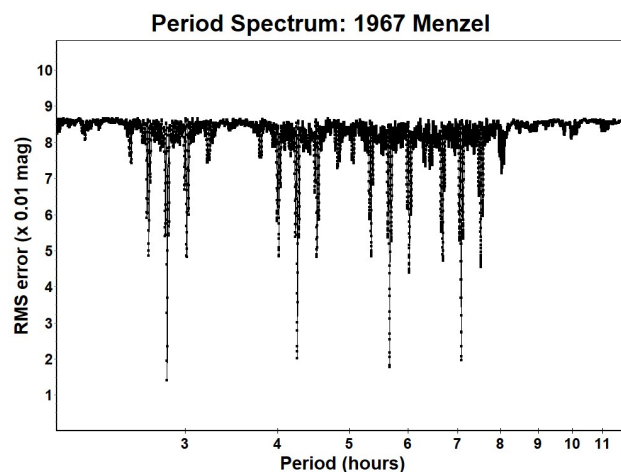
CCD photometric observations of three main-belt asteroids were carried out in June-October 2025 at the Astronomical Observatory of the University of Siena (K54). We used a 0.30-m/ $f/5.6$ Maksutov-Cassegrain telescope, SBIG STL-6303E NABG CCD camera; the pixel scale was 2.30 arcsec when binned at 2×2 pixels. We used a Clear filter and 300 seconds of exposure time.

Data processing and analysis were done with *MPO Canopus* (Warner, 2018). All images were calibrated with dark and flat-field frames and the instrumental magnitudes converted to R magnitudes using solar-colored field stars from a version of the CMC-15 catalogue distributed with *MPO Canopus*. Table I shows the observing circumstances and results.

A search through the asteroid lightcurve database (LCDB; Warner et al., 2009) indicates that our result may be the first reported lightcurve observations and results for 2949 Kaverznev.

1967 Menzel (A905 VC) was discovered by M.F. Wolf at Heidelberg on 1905 November 1. It is an inner main-belt asteroid with a semi-major axis of 2.233 AU, eccentricity 0.139, inclination 3.900° , and an orbital period of 3.34 years. Its absolute magnitude is $H = 12.10$ (JPL, 2025). The NEOWISE satellite infrared radiometry survey (Meinzer et al., 2019) found a diameter $D = 9.588 \pm 0.181$ km using an absolute magnitude $H = 12.21$ and a geometric albedo of 0.251.

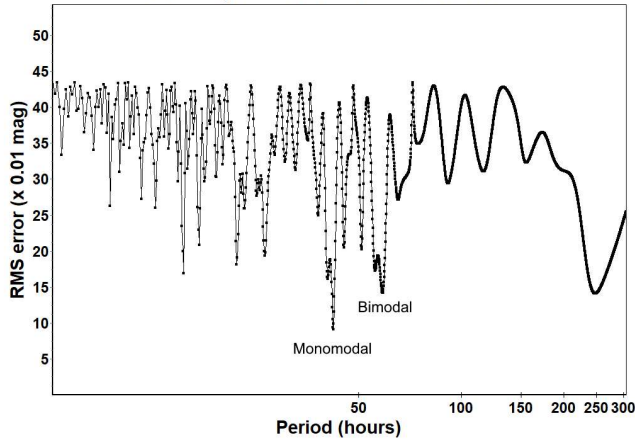
This target was observed within the Photometric Survey for Asynchronous Binary Asteroids under the leadership of Petr Pravec from Ondřejov Observatory, Czech Republic (Pravec et al., 2006; Pravec, 2025web) and their independent analysis confirmed our results. Observations were conducted over six nights and collected 338 data points. The period analysis confirms a rotational period of $P = 2.835 \pm 0.001$ h with an amplitude $A = 0.25 \pm 0.01$ mag, in perfect agreement with the previously results published in the LCDB (Behrend, 2005web, 2015web, 2020web; LeCrone et al., 2006; Pray, 2006; Pravec et al., 2007web, 2010web, 2015web; Higgins, 2008; Clark, 2015; Liu, 2016; Klinglesmith III, 2017; Durech et al., 2019; Pál et al., 2020).



2949 Kaverznev (1970 PR) was discovered on 1970 August 9 by Crimean Astrophysical Observatory at Nauchny and named in memory of Aleksandr Aleksandrovich Kaverznev (1932-1983), Soviet journalist, documentary-film maker and political commentator. It is an inner main-belt asteroid with a semi-major axis of 2.195 AU, eccentricity 0.141, inclination 4.866° , and an orbital period of 3.25 years. Its absolute magnitude is $H = 13.22$ (JPL, 2025). The NEOWISE satellite infrared radiometry survey (Mainzer et al., 2016) found a diameter $D = 6.959 \pm 0.216$ km using an absolute magnitude $H = 13.00$ and a geometric albedo of 0.230.

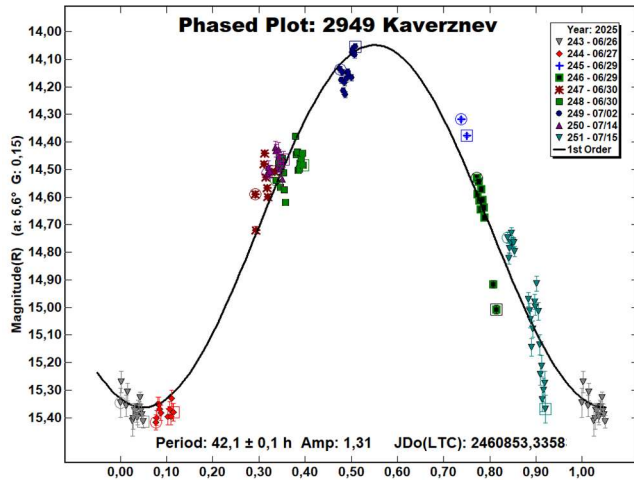
Despite observing this asteroid for six nights and collecting 118 data points, it turned out to be a very slow rotator, and we were unable to cover the entire rotation. The period analysis shows two possible solutions for the synodic rotational period, we present the bimodal one of $P = 84.1 \pm 0.02$ h with an amplitude $A = 1.4 \pm 0.1$ mag as the most likely, but we cannot exclude the monomodal one of $P = 42.1 \pm 0.01$ h with an amplitude $A = 1.3 \pm 0.1$ mag. Further observations are strongly encouraged to nail down the actual period.

Period Spectrum: 2949 Kaverznev

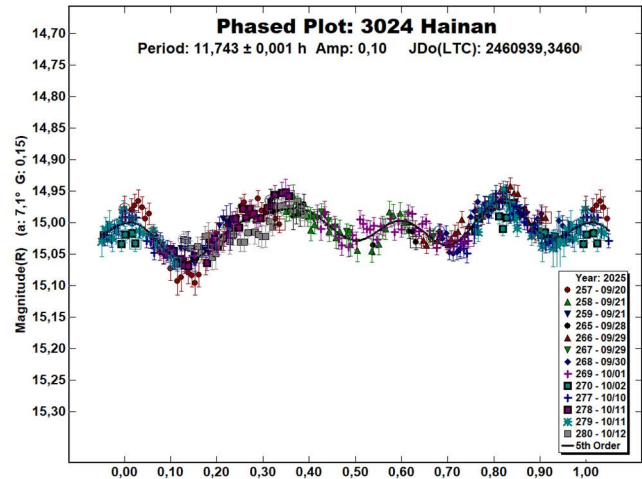
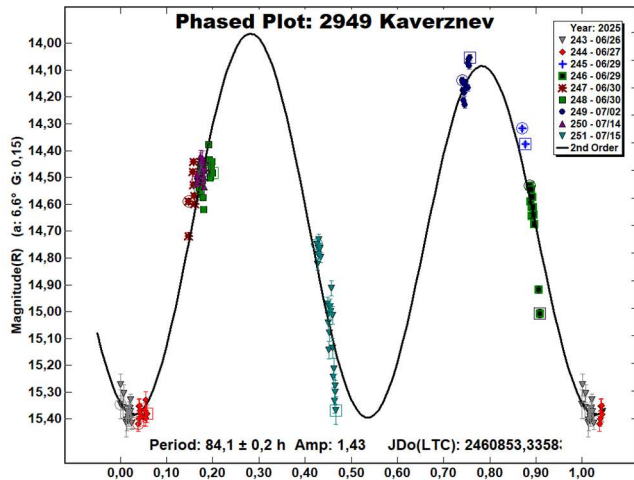
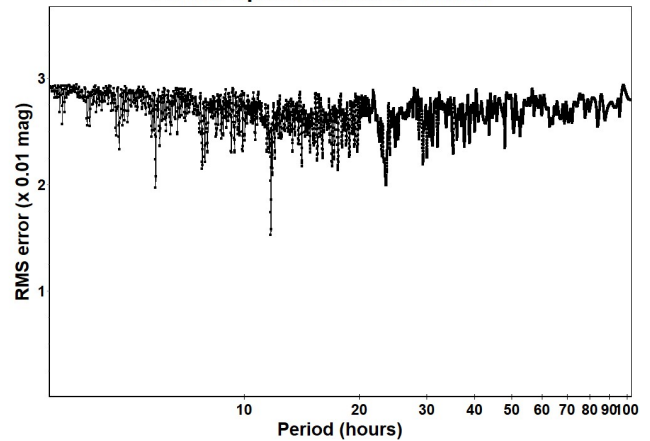


3024 Hainan (1981 UW9) was discovered on 1981 October 23 by Purple Mountain Observatory at Nanking and named for a newly established province in southern China, the Hainan Island. It is an outer main-belt asteroid with a semi-major axis of 3.411 AU, eccentricity 0.131, inclination 14.847° , and an orbital period of 6.30 years. Its absolute magnitude is $H = 11.03$ (JPL, 2025). The NEOWISE satellite infrared radiometry survey (Mainzer et al., 2019) found a diameter $D = 37.189 \pm 0.516$ km using an absolute magnitude $H = 10.7$ and a geometric albedo of 0.067.

Observations were conducted over seven nights and collected 366 data points. The period analysis shows a rotational period of $P = 11.743 \pm 0.001$ h with amplitude $A = 0.10 \pm 0.02$ mag as the most likely quadrimodal solution, which is consistent with those published in the LCDB by Bin et al. (2013) and Simpson et al. (2013) and excludes the one with a halved period published by Pál et al. (2020). Further observations are encouraged to nail down the actual period.



Period Spectrum: 3024 Hainan



Number	Name	2025/mm/dd	Phase	L_{PAB}	B_{PAB}	Period(h)	P.E.	Amp	A.E.	Grp
1967	Menzel	09/19–10/02	11.6, 5.0	14	-4	2.835	0.001	0.25	0.01	MB-I
2949	Kaverznev	06/26–07/15	6.6, 15.8	270	7	84.1	0.2	1.4	0.1	MB-I
3024	Hainan	09/20–10/12	*7.2, 2.1	15	-4	11.743	0.001	0.10	0.02	MB-O

Table I. Observing circumstances and results. The phase angle is given for the first and last date. If preceded by an asterisk, the phase angle reached an extremum during the period. L_{PAB} and B_{PAB} are the approximate phase angle bisector longitude/latitude at mid-date range (see Harris et al., 1984). Grp is the asteroid family/group (Warner et al., 2009).

References

- Behrend, R. (2005web, 2015web, 2020web). Observatoire de Geneve web site.
http://obswww.unige.ch/~behrend/page_cou.html
- Bin, L.; Zhao, H.; Hand, X.L.; Liu, W.; Sun, L.; Shi, J.; Gao, S.Z.H. (2013). "Photometric Observation of 3024 Hainan, 3920 Aubignan, and 5951 Alicemonet." *Minor Planet Bull.* **40**, 43-44.
- Clark, M. (2015). "Asteroid Photometry from the Preston Gott Observatory." *Minor Planet Bull.* **42**, 15-20.
- Durech, J.; Hanus, J.; Vanco, R. (2019). "Inversion of asteroid photometry from Gaia DR2 and the Lowell Observatory photometric database." *Astron. Astrophys* **631**, A2.
- Harris, A.W.; Young, J.W.; Scaltriti, F.; Zappala, V. (1984). "Lightcurves and phase relations of the asteroids 82 Alkmene and 444 Gypsis." *Icarus* **57**, 251-258.
- Higgins, D. (2008). "Asteroid Lightcurve Analysis at Hunters Hill Observatory and Collaborating Stations: April 2007 - June 2007." *Minor Planet Bull.* **35**, 30-32.
- JPL (2025). Small Body Database Search Engine.
<https://ssd.jpl.nasa.gov>
- Klinglesmith III, D.K. (2017). "Asteroids Observed from Estcorn Observatory." *Minor Planet Bull.* **44**, 345-348.
- LeCrone, C.; Duncan, A.; Hudson, E.; Johnson, J.; Mulvihill, A.; Reichert, C.; Ditteon, R. (2006). "2005-2006 fall observing campaign at Rose-Hulman Institute of Technology." *Minor Planet Bull.* **33**, 66-67.
- Liu, J. (2016). "Rotation Period Analysis for 1967 Menzel." *Minor Planet Bull.* **43**, 98-99.
- Mainzer, A.K.; Bauer, J.M.; Cutri, R.M.; Grav, T.; Kramer, E.A.; Masiero, J.R.; Sonnett, S.; Wright, E.L. (2016). "NEOWISE Diameters and Albedos V1.0." *NASA Planetary Data System.*
<https://doi.org/10.26033/ddgd-9m07>
- Mainzer, A.K.; Bauer, J.M.; Cutri, R.M.; Grav, T.; Kramer, E.A.; Masiero, J.R.; Sonnett, S.; Wright, E.L. (2019). "NEOWISE Diameters and Albedos V2.0" *NASA Planetary Data System.*
<https://doi.org/10.26033/18S3-2Z54>
- Pál, A.; Szakáts, R.; Kiss, C.; Bódi, A.; Bognár, Z.; Kalup, C.; Kiss, L.L.; Marton, G.; Molnár, L.; Plachy, E.; Sárneczky, K.; Szabó, G.; Szabó, R. (2020). "Solar System Objects Observed with TESS - First Data Release: Bright Main-belt and Trojan Asteroids from the Southern Survey." *Ap. J. Supl. Ser.* **247**, 26.
- Pray, D.P. (2006). "Lightcurve analysis of asteroids 326, 329, 426, 619, 1829, 1967, 2453, 10518 and 42267." *Minor Planet Bull.* **33**, 4-5.
- Pravec, P.; Scheirich, P.; Kušnirák, P.; Šarounová, L.; Mottola, S.; Hahn, G.; Brown, P.; Esquerdo, G.; Kaiser, N.; Krzeminski, Z.; Pray, D.P.; Warner, B.D.; Harris, A.W.; Nolan, M.C.; Howell, E.S.; Benner, L.A.M.; Margot, J.-L.; Galád, A.; Holliday, W.; Hicks, M.D.; Krugly, Yu.N.; Tholen, D.; Whiteley, R.; Marchis, F.; DeGraff, D.R.; Grauer, A.; Larson, S.; Velichko, F.P.; Cooney, W.R.; Stephens, R.; Zhu, J.; Kirsch, K.; Dyvig, R.; Snyder, L.; Reddy, V.; Moore, S.; Gajdoš, Š.; Világi, J.; Masi, G.; Higgins, D.; Funkhouser, G.; Knight, B.; Slivan, S.; Behrend, R.; Grenon, M.; Burki, G.; Roy, R.; Demeautis, C.; Matter, D.; Waelchli, N.; Revaz, Y.; Klotz, A.; Rieugné, M.; Thierry, P.; Cotrez, V.; Brunetto, L.; Kober, G. (2006). "Photometric survey of binary near-Earth asteroids." *Icarus* **181**, 63-93.
- Pravec, P.; Wolf, M.; Sarounova, L. (2007web, 2010web, 2015web). Ondrejov Asteroid Photometry Project web site.
<http://www.asu.cas.cz/~ppravec/neo.htm>
- Pravec, P. (2025web). Photometric Survey for Asynchronous Binary Asteroids web site.
<http://www.asu.cas.cz/~asteroid/binastphotosurvey.htm>
- Simpson, G.; Chong, E.; Gerhardt, M.; Gorsky, S.; Klaasse, M.; Kodalen, B.; Li, F.; Mader, L.; Moore, R.; Vinson, R.; Ditteon, R. (2013). "Asteroid Lightcurve Analysis at the Oakley Southern Sky Observatory: 2012 August – October." *Minor Planet Bull.* **40**, 146-151.
- Warner, B.D.; Harris, A.W.; Pravec, P. (2009). "The Asteroid Lightcurve Database." *Icarus* **202**, 134-146. Updated 2023 Oct 1.
<https://minplanobs.org/mpinfo/php/lcdb.php>
- Warner, B.D. (2018). MPO Software, MPO Canopus v10.7.7.0. Bdw Publishing. <http://bdwpublishing.com/>

LIGHTCURVES AND ROTATION PERIODS OF FOUR MAIN-BELT ASTEROIDS

Caitlin Bell
Zelie-Louise Bradicich
Kent Montgomery
East Texas A&M University
P.O. Box 3011
Commerce, TX 75429-3011
Kent.Montgomery@etamu.edu

(Received: 2025 October 6)

Aperture photometry was performed on the following asteroids in order to determine their rotational periods: 2778 Tangshan, 3.464 ± 0.002 h; 10022 Zubov, 4.532 ± 0.004 h; (13007) 1984 AU, 12.187 ± 0.001 h; and (31361) 1998 VQ29, 3.223 ± 0.001 h.

This research was conducted in order to determine the lightcurves and the rotational periods of the following asteroids: 2778 Tangshan, 10022 Zubov, (13007) 1984 AU, and (31361) 1998 VQ29. These asteroids were selected using the Collaborative Asteroid Lightcurve Link (CALL) website according to specific parameters. Asteroids needed to have a magnitude between 14 and 16, a positive declination, and an opposition date around two weeks prior to the start of observing.

For an historical perspective, asteroid 2778 Tangshan was discovered in 1979 by the Purple Mountain Observatory at Nanjing. It was first observed on November 28, 1948. This asteroid has a semi-major axis of 2.28 AU, with an orbital eccentricity of 0.122 and an absolute magnitude of 13.49 (JPL, 2025). Asteroid 10022 Zubov was discovered on September 22, 1979, by N.S. Chernykh at the Crimean Astrophysical Observatory. It was first observed on September 18, 1979. This asteroid has a semi-major axis of 2.37 AU, an orbital eccentricity of 0.132, and an absolute magnitude of 14.14 (JPL, 2025). Asteroid (13007) 1984 AU was discovered on January 8, 1984, by J. Wagner at Anderson Mesa, and was first observed on October 23, 1906. It has a semi-major axis of 2.53 AU, an eccentricity of 0.134, and an absolute magnitude of 13.23 (JPL, 2025). The asteroid (31361) 1998 VQ29 was discovered on November 10, 1998, by LINEAR at Socorro. It was first observed on August 13, 1951. Its semi-major axis is 2.62 AU, with an orbital eccentricity of 0.200 and an absolute magnitude of 13.04 (JPL, 2025).

Methods

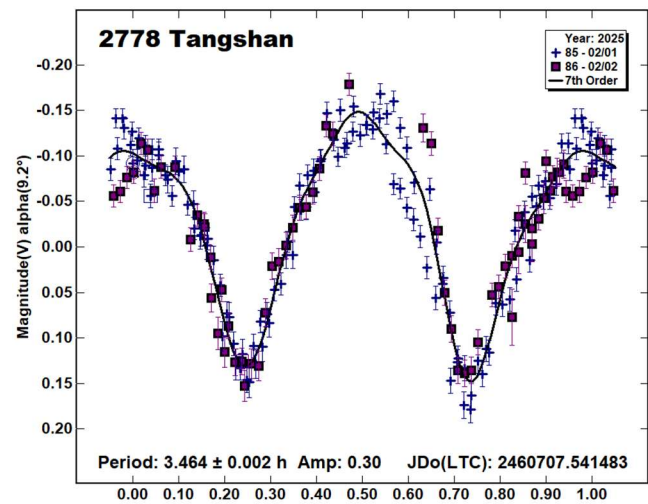
Images of each target field were taken using the Planewave CDK 700 telescope at the East Texas A&M University (ETAMU) Observatory. All images were taken through a luminance filter that blocked both infrared and ultraviolet light, with each image having an exposure time of 180 s. To reduce thermal noise, the detectors

were thermoelectrically cooled to a range between -20°C and -50°C . The telescope was refocused hourly. Observations for each asteroid were collected from 2 to 4 nights.

Calibration images were taken each night. These calibration images included, bias frames, dark frames, and twilight flat field images. Between 20 to 30 bias frames were taken at the beginning of each night. Three dark frames were taken with an exposure time of 180 s, equivalent to the light frame exposure times. Flat field images were taken against the twilight sky. The number and exposure time of flat field images varied for each night of observations. Master images of all the calibration images were created using *Maxim DL* (Diffraction Limited). These master images were then used to reduce all the asteroid images. Aperture photometry was performed on the calibrated images using *MPO Canopus* v.10.8.1.1 software (Warner, 2019). Five comparison stars were chosen based on their magnitude and relative position to the target. The difference in brightness between the asteroid and the average brightness of the reference stars was determined for each image. The resulting magnitudes were then plotted against time to produce the asteroid's lightcurve. Finally, a Fourier transform of the lightcurve was taken to determine the asteroid's best rotation period.

Results

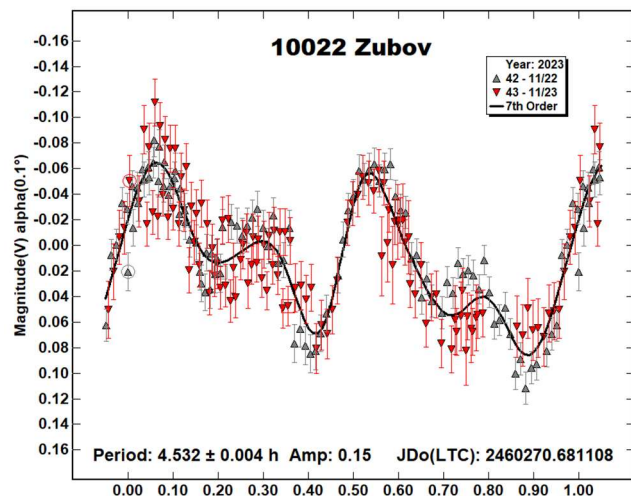
2778 Tangshan is an asteroid in the inner main belt. It was observed on 2025 February 1 and 2025 February 2. A total of 214 images were obtained, with 125 images collected during the first night of observation and the remaining 89 images collected during the second night. Analysis of the resulting lightcurve reveals a rotational period of 3.464 ± 0.002 h with an amplitude variance of 0.30 mag. This is consistent with previous results found by Warner et al. (2022) who found a period of 3.4607 ± 0.002 h and an amplitude variance of 0.30 mag.



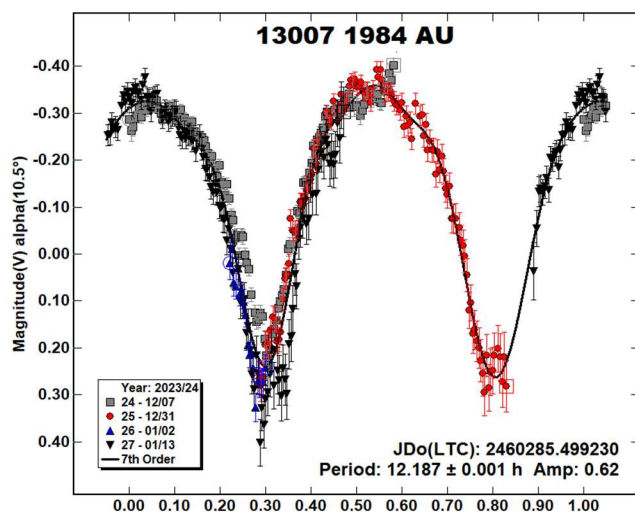
Number	Name	yyyy mm/dd	Phase	L_{PAB}	B_{PAB}	Period(h)	P.E.	Amp	A.E.	Grp
2778	Tangshan	2025 02/01-02/02	0.7, 0.6	132.6	-1.2	3.464	0.002	0.35	0.02	MB-M
10022	Zubov	2023 11/22-11/23	16.0, 15.5	87.8	2	4.532	0.004	0.20	0.03	MB-M
13007	1984 AU	2023/24 12/07-01/13	6.8, 14.7	248.7	-2.0	12.187	0.001	0.29	0.02	MB-I
31361	1998 VQ29	2023 09/21-10/19	9.5, 14.4	152	6	3.223	0.001	0.05	0.03	MB-M

Table I. Observing circumstances and results. The phase angle is given for the first and last date. If preceded by an asterisk, the phase angle reached an extrema during the period. L_{PAB} and B_{PAB} are the approximate phase angle bisector longitude/latitude at mid-date range (see Harris et al., 1984). Grp is the asteroid family/group (Warner et al., 2009).

10022 Zubov was observed for two consecutive nights in November 2023. On November 22, 100 images were collected, and on November 23, an additional 150 images were obtained, totaling 250 images in all. The lightcurve of 10022 Zubov reveals a rotational period of 4.532 ± 0.004 h and an amplitude variance of 0.15 mag. These results are consistent with the findings of Waszczak et al. (2015), who found the rotational period to be 4.564 ± 0.0049 h with no reported amplitude variance.

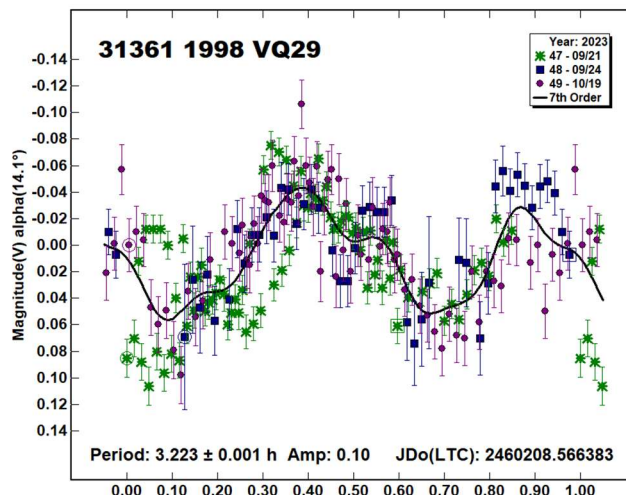


(13007) 1984 AU was observed for four nights with 400 images collected. On 2023 December 7, 150 images were obtained. An additional 120 images were obtained on 2023 December 31, 19 images on 2024 January 2, and the final 130 images were obtained on 2024 January 13. The resulting rotational period is 12.187 ± 0.001 h, with an error in the amplitude of 0.62 mag. This aligns well with previous findings by Ďurech, et al. (2020) who determined the rotational period to be 12.1881 ± 0.0001 h and did not report amplitude variance.



(31361) 1998 VQ29 was observed for three nights with a total of 234 images obtained. The first night on 2023 September 21 with 100 images, 2023 September 24 with 54 images, and 2023 October 19 with 80 images. The rotational period was found to be

3.223 ± 0.001 h with a variance in amplitude of 0.10 mag. The Minor Planet Lightcurve Database (Warner et al., 2009) and the JPL Small-Body Database (JPL, 2025) did not show any previous rotational period results for the asteroid (31361) 1998 VQ29.



References

Collaborative Asteroid Lightcurve Link (CALL): Potential Lightcurve Targets.

http://www.minorplanet.info/PHP/call_OppLCDBQuery.php.

Diffraction Limited MaxIm DL - Astronomy and Scientific Imaging Software.

<https://diffractionlimited.com/product/maxim-dl/>.

Ďurech, J.; Tonry, J.; Erasmus, N.; Denneau, L.; Heinze, A.N.; Flewelling, H.; Vanko, R. (2020), "Asteroid Models Reconstructed from ATLAS Photometry." *Astronomy & Astrophysics* **643**, id.A59, 5 pp.

Harris, A.W.; Young, J.W.; Scaltriti, F.; Zappala, V. (1984). "Lightcurves and phase relations of the asteroids 82 Alkmene and 444 Gytis." *Icarus* **57**, 251-258.

JPL (2025). Small-Body Database Search Engine. <http://ssd.jpl.nasa.gov/sbdb.cgi>.

Warner, B.D.; Harris, A.W.; Pravec, P. (2009). "The Asteroid Lightcurve Database." *Icarus* **202**, 134-146. Updated 2023 Oct. <http://www.MinorPlanet.info/php/lcdb.php>.

Warner, B.D. (2019). MPO Canopus software. Version 10.8.1.1. Bdw Publishing. <http://www.minorplanetobserver.com/>.

Warner, B.D.; Stephens, R.D.; Coley, D.R. (2022). "On Confirmed and Suspected Binary Asteroids at the Center for Solar System Studies: 2022 March-June." *Minor Planet Bull.* **49**, 262-267.

Waszczak, A.; Chang, C.-K.; Ofek, E.O.; Laher, R.; Masci, F.; Levitan, D.; Surace, J.; Cheng, Y.-C.; Ip, W.-H.; Kinoshita, D.; Helou, G.; Prince, T.A.; Kulkarni, S. (2015). "Asteroid Light Curves from the Palomar Transient Factory Survey: Rotation Periods and Phase Functions from Sparse Photometry." *Astron. J.* **150**, A75.

PHOTOMETRIC OBSERVATIONS AND LIGHTCURVE ANALYSIS OF FIVE MAIN-BELT ASTEROIDS FROM SIX OBSERVATORIES

Stephen M. Brincat
Flarestar Observatory (MPC 171)
Fl.5 George Tayar Street,
San Gwann SGN 3160, MALTA
stephenbrincat@gmail.com

Marek Buček
Luckystar Observatory (MPC M55)
Dr. Lučanského 547, Važec, 032 61, SLOVAKIA

Charles Galdies
Znith Observatory
Armonie, E. Bradford Street
Naxxar NXR 2217, MALTA

Vincent Zammit
Stellar Horizon Observatory
No.8, Maranatha, Triq Tal-Fieres
Kirkop KKP 1502, MALTA

Normand Rivard
À la belle étoile Observatory
796, rang des Écossais
Sainte-Brigide-d'Iberville (Québec)
J0J 1X0 CANADA

Martin Mifsud
Manikata Observatory
51, Penthouse 7, Sky Blue Court,
Dun Manwel Grima Street,
Manikata MLH 5013, MALTA

(Received: 2025 September 9)

We present photometric observations of five main-belt asteroids - 1155 Aenna, 1591 Baize, 3066 McFadden, 4016 Sambre, and 11875 Rhone - from six observatories in Malta, Slovakia, and Canada. Synodic rotation periods were determined as 7.9154 h, 7.7956 h, 32.8369 h, 18.235 h, and 5.2100 h, respectively. For 4016 Sambre and 11875 Rhone, these represent the first published lightcurve periods, while the remaining results confirm and refine previous measurements.

We present results from coordinated photometric campaigns of five main-belt asteroids. These campaigns were carried out by a distributed network of observatories situated in Malta (four sites), Slovakia (one site), and Canada (one site), as detailed in Table I. The table provides comprehensive information regarding the instrumental configurations employed and the total number of observation nights allocated to each target.

All instrumentation was remotely operated via internet-based connections to the primary observatory control systems from proximate locations. Two distinct image acquisition platforms were utilized across the network: *NINA - Nighttime Imaging 'N' Astronomy*, (Berg, 2023) was employed at the Slovak and Canadian

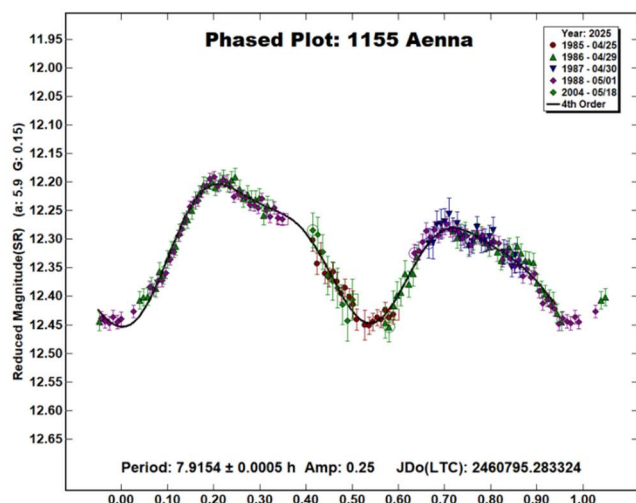
observatories, as well as at the Stellar Horizon Observatory in Malta. The remaining Maltese observatories conducted image acquisition using *Sequence Generator Pro* (Binary Star Software). Observations were conducted in unfiltered mode, utilizing a clear filter with a Sloan r' -band zero-point calibration. All FITS frames were pre-processed through standard calibration procedures, including dark frame subtraction and flat-field correction using master calibration frames.

Image analysis was performed using *MPO Canopus* software versions 10 and 12 (Warner, 2017). Differential aperture photometry was applied to derive light curves, which were subsequently analyzed using Fourier techniques to extract periodicity and other photometric parameters. Comparison stars were selected based on their near-solar colors ($0.5 \leq B - V \leq 0.9$), utilizing the *Comparison Star Selector (CSS)* functionality within *MPO Canopus*. All photometric measurements were calibrated against reference magnitudes from the *Asteroid Terrestrial-impact Last Alert System (ATLAS)* catalog (Tonry et al., 2018).

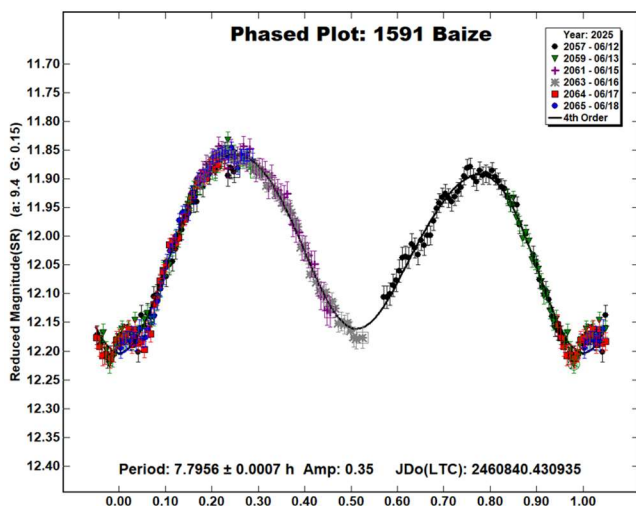
Observatory / Country	Scope and Type	Camera	Observed Asteroids (#Nights)
A la belle étoile Obs. / CANADA	0.20-m MK	Moravian G2-1600	# 4016 (3)
Flarestar Obs. (MPC: 171) / MALTA	0.25-m SCT	Moravian G2-1600	# 1155 (4) # 1591 (6) # 3066 (3) # 4016 (8)
Luckystar Obs. (MPC: M55) / SLOVAKIA	0.25-m SCT	Atik 460EX	# 3066 (17) # 4016 (3) # 11875 (5)
Manikata Obs. / MALTA	0.20-m SCT	ASI2600 MM	# 3066 (1)
Stellar Horizon Obs. / MALTA	0.30-m SCT	ASI6200 MM	# 3066 (3)
Znith Obs. / MALTA	0.20-m SCT	Moravian G2-1600	# 3066 (2) # 4016 (1)

Table I. Instrumentation and Observation Runs. SCT: Schmidt-Cassegrain Telescope, MK: Maksutov-Cassegrain.

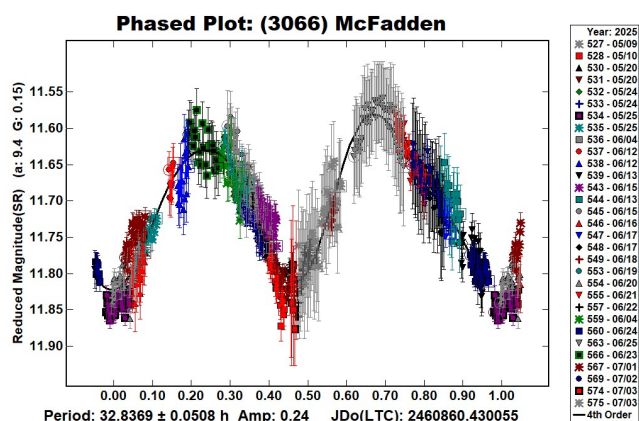
1155 Aenna. This inner main-belt asteroid was discovered on 1928 Jan. 26 by K. Reinmuth at Heidelberg. This artificial name honors the *Astronomische Nachrichten*, one of the oldest continuously published scientific journals in the field of astronomy. Diameter of this asteroid is 9.284 ± 0.524 km with absolute magnitude $H = 12.00$ mag based on the information provided JPL small-body database (JPL, 2025). 1155 Aenna has been observed during its 2025 favorable apparition between 2025 April 25 and May 18 from Flarestar Observatory. Five observation sessions were conducted, yielding 199 data points. Fourier data analysis derived its synodic rotation period as 7.9154 ± 0.0005 h with an amplitude of 0.25 ± 0.02 mag. The LCDB version of 2023 Oct 01, listed 1155 Aenna as having a period of 8.07 ± 0.04 h (Behrend, 2015web) based on a U 2+ quality rating.



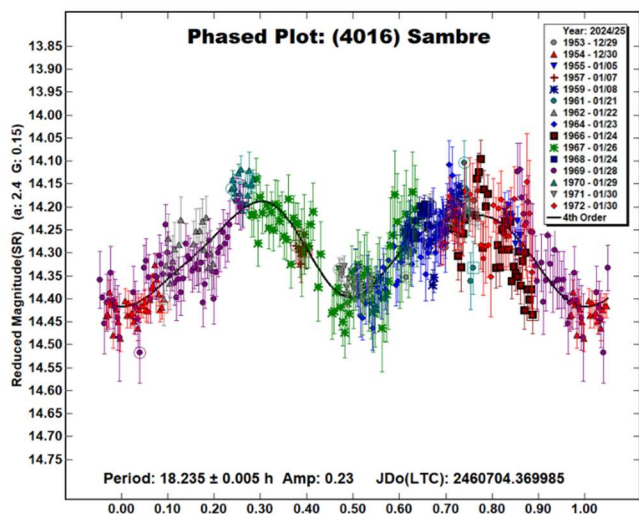
1591 Baize. Baize is a Phocaea family member that has an orbit near the inner main-belt. This 14.41 ± 0.24 km asteroid, based on $H = 11.35$ (JPL, 2025), was discovered in 1951 May 31 by S. Arend at Uccle. Having its best apparition in 2025 over the period from 2020 to 2035, this presented a good opportunity for observation. Baize was observed over six nights from 2025 June 12 to June 18 from Flarestar Observatory. The 347 data point light curve yielded a period of 7.7956 ± 0.0007 h with an amplitude of 0.35 ± 0.02 mag. Our results are consistent with Mas et al. (2018) with period at 7.794 ± 0.001 h (U 3-), and Bentz et al. (2018) with a published period of 7.788 ± 0.002 h (U 3-), (LCDB, 2023).



3066 McFadden. Named in honor of planetary scientist Lucy McFadden, this inner-belt asteroid that was discovered in 1984 March 01 by E. Bowell at Flagstaff (AZ). It has a diameter of 13.526 ± 0.046 km based on H -value of 11.28 (JPL, 2025). 3066 McFadden was observed from 5 observatories over 26 nights between 2025 May 09 to July 03. Our data yielded the derived synodic period to be 32.8369 ± 0.0508 h with an amplitude of 0.24 ± 0.03 mag. Our result is near the periods published by Ďurech et al. (2020) at 32.7524 ± 0.0003 h and Pál et al. (2020) at $P = 32.7314 \pm 0.0005$ (U2), (LCDB, 2025).



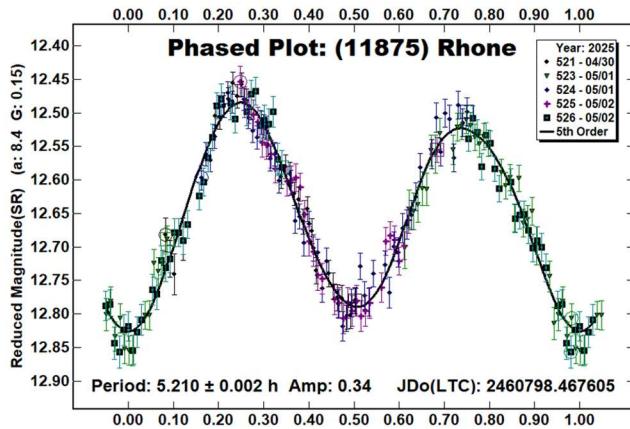
4016 Sambre. This inner main-belt asteroid was discovered on 1979 December 15 by H. Debehogne at La Silla. JPL (2025) lists its diameter as 8.312 ± 0.031 km based on $H = 14.21$. This asteroid was observed between 29 December 2024 and 30 January 2025 from four different observatories: Flarestar Observatory (Malta) over 8 nights, Luckystar Observatory (Slovakia) over 3 nights, Observatoire à la Belle Étoile (Canada) over 3 nights, and Znith Observatory (Malta) for 1 night. In total, 456 individual frames were collected across 15 observational sessions. Our Fourier analysis of these observations allowed us to determine 4016 Sambre's period as $P = 18.235 \pm 0.005$ h with an amplitude of 0.23 ± 0.06 mag. No previous reported period for this asteroid has been found in the LCDB database.



11875 Rhone. This asteroid belongs to the Meliboea asteroid family and was discovered in 1989 December 28 by E.W. Elst at Haute Provence. It has a diameter of 22.222 ± 0.264 km based on H -value of 12.15 (JPL, 2025). The asteroid Rhone has been observed from Luckystar Observatory over five nights from 2025 April 30 to May 02. Fourier analysis through *MPO Canopus* resulted in a period of 5.2100 ± 0.002 h with an amplitude of 0.34 ± 0.02 mag. No published period for this asteroid was found in the LCDB database.

Number	Name	yyyy mm/dd	Phase	L _{PAB}	B _{PAB}	Period(h)	P.E.	Amp	A.E.	Grp
1155	Aenna	2025 04/25-05/18	5.9, 17.1	207	1	7.9154	0.0005	0.25	0.02	MB-inner
1591	Baize	2025 06/12-06/18	16.5, 16.8	34	7	7.7956	0.0007	0.35	0.02	Phocaea
3066	McFadden	2025 05/09-07/03	9.2, 18.0	241	19	32.8369	0.0508	0.24	0.03	MB-inner
4016	Sambre	2024/25 12/29-01/30	2.4, 17.0	103	0	18.235	0.005	0.23	0.06	MB-inner
11875	Rhone	2025 04/30-05/02	8.4, 8.9	210	16	5.210	0.002	0.34	0.02	Meliboea

Table II. Observing circumstances and results. The phase angle is given for the first and last date. L_{PAB} and B_{PAB} are the approximate phase angle bisector longitude and latitude at mid-date range (see Harris et al., 1984). Grp is the asteroid family/group (Warner et al., 2009).



Acknowledgements

We would like to thank Brian Warner for his work in the development of *MPO Canopus* and for his efforts in maintaining the CALL website (Warner, 2016; 2017). This research has made use of the JPL's Small-Body Database (JPL, 2025).

References

- Behrend, R. (2015web). Observatoire de Genève web site. http://obswww.unige.ch/~behrend/page_cou.html. Last accessed 25 July 2025.
- Bentz, M.C.; Abbot, C.; Agudelo, S.; Dassing, S.; Flynn, W.; Gibbs, A.; Gonzalez, L.; Kim, B.; Paredes, L.; Toben, C.; Vrijmoet, H.; Yep, A. (2018). "Filtered Photometric Monitoring of 1591 Baize." *Minor Planet Bulletin* **45**(4), 311-312.
- Berg, S. (2023). *Nighttime Imaging 'N' Astronomy (NINA)* website. <https://nighttime-imaging.eu/>. Last accessed 6 July 2025.
- Durech, J.; Tonry, J.; Erasmus, N.; Denneau, L.; Heinze, A.N.; Flewelling, H.; Vančo, R. (2020). "Asteroid models reconstructed from ATLAS photometry." *Astronomy & Astrophysics* **643**, A59.
- Harris, A.W.; Young, J.W.; Scaltriti, F.; Zappala, V. (1984). "Lightcurves and phase relations of the asteroids 82 Alkmene and 444 Gyptis." *Icarus* **57**, 251-258.
- JPL (2025). Small-Body Database Browser - JPL Solar System Dynamics web site. <http://ssd.jpl.nasa.gov/sbdb.cgi>. Last accessed: 29 July 2025.
- Mas, V.; Fornas, G.; Lozano, J.; Rodrigo, O.; Fornas, A.; Carreño, A.; Arce, E.; Brines, P.; Herrero, D. (2018). "Twenty-one Asteroid Lightcurves at Asteroids Observers (OBAS)-MPPD: Nov 2016-May 2017." *Minor Planet Bulletin* **45**(1), 76-82.
- Pál, A.; Szakáts, R.; Kiss, C.; Bódi, A.; Bognár, Z.; Kalup, C.; Kiss, L.L.; Marton, G.; Molnár, L.; Plachy, E.; Sárneczky, K.; Szabó, G.M.; Szabó, R. (2020). "Solar System Objects Observed with TESS - First Data Release: Bright Main-belt and Trojan Asteroids from the Southern Survey." *Ap. J. Supl. Ser.* **247**, 26-34.
- Tonry, J.; Denneau, L.; Flewelling, H.; Heinze, A.; Onken, C.; Smartt, S.; Stalder, B.; Weiland, H.; Wolf, C. (2018). "The ATLAS All-Sky Stellar Reference Catalog." *Ap. J.* **867**, id. 105.
- Warner, B.D.; Harris, A.W.; Pravec, P. (2009). "The Asteroid Lightcurve Database." *Icarus* **202**, 134-146. Updated 2021 June. <http://www.minorplanet.info/lightcurvedatabase.html>
- Warner, B.D. (2016). Collaborative Asteroid Lightcurve Link website. <http://www.minorplanet.info/call.html>. Last accessed: 6 January 2025.
- Warner, B.D. (2017). MPO Software, *MPO Canopus* version 10.7.10.0. Bdw Publishing. <http://www.minorplanetobserver.com/>

ROTATION PERIODS AND LIGHTCURVE AMPLITUDES FOR ELEVEN MAIN-BELT AND ONE MARS-CROSSING ASTEROID

Milagros Colazo

Astronomical Observatory Institute, Faculty of Physics,
Adam Mickiewicz University,
ul. Słoneczna 36, 60-286 Poznań, POLAND
Grupo de Observadores de Rotaciones de Asteroides (GORA)
ARGENTINA
<https://aoacm.com.ar/gora/index.php>
milirita.colazovinovo@gmail.com

Giuliat Navas

Observatorio Astronómico Nacional Llano del Hato (OAN) -
Centro de Investigaciones de Astronomía Francisco J. Duarte
(CIDA) - Apartaderos (Mérida - VENEZUELA)

Víctor Amelotti

Observatorio Astronómico Naos (GORA NAO) -
Observatorio Astronómico Naos 2 (GORA NA2) -
Observatorio Astronómico Naos 3 (GORA NA3) -
Alta Gracia (Córdoba - ARGENTINA)

Gerard Tàrtalo

Dark Energy Observatory (DEO) -
Dark Energy Observatory 2 (DE2) -
Àger (Lleida - ESPAÑA)

Raúl Melia

Observatorio de Raúl Melia Carlos Paz (GORA RMC) -
Carlos Paz (Córdoba - ARGENTINA)

Damián Scotta

Observatorio de Damián Scotta 1 (GORA ODS) -
Observatorio de Damián Scotta 2 (GORA OD2) -
San Carlos Centro (Santa Fe - ARGENTINA)

Denis Martínez

Observatorio Las Grutas (GORA OLG) -
Las Grutas (Río Negro - ARGENTINA)

Marcos Anzola

Observatorio Astronómico Vuelta por el Universo (GORA OMA)
Córdoba (Córdoba - ARGENTINA)

Bruno Monteleone

Osservatorio Astronomico "La Macchina del Tempo" (MPC M24)
Ardore Marina (Reggio Calabria - ITALIA)

Francisco Santos

Observatorio Astronómico Giordano Bruno (MPC G05) -
Piconcillo (Córdoba - ESPAÑA)

Carlos Colazo

Observatorio Astronómico El Gato Gris (MPC I19) -
Tanti (Córdoba - ARGENTINA)

(Received: 2025 August 3)

Synodic rotation periods and amplitudes are reported for:
845 Naema, 981 Martina, 1365 Henyey, 2232 Altaj,
2675 Tolkien, 2905 Plaskett, 3066 McFadden,
3507 Vilas, 4838 Billmclaughlin, 5778 Jurafrance,
6914 Becquerel, and 7747 Michalowski.

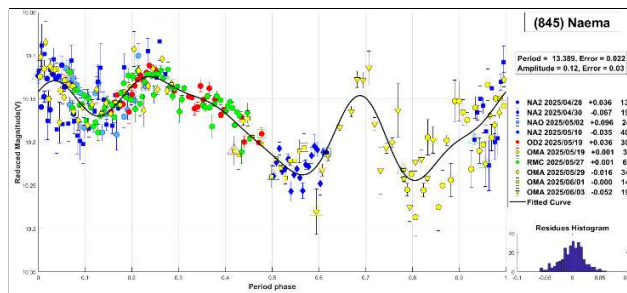
The periods and amplitudes of asteroid lightcurves presented in this paper are the product of collaborative work by the GORA (Grupo de Observadores de Rotaciones de Asteroides) group. In all the studies, we have applied relative photometry assigning V magnitudes to the calibration stars.

The image acquisition was performed without filters and with exposure times of a few minutes. All images used were corrected using dark frames and, in some cases, bias and flat-field corrections were also used. Photometry measurements were performed using *FotoDif* software and for the analysis, we employed *Períodos* software (Mazzone, 2012).

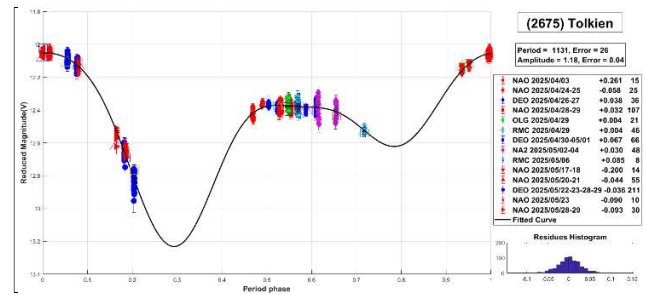
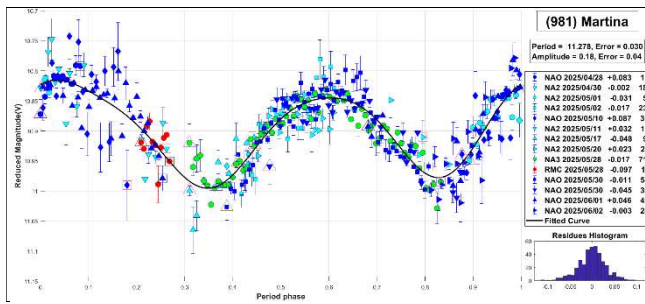
Below, we present the results for each asteroid studied. The lightcurve figures contain the following information: the estimated period and period error and the estimated amplitude and amplitude error. In the reference boxes, the columns represent, respectively, the marker, observatory MPC code, or - failing that - the GORA internal code, session date, session offset, and several data points.

Targets were selected based on the following criteria: 1) those asteroids with magnitudes accessible to the equipment of all participants, 2) those with favorable observation conditions from Argentina, Venezuela, Spain, Italy, or Croatia, i.e. with negative or positive declinations δ , and 3) objects with few periods reported in the literature and/or with Lightcurve Database (LCDB) (Warner et al., 2009) quality codes (U) of less than 3.

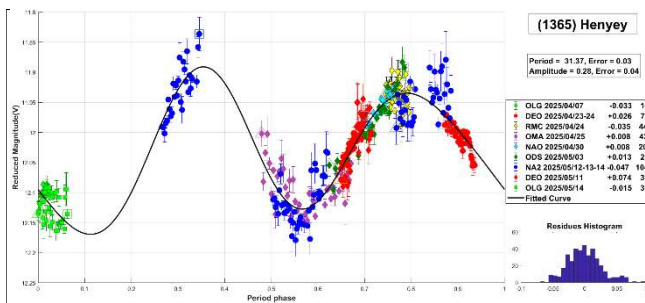
(845) Naema. This main-belt asteroid was discovered in 1916 by M. Wolf. Classified as a C-type asteroid according to the SMASSII taxonomy (Xu et al., 1995; Bus and Binzel, 2002), it is the parent body of the Naema family (Nesvorný et al., 2015). Its estimated diameter is 52.677 km. A previously reported rotational period for this asteroid is $P = 20.892$ h (Bembrick et al., 2008). In this work, we propose a shorter period of $P = 13.389 \pm 0.022$ h, with an amplitude of $\Delta m = 0.12 \pm 0.03$ mag.



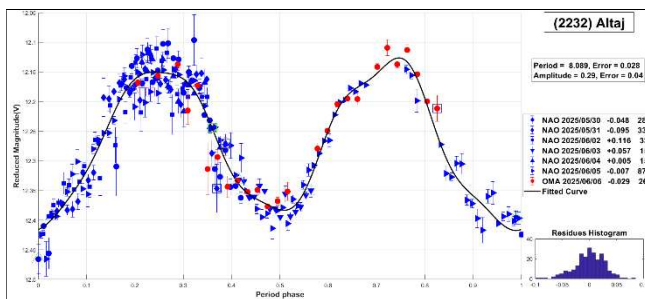
981 Martina. It is a main-belt asteroid discovered in 1917 by S. Belyavskij. It is a member of the Themis family (Nesvorný et al., 2015), with a diameter of 11.267 km. It is a C-type asteroid in the SMASSII spectral type scheme (Xu et al., 1995; Bus and Binzel, 2002). The reported rotational period for this asteroid is 11.267 h (Erasmus et al., 2020). We measured a period of $P = 11.278 \pm 0.030$ h, with $\Delta m = 0.18 \pm 0.04$ mag.



1365 Henyey. Henyey is a main-belt asteroid discovered in 1928 by M. Wolf. It is a member of the Flora family (Nesvorný et al., 2015), with a diameter of 10.958 km. A previously reported rotational period for this asteroid is $P = 18.986$ h (Klingensmith III et al., 2013). In this work, we propose a longer period of $P = 31.37 \pm 0.03$ h, with an amplitude of $\Delta m = 0.28 \pm 0.04$ mag.

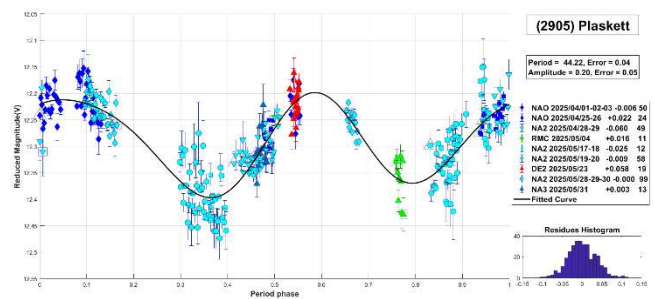


2232 Altaj. Altaj is a main-belt Asteroid with a diameter of 11.78 km, discovered in 1969 by B.A. Burnasheva. The reported rotational period for this asteroid is 8.089 h (Marchini et al., 2022). We also measured a period of $P = 8.089 \pm 0.028$ h, with $\Delta m = 0.29 \pm 0.04$ mag.

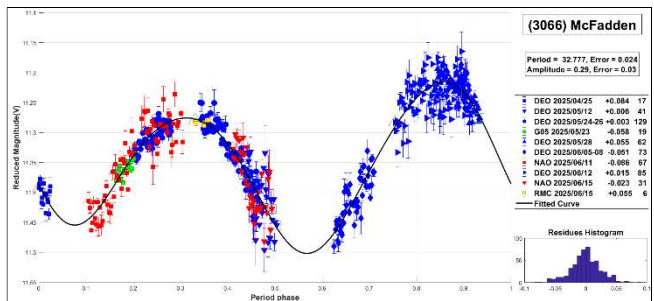


2675 Tolkien. Tolkien is a main-belt asteroid discovered in 1989 by M. Watt. It is classified as a S-type asteroid according to the SMASII spectral type scheme (Xu et al., 1995; Bus and Binzel, 2002), with a diameter of 10.960 km. The reported rotational period for this asteroid is $P = 1060$ h (Durkee et al., 2011). In this work, we propose an even longer period of $P = 1131 \pm 26$ h with $\Delta m = 1.18 \pm 0.04$ mag.

2905 Plaskett. This main-belt asteroid was discovered in 1982 by E. Bowell. Based on the SMASII taxonomy (Xu et al., 1995; Bus and Binzel, 2002), it is classified as an S-type and belongs to the Gefion family (Nesvorný et al., 2015). The asteroid has an estimated diameter of 10.224 km. For this asteroid, we could not find published periods in the literature. In this work, we propose a period of $P = 44.22 \pm 0.04$ h with $\Delta m = 0.20 \pm 0.05$ mag.



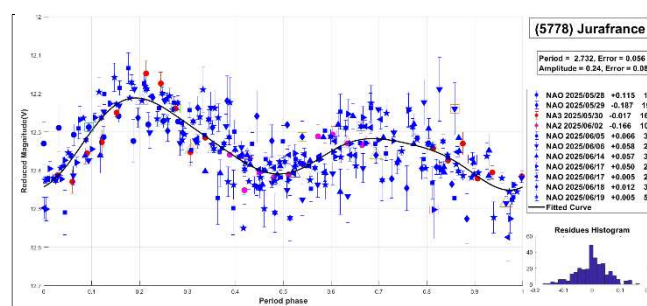
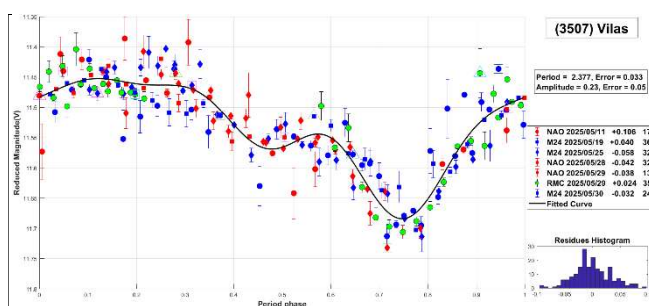
3066 McFadden. Asteroid 3066 McFadden is a main-belt asteroid with a diameter of 13.526 km, discovered in 1984 by E. Bowell. The more recent period published in the literature corresponds to $P = 32.7314$ h (Pál et al., 2020). Our period $P = 32.777 \pm 0.024$ h agrees with the one measured by Pál and collaborators.



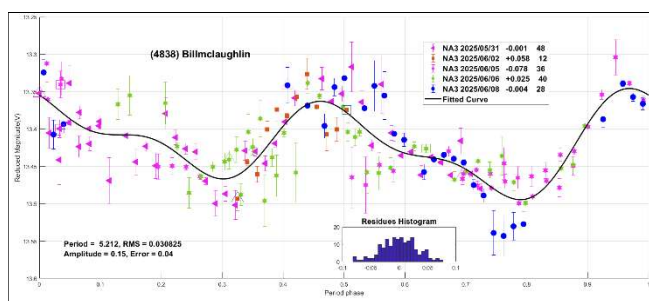
3507 Vilas. Main-belt Asteroid Vilas was discovered in 1982 by E. Bowell, with a diameter of 24.917 km. Classified as a Ch-type asteroid according to the SMAS II taxonomy (Xu et al., 1995; Bus and Binzel, 2002), it is a member of the Themis family (Nesvorný et al., 2015). The reported rotational period for this asteroid is $P = 3.959$ h (Wisniewski et al., 1997). Our observations also support the short-period hypothesis, yielding a value of $P = 2.377 \pm 0.033$ h with $\Delta m = 0.26 \pm 0.05$ mag.

Number	Name	yy/mm/dd-yy/mm/dd	Phase	L_{PAB}	B_{PAB}	Period(h)	P.E.	Amp	A.E.	Grp
845	Naema	25/04/28-25/06/04	*04.5, 09.8	229	-2	13.389	0.022	0.12	0.03	Naem
981	Martina	25/04/28-25/06/03	*07.7, 05.3	239	-1	11.278	0.030	0.18	0.04	Them
1365	Heney	25/04/07-25/05/15	04.4, 21.1	197	-6	31.37	0.03	0.28	0.04	Matt
2232	Altaj	25/05/30-25/06/06	*02.8, 01.9	253	3	8.089	0.028	0.29	0.04	MB-M
2675	Tolkien	25/04/03-25/05/29	*10.4, 16.2	213	-2	1131	26	1.18	0.04	MB-I
2905	Plaskett	25/04/01-25/05/31	*10.8, 15.4	215	-5	44.22	0.04	0.20	0.05	MB-O
3066	McFadden	25/04/25-25/06/15	*12.9, 13.1	241	18	32.777	0.024	0.29	0.03	MB-I
3507	Vilas	25/05/11-25/05/30	08.6, 00.9	249	2	2.377	0.033	0.23	0.05	Them
4838	Billmclaughlin	25/05/31-25/06/08	13.8, 10.4	269	9	5.215	0.029	0.16	0.04	MB-I
5778	Jurafrance	25/05/28-25/06/20	*05.2, 09.1	252	-8	2.732	0.056	0.24	0.08	Maria
6914	Becquerel	25/03/23-25/05/14	*11.3, 17.4	203	-2	16.469	0.035	0.37	0.05	MB-I
7747	Michalowski	25/06/09-25/06/21	11.7, 04.6	274	-2	4.496	0.063	0.50	0.09	M-cros

Table I. Observing circumstances and results. The phase angle is given for the first and last date. If preceded by an asterisk, the phase angle reached an extremum during the period. L_{PAB} and B_{PAB} are the approximate phase angle bisector longitude/latitude at mid-date range (see Harris et al., 1984). Grp is the asteroid family/group (Warner et al., 2009). Naem: 845 Naema; Them: 24 Themis; Matt: 883 Matteredania; MB-M: main-belt middle; MB-I: main-belt inner; MB-O: main-belt outer; Maria: 170 Maria; M-cros: Mars-crosser.

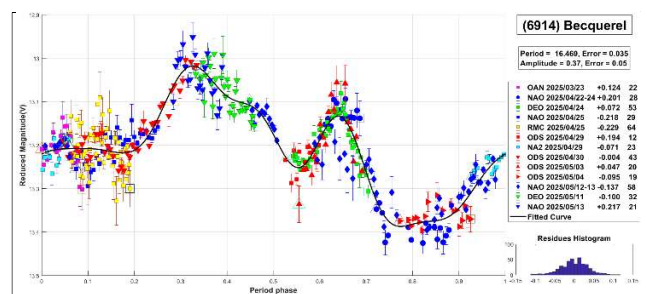


4838 Billmclaughlin. This main-belt asteroid was discovered in 1989 by E.F. Helin and has an estimated diameter of 10.251 km. It is classified as an Xc-type asteroid based on the SMASS II taxonomy (Xu et al., 1995; Bus and Binzel, 2002). A rotational period of $P = 5.199$ h was previously reported for this asteroid (Albers et al., 2010). Our results are consistent with a short rotation period, giving a value of $P = 5.212 \pm 0.031$ h and an amplitude of $\Delta m = 0.15 \pm 0.04$ mag.

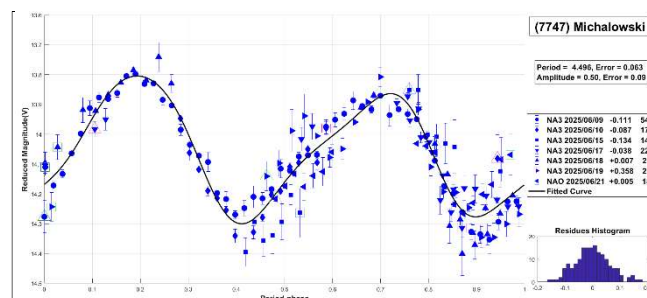


5778 Jurafrance. Main-belt asteroid 5778 was discovered in 1984 by E.W. Elst. It belongs to the Maria family (Nesvorný et al., 2015) and has an estimated diameter of 10.206 km. A previously reported rotational period for this asteroid is 4.14 h (Aznar, 2013web). Our measurements indicate a slightly shorter period of $P = 2.732 \pm 0.056$ h, with a lightcurve amplitude of $\Delta m = 0.24 \pm 0.08$ mag.

6914 Becquerel. Asteroid 6914 orbits in the main belt and was discovered in 1992 by C.S. Shoemaker. For this asteroid, we could not find any published rotational periods in the literature. In this work, we propose a period of $P = 16.469 \pm 0.035$ h with $\Delta m = 0.37 \pm 0.05$ mag.



7747 Michalowski. This Mars-crossing asteroid was discovered in 1987 by E. Bowell, with an estimated diameter of 4.596 km. A previously reported rotational period for this asteroid is $P = 4.5$ h (Waszczak et al., 2015). Our observations also support the short-period interpretation, yielding a value of $P = 4.496 \pm 0.063$ h with a lightcurve amplitude of $\Delta m = 0.50 \pm 0.09$ mag.



Observatory	Telescope	Camera
G05 Obs.Astr.Giordano Bruno	SCT (D=203mm; f=6.3)	CCD Atik 420 m
M24 Oss.Astr.LaMacchina del Tempo	RCT (D250mm; f=8.0)	CMOS ZWO ASI 1600MM
DE0 Dark Energy Observatory	Refractor (D=115mm; f=7.0)	CMOS QHY 294M pro
DE2 Dark Energy Observatory 2	RCT (D=200mm; f=5.4)	CMOS Player One Ares-M
NAO Obs.Astr.Naos	Newtonian (D=250mm; f=4.0)	CMOS ZWO 183
NA2 Obs.Astr.Naos 2	Newtonian (D=200mm; f=5.0)	CMOS ZWO ASI 174
NA3 Obs.Astr.Naos 3	SCT (D=279; f=10)	CMOS QHY 163M
OAN Obs.Astr.Nacional Llano del Hato	Cámara Schmidt (D=1000mm; f=3.0)	CMOS Fujifilm GFX 50R
ODS Obs.Astr.de Damián Scotta 1	Newtonian (D=300mm; f=4.0)	CMOS QHY 174M
OD2 Obs.Astr.de Damián Scotta 2	Newtonian (D=250mm; f=4.0)	CCD SBIG STF-8300M
OLG Observatorio Las Grutas	Newtonian (D=200mm; f=5.0)	CCD ATIK 414EX MONO
OMA Obs.Astr.Vueltaporel Universo	Newtonian (D=150mm; f=5.0)	CMOS POA Neptune-M
RMC Obs.Astr.de Raúl Melia Carlos Paz	Newtonian (D=254mm; f=4.7)	CMOS QHY 174M

Table II. List of observatories and equipment.

Acknowledgements

We want to thank Julio Castellano as we used his *FotoDif* program for preliminary analyses, Fernando Mazzone for his *Períodos* program, which was used in final analyses, and Matías Martini for his *CalculadorMDE_v0.2* used for generating ephemerides used in the planning stage of the observations. We also used Seqplot (<https://www.aavso.org/seqplot>), which proved very effective for checking the magnitudes of the calibration stars. This research has made use of the Small Bodies Data Ferret (<https://sbnapps.psi.edu/ferret/>), supported by the NASA Planetary System. This research has made use of data and/or services provided by the International Astronomical Union's Minor Planet Center.

References

- Albers, K.; Kragh, K.; Monnier, A.; Pligge, Z.; Stolze, K.; West, J.; Yim, A.; Ditteon, R. (2010). "Asteroid Lightcurve Analysis at the Oakley Southern Sky Observatory: 2009 October thru 2010 April." *The Minor Planet Bulletin* **37**(4), 152-158.
- Aznar, A. (2013web). <https://minplanobs.org/mpinfo/php/call.php>
- Bembrick, C.; Allen, B.; Bolt, G. (2008). "The Rotation Periods of 845 Naema, 1607 Mavis, and (30105) 2000 FO3." *Minor Planet Bulletin* **35**(2), 74-75.
- Bus, S.J.; Binzel, R.P. (2002). "Phase II of the small main-belt asteroid spectroscopic survey: A feature-based taxonomy." *Icarus* **158**(1), 146-177.
- Durkee, R.I.; Brinsfield, J.W.; Hornoch, K.; Kuönlirak, P. (2011). "The Long Period of 2675 Tolkien." *Minor Planet Bulletin* **38**(4), 182-183.
- Erasmus, N.; Navarro-Meza, S.; McNeill, A.; Trilling, D.E.; Sickafoose, A.A.; Denneau, L.; Flewelling, H.; Heinze, A.; Tonry, J.L. (2020). "Investigating taxonomic diversity within asteroid families through ATLAS dual-band photometry." *The Astrophysical Journal Supplement Series* **247**(1), 13.
- Harris, A.W.; Young, J.W.; Scaltriti, F.; Zappala, V. (1984). "Lightcurves and phase relations of the asteroids 82 Alkmene and 444 Gyptis." *Icarus* **57**, 251-258.
- Klinglesmith III, D.A.; Hanowell, J.; Risley, E.; Turk, J.; Vargas, A.; Warren, C.A. (2013). "Asteroid Synodic Periods from Etscorn Campus Observatory." *Minor Planet Bulletin* **40**(2), 65-67.
- Marchini, A.; Cavaglioni, L.; Privitera, C.A.; Papini, R.; Salvaggio, F. (2022). "Rotation Period Determination for Asteroids 2232 Altaj, 3699 Milbourn 4101 Ruikou,(6787) 1991 PF15 and 8416 Okada." *Minor Planet Bulletin* **49**(1), 10-13.
- Mazzone, F.D. (2012). *Períodos* Software. version 1.0. <http://www.astrosurf.com/salvador/Programas.html>
- Nesvorný, D.; Brož, M.; Carruba, V. (2015). "Identification and Dynamical Properties of Asteroid Families." In *Asteroids IV* (P. Michel, F. DeMeo, W.F. Bottke, R. Binzel, Eds.). Univ. of Arizona Press, Tucson, also available on astro-ph.
- Pál, A.; Szakáts, R.; Kiss, C.; Bódi, A.; Bognár, Z.; Kalup, C.; Kiss, L.L.; Marton, G.; Molnár, L.; Plachy, E.; Sárneczky, K.; Szabó, G.; Szabó, R. (2020). "Solar System Objects Observed with TESS - First Data Release: Bright Main-belt and Trojan Asteroids from the Southern Survey." *Ap. J. Supl. Ser.* **247**, 26.
- Warner, B.D.; Harris, A.W.; Pravec, P. (2009). "The Asteroid Lightcurve Database." *Icarus* **202**, 134-146. <https://minplanobs.org/mpinfo/php/lcdb.php>
- Waszczak, A.; Chang, C.-K.; Ofek, E.O.; Laher, R.; Masci, F.; Levitan, D.; Surace, J.; Cheng, Y.-C.; Ip, W.-H.; Kinoshita, D.; Helou, G.; Prince, T.A.; Kulkarni, S. (2015). "Asteroid Light Curves from the Palomar Transient Factory Survey: Rotation Periods and Phase Functions from Sparse Photometry." *Astron. J.* **150**, A75.
- Wisniewski, W.Z.; Michałowski, T.M.; Harris, A.W.; McMillan, R.S. (1997). "Photometric observations of 125 asteroids." *Icarus* **126**(2), 395-449.
- Xu, S.; Binzel, R.P.; Burbine, T.H.; Bus, S.J. (1995). "Small main-belt asteroid spectroscopic survey: Initial results." *Icarus* **115**(1), 1-35.

ASTEROID PHOTOMETRY: RESULTS FOR 15 MAIN-BELT ASTEROIDS AND AN APOLLO NEA

Milagros Colazo

Astronomical Observatory Institute, Faculty of Physics,
Adam Mickiewicz University,
ul. Słoneczna 36, 60-286 Poznań, POLAND
Grupo de Observadores de Rotaciones de Asteroides (GORA)
ARGENTINA

<https://aoacm.com.ar/gora/index.php>
milirita.colazovinovo@gmail.com

Gerard Tàrtalo

Dark Energy Observatory (DEO) -
Dark Energy Observatory 2 (DE2) -
Àger (Lleida - ESPAÑA)

Victor Amelotti

Observatorio Astronómico Naos (GORA NAO) -
Observatorio Astronómico Naos 2 (GORA NA2) -
Observatorio Astronómico Naos 3 (GORA NA3) -
Alta Gracia (Córdoba - ARGENTINA)

Marcos Anzola

Observatorio Astronómico Vuelta por el Universo (GORA OMA)
Observatorio Astronómico Vuelta por el Universo 2 (GORA OM2)
Córdoba (Córdoba - ARGENTINA)
Estación Astrofísica Bosque Alegre (MPC 821) -
Departamento Punilla (Córdoba - ARGENTINA)

Raúl Melia

Observatorio de Raúl Melia Carlos Paz (GORA RMC) -
Carlos Paz (Córdoba - ARGENTINA)
Estación Astrofísica Bosque Alegre (MPC 821) -
Departamento Punilla (Córdoba - ARGENTINA)

Giuliat Navas

Observatorio Astronómico Nacional Llano del Hato (OAN) -
Observatorio Astronómico Nacional Llano del Hato (MPC 303) -
Centro de Investigaciones de Astronomía Francisco J. Duarte
(CIDA) - Apartaderos (Mérida - VENEZUELA)

Alejandro Moreschi

Observatorio Chopis (GORA OM3) -
Mercedes - (Buenos Aires - ARGENTINA)

Martín Leiva

Estación Astrofísica Bosque Alegre (MPC 821) -
Departamento Punilla (Córdoba - ARGENTINA)

Paolo Aldinucci

Osservatorio Astronomico Piero Angela (MPC D42) -
Scandicci (Firenze - ITALIA)

Zlatko Orbanic

Osservatorio Explorer (MPC M19) -
Pula (Istria - CROACIA)

José Álvarez

Observatorio Astronómico Corgas (MPC Z65) -
Corgas-Taboadela-Ourense (Galicia - ESPAÑA)

Carlos Colazo

Observatorio Astronómico El Gato Gris (MPC I19) -
Tanti (Córdoba - ARGENTINA)
Estación Astrofísica Bosque Alegre (MPC 821) -
Departamento Punilla (Córdoba - ARGENTINA)

(Received: 2025 October 5)

Synodic rotation periods and amplitudes are reported for:
703 Noemi, 1326 Losaka, 1714 Sy, 1858 Lobachevskij,
1892 Lucienne, 1908 Pobeda, 2359 Debehogne,
2552 Remek, 2949 Kaverznev, 3702 Trubetskaya,
4001 Ptolemaeus, 5676 Voltaire, 6422 Akagi,
6441 Milenajesenska, 6932 Tanigawadake, and (138205)
2000 EZ148.

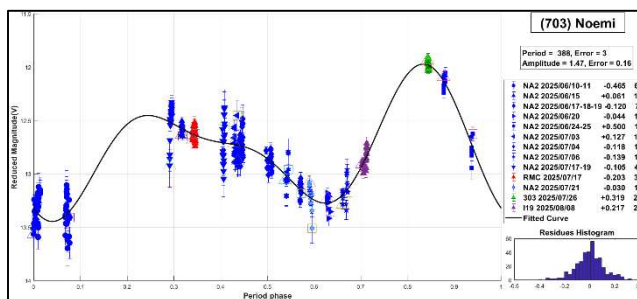
The periods and amplitudes of asteroid lightcurves presented in this paper are the product of collaborative work by the GORA (Grupo de Observadores de Rotaciones de Asteroides) group. In all the studies, we have applied relative photometry assigning V magnitudes to the calibration stars.

The image acquisition was performed without filters and with exposure times of a few minutes. All images used were corrected using dark frames and, in some cases, bias and flat-field corrections were also used. Photometry measurements were performed using *FotoDif* software and for the analysis, we employed *Periodos* software (Mazzone, 2012).

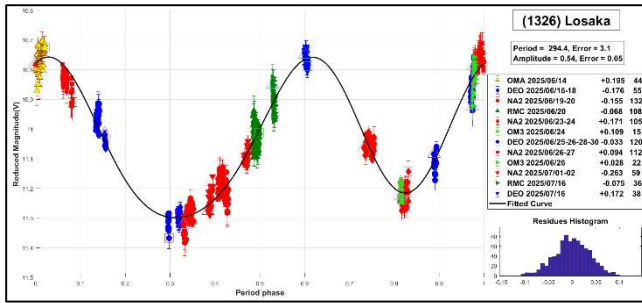
Below, we present the results for each asteroid studied. The lightcurve figures contain the following information: the estimated period and period error and the estimated amplitude and amplitude error. In the reference boxes, the columns represent, respectively, the marker, observatory MPC code, or - failing that - the GORA internal code, session date, session offset, and several data points.

Targets were selected based on the following criteria: 1) those asteroids with magnitudes accessible to the equipment of all participants, 2) those with favorable observation conditions from Argentina, Venezuela, Spain, Italy, or Croatia, i.e. with negative or positive declinations δ , and 3) objects with few periods reported in the literature and/or with Lightcurve Database (LCDB) (Warner et al., 2009) quality codes (U) of less than 3.

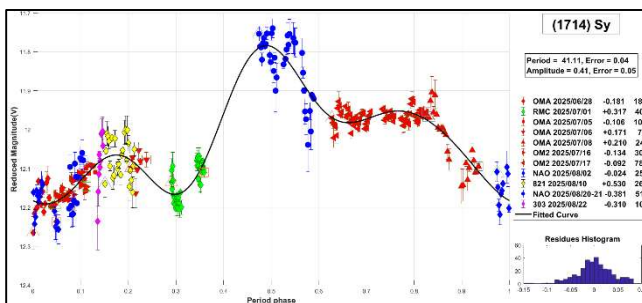
703 Noemi. Noemi is a main-belt asteroid discovered in 1910 by J. Palisa. It is a member of the Flora family (Nesvorný et al., 2015), with a diameter of 7.25 km. A previously reported rotational period for this asteroid is $P = 200$ h (Noschese et al., 2017). In this work, we propose a longer period of $P = 388 \pm 3$ h, with an amplitude of $\Delta m = 1.47 \pm 0.16$ mag.



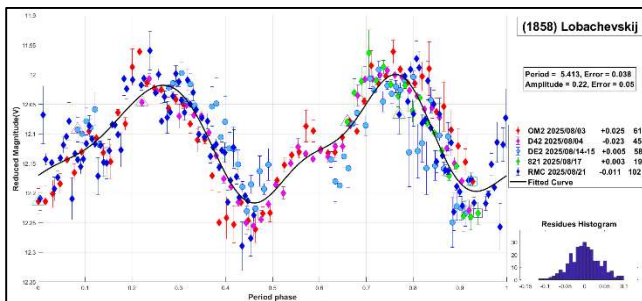
1326 Losaka. This main-belt asteroid was discovered in 1934 by C. Jackson. It is classified as a C-type asteroid according to the SDSS taxonomy (Hasselmann et al., 2012). The reported rotational period for this asteroid is 6.9 h (Warner, 2006). In this work, we propose a long period of $P = 294.4 \pm 3.1$ h with $\Delta m = 0.54 \pm 0.05$ mag.



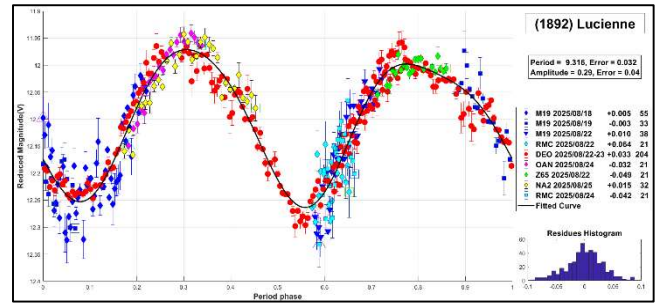
1714 Sy. This main-belt asteroid was discovered in 1951 by L. Boyer. It is classified as a L-type asteroid according to the SDSS-based Asteroid Taxonomy (Hasselmann et al., 2012), with a diameter of 13.998 km. For this asteroid, we could not find any published rotational periods in the literature. In this work, we propose a period of $P = 41.11 \pm 0.41$ h with $\Delta m = 0.41 \pm 0.05$ mag.



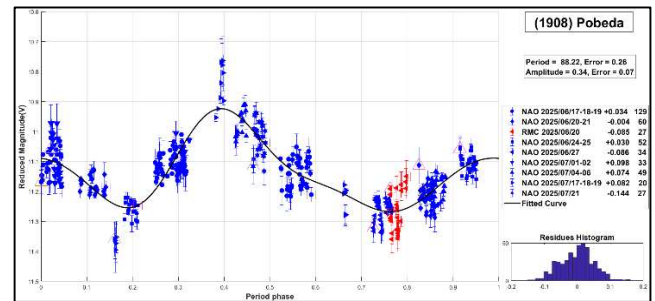
1858 Lobachevskij. This main-belt asteroid was discovered in 1927 by L. Zhuravleva. Based on the SMASSII taxonomy (Xu et al., 1995; Bus and Binzel, 2002), it is classified as an L-type, with a diameter of 10.769 km. The reported rotational period for this asteroid is $P = 5.413$ h (Durech et al., 2016). Our measurement of the period, $P = 5.413 \pm 0.038$ h, with $\Delta m = 0.22 \pm 0.05$, agrees well with the value reported by the authors.



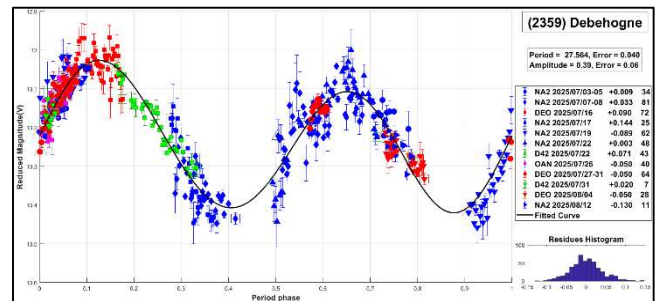
1892 Lucienne. This main-belt asteroid was discovered in 1971 by P. Wild. It is the parent body of the Lucienne family (Nesvorný et al., 2015). The diameter is 9.725 km. Martikainen et al. (2021) measured a rotational period of 9.31 h. Our measurement of the period, $P = 9.316 \pm 0.032$ h, with $\Delta m = 0.29 \pm 0.04$, agrees well with the value reported by the authors.



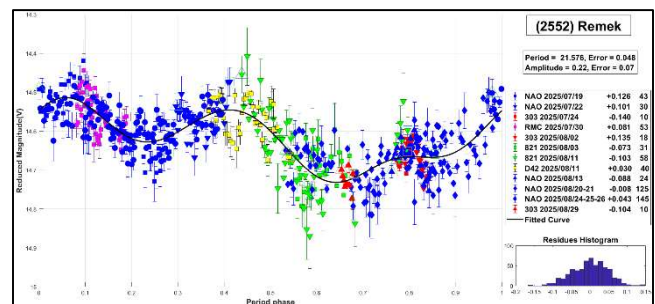
1908 Pobeda. This main-belt asteroid was discovered in 1972 by N. Chernykh, with a diameter of 18.384 km. The reported rotational period for this asteroid is $P = 149.95$ h (Durech et al., 2020). In this work, we propose a considerably shorter period of $P = 88.22 \pm 0.26$ h with $\Delta m = 0.34 \pm 0.07$ mag.



2359 Debehogne. This main-belt asteroid was discovered in 1931 by K. Reinmuth. For this asteroid, we could not find published periods in the literature either. In this work, we propose a period of $P = 27.564 \pm 0.040$ h with $\Delta m = 0.39 \pm 0.06$ mag.



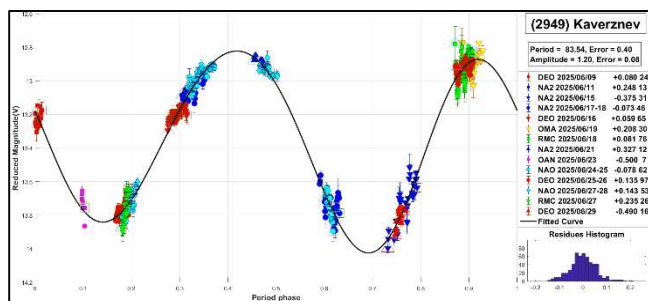
2552 Remek. This main-belt asteroid was discovered in 1978 by A. Mrkos. No published rotational periods for this asteroid were found in the literature. In this work, we propose a period of $P = 21.576 \pm 0.048$ h with $\Delta m = 0.22 \pm 0.07$ mag.



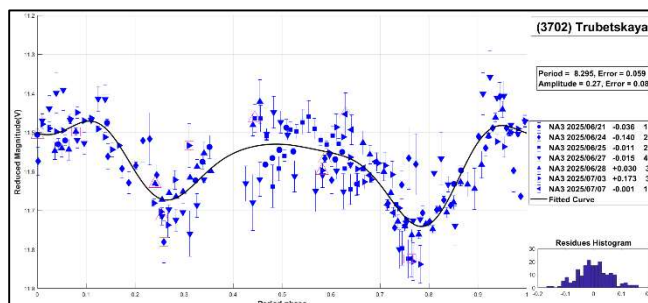
Number	Name	yy/ mm/dd- yy/ mm/dd	Phase	L_{PAB}	B_{PAB}	Period(h)	P.E.	Amp	A.E.	Grp
703	Noemi	25/06/10-25/08/09	*10.5, 19.6	278	3	288	3	1.47	0.16	Flora
1326	Losaka	25/06/14-25/07/16	3.4, 13.7	260	6	294.4	3.1	0.54	0.05	MB-M
1714	Sy	25/06/28-25/08/22	*5.0, 20.5	285	-2	41.11	0.04	0.41	0.05	MB-I
1858	Lobachevskij	25/08/03-25/08/21	*2.5, 06.1	315	2	5.413	0.038	0.22	0.05	MB-O
1892	Lucienne	25/08/18-25/08/25	10.9, 08.2	344	8	9.316	0.032	0.29	0.04	Lucie
1908	Pobeda	25/06/17-25/07/22	*5.9, 09.2	278	-6	88.2	0.26	0.34	0.07	MB-O
2359	Debehogne	25/07/03-25/08/12	*10.9, 11.6	299	6	27.564	0.040	0.39	0.06	MB-I
2552	Remek	25/07/19-25/08/29	*6.8, 19.2	307	-1	21.576	0.048	0.22	0.07	MB-I
2949	Kaverznev	25/06/09-25/06/29	*8.8, 07.4	269	7	83.54	0.40	1.20	0.08	MB-I
3702	Trubetskaya	25/06/21-25/07/07	*6.8, 03.8	281	7	8.295	0.059	0.27	0.08	MB-M
4001	Ptolemaeus	25/07/08-25/07/19	12.5, 06.3	305	2	5.024	0.052	0.45	0.07	Dup
5676	Voltaire	25/07/19-25/08/28	*12.4, 18.4	306	19	8.202	0.034	0.16	0.05	MB-I
6422	Akagi	25/07/08-25/07/18	9.4, 04.3	302	3	7.748	0.041	0.90	0.06	Euno
6441	Milenajesenska	25/07/03-25/07/07	9.3, 07.0	294	3	2.820	0.038	0.40	0.05	Her
6932	Tanigawadake	25/08/22-25/08/22	2.7, 05.3	329	-4	3.794	0.031	0.41	0.04	MB-I
138205	2000 EZ148	25/06/08-25/06/25	46.0, 67.0	263	-39	4.980	0.037	0.26	0.05	NEA

Table I. Observing circumstances and results. The phase angle is given for the first and last date. If preceded by an asterisk, the phase angle reached an extremum during the period. L_{PAB} and B_{PAB} are the approximate phase angle bisector longitude/latitude at mid-date range (see Harris et al., 1984). Grp is the asteroid family/group (Warner et al., 2009). Flora: 8 Flora; MB-M: main-belt middle, MB-I: main-belt inner, MB-O: main-belt outer, Lucie: 1892 Lucienne; Dup: 1338 Duponta; Euno: 15 Eunomia; Her: 135 Hertha; NEA: NEA.

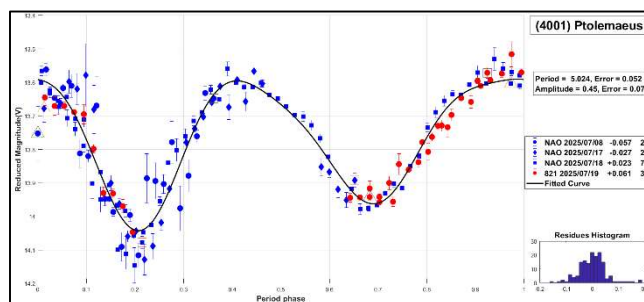
2949 Kaverznev. This main-belt asteroid with a diameter of 6.959 km was discovered in 1970 by the Crimean Astrophysical Observatory. It is classified as an S-type asteroid according to the SMASSII spectral type scheme (Xu et al., 1995; Bus and Binzel, 2002). For this asteroid, we couldn't find published periods in the literature either. Based on our observations and thorough analysis, we propose a long period of $P = 83.54 \pm 0.40$ h and $\Delta m = 1.20 \pm 0.08$ mag.



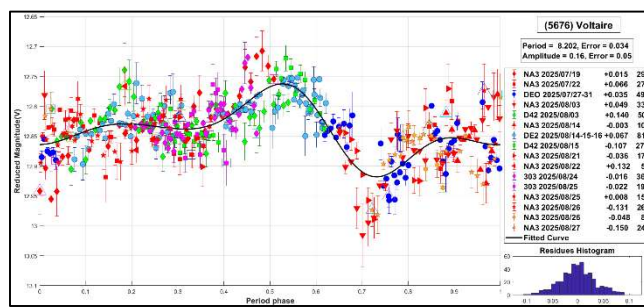
3702 Trubetskaya. This main-belt asteroid was discovered in 1970 by L. Chernykh, with a diameter of 18.158 km. It is classified as a C-type asteroid according to the SDSS taxonomy (Hasselmann et al., 2012). The reported rotational period for this asteroid is $P = 8.2905$ h (Durech et al., 2020). In this work, we measure a period of $P = 8.295 \pm 0.059$ h with $\Delta m = 0.27 \pm 0.08$.



4001 Ptolemaeus. This main-belt asteroid was discovered in 1949 by K. Reinmuth. It is listed as a member of the Flora family (Nesvorný et al., 2015), although its possible association with the Baptistina family has also been noted. Its estimated diameter is 4.641 km. It is an S-type asteroid in the SMASSII spectral type scheme (Xu et al., 1995; Bus and Binzel, 2002). Interestingly, we could not find a reported rotational period for this object in the literature. Based on our observations and thorough analysis, we propose a period of $P = 5.024 \pm 0.052$ h and $\Delta m = 0.45 \pm 0.07$ mag.



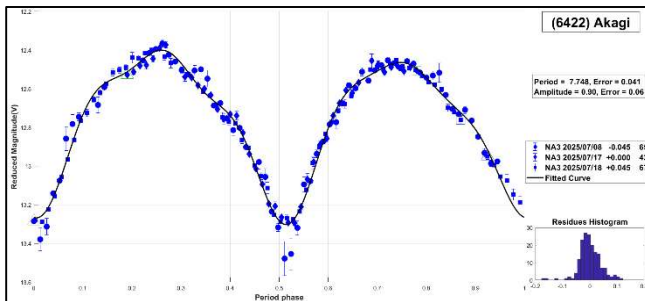
5676 Voltaire. This outer main-belt asteroid, with a diameter of 10.433 km, was discovered in 1986 by L.G. Karachkina. The reported rotational period for this asteroid is $P = 5.039$ h (Pravec et al., 2010web). Our observations suggest a longer period, yielding a value of $P = 8.202 \pm 0.034$ h with $\Delta m = 0.26 \pm 0.05$.



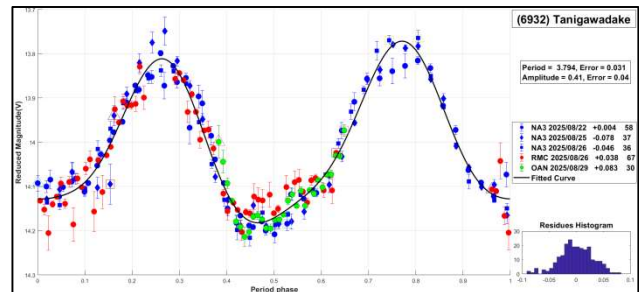
Observatory	Telescope	Camera
303 Obs.Astr.Nacional Llano del Hato	Newtonian (D=1000mm; f=5.5)	CCD FLI PL4240
821 Est.Astrof.Bosque Alegre	Newtonian (D=1540mm; f=4.9)	CCD APOGEE Alta U9
D42 Osservatorio Astronomico Piero Angela	SCT (D=300mm; f=6.2)	CMOS ToupTek 2600 KMA
M19 Osservatorio Explorer	RCT (D=304 mm; f=6.5)	CCD Moravian G2 4000
I19 Obs.Astr.El Gato Gris	SCT (D=355mm; f=10.6)	CCD SBIG STF-8300M
Z65 Obs.Astr.Corgas	Newtonian (D=310mm; f=4.8)	CMOS ZWO ASI 294 MM
DE0 Dark Energy Observatory	Refractor (D=115mm; f=7.0)	CMOS QHY 294M pro
DE2 Dark Energy Observatory 2	RCT (D=200mm; f=5.4)	CMOS Player One Ares-M
NAO Obs.Astr.Naos	Newtonian (D=250mm; f=4.0)	CMOS ZWO 183
NA2 Obs.Astr.Naos 2	Newtonian (D=200mm; f=5.0)	CMOS ZWO ASI 174
NA3 Obs.Astr.Naos 3	SCT (D=279; f=10)	CMOS QHY 163M
OAN Obs.Astr.Nacional Llano del Hato	Cámara Schmidt (D=1000mm; f=3.0)	CMOS Fujifilm GFX 50R
OMA Obs.Astr.Vuelta por el Universo	Newtonian (D=150mm; f=5.0)	CMOS POA Neptune-M
OM2 Obs.Astr.Vuelta por el Universo 2	Newtonian (D=200mm; f=5.0)	CMOS POA Neptune-M
OM3 Obs.Astr.Chopis-Mercedes	Newtonian (D=200mm; f=4.5)	CMOS ZWO ASI 294 MM-PRO
RMC Obs.Astr.de Raúl Melia Carlos Paz	Newtonian (D=254mm; f=4.7)	CMOS QHY 174M

Table II. List of observatories and equipment.

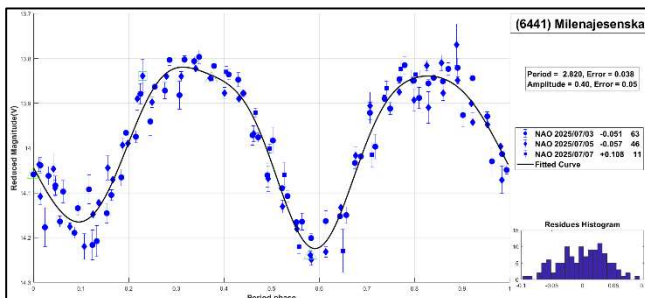
6422 Akagi. This main-belt asteroid was discovered in 1994 by T. Kobayashi. Classified as an L-type asteroid according to the SDSS taxonomy (Hasselmann et al., 2012), it is a member of the Eunomia family (Nesvorný et al., 2015). The diameter is 9.084 km. The reported rotational period for this asteroid is 7.74 h (Pál et al., 2020). Our measurement of the period, $P = 7.748 \pm 0.041$ h, with $\Delta m = 0.40 \pm 0.05$, agrees well with the value reported by the author.



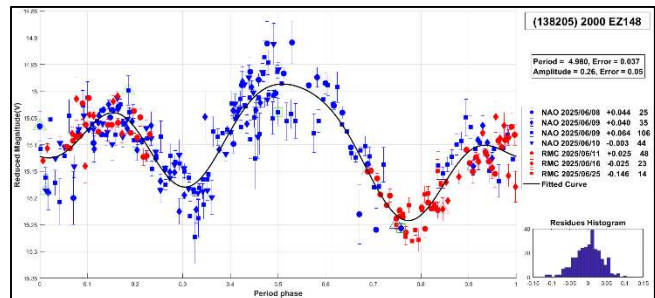
6932 Tanigawadake. This main-belt asteroid with a diameter of 5.211 km, was discovered in 1994 by T. Kobayashi. It is classified as an L-type asteroid according to the SDSS-based Asteroid Taxonomy (Hasselmann et al., 2012). The reported rotational period for this asteroid is 3.79 h (Waszczak et al., 2015). Our measurement of the period, $P = 3.794 \pm 0.031$ h, with $\Delta m = 0.41 \pm 0.04$, agrees well with the value reported by the authors.



6441 Milenajesenska. This main-belt asteroid with a diameter of 4.829 km, was discovered in 1988 by A. Mrkos. It belongs to the Nysa-Polana family (Nesvorný et al., 2015). No published rotational period has been found in the literature for this asteroid. In this work, we propose a short period of $P = 2.820 \pm 0.038$ h with $\Delta m = 0.40 \pm 0.05$ mag, consistent with its small diameter.



(138205) 2000 EZ148. This Apollo near-Earth asteroid was discovered in 2000 by the Catalina Sky Survey. It is classified as an S-type asteroid according to the SMASII spectral type scheme (Xu et al., 1995; Bus and Binzel, 2002). No published rotational periods for this asteroid were found in the literature. In this work, we propose a period of $P = 4.980 \pm 0.037$ h with $\Delta m = 0.26 \pm 0.05$ mag.



Acknowledgements

We want to thank Julio Castellano as we used his *FotoDif* program for preliminary analyses, Fernando Mazzone for his *Periodos* program, which was used in final analyses, and Matías Martini for his *CalculadorMDE_v0.2* used for generating ephemerides used in the planning stage of the observations. We also used Seqplot (<https://www.aavso.org/seqplot>), which proved very effective for checking the magnitudes of the calibration stars. This research has made use of the Small Bodies Data Ferret (<https://sbnapps.psi.edu/ferret/>), supported by the NASA Planetary System. This research has made use of data and/or services provided by the International Astronomical Union's Minor Planet Center.

References

- Bus, S.J.; Binzel, R.P. (2002). "Phase II of the small main-belt asteroid spectroscopic survey: A feature-based taxonomy." *Icarus* **158**(1), 146-177.
- Đurech, J.; Hanuš, J.; Oszkiewicz, D.; Vančo, R. (2016). "Asteroid models from the Lowell photometric database." *Astronomy & Astrophysics* **587**, A48.
- Đurech, J.; Tonry, J.; Erasmus, N.; Denneau, L.; Heinze, A.N.; Flewelling, H.; Vančo, R. (2020). "Asteroid models reconstructed from ATLAS photometry." *Astronomy & Astrophysics* **643**, A59.
- Harris, A.W.; Young, J.W.; Scaltriti, F.; Zappala, V. (1984). "Lightcurves and phase relations of the asteroids 82 Alkmene and 444 Gyptis." *Icarus* **57**, 251-258.
- Hasselmann, P.H.; Carvano, J.M.; Lazzaro, D. (2012). SDSS-based Asteroid Taxonomy V1.1. EAR-A-I0035-5-SDSSTAX-V1.1. NASA Planetary Data System.
- Martikainen, J.; Muinonen, K.; Penttilä, A.; Cellino, A.; Wang, X.B. (2021). "Asteroid absolute magnitudes and phase curve parameters from Gaia photometry." *Astronomy & Astrophysics* **649**, A98.
- Mazzone, F.D. (2012). *Periodos* Software. version 1.0. <http://www.astrosurf.com/salvador/Programas.html>
- Nesvorný, D.; Brož, M.; Carruba, V. (2015). "Identification and Dynamical Properties of Asteroid Families." In *Asteroids IV* (P. Michel, F. DeMeo, W.F. Bottke, R. Binzel, Eds.). Univ. of Arizona Press, Tucson, also available on astro-ph.
- Noschese, A.; Vecchione, A.; D'Avino, L.; Izzo, L. (2017). "Lightcurve Analysis for Minor Planet 703 Noemi." *Minor Planet Bulletin* **44**(3), 177-178.
- Pál, A.; Szakáts, R.; Kiss, C.; Bódi, A.; Bognár, Z.; Kalup, C.; Kiss, L.L.; Marton, G.; Molnár, L.; Plachy, E.; Sárneczky, K.; Szabó, G.; Szabó, R. (2020). "Solar System Objects Observed with TESS - First Data Release: Bright Main-belt and Trojan Asteroids from the Southern Survey." *Ap. J. Supl. Ser.* **247**, 26.
- Pravec, P.; Wolf, M.; Sarounova, L. (2010web). <http://www.asu.cas.cz/~ppravec/neo.html>
- Warner, B.D. (2006). "Asteroid lightcurve analysis at the Palmer Divide Observatory-February-March 2006." *Minor Planet Bulletin* **33**(4), 82-84.
- Warner, B.D.; Harris, A.W.; Pravec, P. (2009). "The Asteroid Lightcurve Database." *Icarus* **202**, 134-146. <https://minplanobs.org/mpinfo/php/lcdb.php>
- Waszczak, A.; Chang, C.-K.; Ofek, E.O.; Laher, R.; Masci, F.; Levitan, D.; Surace, J.; Cheng, Y.-C.; Ip, W.-H.; Kinoshita, D.; Helou, G.; Prince, T.A.; Kulkarni, S. (2015). "Asteroid Light Curves from the Palomar Transient Factory Survey: Rotation Periods and Phase Functions from Sparse Photometry." *Astron. J.* **150**, A75.
- Xu, S.; Binzel, R.P.; Burbine, T.H.; Bus, S.J. (1995). "Small main-belt asteroid spectroscopic survey: Initial results." *Icarus* **115**(1), 1-35.

LIGHTCURVES AND ROTATION PERIODS OF TEN ASTEROIDS

Geoffrey Stone
Dimension Point Observatory
14 Galaxy Point
Mayhill, NM 88339
geoff@first-light-systems.com

(Received: 2025 October 7)

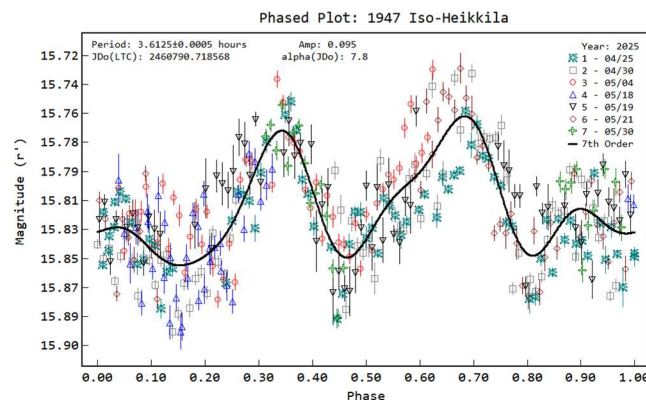
We present lightcurves and synodic rotation periods for ten asteroids observed from March 2025 through October 2025 at Dimension Point Observatory.

Photometric observation of these minor planets was conducted from March 2025 through October 2025 at Dimension Point Observatory (V42). Images were acquired using a 0.61-m f/6.5 Corrected Dall-Kirkham telescope with Finger Lakes Instrumentation Kepler KL400 back-illuminated CMOS camera and a 0.51-m f/8 Ritchey-Chrétien telescope with SBIG AC4040 CMOS camera. The equipment was operated remotely using *ACP Expert* (Denny, 2024) and *MaximDL* (George et al., 2024). Time was synchronized using a local stratum 1 time source and Meinberg NTP client software. Exposures were typically 120 seconds unfiltered or through a yellow blue-blocking long-pass filter with cutoff at 500nm.

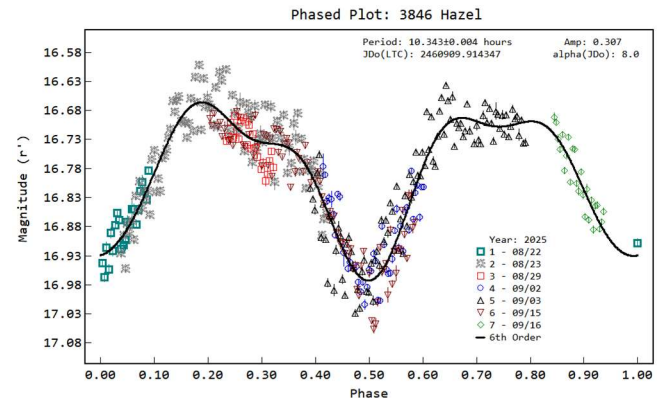
Target selection and observation planning was performed using the authors own Python scripts. Orbital elements, ephemeris and other information were obtained from the Minor Planet Center (MPC) website (<http://www.minorplanet.net>), the JPL Solar System Dynamics website (<http://ssd.jpl.nasa.gov>) (Giorgini et al., 1996), the Lowell Observatory Minor Planet Services website (<http://asteroid.lowell.edu>) (Moskovitz et al., 2022) and the LCDB database (Warner et al., 2009).

Image calibration, plate solving, measurement and period analysis were performed using *Tycho-Tracker* V12.3 (Parrott, 2020). Calibration masters were prepared using *AstroImageJ* (Collins et al., 2017). Comparison stars of near solar color were chosen from the ATLAS refcat2 star catalog using Sloan r' magnitudes (Tonry et al., 2018).

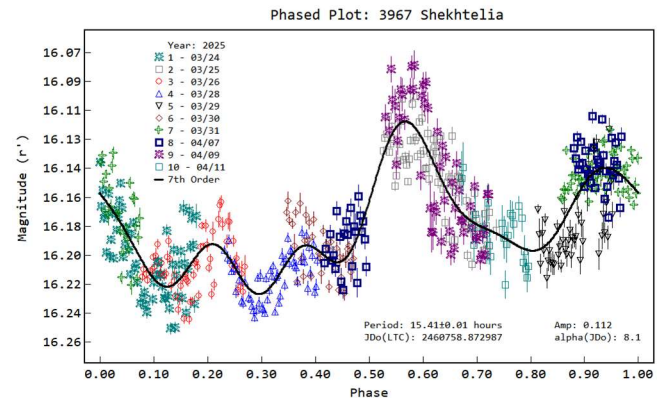
1947 Iso-Heikkila. Galád (2010) previously reported a period of 5.0158 hours. The LCDB quality score U was 1. We found a period of 3.612 ± 0.002 hours with an amplitude of 0.095 ± 0.02 mag, disagreeing with Galád.



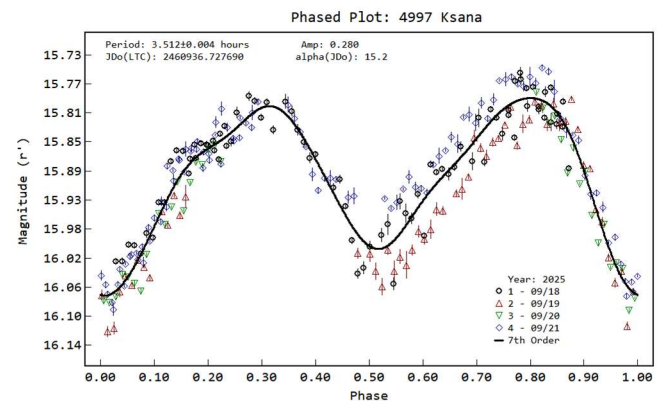
3846 Hazel. We found a best fit period of 10.343 ± 0.004 hours with an amplitude of 0.31 ± 0.03 mag. There are two small gaps in the phase curve so while this is likely the correct period, it could be wrong. We were unable to find any prior rotation period reports.



3967 Shekhtelia. We found a period of 15.41 ± 0.01 hours with an amplitude of 0.11 ± 0.02 mag for this member of the Ursula family. We were unable to find any prior rotation period reports.



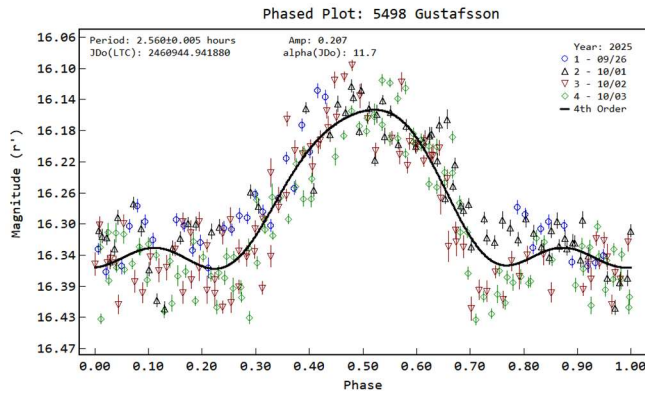
4997 Ksana. We found one prior period report by Behrend (2007web) of 3.4342 ± 0.0003 hours. The LCDB quality score U was 2. We observed Ksana on four nights. Our observations resulted in a best fit period of 3.512 ± 0.004 hours with an amplitude of 0.280 ± 0.03 mag, slightly longer than the Behrend report.



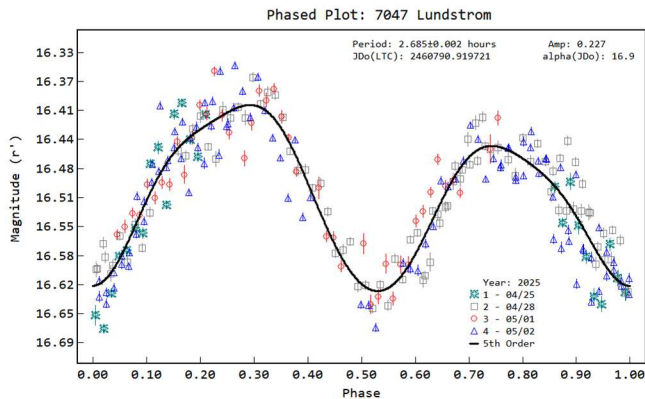
Number	Name	yyyy mm/dd	Phase	L _{PAB}	B _{PAB}	Period(h)	P.E.	Amp	A.E.	Grp
1947	Iso-Heikkila	2025 04/25-05/30	7.9, 16.3	200	13	3.613	0.002	0.09	0.02	Eos
3846	Hazel	2025 08/22-09/16	*8.0, 3.7	349	9	10.343	0.004	0.31	0.03	MB-O
3967	Shekhtelia	2025 03/24-04/09	*8.1, 8.2	192	21	15.41	0.01	0.11	0.02	Urs
4997	Ksana	2025 09/18-09/21	15.2, 13.8	22	3	3.512	0.004	0.28	0.03	Pal
5498	Gustafsson	2025 09/26-10/03	11.7, 7.6	21	1	2.560	0.005	0.21	0.04	MB-I
7047	Lundstrom	2025 04/25-05/02	16.8, 18.0	214	28	2.685	0.002	0.23	0.03	Pho
11875	Rhone	2025 04/21-04/24	7.3, 7.5	209	16	5.215	0.002	0.34	0.03	Mel
13581	1993 QX4	2025 05/29-06/29	*9.9, 12.4	257	20	4.564	0.004	0.15	0.04	Mar
63614	2001 QF77	2025 09/26-10/02	8.2, 10.7	352	9	2.836	0.001	0.13	0.06	Eun
98682	2000 WR180	2025 03/30-04/20	19, 18.7	196	27	5.60	0.01	0.27	0.04	MB-I

Table I. Observing circumstances and results. The phase angle is given for the first and last date. If preceded by an asterisk, the phase angle reached an extrema during the period. L_{PAB} and B_{PAB} are the approximate phase angle bisector longitude/latitude at mid-date range (see Harris et al., 1984). Grp is the asteroid family/group (Warner et al., 2009).

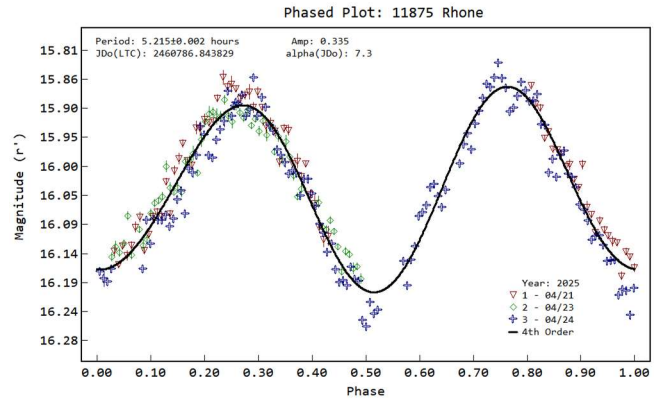
5498 Gustafsson. We found a best fit period of 2.560 ± 0.005 with an amplitude of 0.21 ± 0.04 mag. Alternatively, a bi-modal period of 5.123 is also possible but does not fit as well. We were unable to find any prior rotation period reports.



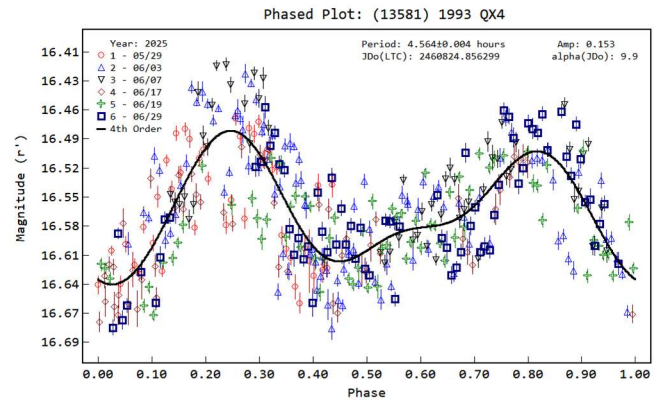
7047 Lundstrom. We found a period of 2.685 ± 0.002 hours with an amplitude of 0.227 ± 0.03 mag for this member of the Phocaea family. We were unable to find any prior rotation period reports.



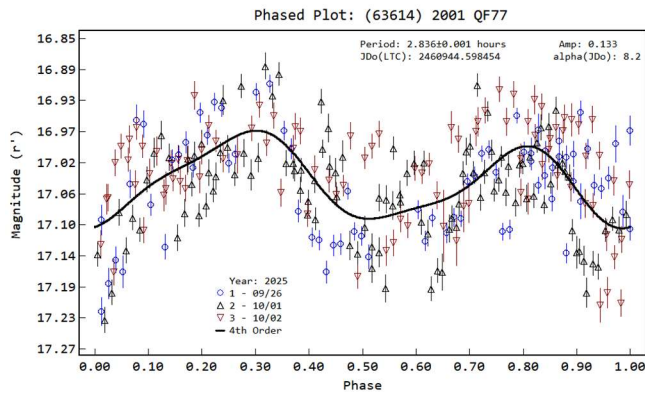
11875 Rhone. We found a period of 5.215 ± 0.002 hours with an amplitude of 0.335 ± 0.0255 mag for this member of the Meliboea family. We were unable to find any prior rotation period reports.



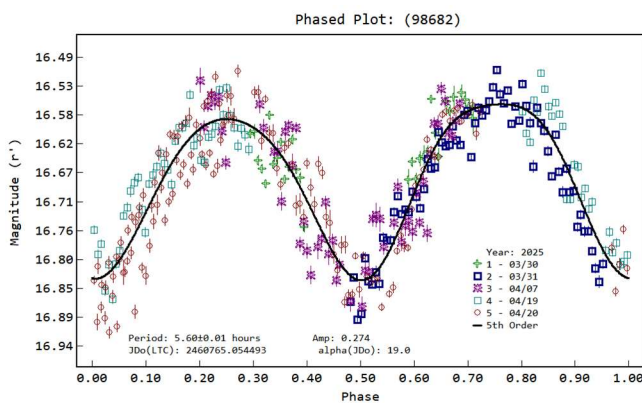
13581 1993 QX4. There is one prior survey report from Pál et al. (2020) of 4.568 hours. We found a best fit period of 4.564 ± 0.004 hours with an amplitude of 0.153 ± 0.038 mag, in agreement with Pál.



63614 2001 QF77. There are two prior survey reports, one from Waszczak et al. (2015) of 2.836 hours and one from Mahlke et al. (2021) of 68.3303 hours. The ALCDEF quality score U was 2. We found a best fit period of 2.836 ± 0.001 hours with an amplitude of 0.133 ± 0.06 mag, in agreement with Waszczak. We could not find a fit for any longer periods such as the report from Mahlke.



98682 2000 WR180. We found a period of 5.60 ± 0.01 hours with an amplitude of 0.27 ± 0.04 mag for this inner main belt asteroid. We were unable to find any prior rotation period reports.



Acknowledgements

This research used data from the Asteroid Terrestrial-impact Last Alert System (ATLAS) project, funded through NASA grants NN12AR55G, 80NSSC18K0284, and 80NSSC18K1575. The ATLAS science products have been made possible through the contributions of the University of Hawaii Institute for Astronomy, the Queen's University Belfast, the Space Telescope Science Institute, and the South African Astronomical Observatory. Funding for PDS observations, analysis, and publication was provided by NASA grant NNX13AP56G. Work on the asteroid lightcurve database (LCDB) was funded in part by National Science Foundation grants AST-1210099 and AST-1507535. Data from the MPC's database is made freely available to the public. Funding for this data and the MPC's operations comes from a NASA PDCO grant (80NSSC22M0024), administered via a University of Maryland - SAO subaward (106075-Z6415201). The MPC's computing equipment is funded in part by the above award, and in part by funding from the Tamkin Foundation. This research used data found on the JPL Solar System Dynamics Website. The JPL Solar System Dynamic group's ephemeris development, maintenance, and improvement tests are part of NASA's Advanced Multi-Mission Operations System, which is funded by NASA's Science Mission Directorate, Planetary Science Division.

References

Behrend, R. (2007web) Observatoire de Geneve web site.
http://obswww.unige.ch/~behrend/page_cou.html

Collins, K.; Kielkopf, J.; Stassun, K.; Hessman, F.; "AstroImageJ: Image Processing and Photometric Extraction for Ultra-Precise Astronomical Light Curves." *The Astronomical Journal* **153**(2), 13pp.

Denny, R. (2024). *ACP Expert* software, version 9.1. DC-3 Dreams.
<https://acpx.dc3.com>

Galád, A. (2010). "Accuracy of calibrated data from the SDSS moving object catalog, absolute magnitudes, and probably lightcurves for several asteroids." *Astronomy and Astrophysics* **514**, id. A55, 10pp.

George, D.; Sharratt, G.; Benson, E.; Browne, H.; Browne, P.; Creery, C.; Boltwood, P.; Mussar, R.; Waring, J.; Lawrence, O.; Robichaud, A. (2024). Maxim DL V6.50.
<https://diffractionlimited.com/>

Giorgini, J.; Yeomans, D.; Chamberlin, A.; Chodas, P.; Jacobson, R.; Keesey, M.; Lieske, J.; Ostro, S.; Standish, E.; Wimberly, R. (1996). "JPL's On-Line Solar System Data Service." *Bulletin of the American Astronomical Society* **28**(3), 1158.

Harris, A.W.; Young, J.W.; Scaltriti, F.; Zappala, V. (1984). "Lightcurves and phase relations of the asteroids 82 Alkmene and 444 Gyptis." *Icarus* **57**, 251-258.

Mahlke, M.; Carry, B.; Denneau, L. (2021). "Asteroid phase curves from ATLAS dual-band photometry." *Icarus* **354**, 114094. DOI: 10.1016/j.icarus.2020.114094

Moskovitz, N.A.; Wasserman, L.; Burt, B.; Schottland, R.; Bowell, E.; Bailen, M.; Granvik, M. (2022). "The astrob database at Lowell Observatory." *Astronomy and Computing*, **41**, id.100661.

Pál, A.; Szakáta, R.; Kiss, C.; Bódi, A.; Bognár, Z.; Kalup, C.; Kiss, L.; Marton, G.; Molnár, L.; Plachy, E.; Sárneczky, K.; Szabó, G.; Szabó, R. (2020). "Solar System Objects Observed with TESS - First Data Release: Bright Main-belt and Trojan Asteroids from the Southern Survey." *The Astrophysical Journal Supplement Series* **247**, id.26. 9pp. *arXiv:2001.05822*

Parrott, D. (2020). "Tycho Tracker: A New Tool to Facilitate the Discovery and Recovery of Asteroids Using Synthetic Tracking and Modern GPU Hardware." *The Journal of the American Association of Variable Star Observers* **48**(2), 262.
<http://www.tycho-tracker.com>

Tonry, J.; Denneau, L.; Flewelling, H.; Heinze, A.; Onken, C.; Smartt, S.; Stalder, B.; Weiland, H.; Wolf, C. (2018). "The ATLAS All-Sky Stellar Reference Catalog." *The Astrophysical Journal* **867**, id.105, 16pp.

Warner, B.D.; Harris, A.W.; Pravec, P. (2009). "The asteroid lightcurve database." *Icarus* **202**, 134-146. Updated 2023 April 24.
<https://www.alcdef.org>

Waszczak, A.; Chang, C.-K.; Ofek, E.O.; Laher, R.; Masci, F.; Levitan, D.; Surace, J.; Cheng, Y.-C.; Ip, W.-H.; Kinoshita, D.; Helou, G.; Prince, T.A.; Kulkarni, S. (2015). "Asteroid Light Curves from the Palomar Transient Factory Survey: Rotation Periods and Phase Functions from Sparse Photometry." *Astron. J.* **150**, A75.

LIGHTCURVE ANALYSIS FOR NINE NEAR-EARTH ASTEROIDS OBSERVED BETWEEN JULY AND SEPTEMBER 2025

Peter Birtwhistle
Great Shefford Observatory
Phlox Cottage, Wantage Road
Great Shefford, Berkshire, RG17 7DA
UNITED KINGDOM
peter@birtwhistle.org.uk

(Received: 2025 October 2)

Lightcurves and amplitudes for nine near-Earth asteroids observed from Great Shefford Observatory during close approaches between July and September 2025 are reported. All are small objects with rotation periods shorter than the spin barrier at ~ 2.2 h. Three are identified as having tumbling rotation.

Photometric observations of near-Earth asteroids during close approaches to Earth between July and September 2025 were made at Great Shefford Observatory using a 0.40-m Schmidt-Cassegrain and Apogee Alta U47+ CCD camera. All observations were made unfiltered and with the telescope operating with a focal reducer at $f/6$. The $1K \times 1K$, 13-micron CCD was binned 2×2 resulting in an image scale of 2.16 arcsec/pix. All the images were calibrated with dark and flat frames and *Astrometrica* (Raab, 2025) was used to measure photometry using G band data from the Gaia DR3 catalogue. *MPO Canopus* (Warner, 2023), incorporating the Fourier algorithm developed by Harris (Harris et al., 1989) was used for lightcurve analysis.

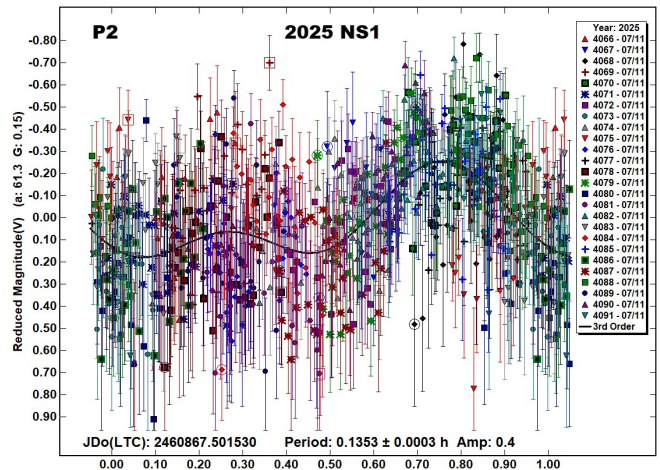
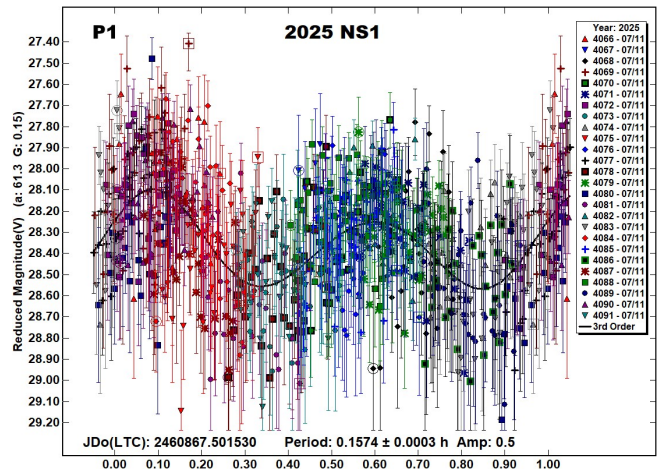
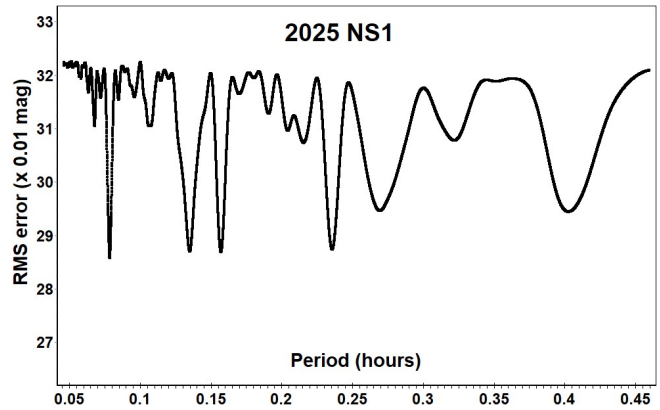
No previously reported results have been found in the Asteroid Lightcurve Database (LCDB) (Warner et al., 2009), from searches via the Astrophysics Data System (ADS, 2025) or from wider searches unless otherwise noted. All size estimates are calculated using H values from the Small-Body Database Lookup (JPL, 2025a), using an assumed albedo for NEAs of 0.2 (LCDB readme.pdf file) and are therefore uncertain and offered for relative comparison only.

2025 NS1. The Z.T.F. Collaboration using the Palomar 1.2-m Schmidt discovered this small Apollo ($H = 26.7$, $D \sim 14$ m) on 2025 Jul 10.36 UTC, 20 hours before it passed Earth at 1.1 Lunar Distances (LD) (Ikari et al., 2025). It was observed for 1.5 h starting at 2025 Jul 11.00 UTC when it had brightened to 15th mag but was at low altitude, at best 26° and with apparent speed > 275 arcsec/min exposures were limited to < 2 s to keep trailing within the measurement annulus used in *Astrometrica*. A period spectrum shows a number of minima, the strongest apparently in integer multiples of ~ 0.08 h and ~ 0.14 h, suggesting that two different periodicities exist and that 2025 NS1 may be tumbling, i.e. non-principal axis rotation (NPAR) is present. The Dual Period Search function in *MPO Canopus* was used to locate potential periods and the best-fit solution gives a pair of NPAR periods of:

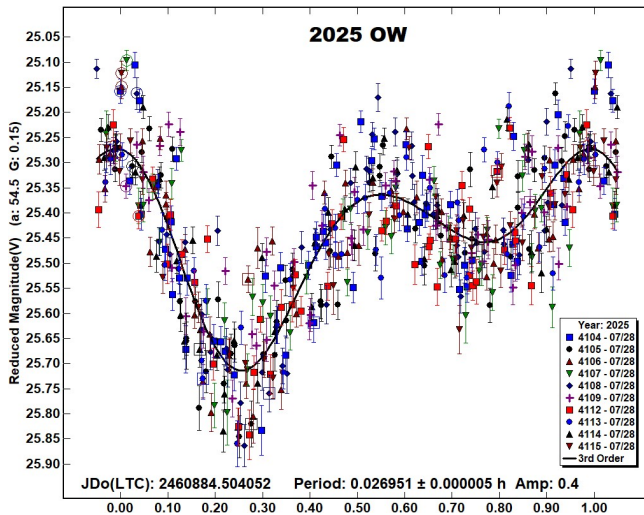
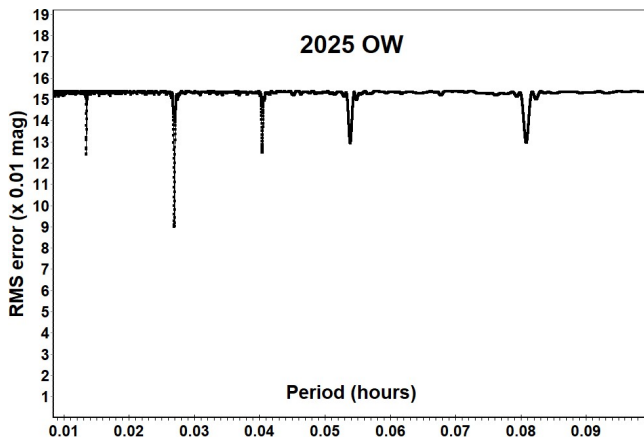
$$P1 = 0.1574 \pm 0.0003 \text{ h}$$

$$P2 = 0.1353 \pm 0.0003 \text{ h}$$

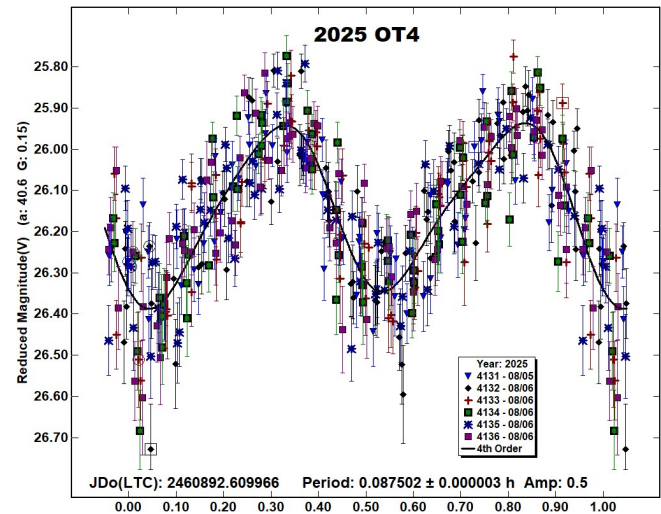
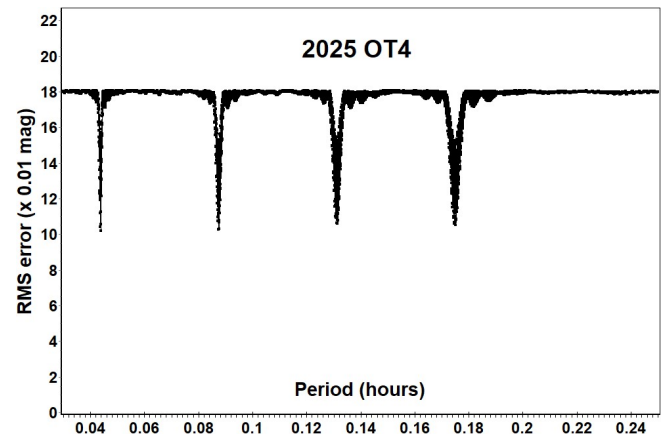
Lightcurves for these are given, labelled P1 and P2. It is noted that a solution using the same P1 period but double the P2 value at 0.273 ± 0.001 h gives an only slightly inferior fit, with an RMS residual 4% larger. Even with the ambiguity in the P2 period it is expected that 2025 NS1 may be assigned a rating of $PAR = -3$ (NPA rotation reliably detected with the two periods resolved. An ambiguity of the periods solution may be tolerated provided the resulting spectrum of frequencies with significant signal is the same for the different solutions) on the PAR scale defined in Pravec et al. (2005). The full amplitude implied by the NPAR lightcurves is 0.9 mag. During the time 2025 NS1 was being observed it completed 9 rotations of the P1 period and 11 of the P2 period.



2025 OW. Pan-STARRS 2 discovered this Apollo ($H = 23.5$, $D \sim 59$ m) on 2025 Jul 21.4 UTC, subsequently more PS2 images were located from 2025 Jul 4 (Bacci et al., 2025a). It approached Earth to 1.6 LD on 2025 Jul 28.8 UTC and was observed by radar from Goldstone as a target-of-opportunity earlier that day (JPL, 2025b). A 41-frame animation of the delay-Doppler images, resolving surface features down to 12 feet (3.75 meters) wide was included in a press release (JPL, 2025c) which also stated that 2025 OW rotates every $1\frac{1}{2}$ to 3 minutes and suggests a diameter of ~ 60 m. It was observed from Great Shefford for 2.1 h starting on 2025 Jul 28.00 UTC when it was moving between 65-80 arcsec/min and exposures were limited to 8 s or less to reduce image trailing. The period spectrum reveals a well-defined solution with a period of 0.026951 ± 0.000005 hours (~ 1.6 min), which agrees well with the radar estimate and produces an asymmetric, bimodal lightcurve. 2025 OW completed 79 rotations while under observation.



2025 OT4. This Apollo ($H = 24.8$, $D \sim 33$ m) was an ATLAS Haleakala discovery made on 2025 Jul 28.4 UTC and it approached Earth to 4 LD on 2025 Aug 7.7 UTC (Fumagalli et al., 2025). It was also observed by radar from Goldstone as a target-of-opportunity on 2025 Aug 6 (JPL, 2025b) but this resulted in a much weaker detection than achieved for 2025 OW. Photometry was obtained for 14 minutes starting on 2025 Aug 5.11 UTC and again for 99 minutes starting 2025 Aug 6.05 UTC and the resulting period spectrum from a 4th order analysis of both nights combined gives the best-fit solution at 0.088 h and an almost symmetrical lightcurve. 2025 OT4 was observed to complete 2.7 rotations on the first night and 19 rotations on the second night.



2025 PE. The ATLAS system on Mauna Loa discovered this Apollo ($H = 23.9$, $D \sim 48$ m) on 2025 Aug 1.4 UTC (Bacci et al., 2025b), some 29 h after it had passed Earth at 2.1 LD. It was observed for 2.2 h starting on 2025 Aug 1.91 UTC and again for 5.3 h starting 2025 Aug 2.88 UTC. Due to the two sets of measurements being separated by a day, the period spectrum shows “beating” in each of the main minima around 0.56, 0.81, 1.1, 1.6 and 2.4 h. Those minima are all integer multiples of the first two values and suggest tumbling motion may be present. The Dual Period Search function in *MPO Canopus* resolved the best-fit pair of NPAR periods to be:

$P1 = 1.1172 \pm 0.0003$ h, amplitude 0.6

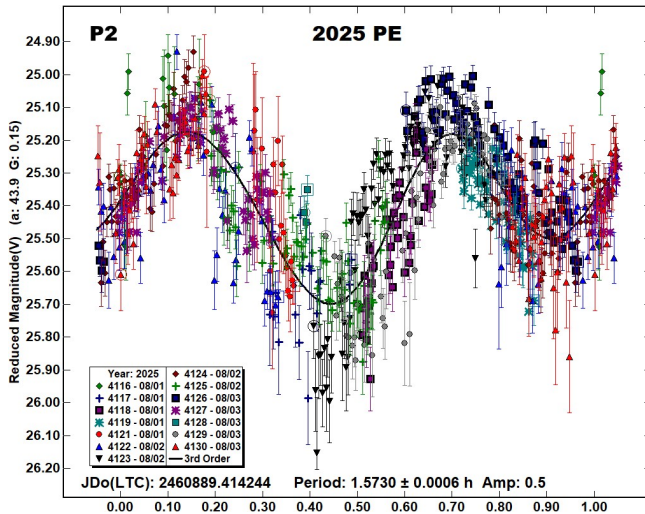
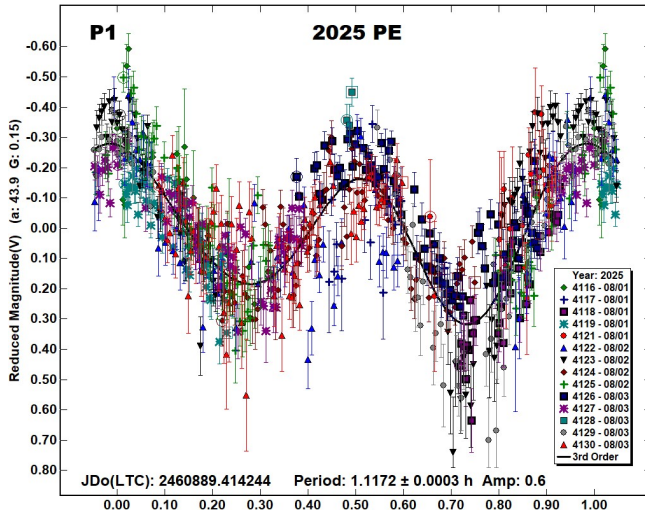
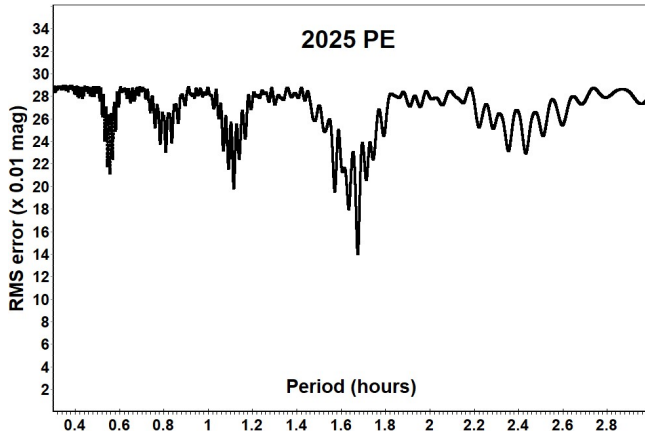
$P2 = 1.5730 \pm 0.0006$ h, amplitude 0.5

and lightcurves for these are given labelled P1 and P2. However, even though the P1 period appears to be well determined there are several other possible solutions for the second period with only slightly inferior RMS residuals, e.g.:

$P3 = 1.6787 \pm 0.0006$ h, amplitude 0.6

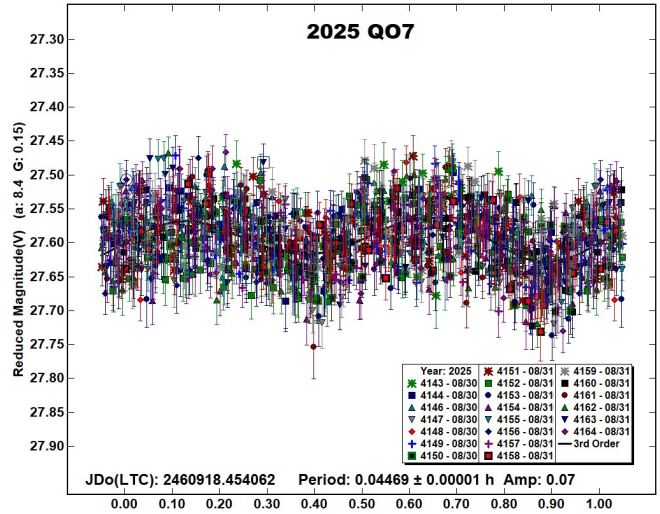
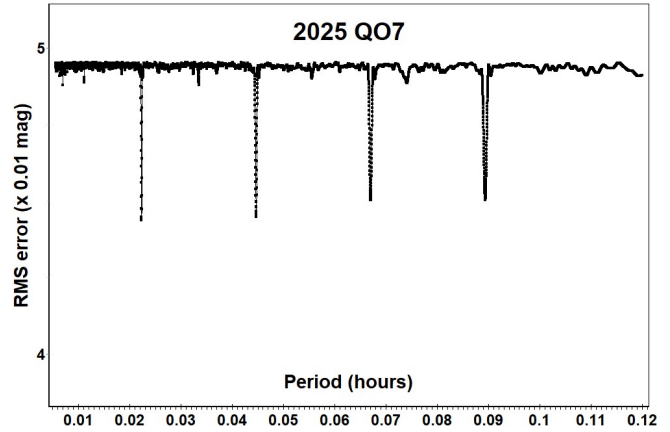
$P4 = 1.6246 \pm 0.0006$ h, amplitude 0.5

Solutions for the second period around 2.4 h give implausible trimodal lightcurves and are discounted. Due to the ambiguity in the P2 period it is expected that a rating of $PAR = -2$ (NPA rotation detected based on deviations from a single period but the second period is not resolved) may be appropriate on the PAR scale defined in Pravec et al. (2005). The full amplitude implied by the P1 & P2 NPAR lightcurves is 1.1 mag.



2025 QO7. Discovered from Observatorio Campo dos Amarais in Brazil on 2025 Aug 26.0 UTC this Apollo ($H = 27.0$, $D \sim 12$ m) subsequently approached Earth to 0.7 LD on 2025 Aug 31.58 UTC (Linder et al., 2025a). 2025 QO7 was also a radar target-of-opportunity from Goldstone on 2025 Sep 2 and although observations went ahead it was not detected (JPL, 2025b). It was observed from Great Shefford for 2.8 h starting on 2025 Aug 30.95 UTC when it was at opposition, the phase angle reaching a minimum of 7.7° midway through the session. The period spectrum

shows that a monomodal solution at 0.0224 h (~ 80.5 s) and a bimodal solution at 0.0447 h (~ 160.9 s) have virtually identical RMS residuals, with the bimodal solution here assumed more likely. 2025 QO7 completed 63 rotations while under observation.



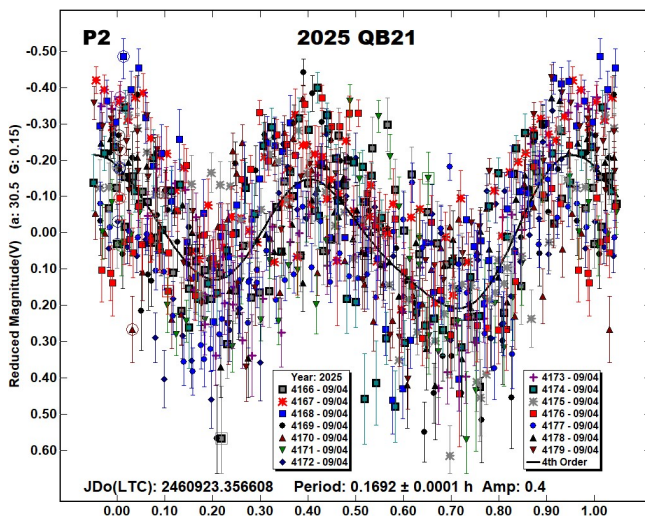
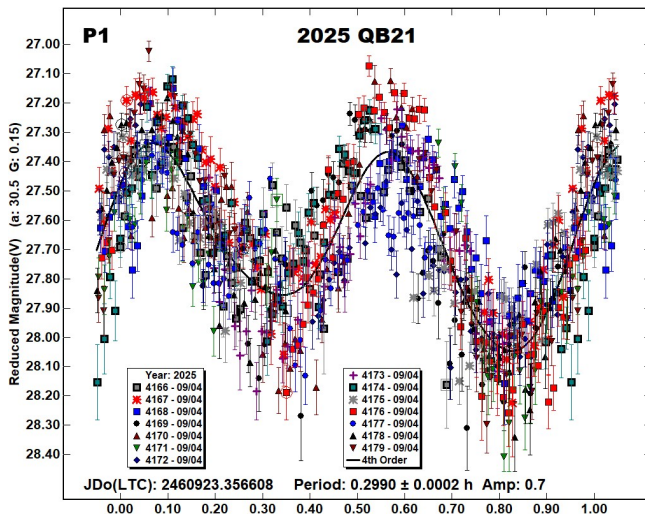
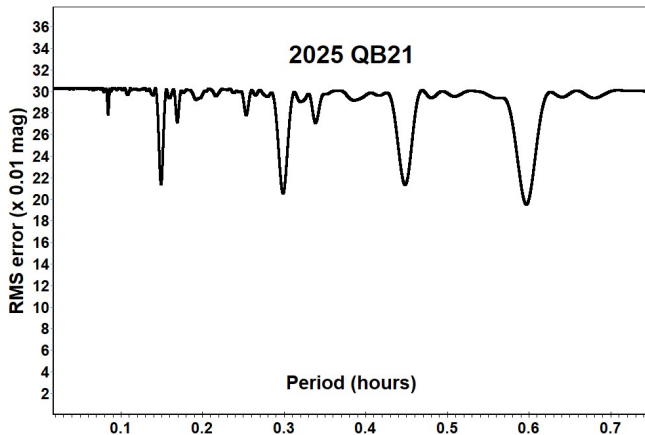
P. Pravec also obtained a period of 0.044710 ± 0.000002 h and amplitude 0.11 from observations spanning 2025 Aug 28.1 - 29.3 UTC using the 1.54-m Danish Telescope at La Silla, at somewhat larger phase angles, $24.7^\circ - 26.6^\circ$ (Pravec, 2025). The period and amplitude found is in good agreement with the result in this paper. However, Pravec assigned it a PAR code of -2, indicating that there was possible evidence of non-principal axis rotation. No suggestion of tumbling is found in the current analysis, but with the amount of scatter being a significant fraction of the amplitude, it is unlikely that low-level tumbling would be detectable even if present.

2025 QB21. The ATLAS South Africa, Sutherland survey discovered this Apollo ($H = 26.4$, $D \sim 15$ m) on 2025 Aug 31.9 UTC (Hoegner et al., 2025) a week before it approached Earth to 1.6 LD on 2025 Sep 6.0 UTC. Photometry was obtained for 3.1 h starting on 2025 Sep 4.86 UTC when it was at 2.2 LD. The period spectrum shows two sets of equally spaced minima, the strongest at multiples of 0.15 h and a weaker set at multiples of 0.085 h, suggesting that tumbling rotation is present. The best-fit NPAR solution using the Dual Period Search function in *MPO Canopus* gives:

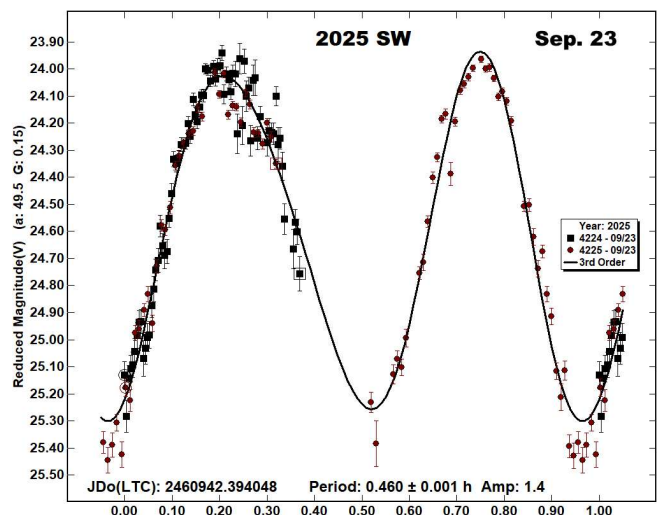
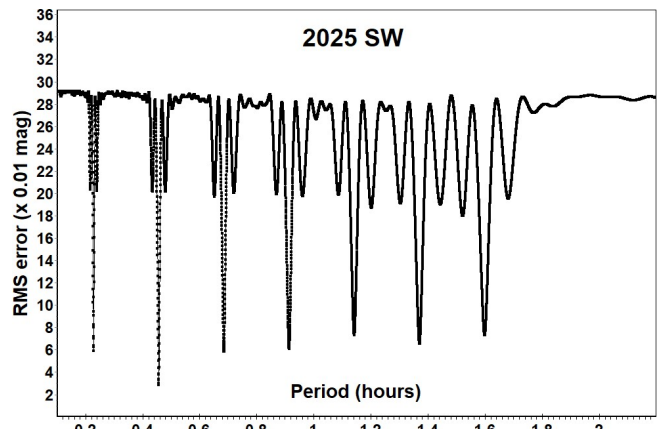
P1 = 0.2990 ± 0.0002 h (~ 17.9 min), amplitude 0.7

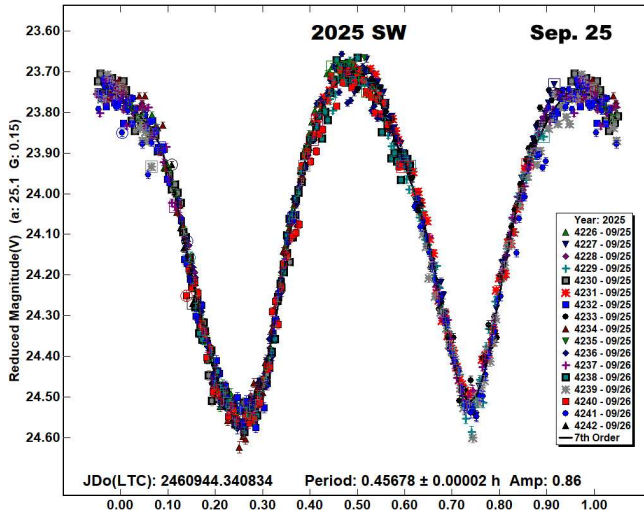
P2 = 0.1692 ± 0.0001 h (~ 10.2 min), amplitude 0.4

Lightcurves for these are labelled P1 and P2. It is expected that 2025 QB21 may be assigned a rating of PAR = -3 (NPA rotation reliably detected with the two periods resolved) on the PAR scale defined in Pravec et al. (2005). The full amplitude implied by the NPAR lightcurves is 1.1 mag and during the time was being observed it completed 10 rotations of the P1 period and 18 of the P2 period.

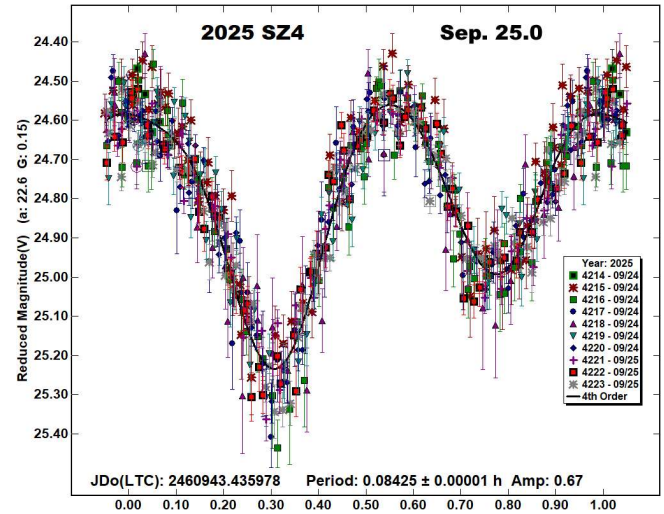
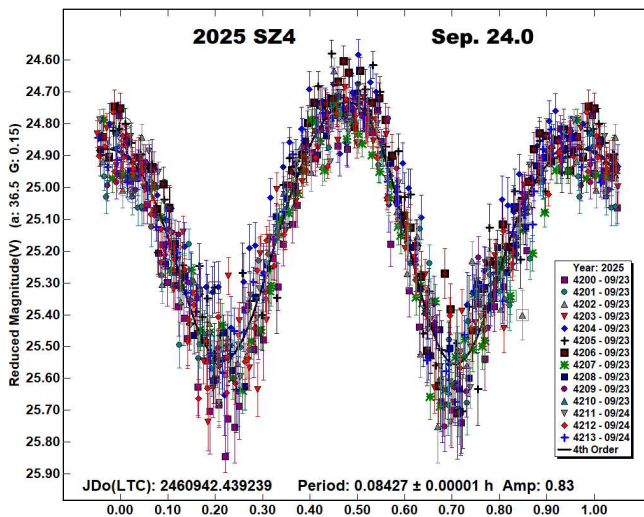
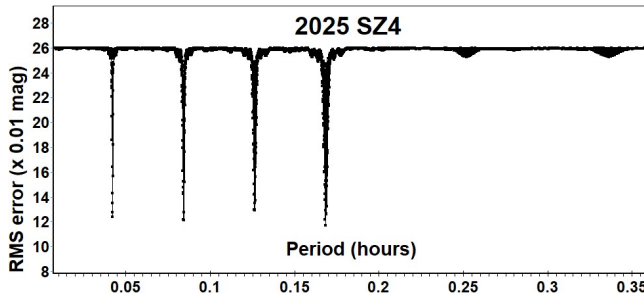


2025 SW. The ATLAS Chile, Rio Hurtado station discovered this Apollo (H = 22.9, D ~77 m) on 2025 Sep. 17.1 UTC and it made an approach to 4 LD from Earth on 2025 Sep. 25.7 UTC (Linder et al., 2025b). It was observed for 36 min starting on 2025 Sep. 23.89 UTC and then again for a total of 3.4 h over a period of 6 h starting 2 nights later on 2025 Sep. 25.84 UTC. The shorter session shows three well-defined maxima and two minima. A phased light curve is labelled Sep 23, indicating a period just under 30 minutes and an amplitude of approximately 1.4 magnitudes at a phase angle of 50°. On the second night of observation, the phase angle decreased to a minimum of 24.7° for this apparition. The light curve labelled "Sep 25" shows a reduced amplitude of 0.86 at the smaller phase angle and the period spectrum is from the same 7th order fit. 2025 SW completed 7.5 rotations during the 3.4 h it was under observation on the second night.



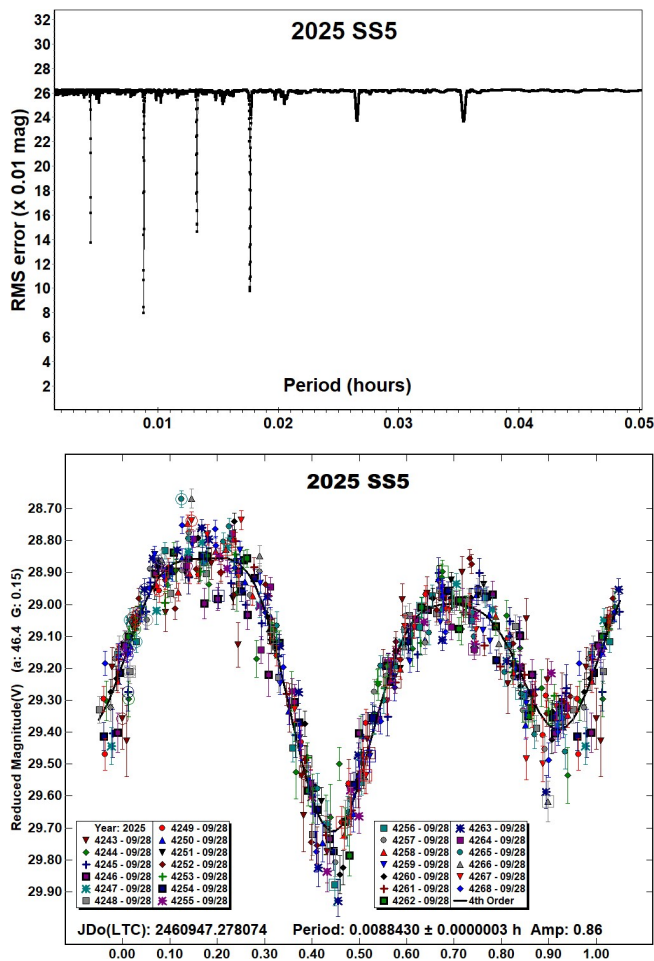


2025 SZ4. The ATLAS South Africa, Sutherland station discovered this Apollo ($H = 23.9$, $D \sim 49$ m) on 2025 Sep 23.0 UTC and it passed Earth at 5 LD 18 hours later (Kowalski et al., 2025). It was observed for 1.9 h starting on 2025 Sep 23.94 UTC and then again for 2.3 h starting on 2025 Sep 24.94 UTC. Although on both dates it was receding from Earth, the apparent magnitude remained fairly constant at +16 as the phase angle reduced to a minimum for the apparition at 22.1° on Sep. 24.75 UTC. A period spectrum using photometry from both dates indicates a well-defined best-fit period at 0.0843 h (~ 5.1 min) and lightcurves from the two dates show amplitude reducing with phase angle while asymmetry in the bimodal curve increased. It completed 22 rotations during observation on the first night and 27 rotations on the second night.



2025 SS5. The Mt. Lemmon Survey discovered this small Apollo ($H = 27.8$, $D \sim 8$ m) on 2025 Sep. 23.3 UTC and it made a very close approach to Earth, to within 0.3 LD on 2025 Sep 28.9 UTC (Leonard et al., 2025). It is listed as a virtual impactor by impact monitoring services Sentry (JPL, 2025d), Clomon-2 (NEODyS, 2025) and Aegis (ESA, 2025), each indicating ~ 50 very low probability potential impacts, the earliest in 2078. It was observed starting at 2025 Sep 28.72 UTC for 57 minutes when it was at a distance of 0.35 LD and still on its approach. With its apparent speed increasing above 540 arcsec/min, exposures were reduced from 1.2 to 0.9 seconds to limit image trailing. The period spectrum shows a clear best-fit solution at 0.009 hours. Other significant minima appear at multiples of this period — specifically at $\frac{1}{2}$, $\frac{1}{3}$, 2, 3, and 4 times 0.009 h. These correspond to monomodal, trimodal and other harmonic solutions of the bimodal best-fit period. Very weak minima visible in the range 0.005 - 0.21 h are suggestive of tumbling rotation but attempts to isolate an NPAR solution are inconclusive. A small systematic trend in the measured magnitudes was corrected by making small adjustments to the zero-points of the 26 sessions in MPO Canopus to minimise the overall RMS fit of the lightcurve, the RMS of those corrections was 0.053 mag. The trend — a linear 0.17 mag fade — was observed even though the magnitude was predicted to remain constant to within 0.02 mag using an ephemeris based on $H = 27.9$ and $G = 0.15$. This fading may be due to increasing apparent speed (leading to shorter exposure times), changing viewing geometry, or possibly an unusual shadowing effect as the phase angle increased.

The best-fit period is found to be 0.0088430 ± 0.0000003 h (~ 31.8 seconds) indicating that 2025 SS5 completed 107 rotations while under observation.



Number	Name	Integration times	Max intg/Pd	Min a/b	Pts	Flds
2025	NS1	1.4–1.9	0.004 ¹	1.3*	819	26
2025	OW	6.8–8.0	0.082	1.2*	469	10
2025	OT4	10–15	0.048	1.2*	405	6
2025	PE	10–30	0.007 ¹	1.6*	747	14
2025	QO7	3.9–5.2	0.032	1.1	1234	21
2025	QB21	8.4–10.5	0.017 ¹	1.7	789	14
2025	SW	6–13.6	0.008	1.6	1165	19
2025	SZ4	2.5–8.8	0.029	1.4	1436	24
2025	SS5	0.9–1.2	0.038	1.4*	500	26

Table I. Ancillary information, listing the integration times used (seconds), the fraction of the period represented by the longest integration time (Pravec et al., 2000), the calculated minimum elongation of the asteroid (Zappala et al., 1990), the number of data points used in the analysis and the number of times the telescope was repositioned to different fields. Note: * = Value uncertain, based on phase angle $> 40^\circ$, 1 = Calculated using the shorter of the NPAR periods.

Acknowledgements

The author is indebted to Dr. Petr Pravec, Astronomical Institute, Czech Republic for his help in reviewing the analyses of tumbling asteroids in this paper. The author also gratefully acknowledges a Gene Shoemaker NEO Grant from the Planetary Society (2005) and a Ridley Grant from the British Astronomical Association (2005), both of which facilitated upgrades to observatory equipment used in this study. This work has made use of data from the European Space Agency (ESA) mission Gaia (<https://www.cosmos.esa.int/gaia>), processed by the Gaia Data Processing and Analysis Consortium (DPAC, <https://www.cosmos.esa.int/web/gaia/dpac/consortium>). Funding for the DPAC has been provided by national institutions, in particular the institutions participating in the Gaia Multilateral Agreement.

References

- ADS (2025). Astrophysics Data System.
<https://ui.adsabs.harvard.edu/>
- Bacci, P.; Maestrupieri, M.; Giovannetti, T.; Greco, N.; Lowe, T.; Minguez, P.; Schultz, A.; Smith, I.; Chambers, K.; de Boer, T.; Fairlamb, J.; Gao, H.; Huber, M.; Lin, C.-C.; Magnier, E. and 7 colleagues (2025a). “2025 OW.” MPEC 2025-O41.
<https://www.minorplanetcenter.net/mpec/K25/K25O41.html>
- Bacci, P.; Maestrupieri, M.; Wiggins, P.; Dupouy, P.; Laborde, J.; Jaeger, M.; Rhemann, G.; Prosperi, E.; Thinius, B.; Holmes, R.; Linder, T.; Hutton, L.; Losse, F.; Briggs, D.; Birtwhistle, P. and 28 colleagues (2025b). “2025 PE.” MPEC 2025-P53.
<https://www.minorplanetcenter.net/mpec/K25/K25P53.html>
- ESA (2025) Risk List.
<https://neo.ssa.esa.int/risk-list>
- Fumagalli, A.; Testa, A.; Ikari, Y.; Dupouy, P.; Lowe, T.; Minguez, P.; Schultz, A.; Smith, I.; Chambers, K.; de Boer, T.; Fairlamb, J.; Gao, H.; Huber, M.; Lin, C.-C.; Magnier, E. and 22 colleagues (2025). “2025 OT4.” MPEC 2025-O125.
<https://www.minorplanetcenter.net/mpec/K25/K25OC5.html>
- Harris, A.W.; Young, J.W.; Scaltriti, F.; Zappala, V. (1984). “Lightcurves and phase relations of the asteroids 82 Alkmene and 444 Gyptis.” *Icarus* **57**, 251-258.
- Harris, A.W.; Young, J.W.; Bowell, E.; Martin, L.J.; Millis, R.L.; Poutanen, M.; Scaltriti, F.; Zappala, V.; Schober, H.J.; Debehogne, H.; Zeigler, K. (1989). “Photoelectric Observations of Asteroids 3, 24, 60, 261, and 863.” *Icarus* **77**, 171-186.
- Hoegner, C.; Ludwig, F.; Hartmann, M.; Stecklum, B.; Ikari, Y.; Z.T.F. Collaboration; Ye, Q.-Z.; Birtwhistle, P.; Denneau, L.; Tonry, J.; Weiland, H.; Erasmus, N.; Fitzsimmons, A.; Licandro, J.; Ngwane, T. and 11 colleagues (2025). “2025 QB21.” MPEC 2025-R05. <https://www.minorplanetcenter.net/mpec/K25/K25R05.html>

Number	Name	yyyy mm/dd	Phase	L _{PAB}	B _{PAB}	Period(h)	P.E.	Amp	A.E.	PAR	H
2025	NS1	2025 07/11–07/11	61.4, 68.4	321	1	0.1574 0.1353	0.0003 0.0003	0.5 0.4	0.4 0.4	–3	26.7
2025	OW	2025 07/28–07/28	54.4, 55.9	307	28	0.026951	0.000005	0.4	0.1		23.5
2025	OT4	2025 08/05–08/06	40.5, 44.2	334	5	0.087502	0.000003	0.5	0.1		24.8
2025	PE	2025 08/01–08/03	43.9, 36.9	317	20	1.1172 1.5730	0.0003 0.0006	0.6 0.5	0.2 0.2	–2	23.9
2025	QO7	2025 08/30–08/31	*8.2, 8.2	336	3	0.04469	0.00001	0.07	0.06		27.0
2025	QB21	2025 09/04–09/04	30.2, 31.0	348	14	0.2990 0.1692	0.0002 0.0001	0.7 0.4	0.2 0.2	–3	26.4
2025	SW	2025 09/23–09/23	49.6, 49.4	335	0	0.460	0.001	1.4	0.1		22.9
		2025 09/25–09/26	*25.0, 24.7	357	11	0.45678	0.00002	0.86	0.04		
2025	SZ4	2025 09/23–09/24	36.7, 34.0	18	–7	0.08427	0.00001	0.83	0.13		23.9
		2025 09/24–09/25	*22.6, 23.1	9	9	0.08425	0.00001	0.67	0.10		
2025	SS5	2025 09/28–09/28	46.2, 56.0	1	25	0.0088430	0.0000003	0.86	0.11		27.8

Table II. Observing circumstances and results. The phase angle is given for the first and last date. If preceded by an asterisk, the phase angle reached an extrema during the period. L_{PAB} and B_{PAB} are the approximate phase angle bisector longitude/latitude at mid-date range (see Harris et al., 1984). Amplitude error (A.E.) is calculated as $\sqrt{2} \times$ (lightcurve RMS residual). PAR is the expected Principal Axis Rotation quality detection code (Pravec et al., 2005) and H is the absolute magnitude at 1 au from Sun and Earth taken from the Small-Body Database Lookup (JPL, 2025a).

Ikari, Y.; Z.T.F. Collaboration; Wagh, Y.; Ye, Q.-Z.; Duev, D.A.; Helou, G.; Lin, H.-W.; Mahabal, A.A.; Masci, F.J.; Prince, T.A.; Denneau, L.; Siverd, R.; Tonry, J.; Weiland, H.; Erasmus, N. and 2 colleagues (2025). “2025 NS1.” MPEC 2025-N85.
<https://www.minorplanetcenter.net/mpec/K25/K25N85.html>

JPL (2025a). Small-Body Database Lookup.
https://ssd.jpl.nasa.gov/tools/sbdb_lookup.html

JPL (2025b). Asteroid Radar Research Schedule & Planning Pages.
https://echo.jpl.nasa.gov/asteroids/goldstone_asteroid_schedule.html?schedule=past

JPL (2025c). NASA's Goldstone Planetary Radar Observes Fast-Spinning Asteroid.
<https://photojournal.jpl.nasa.gov/catalog/PIA26587>

JPL (2025d). Sentry: Earth Impact Monitoring.
<https://cneos.jpl.nasa.gov/sentry/>

Kowalski, R.A.; Beuden, T.; Carvajal, V.F.; Fay, D.; Fazekas, J.B.; Fuls, D.C.; Gibbs, A.R.; Grauer, A.D.; Groeller, H.; Hogan, J.K.; Larson, S.M.; Leonard, G.J.; Loewen, C.J.; Rankin, D.; Seaman, R.L. and 36 colleagues (2025). “2025 SZ4.” MPEC 2025-S194.
<https://www.minorplanetcenter.net/mpec/K25/K25SJ4.html>

Leonard, G.J.; Beuden, T.; Carvajal, V.F.; Fay, D.; Fazekas, J.B.; Fuls, D.C.; Gibbs, A.R.; Grauer, A.D.; Groeller, H.; Hogan, J.K.; Kowalski, R.A.; Larson, S.M.; Rankin, D.; Seaman, R.L.; Shelly, F.C. and 4 colleagues (2025). “2025 SS5.” MPEC 2025-S204.
<https://www.minorplanetcenter.net/mpec/K25/K25SK4.html>

Linder, T.; Holmes, R.; Hutton, L.; Urbanik, M.; Vilquin Barrajon, A.; Gilmore, A.C.; Kilmartin, P.M.; Denneau, L.; Tonry, J.; Weiland, H.; Erasmus, N.; Fitzsimmons, A.; Robinson, J.; Amaral, L.S.; Ramos, B.M. and 3 colleagues (2025a). “2025 QO7.” MPEC 2025-Q178.
<https://www.minorplanetcenter.net/mpec/K25/K25QH8.html>

Linder, T.; Holmes, R.; Hutton, L.; Hidas, A.; Bannister, A.; Aletti, A.; Bellini, F.; Buzzi, L.; Galli, G.; Denneau, L.; Tonry, J.; Weiland, H.; Erasmus, N.; Fitzsimmons, A.; Licandro, J. and 5 colleagues (2025b). “2025 SW.” MPEC 2025-S85.
<https://www.minorplanetcenter.net/mpec/K25/K25S85.html>

NEODyS (2025) Risk List.
<https://newton.spacedys.com/neodys/index.php?pc=4.1>

Pravec, P.; Hergenrother, C.; Whiteley, R.; Sarounova, L.; Kusnirak, P.; Wolf, M. (2000). “Fast Rotating Asteroids 1999 TY2, 1999 SF10, and 1998 WB2.” *Icarus* **147**, 477–486.

Pravec, P.; Harris, A.W.; Scheirich, P.; Kušnirák, P.; Šarounová, L.; Hergenrother, C.W.; Mottola, S.; Hicks, M.D.; Masi, G.; Krugly, Yu. N.; Shevchenko, V.G.; Nolan, M.C.; Howell, E.S.; Kaasalainen, M.; Galád, A. and 5 colleagues. (2005). “Tumbling Asteroids.” *Icarus* **173**, 108–131.

Pravec, P. (2025). “Prepublished” periods of asteroids.
<https://space.asu.cas.cz/~ppravec/newres.htm>

Raab, H. (2025). Astrometrica software, version 4.16.4.468.
<http://www.astrometrica.at/>

Warner, B.D.; Harris, A.W.; Pravec, P. (2009). “The Asteroid Lightcurve Database.” *Icarus* **202**, 134–146. Updated 2023 Oct.
<https://www.minorplanet.info/php/lcdb.php>

Warner, B.D. (2023). MPO Software, Canopus version 10.8.6.20. Bdw Publishing, Colorado Springs, CO.
<https://minplanobs.org/BdwPub/>

Zappala, V.; Cellini, A.; Barucci, A.M.; Fulchignoni, M.; Lupishko, D.E. (1990). “An analysis of the amplitude-phase relationship among asteroids.” *Astron. Astrophys.* **231**, 548–560.

LIGHTCURVE ANALYSIS FOR TWELVE MAIN-BELT ASTEROIDS

Gonzalo Fornas (J57)
Asociación Valenciana de Astronomía
(Centro Astronómico Alto Turia)
C/ Profesor Blanco 16. 46014 Valencia, SPAIN
gon@iicv.es

Alfonso Carreño (Y76)
Nova Canet Observatory

(Received: 2025 September 11)

Photometric observations for twelve main-belt asteroids are reported. We derived the following rotational synodic periods: 123 *Brunhild*, 9.8561 ± 0.0014 h; 490 *Veritas*, 7.965 ± 0.005 h; 689 *Zita*, 6.4264 ± 0.0016 h; 872 *Holda*, 5.94499 ± 0.0011 h; 1130 *Skuld*, 4.802 ± 0.002 h; 1152 *Pawona*, 3.41499 ± 0.0001 h; 1257 *Mora*, 5.29574 ± 0.00034 h; 1588 *Descamisada*, 3.8236 ± 0.0006 h; 1648 *Shajna*, 6.412 ± 0.002 h; 2159 *Kukkamaki*, 3.7909 ± 0.0002 h; 2501 *Lohja*, 3.8080 ± 0.0002 h; 6441 *Milenajesennska*, 2.8135 ± 0.0008 h.

We report on the photometric analysis for twelve main-belt asteroids. The data were obtained during 2025. We present graphic results of data analysis, mainly lightcurves, with the plot phased according to a given period solution. We managed to obtain several accurate and complete lightcurves and calculated their rotation periods as accurately as possible.

Observatory	Telescope (meters)	CCD
Y76	SC 9.25"	ATIK 314L+

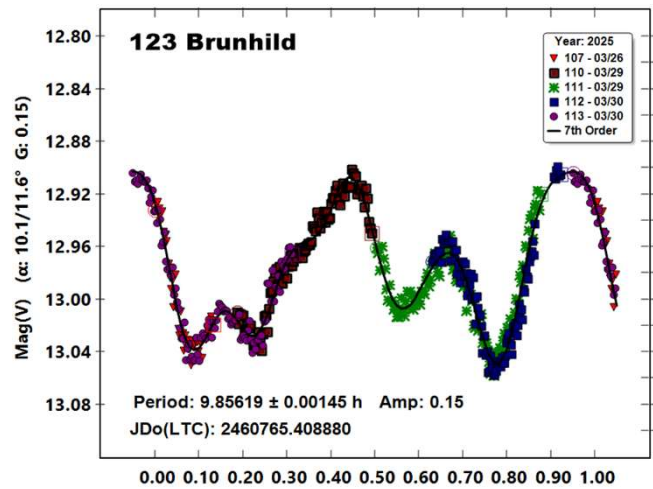
Table I. List of instruments used for the observations.

The targets were selected from the Minor Planet Center (<http://www.minorplanet.net>), Collaborative Asteroid Lightcurve (CALL) website (<http://www.minorplanet.info/call.html>), and Warner et al. (2025). The Asteroid Lightcurve Database (LCDB; Warner et al., 2009) was consulted to locate previously published results.

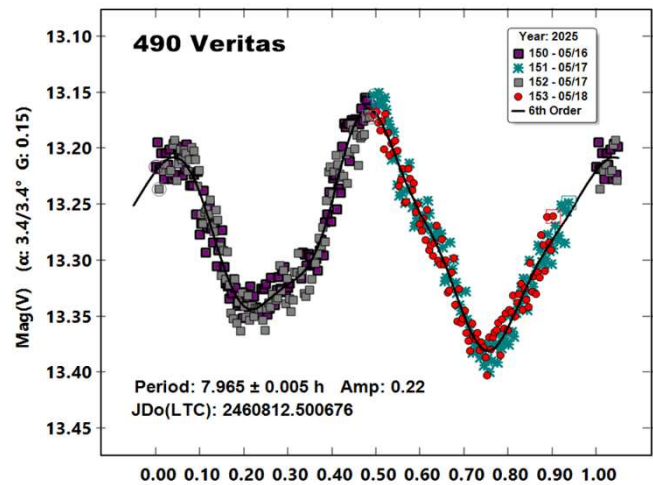
Images were measured using *MPO Canopus* (Bdw. Publishing) with a differential photometry technique. The comparison stars were restricted to near solar color to minimize color dependencies, especially at larger air masses. The lightcurves show the synodic rotation period. The amplitude (peak-to-peak) that is shown is that for the Fourier model curve and not necessarily the true amplitude.

Results

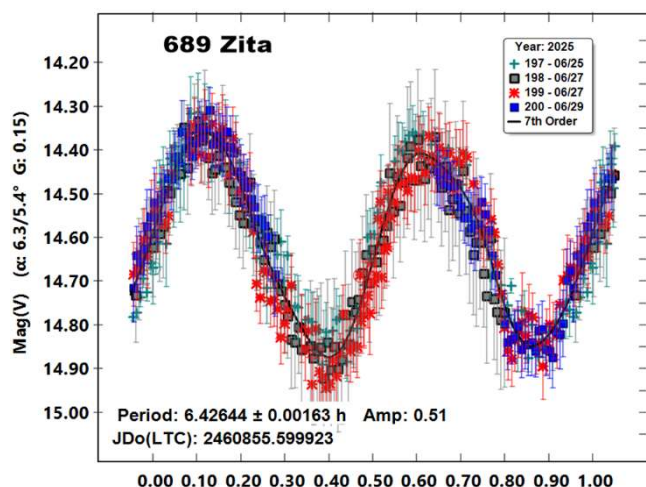
123 *Brunhild*. This middle main-belt asteroid was discovered on 1872 Jul 31 at Clinton by C.H.F. Peters. We made observations on 2025 March 26 to 30. From our data we derive a synodic rotation period of 9.8561 ± 0.0015 h and an amplitude of 0.15 mag. The data provides an unsymmetric lightcurve, such as Pilcher (Pilcher, 2016) found. Barucci and Di Martino (1984) found a period of 10.04 hours; and Behrend (Behrend, 2010web), 9.8 hours.



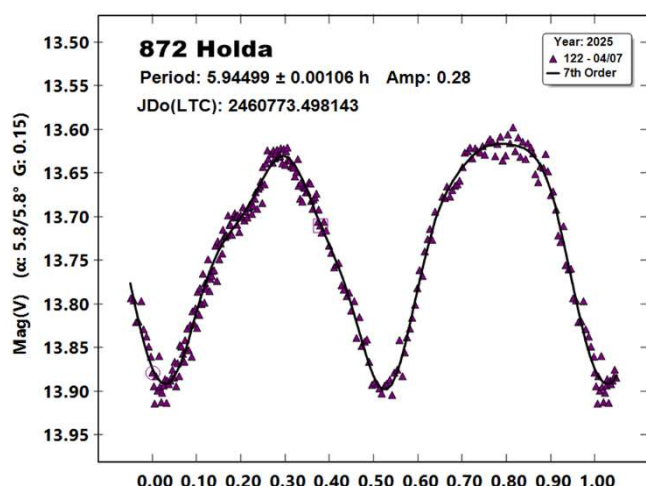
490 *Veritas*. This outer main-belt asteroid was discovered on 1902 Sep 3 at Heidelberg by M.F. Wolf. We made observations on 2025 Jun 6 to 18. From our data we derive a synodic rotation period of 7.965 ± 0.005 h and an amplitude of 0.22 mag. Behrend (2007web) found a period of 7.927 h. Koff and Brincat (2001) found 7.93 h. Klinglesmith et al. (2015) found 7.927 h. All of them are consistent with our results.



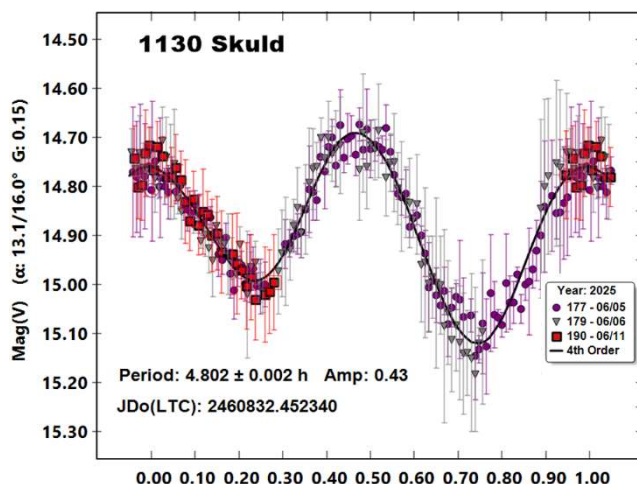
689 *Zita*. This inner main-belt asteroid was discovered on 1909 Sep 12 at Vienna by K. Palisa. We made observations on 2025 Jun 25-29. From our data we derive a synodic rotation period of 6.4264 ± 0.0016 h and an amplitude of 0.51 mag. Behrend (2004web, 2022web) found a period of 6.4, 6.4171 and 6.4 h. Higgins (2005) found 6.425 h, all reaching consistent conclusions.



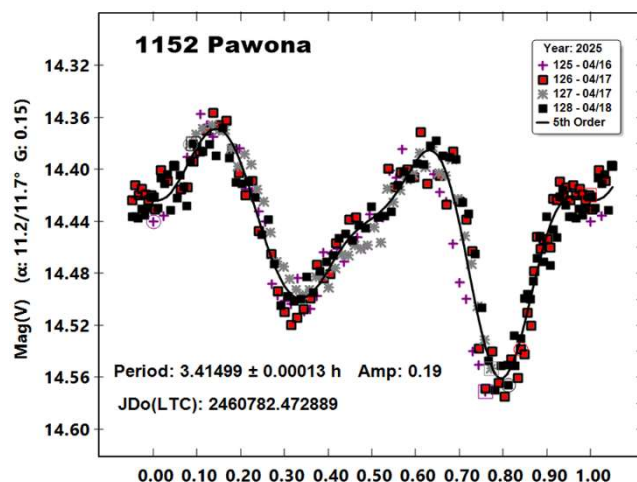
872 Holda. This middle main-belt asteroid was discovered on 1917 May 21 at Deidelberg by M.F. Wolf. We made observations on 2025 April 7. From our data we derive a synodic rotation period of 5.94499 ± 0.00105 h and an amplitude of 0.28 mag. Behrend (2002web, 2004web) found a period of 5.94 and 5.945 h. Brinsfield (2007) found 5.943 h and Fauerbach et al. (2008) found 5.941h. Sheridan (2009) got a period of 5.9405 h. Waszczak et al. (2015) got 5.927 h; a long series of consistent results.



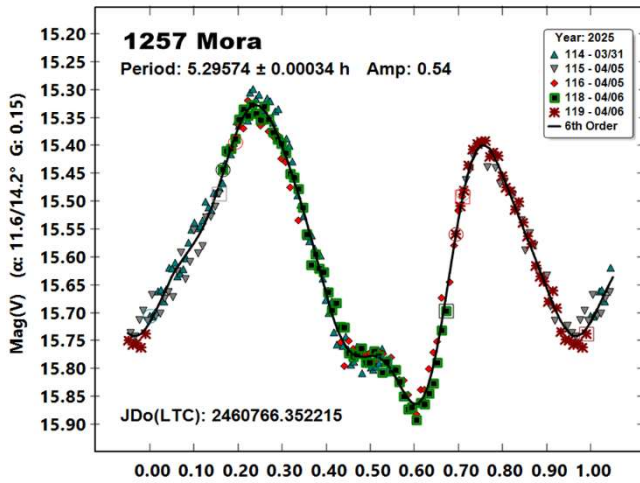
1130 Skuld. This inner main-belt asteroid was discovered on 1929 Sep 2 at Heidelberg by K. Reinmuth. We made observations on 2025 June 6 to 11. From our data we derive a synodic rotation period of 4.802 ± 0.002 h and an amplitude of 0.43 mag. Behrend (2004web, 2011web, 2017web, 2019web) found a period of 4.75, 4.810, 4.8096 and 4.8058 h. Buchheim (2010) got a period of 4.807 h. Kryszczyńska et al. (2012) found 4.8079 h. Dose (2020) found 4.808 h; providing a range of consistent results.



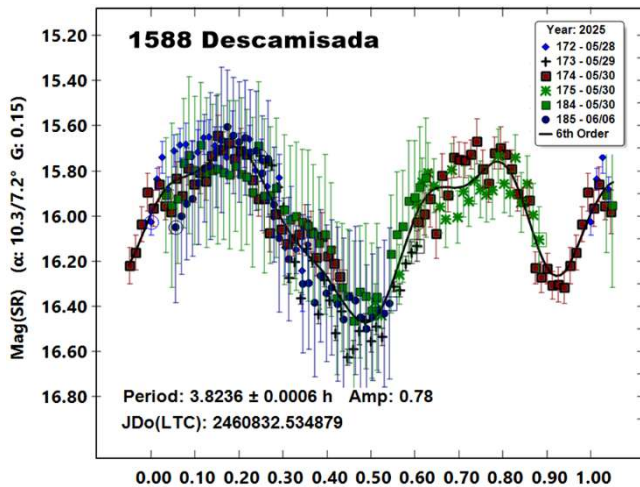
1152 Pawona. This inner main-belt asteroid was discovered on 1930 Jan 8 at Heidelberg by K. Reinmuth. We made observations on 2025 April 16 to 18. From our data we derive a synodic rotation period of 3.41499 ± 0.0001 h and an amplitude of 0.19 mag. Behrend (2006web, 2011web) found a period of 3.4154 and 3.41500 h. Koff and Clark (2002) found a period of 3.418 h. Schmidt (2017) got 3.4151 h and Klinglesmith et al. (2017) got 3.425 h. Franco et al. (2021) found 3.4152 h; all consistent results.



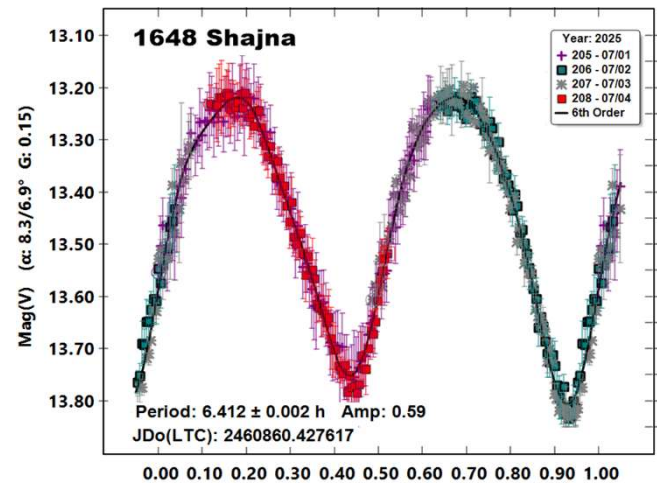
1257 Mora. This inner main-belt asteroid was discovered on 1932 Aug 08 at Heidelberg by K. Reinmuth. From our data we derive a synodic rotation period of 5.29574 ± 0.00034 h and an amplitude of 0.54 mag. Behrend (2009web, 2011web) found a period of 5.3 and 5.2948 h. Binzel (1987) got a period of 5.28 h, Stephens et al. (2021) found a period of 5.298 h; all consistent results.



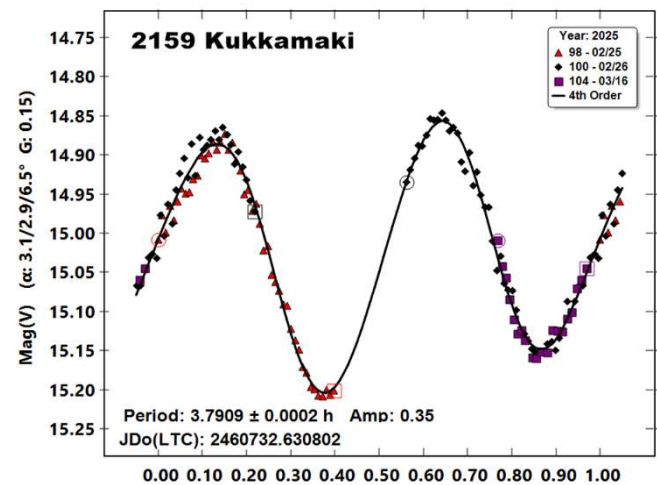
1588 Descamisada. This outer main-belt asteroid of the Eos family was discovered on 1951 June 27 at La Plata by Itzigsohn. We made observations on 2025 May 28 to Jun 6. From our data we derive a synodic rotation period of 3.8236 ± 0.0006 h and an amplitude of 0.78 mag. Durech et al. (2019) found a sidereal period of 4.606795 h, which does not match our calculation.



1648 Shajna. This inner main-belt asteroid was discovered on 1935 Sep 5 at Simeis by P.F. Shajna. We made observations on 2025 July 1 to 4. From our data we derive a synodic rotation period of 6.412 ± 0.002 h and an amplitude of 0.59 mag. Behrend (2005web, 2021web) found a period of 6.4140 and 6.41h. Skiff (2018web) got 6.4156 h. Waszczak et al. (2015) found 6.414 and 6.425 h.



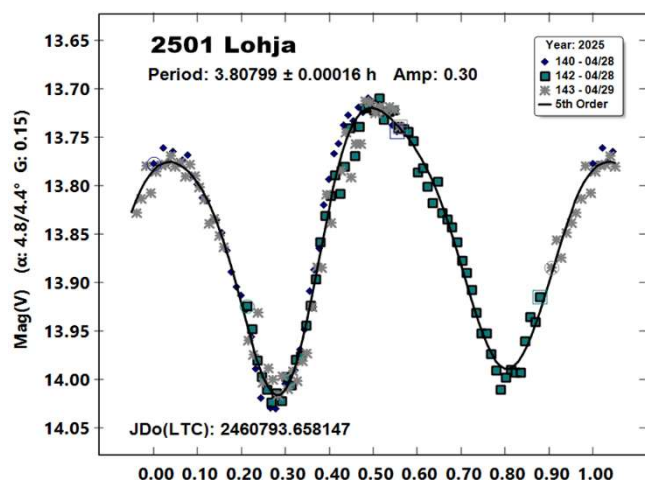
2159 Kukkamaki. This inner main-belt asteroid was discovered on 1941 Oct 16 at Turku by L. Oterma. We made observations on 2025 February 25 to March 16. From our data we derive a synodic rotation period of 3.7909 ± 0.0002 h and an amplitude of 0.35 mag. Behrend (2021web) found a period of 3.867 h. Binzel (1987) got results of 4.06 ± 0.02 h, slightly over estimating the later confirmed value.



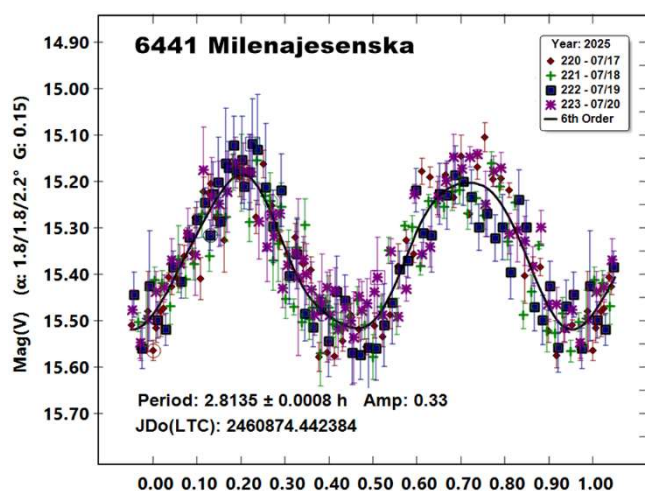
2501 Lohja. This inner main-belt asteroid was discovered on 1952 Apr. 14 at Turku by L. Oterma. We made observations on 2025 April 28 to 29. From our data we derive a synodic rotation period of 3.8080 ± 0.0002 h and an amplitude of 0.30 mag. Pravec (2006web, 2007web, 2010web and 2011web) found 8.8040, 8.80848, 8.80824 and 3.80912 h. Behrend (2006web, 2021web, 2022web) found a period of 8.807, 8.80847 and 3.8040 h. Husarik (2018) got 3.8081 h. Higgins (2005, 2011) found 3.8084 and 3.80865 h. Waszczak (2015) found 3.806 and 3.808 h. Franco et al. (2017) got 3.809 h. Overall, our data and most other results point most strongly to the 3.8 h values.

Number	Name	yyyy mm/dd	Phase	L _{PAB}	B _{PAB}	Period(h)	P.E.	Amp	A.E.	Grp
123	Brunhild	2025/03/26-30	9.8, 11.3	163.45	-5.35	9.8562	0.0015	0.15	0.03	MB-M
490	Veritas	2025/06/16-28	10.2, 12.3	235.90	9.80	7.965	0.005	0.22	0.03	MB-O
689	Zita	2025/06/25-29	6.6, 5.4	280.40	7.90	6.4264	0.0016	0.51	0.03	MB-I
872	Holda	2025/04/07	25.5	266.90	6.40	5.94499	0.00106	0.28	0.05	MB-M
1130	Skuld	2025/06/05-11	12.7, 15.6	233.20	1.25	4.802	0.002	0.43	0.05	MB-I
1152	Pawona	2025/04/16-18	10.8, 11.7	185.95	-4.40	3.41499	0.0001	0.19	0.03	MB-I
1257	Mora	2025/03/31-04/06	11.2, 13.8	168.65	-3.25	5.29574	0.00034	0.54	0.05	MB-I
1588	Descamisada	2025/05/28-06/06	10.3, 7.2	272.15	2.60	3.8236	0.0006	0.78	0.05	MB-O
1648	Shajna	2025/07/01-04	8.8, 6.9	290.20	3.10	6.412	0.002	0.59	0.03	MB-I
2159	Kukkamaki	2025/02/25-03/16	3.5, 6.1	163.20	0.55	3.7909	0.0002	0.35	0.05	MB-I
2501	Lohja	2025/04/28-29	4.9, 4.4	224.30	-2.60	3.8080	0.0002	0.30	0.03	MB-I
6441	Milenajesenska	2025/7/17-20	1.9, 2.1	295.40	2.45	2.8135	0.0008	0.33	0.05	MB-I

Table I. Observing circumstances and results. The phase angle is given for the first and last date. If preceded by an asterisk, the phase angle reached an extrema during the period. L_{PAB} and B_{PAB} are the approximate phase angle bisector longitude/latitude at mid-date range (see Harris et al., 1984). Grp is the asteroid family/group (Warner et al., 2009).



6441 Milenajesenska. This inner main-belt asteroid was discovered on 1988 Sep 9 at Klet by A. Mrkos. We made observations on 2025 July 17 to 20. From our data we derive a synodic rotation period of 2.8135 ± 0.0008 h and an amplitude of 0.33 mag. We have no previous information about its rotation period.



References

- Barucci, M.A.; Di Martino, M. (1984). "Rotational rates of very small asteroids - 123 Brunhild, 376 Geometria, 437 Rhodia and 1224 Fantasia." *Astron. Astrophys. Suppl. Ser.* **57**, 103-106.
- Behrend, R. (2002web, 2004web, 2005web, 2006web, 2007web, 2009web, 2010web, 2011web, 2017web, 2019web, 2021web, 2022web) Observatoire de Geneve web site.
http://obswww.unige.ch/~behrend/page_cou.html
- Binzel, R.P. (1987). "A photoelectric survey of 130 asteroids." *Icarus* **72**, 135-208.
- Brinsfield, J.W. (2007). "The Rotation Periods of 873 Holda, 3028 Zhangguoxi 3497 Innanen, 5484 Inoda, 5654 Terni, and 7304 Namiki." *Minor Planet Bull.* **34**, 108-110.
- Buchheim, R.K. (2010). "Lightcurve and Phase Curve of 1130 Skuld." *Minor Planet Bull.* **37**, 41-42.
- Dose, E.V. (2020). "A New Photometric Workflow and Lightcurves of Fifteen Asteroids." *Minor Planet Bull.* **47**, 324-330.
- Durech, J.; Hanus, J.; Vanco, R. (2019). "Inversion of asteroid photometry from Gaia DR2 and the Lowell Observatory photometric database." *Astron. Astrophys.* **631**, A2.
- Fauerbach, M.; Marks, S.A.; Lucas, M.P. (2008). "Lightcurve Analysis of Ten Main-belt Asteroids." *Minor Planet Bull.* **35**, 44-46.
- Franco, L.; Baj, G.; Tinella, V.; Bachini, M.; Succi, G.; Casalnuovo, G.B.; Bacci, P. (2017). "Rotation Periods for Three Main-belt Asteroids." *Minor Planet Bull.* **44**, 311-312.
- Franco, L.; Marchini, A.; Cavaglioni, L.; Papini, R.; Privitera, C.A.; Baj, G.; Galli, G.; Scarfi, G.; Aceti, P.; Banfi, M.; Bacci, P.; Maestripieri, M.; Mannucci, M.; Montigiani, N.; Tinelli, L.; Mortari, F. (2021). "Collaborative Asteroid Photometry from UAI: 2021 January-March." *Minor Planet Bull.* **48**, 219-222.
- Harris, A.W.; Young, J.W.; Scaltriti, F.; Zappala, V. (1984). "Lightcurves and phase relations of the asteroids 82 Alkmene and 444 Gypsis." *Icarus* **57**, 251-258.

Higgins, D.J. (2005). "Lightcurve periods for 1701 Okavango, 689 Zita, 981 Martina and (14653) 1998 YV11." *Minor Planet Bull.* **32**, 13-14.

Higgins, D.; Oey, J.; Pravec, P. (2011). "Period Determination of Binary Asteroid Targets Observed at Hunters Hill Observatory: May-September 2009." *Minor Planet Bull.* **38**, 46-49.

Husarik, M. (2018). "Shape model of the asteroid (2501) Lohja from long-term photometric observations." *Contrib. Astron. Obs. Skalnaté Pleso* **48**, 319-328. *arXiv:1803.00238*.

Klinglesmith, D.A., III; DeHart, A.; Hanowell, J.; Warrern, C.A. (2015). "Asteroids at Etscom: 490 Veritas, 3039 Yangel, 5492 Thoma." *Minor Planet Bull.* **42**, 12-13.

Klinglesmith III, D.A.; Hendrickx, S.; Kimber, C.; Madden, K. (2017). "CCD Asteroid Photometry from Etscom Observatory." *Minor Planet Bull.* **44**, 244-246.

Koff, R.A.; Brincat, S.M. (2001). "Lightcurve Photometry of Asteroid 490 Veritas." *Minor Planet Bull.* **28**, 67.

Koff, R.A.; Clark, M. (2002). "Lightcurve Photometry of 1152 Pawona." *Minor Planet Bull.* **29**, 49-50.

Kryszczyńska, A.; Colas, F.; Polinska, M.; Hirsch, R. and 26 colleagues (2012). "Do Slivan states exist in the Flora family? I. Photometric survey of the Flora region." *Astron. Astrophys.* **546**, A72.

Pilcher, F. (2016). "Rotation Period Determinations for 123 Brunhild, 314 Rosalia 346 Hermentaria, 633 Zelima, and 730 Athanasia." *Minor Planet Bull.* **43**, 222-224.

Pravec, P.; Wolf, M.; Sarounova, L. (2006web, 2007web, 2010web, 2011web). <http://www.asu.cas.cz/~ppravec/neo.htm>

Schmidt, R.E. (2017); "Near-IR Minor Planet Photometry from Burleigh Observatory." *Minor Planet Bull.* **44**, 191-192.

Sheridan, E.E. (2009). "Lightcurve Results for 99 Dike, 313 Chaldaea, 872 Holda 1274 Delporia, and 7304 Namiki." *Minor Planet Bull.* **36**, 55-56.

Skiff, B.A. (2018). Posting on CALL web site:
<https://minplanobs.org/MPInfo/php/call.php>

Stephens, R.D.; Coley, D.R.; Warner, B.D. (2021). "Main-belt Asteroids Observed from CS3: 2021 April-May." *Minor Planet Bull.* **48**, 380-387.

Warner, B.D.; Harris, A.W.; Pravec, P. (2009); "The Asteroid Lightcurve Database." *Icarus* **202**, 134-146. Updated 2016 Sep. <http://www.minorplanet.info/lightcurvedatabase.html>

Warner, B.D.; Harris, A.W.; Durech J.; Lance, A.M. (2025). "Lightcurve Photometry Opportunities: 2025 January - April." *Minor Planet Bull.* **52**, 90-93.

Waszczak, A.; Chang, C.-K.; Ofek, E.O.; Laher, R.; Masci, F.; Levitan, D.; Surace, J.; Cheng, Y.-C.; Ip, W.-H.; Kinoshita, D.; Helou, G.; Prince, T.A.; Kulkarni, S. (2015). "Asteroid Light Curves from the Palomar Transient Factory Survey: Rotation Periods and Phase Functions from Sparse Photometry." *Astron. J.* **150**, A75.

RESULTS OF OBSERVATIONS AND LIGHTCURVES FOR SIX ASTEROIDS

Rafael González Farfán (Z55)
Observatorio Uraniborg
Écija, Sevilla, SPAIN
uraniborg16@gmail.com

Faustino García de la Cuesta (J38)
La Vara, Valdés
Asturias, SPAIN

Javier Ruiz Fernández (J96)
Lucía Sánchez Blanco
Observatorio de Cantabria
Cantabria, SPAIN

Fernando Limón Martínez (Z50)
Observatorio Mazariegos
Mazariegos, Palencia, SPAIN

Carlos Botana Albá (Y85)
Observatorio en Magalofes
Fene, A Coruña, SPAIN

Esteban Reina Lorenz (232)
Masquefa, Can Parellada
Barcelona, SPAIN

Javier De Elías Cantalapiedra (L46)
Observatorio en Majadahonda
Madrid SPAIN

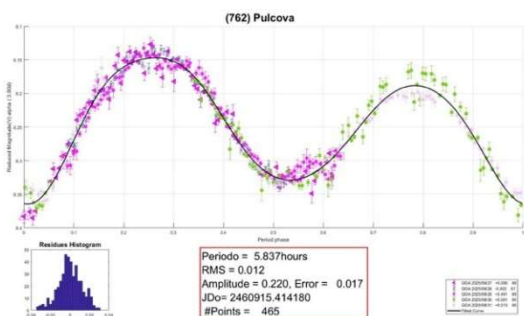
(Received: 2025 September 5)

We present results for six asteroids observed between May and August 2025: 762 Pulcova (5.837 h), 1818 Brahms (5.356 h), 1856 Ruzena (5.957 h), 3957 Sugie (9.731 h), 4117 Wilke (3.021 h) and 6015 Paularego (3.009 h).

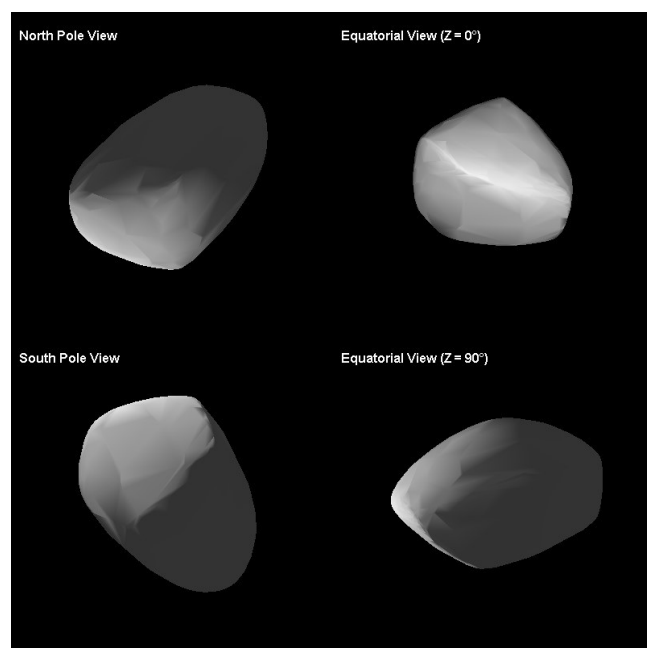
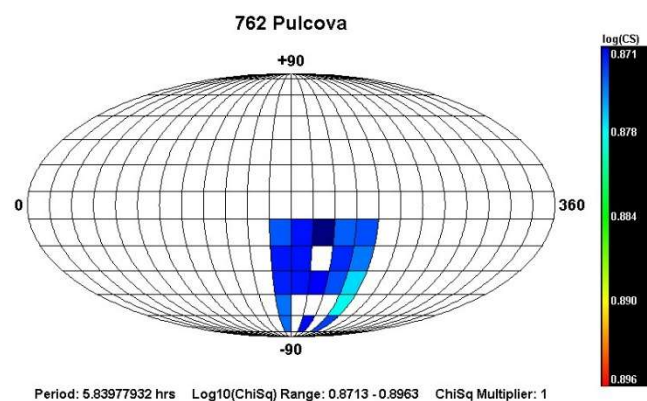
Here, we present a study of the rotation lightcurves of six asteroids conducted by our team between May and August 2025. As data on the rotation periods of most of these asteroids could not be found in the literature, we present our results in the hope that other observers will be able to confirm or refute them.

As on other occasions, the images obtained were calibrated in the conventional mode, without photometric filter, and with the application of darks, bias and flats. Data analysis and processing were performed using *FotoDif* (2021), *Tycho Tracker* (2023) and *Periodos* (2020) software. Besides, all data were light-time corrected. The results are summarized below. Individual light curve plots along additional comments as required are also presented.

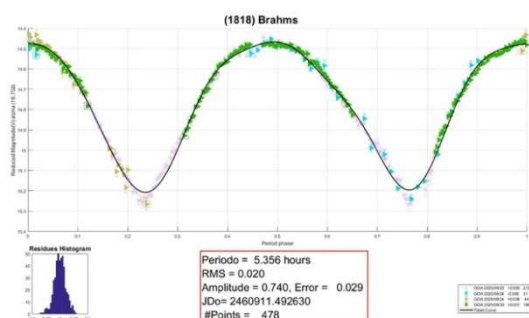
762 Pulcova. There is a wealth of information about this asteroid in the literature. We located one of the most recent light curves in the work of Martikainen et al. (2021). The results achieved by our team in August 2025 are consistent with those published previously: $P = 5.837 \pm 0.012$ hours, and $A = 0.220 \pm 0.017$ mag.



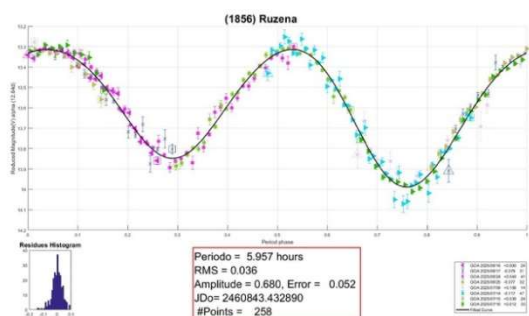
Furthermore, we combined our data with that published by ALCDEF in 2006 and 2020 and DAMIT, to propose a subsequent 3D model applying the lightcurve inversion method (Kaasalainen and Torppa, 2001) implemented in the MPO package *LCInvert* (BDW Publishing, 2016). We obtained a spin axis of $\Lambda = 192.398$, $B = -50.216$ and $P = 5.83977932$.



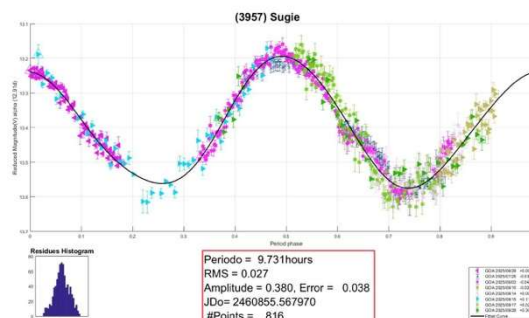
1818 Brahms. When we reached these results, we could not find any published data on the rotation of this asteroid or any 3D models in the literature. Our observations were carried out in August 2025. These allowed us to deduce a rotation period of $P = 5.356 \pm 0.020$ hours, and $A = 0.740 \pm 0.029$.



1856 Ruzena. The latest published work on the rotation period and lightcurve of this asteroid can be found in the paper by Lorea-González et al. (2019). These results are not significantly different to those obtained by our team in June 2025 or to those published in JPL or ALCDEF. Our observations enabled us to deduce the period, $P = 5.957 \pm 0.036$ hours, and $A = 0.680 \pm 0.052$.



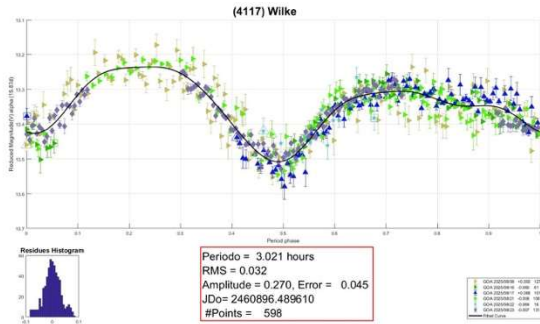
3957 Sugie. Our team observed this asteroid during June and August 2025. Until then, we had not found any published rotation curves, 3D models or periods in the literature, so we plotted its lightcurve. We were able to deduce a period $P = 9.731 \pm 0.027$ hours, and $A = 0.380 \pm 0.038$.



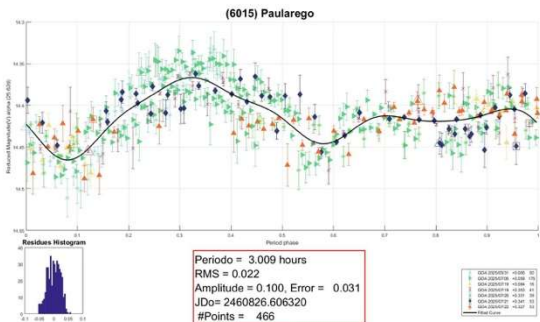
4117 Wilke. Although it was discovered in September 1982, we have been unable to find any publication of its lightcurve in the literature. We have also been unable to find any data on its rotation period or 3D model. We conducted an observation campaign for this asteroid in August 2025. Thanks to this, we were able to plot its light curve and deduce a rotation period of $P = 3.021 \pm 0.032$ hours, and $A = 0.270 \pm 0.045$.

Number	Asteroid	20yy mm/dd	Phase	Period(h)	P.E.	Amp	A.E.
762	Pulcova	25/08/27–25/08/31	4.0–3.4	5.837	0.012	0.220	0.017
1818	Brahms	25/08/25–25/08/30	17.7–14.9	5.356	0.020	0.740	0.029
1856	Ruzena	25/06/16–25/07/16	34.6–31.7	5.957	0.036	0.680	0.052
3957	Sugie	25/06/28–25/08/29	12.9–14.2	9.731	0.027	0.380	0.038
4117	Wilke	25/08/08–25/08/22	15.9–8.9	3.021	0.032	0.270	0.045
6015	Paularego	25/05/09–25/08/15	28.3–10.4	3.009	0.022	0.100	0.031

Table I. Observing circumstances and results. Phase is the solar phase angle given at the start and end of the date range. If preceded by an asterisk, the phase angle reached an extrema during the period.



6015 Paularego. In June 2025, our team observed this asteroid. Until then, we had found no published results in the literature regarding its rotation period, lightcurve or 3D model. Our work enabled us to deduce a rotation period $P = 3.009 \pm 0.022$ hours and an amplitude $A = 0.100 \pm 0.031$ magnitudes.



Observer	Telescope	Camera
Botana Alba, Carlos (Y85)	Newton 8"	ZWO ASI183M Pro
De Elias Cantalapiedra, Javier (L46)	CDK 12.5"	QHY 268m
García de la Cuesta, Faustino (J38)	RCX 10"	SBIG ST8XE
González Farfán, Rafael (Z55)	SC 11"	Atik414ex m
Limón Martínez, Fernando (Z50)	SC 8"	ZWO ASI533MM Pro
Reina Lorent, Esteban (Z32)	SC 10"	ZWO 294MM
Ruiz Fernández, Javier (J96) Lucía Sánchez Blanco	RC 16"	SBIG ST8XME

Table II. Observers and equipment used.

References

ALCDEF. Asteroid Lightcurve Data Exchange Format web site.
<http://alcdef.org>

DAMIT. <https://damit.cuni.cz/>

FotoDif (2021) software.
<http://astrosurf.com/orodeno/fotodif/index.htm>

JPL. Small-Body Database Lookup.
https://ssd.jpl.nasa.gov/tools/sbdb_lookup.html#/?sstr=52768

Kaasalainen, M.; Torppa, J. (2001). "Optimization Methods for Asteroid Lightcurve Inversion. I. Shape Determination." *Icarus* **153**, 24-36.

Loera-González, P.; Olguín, L.; Contreras, M.E.; Saucedo Morales, J.; Schuster, W.; Sada, P.V. (2019). "Results of the First Semester of the 2018 Mexican Asteroid Photometry Campaign." *Minor Planet Bull.* **46**, 283-285.

Martikainen, J.; Muinonen, K.; Penttilä, A.; Cellino, A.; Wang, X.-B. (2021). "Asteroid absolute magnitudes and phase curve parameters from Gaia photometry." *Astron. Astrophys.* **649**, A98.

MPO Canopus software.
<https://minplanobs.org/bdwpub/php/mpocanopus.php>

Períodos software (2020).
<http://www.astrosurf.com/salvador/Programas.html>

Tycho Tracker software (2023).
<https://www.tycho-tracker.com>

ROTATIONAL PERIODS AND LIGHTCURVES OF SEVEN ASTEROIDS

Sierra Kunigis
Kent Montgomery
East Texas A&M University
P.O. Box 3011
Commerce, TX 75429-3011
Kent.Montgomery@etamu.edu

(Received: 2025 October 6)

Rotational lightcurve period results were determined for seven main-belt asteroids through aperture photometry conducted with 1-meter class telescopes. 1276 Uccia: 4.8878 ± 0.0018 h, 1688 Wilkens: 7.246 ± 0.001 h, 5132 Maynard: 3.609 ± 0.001 h, 5656 Oldfield: 4.778 ± 0.001 h, 6377 Cagney: 4.185 ± 0.001 h, (7930) 1989 VD: 4.887 ± 0.001 h, and (17006) 1999 CH63 4.040 ± 0.008 h.

Introduction

Telescope research was conducted to determine the rotational periods and lightcurves of the following asteroids: 1276 Uccia, 1688 Wilkens, 5132 Maynard, 5656 Oldfield, 6377 Cagney, (7930) 1989 VD, and (17006) 1999 CH63. These asteroids were found in the MinorPlanet.info database (JPL, 2025) with their opposition date taking place roughly two weeks prior to the observation date, a magnitude between 15 and 16, an approximate declination between -15 and $+15$ degrees, and when known, a rotational period below 10 hours. *Airmass.org* (Wesson, 2025) was utilized to determine the relative air mass of the asteroid at any given time throughout the night. *TheSkyX Professional Edition v10.5.0* software (Software Bisque, 2024) was then used to determine if the asteroids would travel close to a brighter star within the observing field during its observational period.

As a brief historical summary, asteroid 1276 Uccia was discovered by E. Delporte on January 24, 1933, at the Royal Observatory of Belgium, located in the Uccle municipality of Brussels. It has a semi-major axis of 3.18 AU, an orbital eccentricity of 0.091, and an absolute magnitude of 10.81 (JPL, 2025). Asteroid 1688 Wilkens was discovered by M. Itzigsohn on March 3, 1951, at La Plata Astronomical Observatory, located in Buenos Aires, Argentina. It has a semi-major axis of 2.62 AU, an orbital eccentricity of 0.241, and an absolute magnitude of 12.75 (JPL, 2025). Asteroid 5132 Maynard was discovered by H.E. Holt on June 22, 1990, at the Palomar Observatory in San Diego, California. It has a semi-major axis of 2.67 AU, an orbital eccentricity of 0.115, and an absolute magnitude of 12.60 (JPL, 2025). Asteroid 5656 Oldfield was discovered by W. Baade on October 8, 1920, at the Hamburg Observatory located in the Bergedorf borough of the city of

Hamburg. It has a semi-major axis of 2.46 AU, an orbital eccentricity of 0.263, and an absolute magnitude of 14.50 (JPL, 2025). Asteroid 6377 Cagney was discovered by A. Mrkos on June 25, 1987, at the Klet' Observatory located in the Czech Republic. It has a semi-major axis of 2.62 AU, an orbital eccentricity of 0.162, and an absolute magnitude of 12.65 (JPL, 2025). Asteroid (7930) 1989 VD was discovered by S. Ueda and H. Kaneda on November 15, 1987, at the Kushiro City Marsh Observatory located in Japan. It has a semi-major axis of 2.25 AU, an orbital eccentricity of 0.253, and an absolute magnitude of 14.79 (JPL, 2025). Lastly, asteroid (17006) 1999 CH63 was discovered by LINEAR (Lincoln Near-Earth Asteroid Research) on February 12, 1999, at Socorro located in New Mexico. It has a semi-major axis of 2.59 AU, an orbital eccentricity of 0.187, and an absolute magnitude of 13.37 (JPL, 2025).

Methods

Imaging of the target fields was performed using both the Planewave CDK 700 27-inch telescope and the Planewave CDK 600 24-inch telescope located at the East Texas A&M University (ETAMU) Observatory, as well as the 0.6-m Cerro Tololo Inter-American Observatory (CTIO) telescope located in Chile. All three telescopes were equipped with Apogee Andor CCD cameras. The two cameras used at the ETAMU Observatory were thermoelectrically cooled to a temperature ranging between -20°C to -30°C . The camera used in Chile was thermoelectrically cooled to a temperature of -75°C . The light passed through a luminance filter before hitting the CCD camera for all three telescopes. On most nights, the telescopes were refocused every hour to account for the change in air mass and humidity. Every asteroid was observed over two to four nights.

New calibration images were taken each night including bias frames, dark frames, and twilight flat field images. Bias frames were taken at the start of each observation. Five to seven dark frames were captured using 180 second exposures to match the duration of the light frames with the exception of (17006) 1999 CH63 with 240 second exposures. Flat field images were taken during twilight ranging from an exposure time of 5 to 19 seconds. The number of flat field images obtained varied each night. A master image was created for each calibration type using *MaxIm DL* (Diffraction Limited). The master images were used to reduce the data for all the asteroid images.

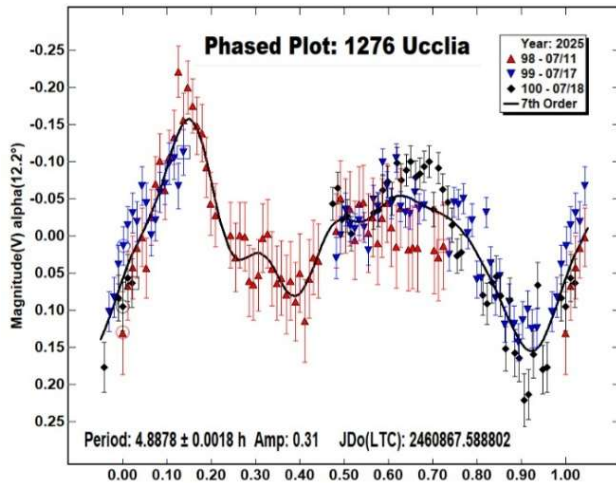
Aperture photometry was utilized to measure the relative brightness of the asteroids using five comparison stars in each image with *MPO Canopus v.10.8.1.1* software (Warner, 2011). For each 3-to-4-minute exposure, the difference in brightness between the asteroid and its comparison stars was calculated. These values were then plotted versus time to generate a lightcurve. If the asteroid was observed passing near or in front of a star, the data points were removed. A Fourier Transform was applied to the lightcurve to identify the most likely rotational period for each asteroid.

Number	Name	yyyy mm/dd	Phase	L_{PAB}	B_{PAB}	Period(h)	P.E.	Amp	A.E.	Grp
1276	Uccia	2025 07/11-07/18	12.1, 13.4	252	16.5	4.8878	0.0018	0.31	0.03	MB-O
1688	Wilkens	2024 09/27-10/03	13.7, 15.5	345.2	15.2	7.246	0.001	0.67	0.01	MB-M
5132	Maynard	2025 07/16-07/20	14.5, 15.8	267.7	13.5	3.609	0.001	0.63	0.01	MB-M
5656	Oldfield	2024 10/05-10/10	13.8, 16.2	354.1	5.5	4.778	0.001	0.23	0.03	MB-I
6377	Cagney	2025 06/17-06/25	15.5, 17.8	244.8	16.6	4.185	0.001	0.26	0.05	MB-M
7930	1987 VD	2024 09/14-09/26	18.4, 23.9	332.8	7.4	4.887	0.001	0.19	0.05	MB-I
17006	1999 CH63	2025 07/22-07/24	21.7, 22.2	263.4	17.1	4.040	0.008	0.15	0.05	MB-M

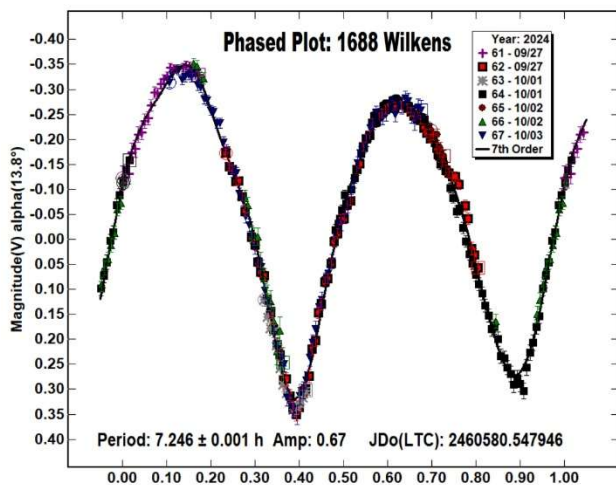
Table I. Observing circumstances and results. The phase angle is given for the first and last date. If preceded by an asterisk, the phase angle reached an extrema during the period. L_{PAB} and B_{PAB} are the approximate phase angle bisector longitude/latitude at mid-date range (see Harris et al., 1984). Grp is the asteroid family/group (Warner et al., 2009).

Results

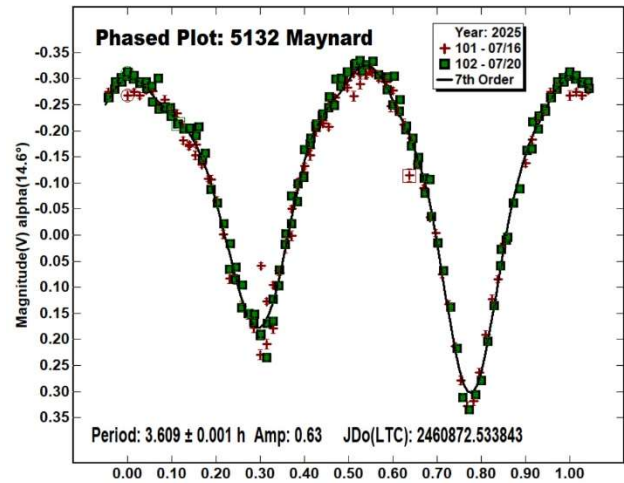
1276 Uccia. A total of 194 images were obtained over a three-night period using the ETAMU 24-inch telescope. The first night of observation was 2025, July 11 with a total of 69 images. The second night was 2025, July 17 with a total of 62 images. The third night was 2025, July 18 with a total of 63 images. The lightcurve analysis indicates a rotational period of 4.8878 ± 0.0018 h and an amplitude of 0.31 mag. This is slightly off compared to the most recent results of a previous study done by Galad et al. (2010) who found a rotational period of 4.9073 ± 0.0004 h.



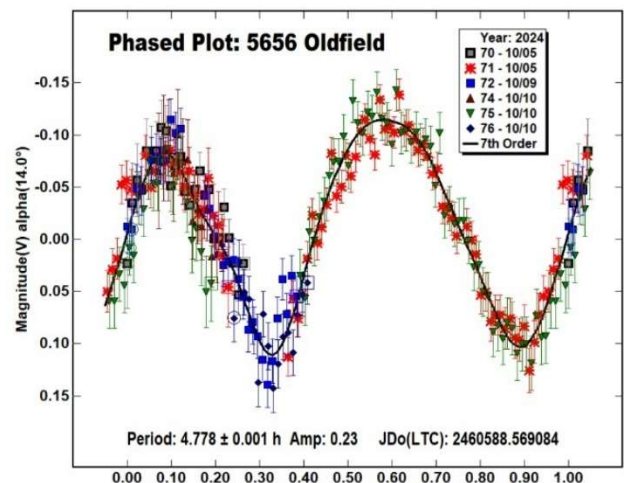
1688 Wilkens. A total of 390 images were obtained over a four-night period using the ETAMU 24-inch telescope. The first night of observation was 2024, September 27 with a total of 105 images. The second night was 2024, October 1 with a total of 100 images. The third night was 2024, October 2 with a total of 105 images. The fourth night was 2024, October 3 with a total of 80 images. The lightcurve analysis indicates a rotational period of 7.246 ± 0.001 h and an amplitude of 0.67 mag. This was extremely close to the rotational period found by Franco (2012) who found a rotational period of 7.248 ± 0.001 h and an amplitude of 0.23 mag.



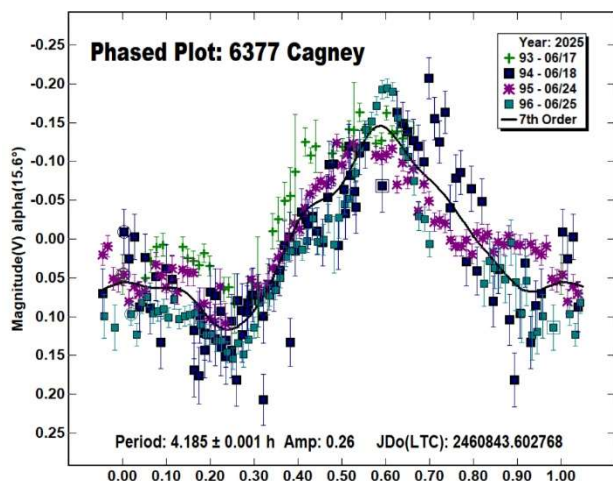
5132 Maynard. A total of 257 images were obtained over a two-night period using the 0.6-m CTIO telescope located in Chile. The first night of observation was 2025, July 16 with a total of 122 images. The second night was 2025, July 20 with a total of 135 images. The lightcurve analysis indicates a rotation period of 3.609 ± 0.001 h and an amplitude of 0.63 mag. This was similar to a previous study done by Pál et al. (2020) that did a result based on less than full coverage of its rotational period. The rotational period of 5132 Maynard was listed to be 3.6113 h in the Minor Planet Lightcurve Database (Warner et al., 2009).



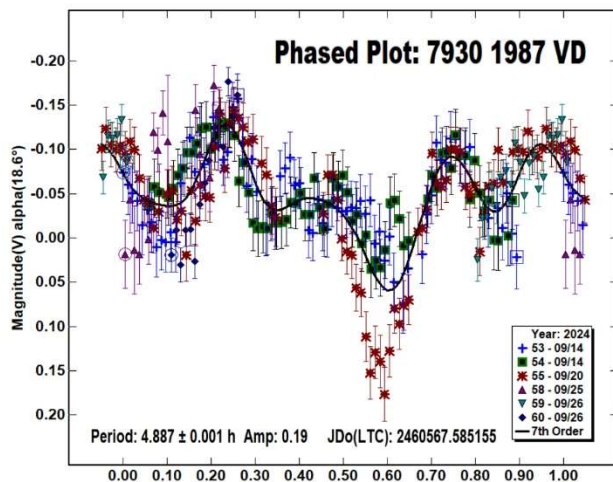
5656 Oldfield. A total of 254 images were obtained over a three-night period using the ETAMU 24-inch telescope and the ETAMU 27-inch telescope. The first night of observation was 2024, October 5 with a total of 105 images using the 24-inch telescope. The second night was 2024, October 9 with a total of 35 images using the 27-inch telescope. The third night of observation was 2024, October 10 with a total of 98 images using the 24-inch telescope and 16 images using the 27-inch telescope. The lightcurve analysis indicates a rotational period of 4.778 ± 0.001 h and an amplitude of 0.23 mag. No previous rotational period data for asteroid 5656 Oldfield was found in the Minor Planet Lightcurve Database (Warner et al., 2009) or the JPL Small-Body Database (JPL, 2025).



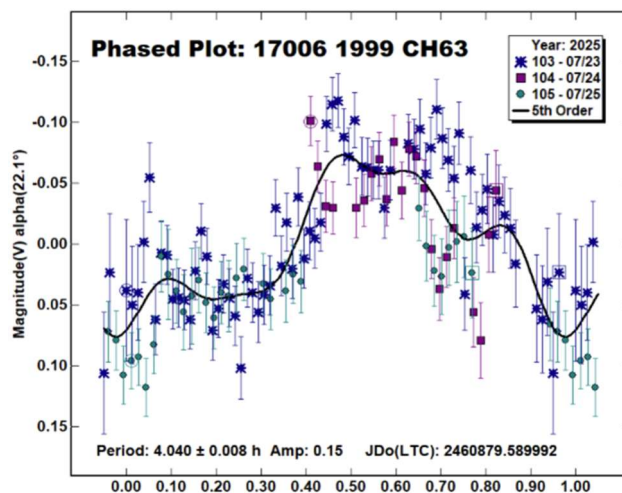
6377 Cagney. A total of 324 images were obtained over a four-night period using the ETAMU 24-inch telescope and the 0.6-m CTIO telescope located in Chile. The first night of observation was 2025, June 17 with a total of 44 images using the ETAMU 24-inch telescope. The second night was 2025, June 18 with a total of 113 images using the 0.6-m CTIO telescope. The third night of observation was 2025, June 24 with a total of 87 images using the 24-inch ETAMU telescope. The fourth night of observation was 2025, June 25 with a total of 80 images using the 24-inch ETAMU telescope. The lightcurve analysis indicates a rotational period of 4.185 ± 0.001 h and an amplitude of 0.26 mag. This was close to a previous study done by Galad (2009) who found a period of 4.171 ± 0.003 h.



7930 1987 VD. A total of 357 images were obtained over a four-night period using the ETAMU 24-inch telescope and the ETAMU 27-inch telescope. The first night of observation was 2024, September 14 with a total of 99 images using the 24-inch telescope and 82 images using the 27-inch telescope. The second night was 2024, September 20 with a total of 80 images using the 27-inch telescope. The third night of observation was 2024, September 25 with a total of 26 images using the 24-inch telescope. The fourth night of observation was 2024, September 26 with a total of 70 images on the 27-inch telescope. The lightcurve analysis indicates a rotational period of 4.887 ± 0.001 h and an amplitude of 0.19 mag. No previous rotational period data for asteroid 7930 1987 VD was found in the Minor Planet Lightcurve Database (Warner et al., 2009) or the JPL Small-Body Database (JPL, 2025).



(17006) 1999 CH63. A total of 170 images were obtained over a three-night period using the ETAMU 24-inch telescope. The first night of observation was 2025, July 23 with a total of 72 images. The second night was 2025, July 24 with a total of 52 images. The third night was 2025, July 25 with a total of 46 images. The lightcurve analysis shows a rotational period of 4.040 ± 0.008 h and an amplitude of 0.15 mag. This data is very tentative, as more than one rotational period equally fits the data. No previous rotational period data for asteroid (17006) 1999 CH63 was found in the Minor Planet Lightcurve Database (Warner et al., 2009) or the JPL Small-Body Database (JPL, 2025).



Acknowledgements

The National Science Foundation (NSF) grant no. 2050277 fully funded this research. This research was conducted as part of the Physics and Astronomy Research Experience for Undergraduates (REU) program at East Texas A&M University. This research was made possible through the use of the Cerro Tololo Inter-American Observatory and the East Texas A&M University Observatory.

References

- Diffraction Limited MaxIm DL - Astronomy and Scientific Imaging Software.
<https://diffractionlimited.com/product/maxim-dl/>
- Franco, L. (2012). "Lightcurve Photometry of 1688 Wilkens." *Minor Planet Bull.* **39**, 50.
- Galad, A. (2009). "Digest of Ten Lightcurves from Modra." *Minor Planet Bull.* **36**, 42-44.
- Galad, A.; Kornos, L.; Vilagi, J. (2010). "An Ensemble of Lightcurves from Modra." *Minor Planet Bull.* **37**, 9-15.
- Harris, A.W.; Young, J.W.; Scaltriti, F.; Zappala, V. (1984). "Lightcurves and phase relations of the asteroids 82 Alkmene and 444 Gyptis." *Icarus* **57**, 251-258.
- JPL (2025). Small-Body Database Search Engine.
<http://ssd.jpl.nasa.gov/sbdb.cgi>
- Pál, A.; Szakáts, R.; Kiss, C.; Bódi, A.; Bognár, Z.; Kalup, C.; Kiss, L.L.; Marton, G.; Molnár, L.; Plachy, E.; Sárneczky, K.; Szabó, G.; Szabó, R. (2020). "Solar System Objects Observed with TESS - First Data Release: Bright Main-belt and Trojan Asteroids from the Southern Survey." *Ap. J. Supl. Ser.* **247**, 26.

Software Bisque (2024). TheSkyX Professional Edition. Version 10.5.0. <https://www.bisque.com/product/theskysx-pro/>

Warner, B.D.; Harris, A.W.; Pravec, P. (2009). “The Asteroid Lightcurve Database.” *Icarus* **202**, 134-146. Updated 2023 Oct. <http://www.MinorPlanet.info/php/lcdb.php>

Warner, B.D. (2011). MPO Canopus software. Version 10.8.1.1. Bdw Publishing. <http://www.minorplanetobserver.com/>

Wesson, R. (2025). Airmass.org. National Optical-Infrared Astronomy Research Laboratory. <https://airmass.org/>. Accessed 2025.

COLLABORATIVE ASTEROID PHOTOMETRY FROM UAI: 2025 JULY - SEPTEMBER

Riccardo Papini, Marco Iozzi, Lorenzo Franco
UAI - Unione Astrofili Italiani, Rome, ITALY
riccardopapini.me@gmail.com

Giulio Scarfi
Iota Scorpis Observatory (K78), La Spezia, ITALY

Nello Ruocco
Osservatorio Astronomico Nastro Verde (C82), Sorrento, ITALY

Luca Buzzi
Schiaparelli Observatory (204), Varese, ITALY

Alessandro Marchini
Astronomical Observatory, University of Siena (K54)
Via Roma 56, 53100 - Siena, ITALY

Marco Iozzi
HOB Astronomical Observatory (L63)
Capraia Fiorentina, ITALY

Matteo Lombardo, Niccolò Lombardo
Zen Observatory (M26), Scandicci, ITALY

Gianni Galli
GiaGa Observatory (203), Pogliano Milanese, ITALY

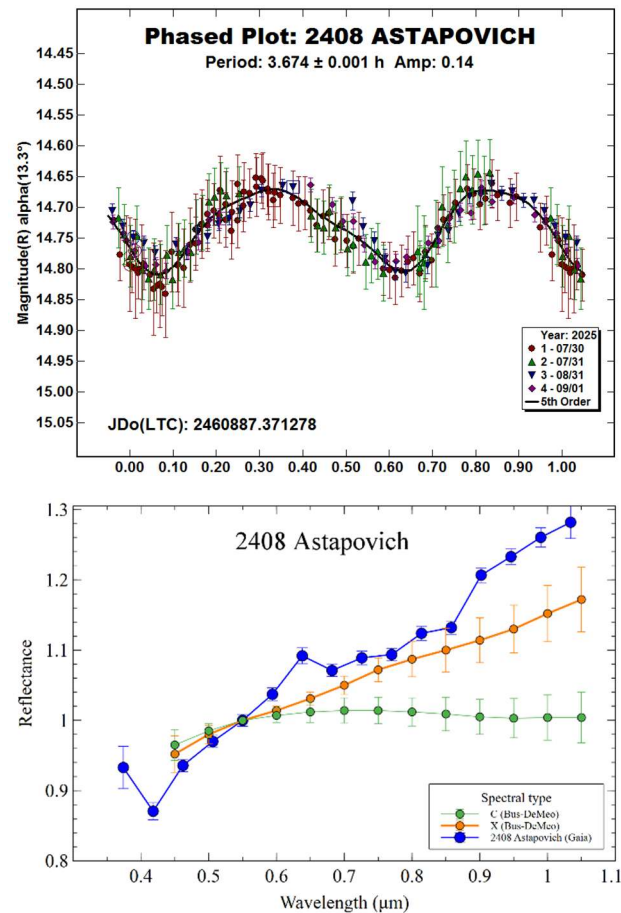
(Received: 2025 October 14)

Photometric observations of four asteroids were made in order to acquire lightcurves for shape/spin axis modeling. Lightcurves were acquired for 2408 Astapovich, 3578 Carestia, (19261) 1995 MB, and (35107) 1991 VH.

Collaborative asteroid photometry was done inside the Italian Amateur Astronomers Union (UAI, 2025) group. The targets were selected mainly in order to acquire lightcurves for shape/spin axis modeling. Table I shows the observing circumstances and results.

The CCD observations were made in 2025 July-September using the instrumentation described in Table II. Lightcurve analysis was done by R. Papini and M. Iozzi, belonging to the UAI group, with *MPO Canopus* (Warner, 2023). All the images were calibrated with dark and flat frames and converted to standard magnitudes using solar colored field stars from CMC15 and ATLAS catalogues, distributed with *MPO Canopus*. For brevity, “LCDB” is a reference to the asteroid lightcurve database (Warner et al., 2009)

2408 Astapovich is a low albedo middle main-belt asteroid. Collaborative observations were made over four nights. We found a bimodal solution with a synodic period of $P = 3.674 \pm 0.001$ h and an amplitude $A = 0.14 \pm 0.02$ mag. The period is close to the previously published results in the LCDB. The reflectance spectrum for 2408 Astapovich, extracted from Gaia ESA Archive (2025), is close to a X-type when compared with the Bus-DeMeo taxonomy (DeMeo et al., 2009) and agree also with the taxonomic attribution by Franco (2025).

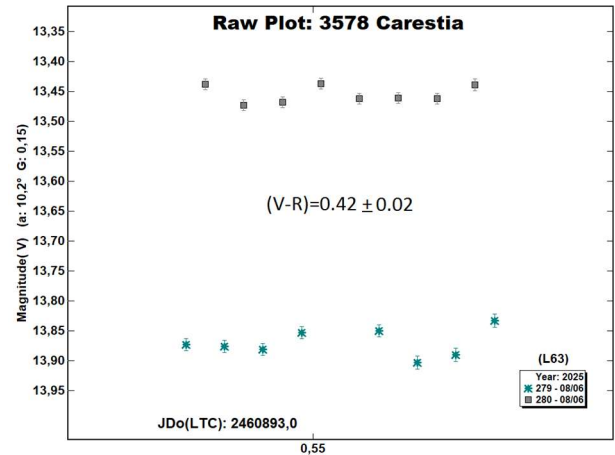
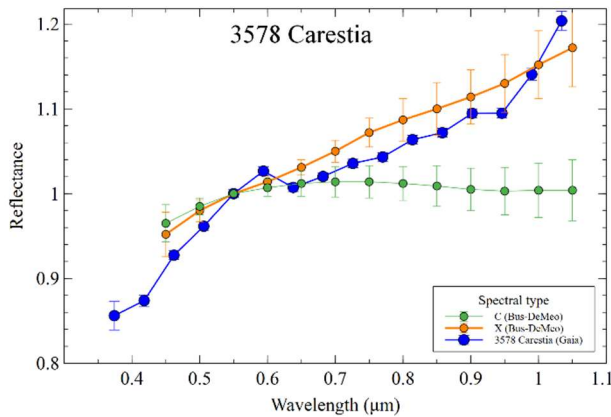
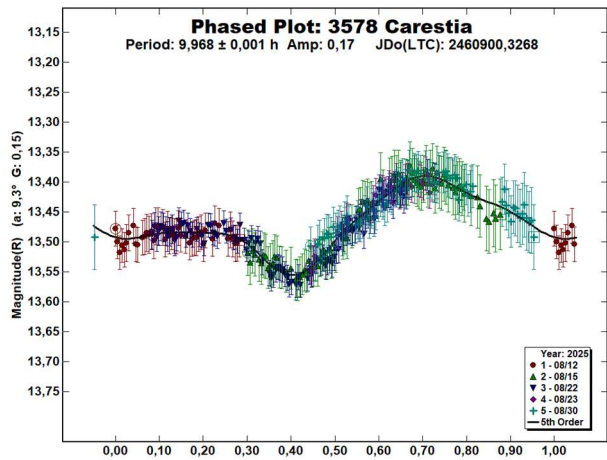


3578 Carestia is a low albedo outer main-belt asteroid. In September 2008, a rotational lightcurve was obtained from photometric observations made by Italian amateur astronomer Federico Manzini. It rendered it a rotation period of 9.93 ± 0.01 hours with a brightness variation of 0.13 in magnitude (Behrend, 2016web). Previously, a fragmentary lightcurve from the 1990s,

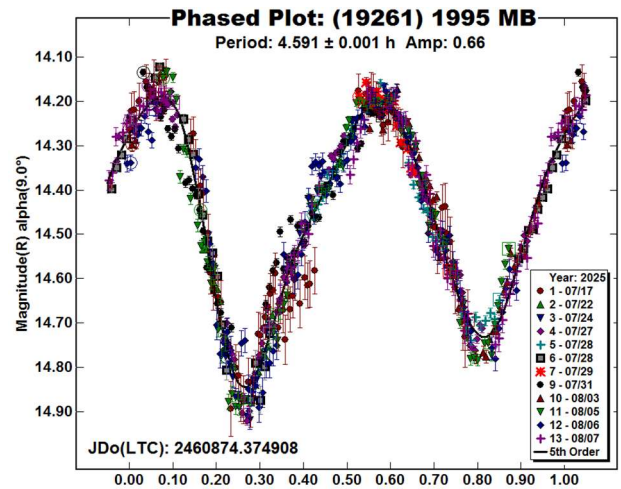
Number	Name	2025 mm/dd	Phase	L _{PAB}	B _{PAB}	Period(h)	P.E.	Amp	A.E.	Grp
2408	Astapovich	07/30-09/01	*13.3, 5.7	329	7.6	3.674	0.001	0.14	0.02	MB-M
3578	Carestia	08/12-08/30	* 9.2, 10.6	326	19	9.968	0.001	0.17	0.03	MB-O
19261	1995 MB	07/17-08/07	9.2, 17.0	297	14.8	4.591	0.001	0.66	0.07	MB-I
35107	1991 VH	07/09-07/14	80.0, 84.1	317	41	2.625	0.001	0.16	0.02	NEA

Table I. Observing circumstances and results. The first line gives the results for the primary of a binary system. The second line gives the orbital period of the satellite and the maximum attenuation. The phase angle is given for the first and last date. If preceded by an asterisk, the phase angle reached an extrema during the period. L_{PAB} and B_{PAB} are the approximate phase angle bisector longitude/latitude at mid-date range (see Harris et al., 1984). Grp is the asteroid family/group (Warner et al., 2009).

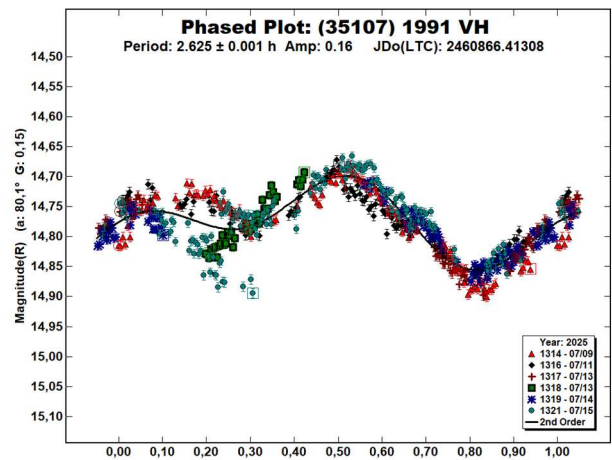
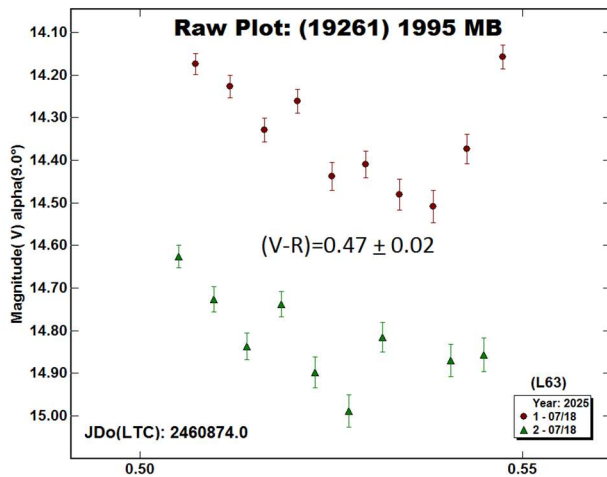
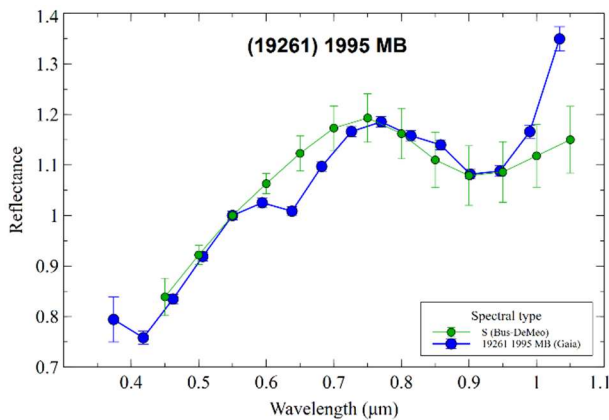
gave a shorter period of 7.1 hours with an amplitude of 0.25 (Holliday, 1997). Our collaborative observations were made over six nights. We found a bimodal solution with a synodic period of $P = 9.968 \pm 0.001$ h and an amplitude $A = 0.17 \pm 0.03$ mag. The reflectance spectrum for 3578 Carestia, extracted from Gaia ESA Archive (2025), is close to a X-type when compared with the Bus-DeMeo taxonomy (DeMeo et al., 2009) and agree also with the taxonomic attribution by Franco (2025). Multiband photometry was acquired by M. Iozzi (L63) on 2025 August 5, from which we found a color index $V-R = 0.42 \pm 0.02$, consistent with a M-Type asteroid (Shevchenko and Lupishko, 1998; 0.42 ± 0.04).



(19261) 1995 MB is an inner main-belt asteroid. Collaborative observations were made over eleven nights. We found a bimodal solution with a synodic period of $P = 4.591 \pm 0.001$ h and an amplitude $A = 0.66 \pm 0.07$ mag, which is in agreement with the previously published results in the LCDB. The reflectance spectrum for (19261) 1995 MB, extracted from Gaia ESA Archive (2025), is close to a S-type when compared with the Bus-DeMeo taxonomy (DeMeo et al., 2009) and agree also with the taxonomic attribution by Franco (2025). Multiband photometry was acquired by M. Iozzi (L63) on 2025 July 18 and by M. Lombardo (M26) on 2025 August 5, from which we found a mean color index $V-R = 0.47 \pm 0.02$, consistent with a S-Type asteroid (Shevchenko and Lupishko, 1998; 0.49 ± 0.05).



Observatory (MPC code)	Telescope	CCD	Filters	Observed Asteroids (#Sessions)
Iota Scorpii (K78)	0.40-m RCT f/6.1	Player One 455M Pro (bin 4×4)	Rc	19261 (2), 3578 (5), 2408 (2)
Osservatorio Astronomico Nastro Verde (C82)	0.35-m SCT f/6.3	SBIG ST10XME (bin 2×2)	C	19261 (8)
Schiaparelli Observatory (204)	0.84-m NRT f/3.5	Moravian C3-61000 PRO (bin 4×4)	C	35107 (4)
Astronomical Observatory, University of Siena (K54)	0.30-m MCT f/5.6	SBIG STL-6303e (bin 2×2)	C	2408 (2)
HOB Astronomical Observatory (L63)	0.20-m SCT f/6.0	ATIK 383L+ (bin 2×2)	V,Rc	19261 (1), 3578 (1)
Zen Observatory (M26)	0.30-m RCT f/7.4	ATIK 383L+ (bin 2×2)	C,V,Rc	19261 (2)
GiaGa Observatory (203)	0.36-m SCT f/5.8	Moravian G2-3200	C	19261 (1)



References

- Behrend, R. (2016web). "Asteroids and comets rotation curves - (3578) Ceresia." Observatoire de Geneve web site. http://obswww.unige.ch/~behrend/page_cou.html
- Bus, S.J.; Binzel, R.P. (2002). "Phase II of the Small Main-Belt Asteroid Spectroscopic Survey: A Feature-Based Taxonomy." *Icarus* **158**, 146-177.
- DeMeo, F.E.; Binzel, R.P.; Slivan, S.M.; Bus, S.J. (2009). "An extension of the Bus asteroid taxonomy into the near infrared." *Icarus* **202**, 160-180.
- Franco, L. (2025). "On The Gaia Reflectance Spectra." *Minor Planet Bulletin* **52**, 351-354.
- Gaia ESA Archive (2025), version 3.7. <https://gea.esac.esa.int/archive/>
- Harris, A.W.; Young, J.W.; Scaltriti, F.; Zappala, V. (1984). "Lightcurves and phase relations of the asteroids 82 Alkmene and 444 Gypsis." *Icarus* **57**, 251-258.
- Holliday, B. (1997). "Photometric Observations of Minor Planet 3578 Ceresia." *The Minor Planet Bulletin* **24**, 1.
- JPL (2025). Small Body Database Search Engine. <https://ssd.jpl.nasa.gov>

(35107) 1991 VH is a binary near-Earth asteroid and potentially hazardous of the Apollo group. Discovered in 1991, by Australian astronomer Robert McNaught at Siding Spring Observatory, this binary system is composed of a roughly-spheroidal primary body and an elongated natural satellite. (Naidu et al., 2018). Photometric observations in 1997 determined a primary rotation period of 2.624 hours, with a lightcurve amplitude of 0.08 ± 0.01 magnitudes ($U=3$) (Pravec et al., 1998). Observations by L. Buzzi (204) were made over four nights. We found a bimodal solution with a synodic period of $P = 2.265 \pm 0.001$ h and an amplitude $A = 0.16 \pm 0.02$ mag. The folded lightcurve shows evidence of eclipsing events but the data are not enough to working out a precise orbital period of the satellite.

Naidu, S.; Margot, J.-L.; Benner, L.; Taylor, P.A.; Nolan, M.C.; Magri, C.; et al. (2018). “Radar Observations and Characterization of Binary Near-Earth Asteroid (35107) 1991 VH.” AAS, DPS Meeting #50, id.312.09.

Pravec, P.; Harris, A.W.; Kušnirák, P.; Galád, A.; Hornoch, K. (2012). “Absolute magnitudes of asteroids and a revision of asteroid albedo estimates from WISE thermal observations.” *Icarus* **221**, 365-387.

Shevchenko, V.G.; Lupishko, D.F. (1998). “Optical properties of Asteroids from Photometric Data.” *Solar System Research* **32**, 220-232.

UAI (2025). “Unione Astrofili Italiani” web site. <https://www.uai.it>

Warner, B.D.; Harris, A.W.; Pravec, P. (2009). “The Asteroid Lightcurve Database.” *Icarus* **202**, 134-146. Updated 2016 Sep. <http://www.minorplanet.info/lightcurvedatabase.html>

Warner, B.D. (2023). MPO Software, MPO Canopus v10.8 Bdw Publishing. <http://minorplanetobserver.com>

LIGHTCURVES AND ROTATION PERIODS OF 1858 LOBACHEVSKIJ AND 6394 1990 QM2

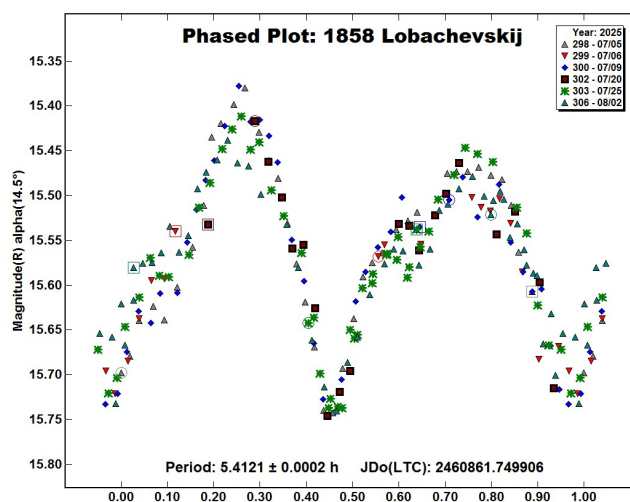
Frederick Pilcher
Organ Mesa Observatory (G50)
4438 Organ Mesa Loop
Las Cruces, NM 88011 USA
fpilcher35@gmail.com

(Received: 2025 August 25)

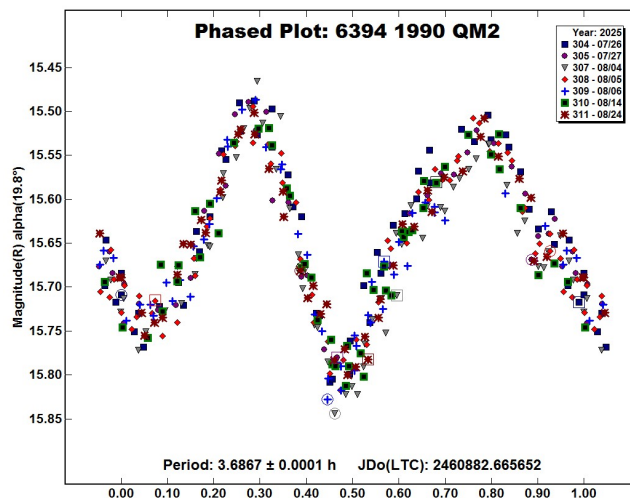
Synodic rotation periods and amplitudes are found for 1858 Lobachevskij 5.4121 ± 0.0002 hours, 0.30 ± 0.02 magnitudes; and (6394) 1990 QM2 3.6867 ± 0.0001 hours, 0.28 ± 0.03 magnitudes.

The new observations to produce the results reported in this paper were made at the Organ Mesa Observatory with a Meade 35 cm LX200 GPS Schmidt-Cassegrain, SBIG STL-1001E CCD, 120 second exposures, unguided, clear filter. Image measurement and lightcurve construction were with *MPO Canopus* software with calibration star magnitudes for solar colored stars from the CMC15 catalog reduced to the Cousins R band. Zero-point adjustments of a few $\times 0.01$ magnitude were made for best fit. To reduce the number of data points on the lightcurves and make them easier to read, data points have been binned in sets of 3 with maximum time difference 6 minutes.

1858 Lobachevskij. Ditteon et al. (2002) published a period of 7.00 hours based on data 2002 May 2-4. A second set of sessions by Ditteon et al. (2012) found a period of 5.413 hours based on data 2011 May 25-28. In this same paper the 7.00-hour period found in 2002 was corrected to 5.435 hours. Waszczak et al. (2015), based entirely on sparse data from the Palomar transient factory survey during the 2012 opposition, published a period of 5.414 hours. New observations on six nights 2025 July 5 - August 2 provide a good fit to a period 5.4121 ± 0.0002 hours, amplitude 0.30 ± 0.02 magnitudes. This new result is compatible with the periods found by Ditteon et al. 2011 observations, by Waszczak et al. 2015 observations, and fairly close to the period by Ditteon et al. 2001 observations, as corrected.



(6394) 1990 QM2. Six separate studies of the rotation period of this object, well distributed around the sky, all but one of which found values between 3.681 hours and 3.6888 hours, have been referenced by Warner et al. in “The Asteroid Lightcurve Database,” (2009, updated 2023 October). New observations on seven nights 2025 July 26 - August 24 provide a good fit to a period 3.6867 ± 0.0001 hours, amplitude 0.28 ± 0.03 magnitudes, and representing 190 rotational cycles. This value is compatible with many other published values.



Number	Name	yyyy/mm/dd	Phase	L _{PAB}	B _{PAB}	Period(h)	P.E	Amp	A.E
1858	Lobachevskij	2025/07/05–2025/08/02	14.5 – 2.8	314	1	5.4121	0.0002	0.30	0.02
6394	1990 QM2	2025/07/26–2025/08/24	19.8 – 7.6	326	13	3.6867	0.0001	0.28	0.03

Table I. Observing circumstances and results. The phase angle is given for the first and last date, unless a minimum (second value) was reached. L_{PAB} and B_{PAB} are the approximate phase angle bisector longitude and latitude at mid-date range (see Harris et al., 1984).

References

- Ditteon, R.; Bixby, A.R.; Sarros, A.M.; Waters, C.T. (2002). “Rotational periods and lightcurves of 1858 Lobachevskij, 2384 Schulhof, and (5515) 1989 EL1.” *Minor Planet Bull.* **29**, 69.
- Ditteon, R.; Horn, L.; Kamperman, A.; Vorjohan, B.; Kirkpatrick, E. (2012). “Asteroid lightcurve analysis at the Oakley Southern Sky Observatory, 2011 April to May.” *Minor Planet Bull.* **39**, 26-28.
- Harris, A.W.; Young, J.W.; Scaltriti, F.; Zappala, V. (1984). “Lightcurves and phase relations of the asteroids 82 Alkmene and 444 Gyptis.” *Icarus* **57**, 251-258.
- Warner, B.D., Harris, A.W., Pravec, P. (2009). “The Asteroid Lightcurve Database.” *Icarus* **202**, 134-146. Updated 2023 Oct. <https://minplanobs.org/MPInfo/php/lcdb.php>
- Waszczak, A.; Chang, C.-K.; Ofeck, E.O.; Laher, F.; Masci, F.; Levitan, D.; Surace, J.; Cheng, Y.-C.; Ip, W.-H.; Kinoshita, D.; Helou, G.; Prince, T.A.; Kulkarni, S. (2015). “Asteroid light curves from the Palomar transient factory survey: rotation periods and phase functions from sparse photometry.” *The Astronomical Journal* **150**, 75pp. <https://dx.doi.org/10.1088/0004-6256/150/3/75>

PHOTOMETRIC OBSERVATIONS OF THE MARTIAN TROJAN ASTEROID (311999) 2007 NS2

Galin Borisov

Institute of Astronomy and National Astronomical Observatory,
Bulgarian Academy of Sciences
72 Tsarigradsko Chaussée Blvd., BG-1784 Sofia, BULGARIA
gborisov@nao-rozhen.org

Apostolos A. Christou

Armagh Observatory and Planetarium,
Armagh, BT61 9DG, Northern Ireland, UK

(Received: 2025 September 30)

We present R filter photometry of the Martian Trojan asteroid (311999) 2007 NS2, carried out with the two-channel Focal Reducer Rozhen (FoReRo2) at the 2-m Ritchey-Chrétien-Coude (2mRCC) telescope of the Bulgarian National Astronomical Observatory (BNAO) Rozhen for 3 nights in August 2024. The lightcurve analysis suggests a rotation period of $P=6.864\pm0.067$ h with an amplitude $A=0.14$ mag.

The asteroid (311999) 2007 NS2 (NS2 hereafter) is an L_S Martian Trojan (MT), trailing $\sim 60^\circ$ behind the planet as it orbits the Sun. The asteroid is also the second largest member - after (5261) Eureka - of a small dynamical family of L_S Trojan asteroids (Christou, 2013; de la Fuente Marcos & de la Fuente Marcos, 2013) that may be the product of rotational spin-up and fission due to the YORP effect, or collisional fragmentation of a Trojan progenitor (Christou, 2013; Čuk et al., 2015; Christou et al., 2017; 2020; 2025). To test

these hypotheses, it is important to determine the rotational states of MTs. Rotational state information already exists for (5261) Eureka (Koehn et al., 2014) and a photometric campaign that we began in 2015 has produced rotational period estimates for all other MTs with $H<19$ (Borisov et al., 2016; Borisov et al., 2018; Christou et al., 2020).

We observed NS2 during 3 nights in August 2024 with the 2-m Ritchey-Chrétien-Coude (2mRCC) telescope at the Bulgarian National Astronomical Observatory (BNAO) in Rozhen equipped with a two-channel Focal Reducer Rozhen (FoReRo2) and Bessell R filter. Standard data reduction with bias and flat fields was performed on the raw data. Aperture photometry was carried out with an aperture size of $2\times\text{FWHM}$ to maximize the obtained S/N.

Before the period analysis, we compute the average R magnitude of the target for each night and use these averages to shift the measurements for all nights to the same zero datum. We then perform a Levenberg-Marquardt least-squares fit of these relative measurements to a Fourier function of order 5. We obtain a rotational period of $P = 6.86 \pm 0.02$ h and an amplitude of $A = 0.14$ mag. We then perform a χ -squared minimization with the same Fourier function and probe periods in the range from 6.4 to 7.4 hours around the initial estimate. The results, shown on the bottom panel of Figure 1, are as follows: $P = 6.864$ h with $1-\sigma = -0.065$ h, $+0.069$ h; $2-\sigma = -0.085$ h; $+0.088$ h; $3-\sigma = -0.107$ h; $+0.105$ h. A statistically identical estimate was obtained by processing the photometric data with an online implementation of the Lomb-Scargle (L-S) algorithm (Scargle, 1982) available through the NASA Exoplanet Archive (Christiansen et al., 2025). This method estimates the period of a harmonic function with a single minimum and maximum (See Figure 1 - top panel).

Number	Name	yyyy/mm/dd	Phase	L _{PAB}	B _{PAB}	Period(h)	P.E.	Amp	A.E.	Grp
311999	2007 NS2	2024 08/01–08/03	24.16, 23.40	329	21	6.864	0.067	0.14	–	EUR

Table I. Observing circumstances and results. The phase angle is given for the first and last date. If preceded by an asterisk, the phase angle reached an extrema during the period. L_{PAB} and B_{PAB} are the approximate phase angle bisector longitude/latitude at mid-date range (see Harris et al., 1984). Grp is the asteroid family/group (Warner et al., 2009) EUR Eureka family Martian Trojans.

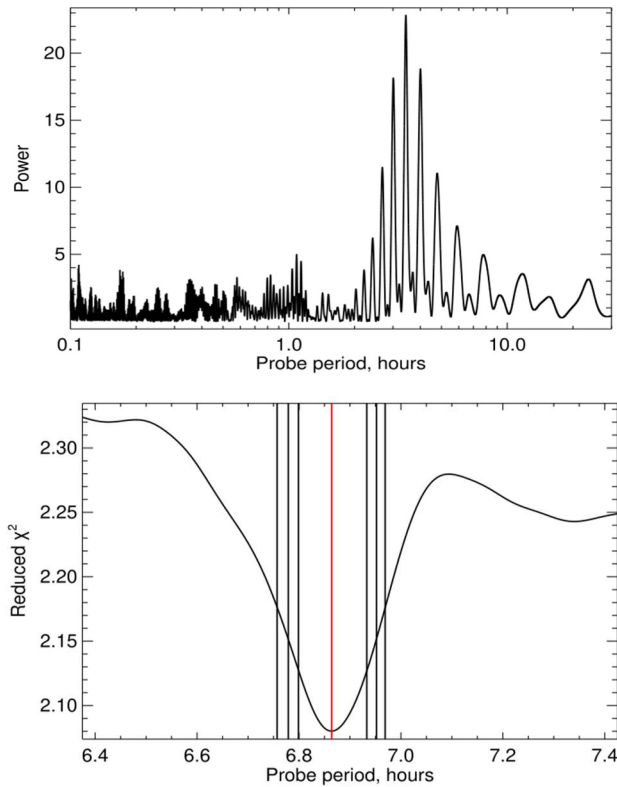


Figure 1. *Top panel:* Power spectrum of the photometric data using the NASA Exoplanet Archive online periodogram tool. *Bottom panel:* Reduced χ -square function around the estimated rotational period (red vertical line) and 1-, 2- and 3- σ uncertainties (black vertical lines).

The final lightcurve and fitted Fourier function of order 5 are presented at Figure 2. We assign to our determined period solution a quality code U=2 (Warner et al., 2009) as it is unlikely that our nominal estimates are off by a factor of 2 or more.

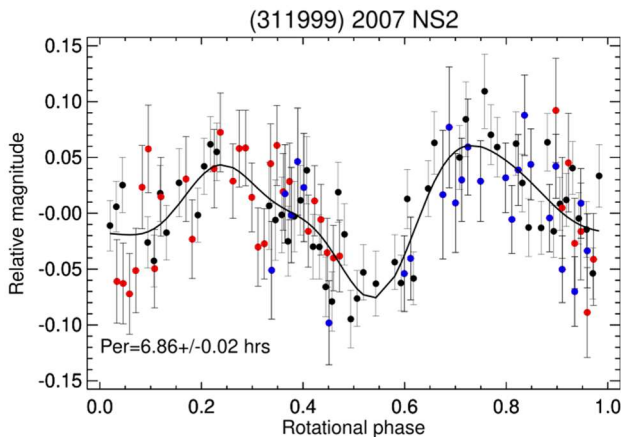


Figure 2. Lightcurve of the Martian Trojan asteroid (311999) 2007 NS2 with fitted Fourier function of order 5 and rotational period solution. Different colours indicate the observing night: black, red and blue for 1, 2 and 3 August 2024, respectively.

Acknowledgments

G.B. acknowledges partial support from grant KP-06-H88/5 by the Bulgarian National Science Fund. Authors gratefully acknowledge observing grant support from the Institute of Astronomy and

Rozhen National Astronomical Observatory, Bulgarian Academy of Sciences. This research has made use of the NASA Exoplanet Archive, operated by the California Institute of Technology, under contract with the National Aeronautics and Space Administration under the Exoplanet Exploration Program. Astronomical research at the Armagh Observatory and Planetarium is grant-aided by the Northern Ireland Department for Communities (DfC).

References

- Borisov, G.; Christou, A.A.; Unda-Sanzana, E. (2016). "Photometric Observations of Martian Trojan Asteroids." *Minor Planet Bull.* **43**, 216-217.
- Borisov, G.; Christou, A.A.; Colas, F.; Bagnulo, S.; Cellino, A.; Dell'Oro, A. (2018). "(121514) 1999 UJ₇: A Primitive, Slow-rotating Martian Trojan." *Astron. Astrophys.* **618**, A178, 8pp.
- Christiansen, J.L.; McElroy, D.L.; Harbut, M.; Ciardi, D.R.; Crane, M.; Good, J.; Hardegree-Ullman, K.K.; Kesseli, A.Y.; Lund, M.B.; Lynn, M.; Muthiar, A.; Nilsson, R.; Oluyide, T.; Papin, M.; Rivera, A.; Swain, M.; Susemihl, N.D.; Tam, R.; van Eyken, J.; Beichman, C. (2025). "The NASA Exoplanet Archive and Exoplanet Follow-up Observing Program: Data, Tools, and Usage." *Planet. Sci. J.* **6**, 186, 14pp.
<https://exoplanetarchive.ipac.caltech.edu/cgi-bin/Pgram/nph-pgram>
- Christou, A.A. (2013). "Orbital Clustering of Martian Trojans: An Asteroid Family in the Inner Solar System?" *Icarus* **224**, 144-153.
- Christou, A.A.; Borisov, G.; Dell'Oro, A.; Cellino, A.; Bagnulo, S. (2017). "Is the Eureka Cluster a Collisional Family of Mars Trojan Asteroids?" *Icarus* **293**, 243-258.
- Christou, A.A.; Borisov, G.; Dell'Oro, A.; Jacobson, S.A.; Cellino, A.; Unda-Sanzana, E. (2020). "Population Control of Mars Trojans by the Yarkovsky & YORP Effects." *Icarus* **335**, 113370.
- Christou, A.A.; Georgakarakos, N.; Marshall-Lee, A.; Humpage, A.; Ćuk, M.; Dell'Oro, A. (2025). "New Asteroid Clusters and Evidence of Collisional Fragmentation in the L₅ Trojan Cloud of Mars." *Astron. Astrophys.* **698**, A42, 11pp.
- Ćuk, M.; Christou, A.A.; Hamilton, D.P. (2015). "The Yarkovsky-driven Spreading of the Eureka Family of Mars Trojans." *Icarus* **252**, 339-346.
- de la Fuente Marcos, C.; de la Fuente Marcos, R. (2013). "Three New Stable L₅ Martian Trojans." *Mon. Not. Royal Astron. Soc.* **432**, 31-35.
- Harris, A.W.; Young, J.W.; Scaltriti, F.; Zappala, V. (1984). "Lightcurves and phase relations of the asteroids 82 Alkmene and 444 Gyptis." *Icarus* **57**, 251-258.
- Koehn, B.W.; Bowell, E.G.; Skiff, B.A.; Sanborn, J.J.; McLelland, K.P.; Pravec, P.; Warner, B.D. (2014). "Lowell Observatory Near-Earth asteroid photometric survey (NEAPS) - 2009 January through 2009 June." *Minor Planet Bull.* **41**, 286-300.
- Scargle, J.D. (1982). "Studies in Astronomical Time Series Analysis II: Statistical Aspects of Spectral Analysis of Unevenly Spaced Data." *Astrophys. J.* **26**, 835-853.
- Warner, B.D.; Harris, A.W.; Pravec, P. (2009). "The Asteroid Lightcurve Database." *Icarus* **202**, 134-146.

ASTEROID PHOTOMETRY FROM THE DUNWURKIN OBSERVATORY

Dr. Maurice Clark
ozprof@yahoo.com

(Received: 2025 August 13)

Asteroid period and amplitude results obtained at the Dunwurkin Observatory in Koorda Western Australia during January 2024 and June 2025 are presented.

During January 2024 and June 2025, I was able to visit my observatory in Koorda, Western Australia. The main instrument used for the results presented here was a 14" $f/11$ Schmidt-Cassegrain with an $f/6.3$ focal reducer, giving an effective focal length of $f/7$, and an SBIG STL-1001E CCD. Also used was a 5" $f/5$ refractor with an SBIG ST8XE CCD. The 14" images were unfiltered while the 5" images were taken using a clear filter. All images were reduced with dark frames and twilight sky flats.

Image analysis was accomplished using differential aperture photometry with *MPO Canopus*. Period analysis was also done in Canopus. Differential magnitudes were calculated using reference stars from the UCAC4 catalog. The results are summarized in the table below, and the lightcurve plots are presented at the end of the paper.

2778 Tangshan. Observations of this asteroid were made on 2 nights when it was in the same field as another asteroid I was observing. The derived period is in close agreement with those recorded on the Asteroid Lightcurve Database. (LCDB, Warner et al., 2009).

4620 Bickley. Observations were made over 3 nights. The resulting lightcurve was very asymmetric and is uncertain. A search of the Asteroid Lightcurve Database did not reveal any previously reported period for this asteroid.

4671 Drtikol. Observations of this asteroid were made on 5 nights when it was in the same field as another asteroid I was observing. Despite a large scatter in the data, the derived period is in close agreement with that derived by Benishek (2024).

4685 Karetnikov. Observations were made over 8 nights. The resulting lightcurve was very scattered and the period result is highly uncertain. A search of the Asteroid Lightcurve Database did not reveal any previously reported period for this asteroid.

5602 1991 VM1. Observations of this asteroid were made on 3 nights. A search of the Asteroid Lightcurve Database did not reveal any previously reported period for this asteroid.

6735 Madhatter. Observations were made over 5 nights. The resulting lightcurve was very scattered and yields uncertain results for the period. A search of the Asteroid Lightcurve Database did not reveal any previously reported period for this asteroid.

7068 Minowa. Observations were made over 5 nights. The resulting lightcurve was very scattered and yields an uncertain period result. A search of the Asteroid Lightcurve Database did not reveal any previously reported period for this asteroid.

8132 Vitginzburg. Observations of this asteroid were made on 2 nights when it was in the same field as another asteroid I was observing. The derived period is in close agreement with previous results listed on the ALCDEF.

9010 Candelo. Observations were made over 5 nights. The resulting lightcurve was very asymmetric and is uncertain. A search of the Asteroid Lightcurve Database did not reveal any previously reported period for this asteroid.

16788 Alyssarose. Observations were made over 7 nights. A search of the Asteroid Lightcurve Database did not reveal any previously reported period for this asteroid.

(18489) 1996 BV2. Observations were made over 4 nights. A search of the Asteroid Lightcurve Database did not reveal any previously reported period for this asteroid.

(24029) 1999 RT198. Observations of this asteroid were made on 7 nights when it was in the same field as another asteroid I was observing. The derived period is in close agreement with previous results listed on the ALCDEF.

(25241) 1998 UF14. Observations of this asteroid were made on 3 nights when it was in the same field as another asteroid I was observing. The derived period is in close agreement with previous results listed on the ALCDEF.

Number	Name	2024/2025 mm/dd	Phase	L _{PAB}	B _{PAB}	Period(h)	P.E.	Amp	A.E.	Grp
2778	Tangshan	01/25-01/26	5.5	115.0	2.7	3.4633	0.0042	0.29	0.05	MBA
4620	Bickley	01/18-01/26	7.3	114.9	2.5	3.6588	0.0012	0.21	0.1	MBA
4671	Drtikol	01/27-02/02	2.7	135.4	3.6	3.8301	0.0011	0.41	0.2	MBA
4685	Karetnikov	01/08-01/29	3.3	117.2	1.9	5.7464	0.0011	0.14	0.2	MBA
5602	1991 VM1	05/21-05/27	5.5	115.0	2.7	3.3492	0.0012	0.16	0.05	MBA
6735	Madhatter	01/27-02/02	4.0	135.4	3.6	8.4813	0.0001	0.12	0.2	MBA
7068	Minowa	01/08-01/18	1.7	116.7	1.9	6.048	0.003	0.11	0.2	MBA
8132	Vitginzburg	05/21-05/24	7.5	228.7	7.1	7.288	0.009	0.53	0.05	MBA
9010	Candelo	01/27-02/02	3.9	135.5	3.4	5.6931	0.0031	0.13	0.1	MBA
16788	Alyssarose	12/31-01/11	0.2	105.5	-0.5	5.16231	0.00001	0.36	0.1	MBA
18489	1996 BV2	01/29-02/03	7.4	142.6	8.7	5.0019	0.0025	0.21	0.05	MBA
24029	1999 RT198	01/05-01/18	35.7	60.1	-25.5	5.4209	0.0005	0.57	0.1	MBA
25241	1998 UF14	01/25-01/26	4.1	114.3	2.7	4.650	0.008	0.38	0.15	MBA
29386	1996 JC5	02/01-02/02	2.6	136.0	3.5	3.382	0.009	0.53	0.2	MBA
45487	2000 AR237	01/30-02/02	3.2	132.2	6.1	3.0374	0.0012	0.74	0.1	MBA
69649	1998 FK98	01/04-01/08	0.6	105.4	-0.5	2.181	0.001	1.22	0.2	MBA
137414	1999 TB190	01/08	0.7	105.5	-0.2	2.876	0.001	0.97	0.2	MBA

Table I. Observing circumstances and results. The phase angle is given for the first and last date. L_{PAB} and B_{PAB} are the approximate phase angle bisector longitude and latitude at mid-date range (see Harris et al., 1984). Grp is the asteroid family/group (Warner et al., 2009).

(29386) 1996 JC5. Observations of this asteroid were made on 2 nights when it was in the same field as another asteroid I was observing. The derived lightcurve was very scattered and is extremely uncertain. A search of the Asteroid Lightcurve Database did not reveal any previously reported period for this asteroid.

(45487) 2000 AR237. Observations of this asteroid were made on 2 nights when it was in the same field as another asteroid I was observing. A search of the Asteroid Lightcurve Database did not reveal any previously reported period for this asteroid.

(69649) 1998 FK98. Observations of this asteroid were made on 3 nights when it was in the same field as another asteroid I was observing. A search of the Asteroid Lightcurve Database did not reveal any previously reported period for this asteroid.

(137414) 1999 TB190. Observations of this asteroid were made on 1 night when it was in the same field as another asteroid I was observing. The derived lightcurve is very uncertain. A search of the Asteroid Lightcurve Database did not reveal any previously reported period for this asteroid.

Acknowledgments

I would like to thank Brian Warner for all of his work with the program *MPO Canopus* and for his efforts in maintaining the “CALL” website.

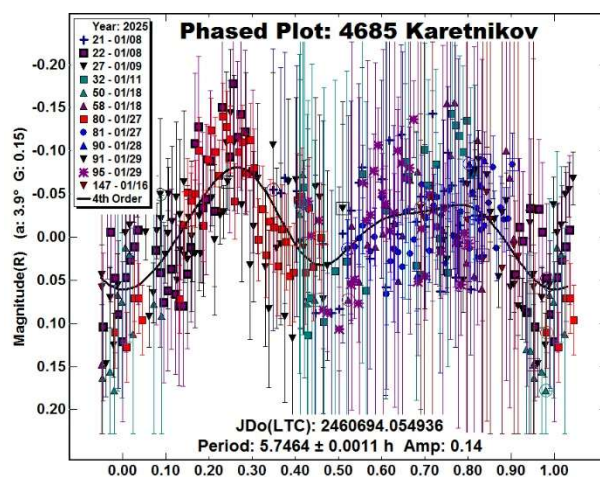
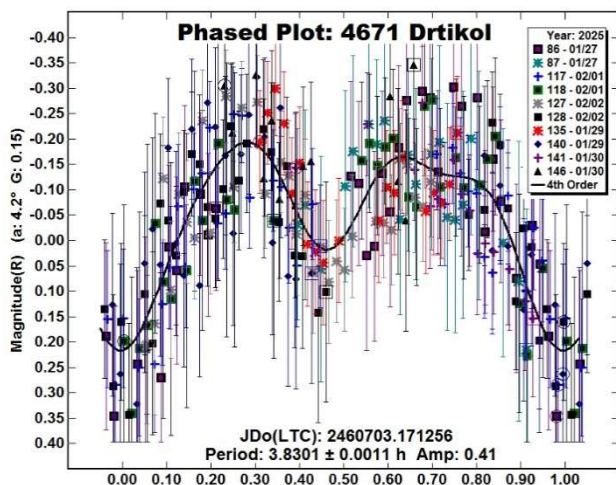
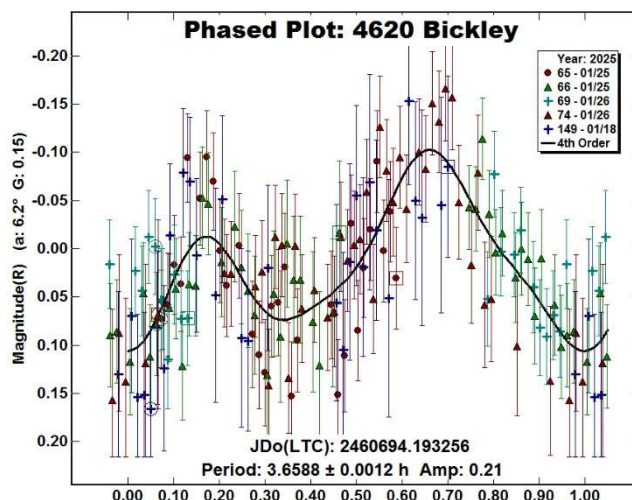
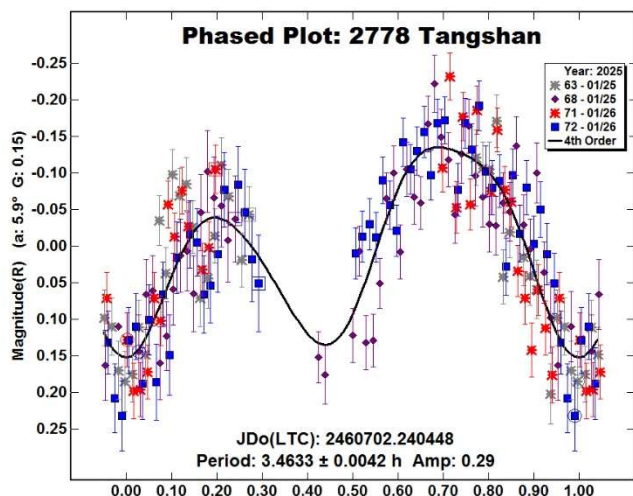
References

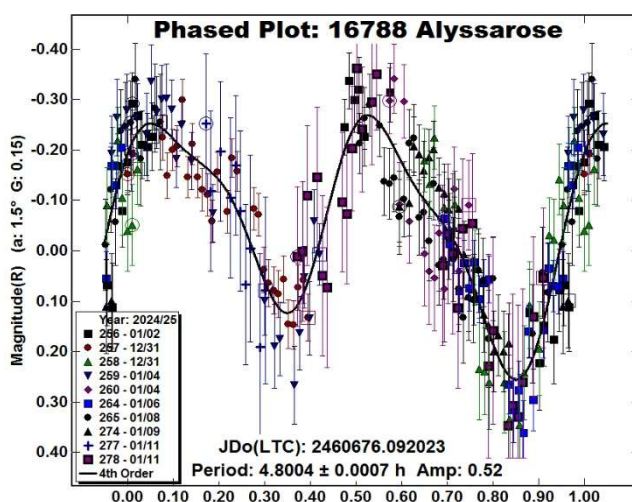
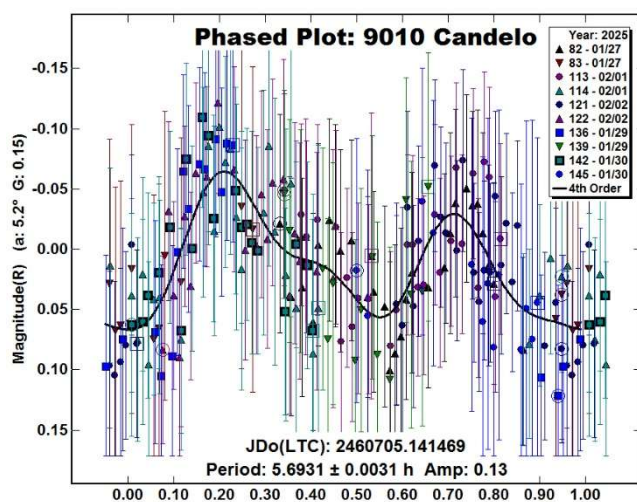
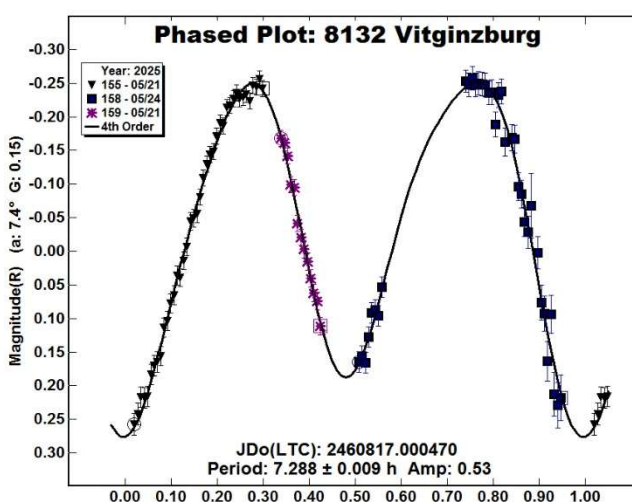
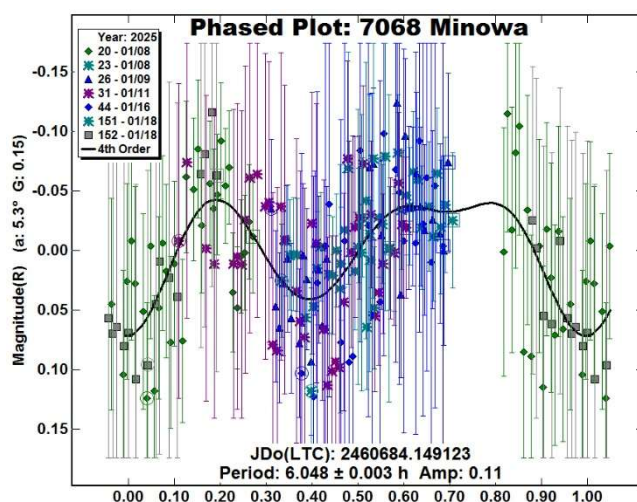
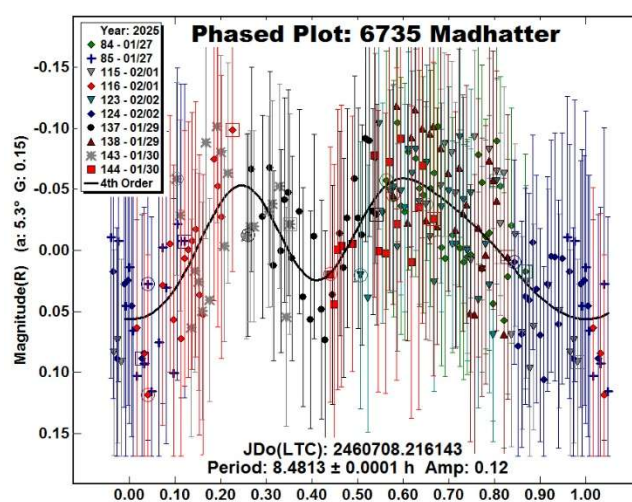
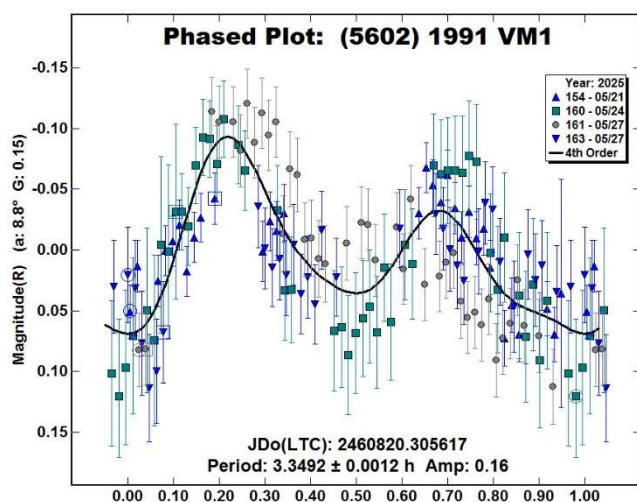
Benishek, V. (2024). “Lightcurves and Synodic Rotation Periods for 30 Asteroids from Sopot Astronomical Observatory: 2023 April. – December.” *Minor Planet Bull.* **51**, 151-156.

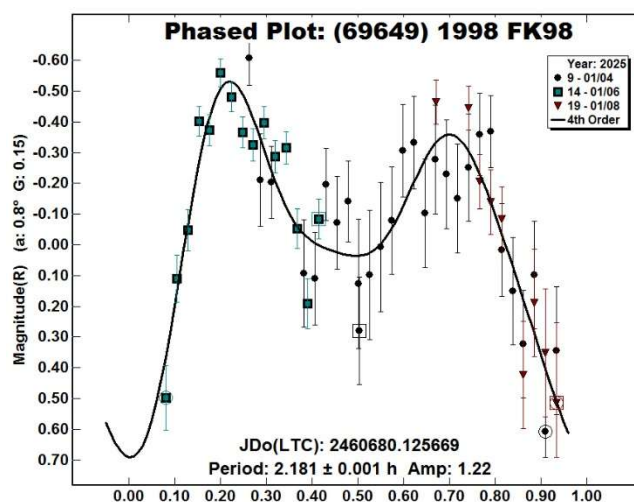
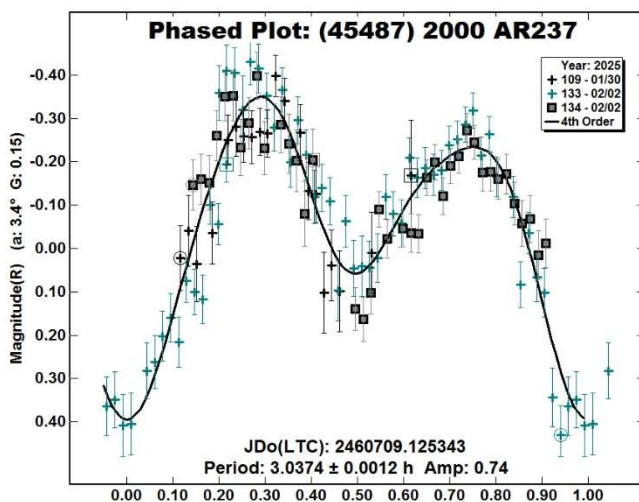
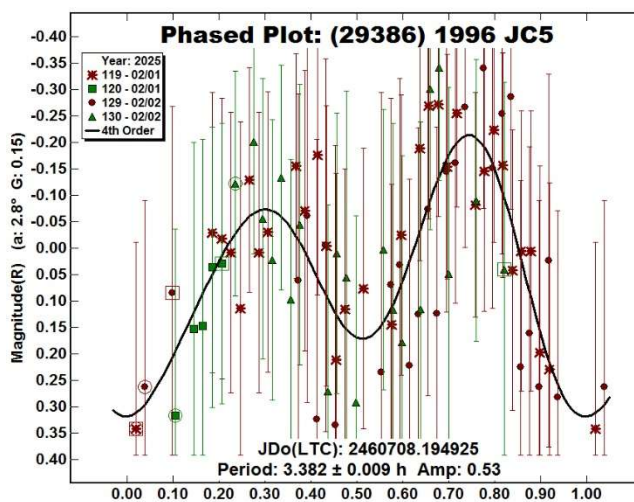
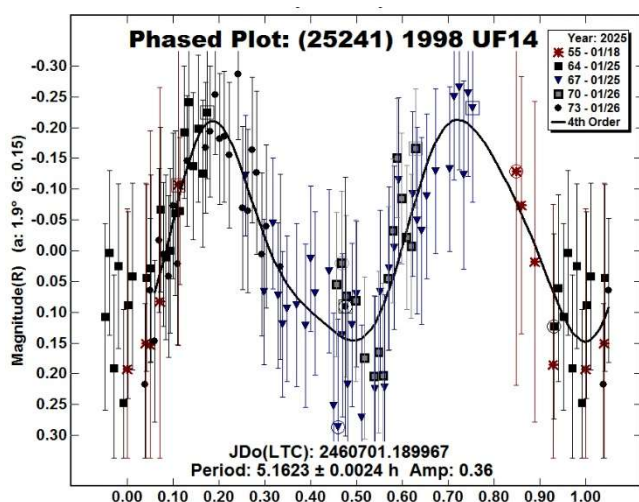
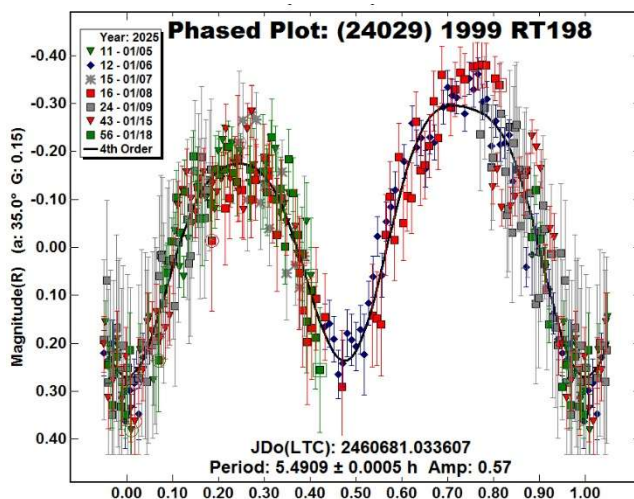
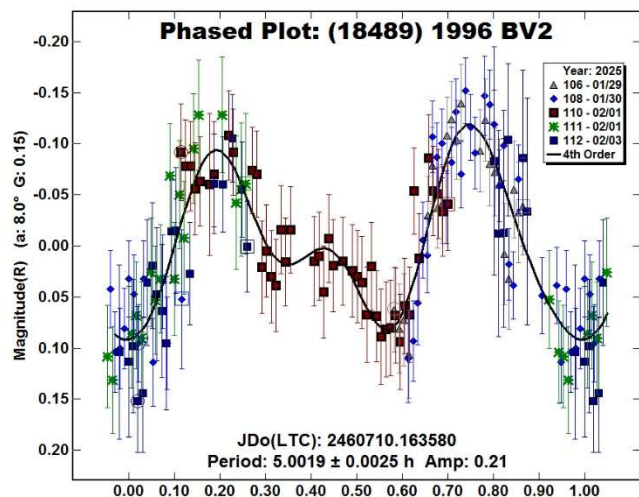
Harris, A.W.; Young, J.W.; Scaltriti, F.; Zappala, V. (1984). “Lightcurves and phase relations of the asteroids 82 Alkmene and 444 Gyptis.” *Icarus* **57**, 251-258.

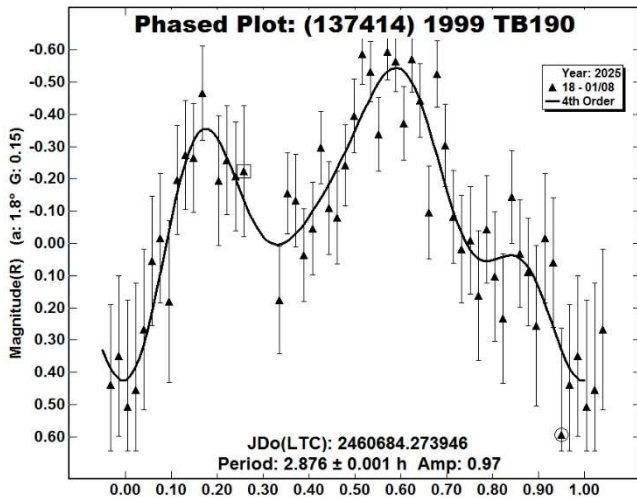
Warner, B.D.; Harris, A.W.; Pravec, P. (2009). “The Asteroid Lightcurve Database.” *Icarus* **202**, 134-146. Updated 2021 June. <http://www.minorplanet.info/lightcurvedatabase.html>

Warner, B.D. (2019). MPO Software, MPO Canopus v10.8.6.20. Bdw Publishing. <http://minorplanetobserver.com>









ASTEROID DIAMETERS FROM THE GAIA DR3 REFLECTANCE SPECTRA

Lorenzo Franco
Balzaretto Observatory (A81), Rome, ITALY
lor_franco@libero.it

(Received: 2025 September 8)

We present a study on indirectly deriving the diameters of the asteroids previously subject to the taxonomic classification from the ESA Gaia DR3 reflectance spectra by the same author. The approach was to use data from the AKARI IRC all-sky survey, combined with the SMASSII taxonomy, to determine the mean albedo distribution for each spectral class. Absolute magnitude H values derived from the JPL Small-Body Database were also used and appropriately corrected to eliminate a systematic trend. Finally, the diameters of 14926 main-belt asteroids were derived.

This study aims to derive indirectly the diameters of the asteroids classified using the reflectance spectra of Gaia DR3, as described in a previous article of the same author (Franco, 2025), of which the present article represents a natural continuation. The diameter (D) is related to the absolute magnitude (H) and the geometric albedo (pV) according to the relation (Pravec and Harris, 2007):

$$D \text{ (km)} = 1329 / \sqrt{pV} * 10^{(-H/5)} \quad (1)$$

For this study, we used the absolute magnitudes extracted from the JPL Small-Body Database Query (JPL SBDB, 2025) and the albedo values extracted from the AKARI IRC all-sky survey (Alí-Lagoa et al., 2018). For further details and references, we refer to the latter source. For the data analysis, we used Orange 3.34 (Demsar et al., 2013).

The AKARI survey data were downloaded from the CDS AKARI IRC (2018) and consist of 8097 records for a total of 5198 asteroids. These include mainly: asteroid designation (d), absolute magnitude (H), visible geometric albedo (pV), equivalent diameter (D), as well as Modified Julian Date (MJD) and phase angle (alpha) at time of the observation. The detailed information on multiple records for the same asteroid in this database isn't crucial for this study. Therefore, we decided to average the values for albedo and diameter related to each asteroid.

For the absolute magnitude (H), we used data from the JPL Small-Body Database (JPL SBDB, 2025), provided by the Minor Planet Center. However, it should be noted that the H values from AKARI are considered more accurate as they were obtained using photometric methods, unlike the JPL values which were obtained astrometrically.

To verify any differences between these two data sets, we selected the common set, consisting of 3763 asteroids, and plotted the difference ($H_{\text{akari}} - H_{\text{jpl}}$) vs H_{jpl} (Figure 1a). This plot shows that the H values from JPL are systematically greater for increasing H, so the difference ($H_{\text{akari}} - H_{\text{jpl}}$) grows, following a linear relationship:

$$(H_{\text{akari}} - H_{\text{jpl}}) = -0.0215 * H_{\text{jpl}} + 0.0489 \quad (2)$$

The Figure 1b shows the same data set after applying that linear correction.

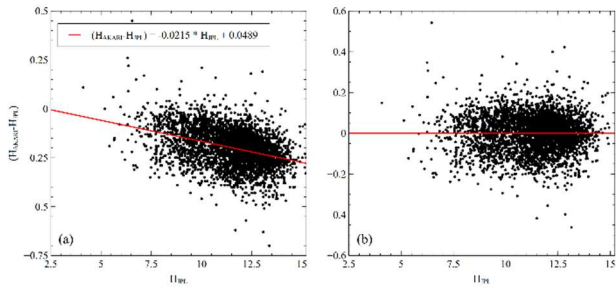


Figure 1: Comparison of the H-values from a common set of 3763 asteroids from the AKARI and the JPL Small-Body Database. The left panel (a) shows a systematic linear trend for $(H_{\text{akari}} - H_{\text{jpl}})$ vs H_{jpl} , while the right panel (b) shows the effects of applying a linear correction.

To determine the albedo for each taxonomic class, the albedo from the AKARI IRC all-sky survey (Ali-Lagoa et al., 2018) was correlated with the SMASSII spectral class data (Bus and Binzel, 2002) for a total of 876 asteroids in common.

In detail, the sub-classes S, C, X have been merged into their broader complex. For each taxonomic class, the mean albedo and relative standard deviation have been calculated, as reported in Table I, while Figure 2 represents the same results in graphical form. It is worth noting the wide distribution of albedo values for the taxonomic X-class.

SMASSII		AKARI	
Spectral Type	pV mean	pV sigma	count
A	0.272	0.058	9
B	0.072	0.036	46
C	0.058	0.025	292
D	0.081	0.031	7
K	0.152	0.036	28
L	0.129	0.047	28
Q	0.315	0.071	2
S	0.241	0.055	255
V	0.307	0.069	2
X	0.123	0.114	207

Table I. The mean albedo distribution for each spectral class from a common set of 876 asteroids selected from the AKARI and the SMASSII taxonomy.

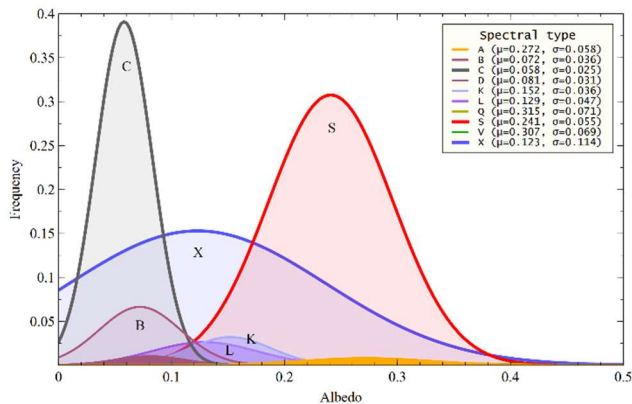


Figure 2: Mean albedo distribution for spectral classes.

Finally, for our data set of 14926 main-belt asteroids, classified using the reflectance spectra from Gaia DR3 (Franco, 2025), the diameters were calculated using the relation (1). We used H values from JPL that were corrected for the systematic trend with the relation (2), along with the albedo value corresponding to each spectral class, as reported in Table I.

To verify these results, the diameters of the AKARI survey were compared with those derived from Gaia, using a common set of 825 asteroids. The plot in Figure 3 shows the overall trend of AKARI diameters compared to the Gaia-derived ones.

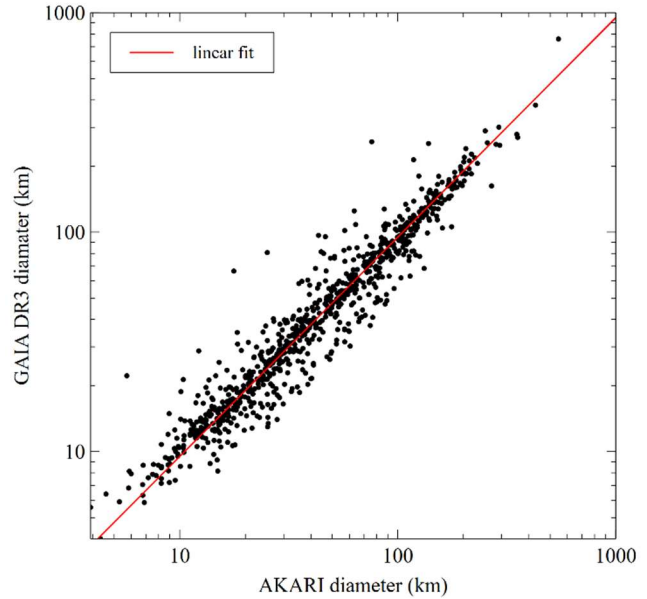


Figure 3: Diameters derived from GAIA compared with those from AKARI for a common set of 825 asteroids.

For a more in-depth analysis, the differences between the diameters from the two data sets were grouped by spectral type, and the distribution of the relative differences $(D_{\text{akari}} - D_{\text{gaia}}) / D_{\text{akari}}$ was plotted (Figure 4, Table II).

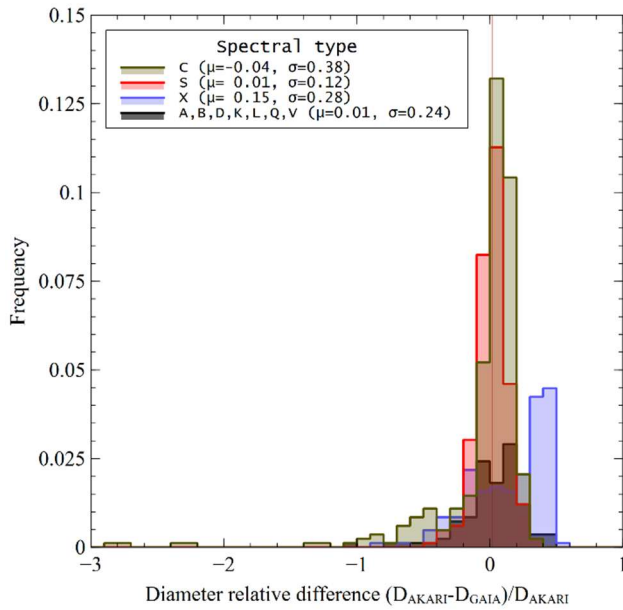


Figure 4: Relative differences distribution of diameters for a common set of 825 asteroids derived from GAIA and compared with AKARI.

Diameter relative difference			
Spectral type	mean	sigma	count
C	-0.04	0.38	316
S	0.01	0.12	246
X	0.15	0.28	168
A, B, D, K, L, Q, V	0.01	0.24	95

Table II. Relative diameter difference for spectral type.

It is notable that for X-type asteroids, there is an isolated peak near 0.4-0.5 in the relative diameter difference. This is caused by a low albedo value (around 0.05) assigned by the AKARI survey. Conversely, the negative values for C-type asteroids are due to isolated cases where a high albedo value (ranging from 0.12-0.71) was assigned by AKARI. We can assume the percentage uncertainties in the estimated diameters are a function of the spectral type, based on the sigma values reported in Table II. Furthermore, the diameters derived from the Gaia spectra were compared (Figure 5) with those obtained directly from the occultations (Herald et al., 2020) with a common sub-set of 101 asteroids. The derived diameters agree with an uncertainty of 20% (1 sigma).

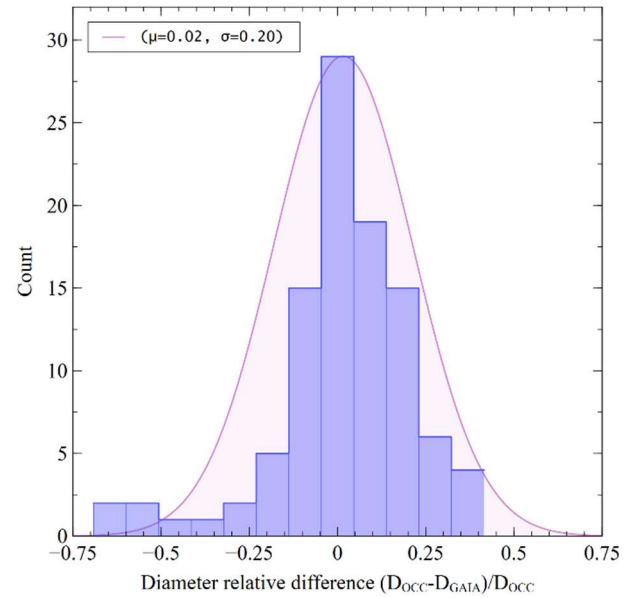


Figure 5: Relative differences distribution of diameters for a common set of 101 asteroids derived from GAIA and compared with diameters directly measured from the occultations. A normal distribution is superimposed to the relative difference with the same sigma.

To conclude, we plotted the cumulative distribution of diameters, which follows a power law (Figure 6). The flat trend below the ~4 km diameter limit is due to the incompleteness of the sample we used (14926 main-belt asteroids from the reflectance spectra of Gaia DR3).

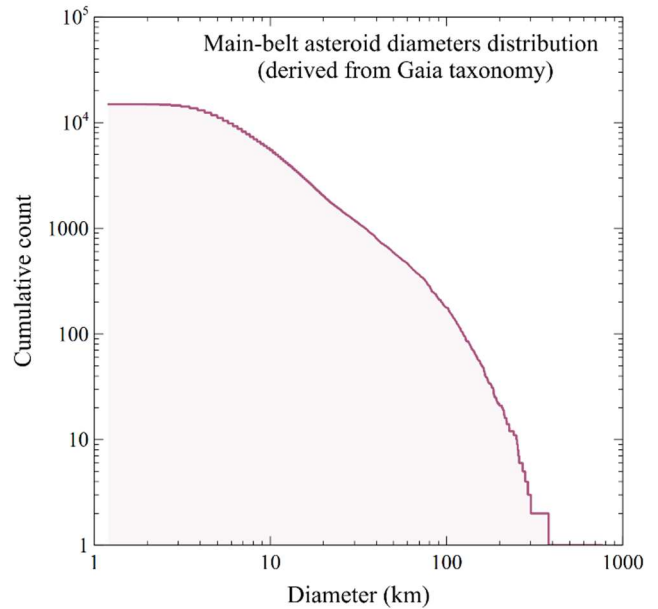


Figure 6: Cumulative distribution for the diameters derived from Gaia.

The catalogue of the derived diameters is available in a .csv file format, with the following data fields: Num, Denomination, H, pV, Diameter (Gaia Diameters@Balzaretto Observatory, 2025).

References

Ali-Lagoa, V.; Müller, T.G.; Usui, F.; Hasegawa, S. (2018). “The AKARI IRC asteroid flux catalogue: updated diameters and albedos.” *Astronomy & Astrophysics* **612**, A85.

Bus, S.J.; Binzel, R.P. (2002). “Phase II of the Small Main-Belt Asteroid Spectroscopic Survey - A Feature-Based Taxonomy.” *Icarus* **158**, 146-177.

CDS AKARI IRC (2018).
<https://cdsarc.cds.unistra.fr/ftp/J/A+A/612/A85/>

Demsar, J.; Curk, T.; Erjavec, A.; Gorup, C.; Hocevar, T.; Milutinovic, M.; Mozina, M.; Polajnar, M.; Toplak, M.; Staric, A.; Stajdohar, M.; Umek, L.; Zagar, L.; Zbontar, J.; Zitnik, M.; Zupan, B. (2013). Orange: “Data Mining Toolbox in Python.” *Journal of Machine Learning Research* **14**, 2349-2353.

Franco, L. (2025). “On the GAIA DR3 Reflectance Spectra.”, *Minor Planet Bulletin* **52**, 351-353.

Gaia Diameters@Balzaretto Observatory (2025).
https://digidownload.libero.it/A81_Observatory/data/gaia_asteroid_diameters.csv

Herald, D.; Gault, D.; Anderson, R.; Dunham, D.; Frappa, E.; Hayamizu, T.; Kerr, S.; Miyashita, K.; Moore, J.; Pavlov, H.; Preston, S.; Talbot, J.; Timerson, B. (2020). “Precise astrometry and diameters of asteroids from occultations - a data set of observations and their interpretation.” *Monthly Notices of the Royal Astronomical Society* **499**, 4570-4590.

JPL SBDB (2025). “JPL Small-Body Database Query.”
https://ssd.jpl.nasa.gov/tools/sbdb_query.html

Pravec, P.; Harris, A.W. (2007). “Binary asteroid population. 1. Angular momentum content.” *Icarus* **190**, 250-259.

EDITOR'S NOTE: SALUTING BRIAN WARNER AND OBSERVING OPPORTUNITIES

Calling attention to particularly favorable or high scientific value observing opportunities has been a hallmark of *The Minor Planet Bulletin* since its inception five decades ago by the Minor Planets Section founder, Richard G. Hodgson. For decades this service has been performed by the Section Coordinator, Professor Frederick Pilcher, highlighting favorable elongations for each year. Photometric opportunities have similarly been highlighted in each issue, with these lists being organized and prioritized by Associate Editor Brian Warner for more than two decades.

Long-time readers will carefully note the sea change in the *Photometry Opportunities* beginning with this volume (Volume 53) and moving forward. Rather than preparing detailed lists, the tools are now being highlighted. Scientific interests and motivations are quite varied among individual observers. Thus, by providing guidance to the available tools, an individual observer can identify targets matching their own available time, equipment, and interests.

With this sea change, it is an opportunity to illuminate the long history of Brian Warner's service to fellow observers; service beyond the software tools of *MPO Canopus* that have facilitated a tidal wave of lightcurve observations and their publication (well illustrated in charting the number of objects and pages published in *The Minor Planet Bulletin* over the recent decades). Observing opportunities, including finder charts (!), were published by Warner in the *Minor Planet Observer (MPO)* through the full decade of the 1990s. (The *MPO* was a worthy successor to the pioneering *Tonight's Asteroids* published by J.U. Gunter beginning in the 1970's.) After the conclusion of the *MPO* publication, in 2004 Warner became the lead author of the *Photometry Opportunities* appearing in these pages. However, his contributions to the *MPB* photometry observations listings began as early as 2001. Thus, at this time, in the ever-evolving methods for our field, it is a time for appropriate reflection and appreciation. Please join me in thanking and saluting Brian Warner for 25 years in this service to *The Minor Planet Bulletin*!

Richard P. Binzel, Editor

LIGHTCURVE PHOTOMETRY OPPORTUNITIES: RESOURCES FOR OBSERVERS

Brian D. Warner
Center for Solar System Studies (CS3)
446 Sycamore Ave.
Eaton, CO 80615 USA
brian@MinPlanObs.org

Alan W. Harris
Center for Solar System Studies (CS3)
La Cañada, CA 91011-3364 USA

Josef Ďurech
Astronomical Institute
Charles University
18000 Prague, CZECH REPUBLIC
durech@sirrah.troja.mff.cuni.cz

Lance A.M. Benner
Jet Propulsion Laboratory
Pasadena, CA 91109-8099 USA
lance.benner@jpl.nasa.gov

(Received: 2025 October 15)

In light of changing circumstances, opportunities, and observer capabilities, we forgo lists of selected objects. Instead, we refer to some on-line resources that allow observers to select objects that fit their objectives. In part, this helps reduce some biases that favored the easier, brighter targets.

After some months of internal discussions, we have opted to forgo the usual lists of targets. While those lists served as a good starting point for observers, they also tended to favor brighter asteroids, those $V < 15.5$, and didn't always challenge the more experienced or adventurous observers to chase lesser observed objects.

For reference, those lists – which still serve well as broad topics of research – are:

Favorable Apparitions, which includes objects reaching one of the five brighter (favorable) apparitions from 1995 and 2050 and rated $U < 3$ – in the LCDB (Warner et al., 2009).

No Pole Solutions, which includes objects rated $U > 2+$ but do not have a pole indicated on the LCDB summary line. This list is the most likely needing further confirmation by checking the DAMIT web site, which grows in spurts large and small quite frequently and so the LCDB can lag considerably.

Poor Pole Solutions, which includes objects rated $U < 3$ – that have a pole solution on the summary line. In this case, the period is often based on using sparse survey data, with or without support of dense lightcurve data. An additional set of dense data may help elevate both the U rating and the quality of the pole solution.

Low Phase Angles, which includes objects, regardless of U rating or even having a period, that reach a solar phase angle $< 1^\circ$. You should refer to Warner et al. (2023) to review important information about low solar phase angle work.

Long Periods, which includes objects with $P \geq \sim 24$ hours. These are often overlooked because they are very difficult for a single-station campaign. However, they are ideal for collaborations, especially those with stations well-separated in longitude.

NEAs (aka Radar Target) is limited to *known* near-Earth asteroids that might be on the radar team's radar (pun intended). It is common for newly discovered objects to move into or out of the list. We recommend that you keep up with the latest discoveries by using the Minor Planet Center observing tools.

We refer the reader to the lightcurve photometry opportunities article in *Minor Planet Bulletin* 51-4 (Warner et al., 2024) for a detailed discussion on the evolution of the lists and the purpose behind each one. In addition, we refer the reader to other prior releases of this paper (e.g., Warner et al., 2023) for more detailed discussions about the requirements and considerations when choosing a target and to Warner et al. (2021a; 2021b).

On-Line Planning Tool

The ephemeris generator on the <https://MinorPlanet.info> web site allows creating custom lists for numbered objects reaching $V \leq 18.0$ during a given month from 2020 through 2035 by setting search parameters based on a number of parameters.

<https://www.minorplanet.info/php/callopplcdbquery.php>

In fact, the underlying databases used by this page are the same ones used to generate the lists in the past.

The next few pages feature screen shots of that page at start up and after initiating a search. Figure 1 shows the initial page. It's important to note that this page *covers only numbered objects*. The reason for this is that the underlying oppositions database used to find objects reaching brightest is limited the same way. Otherwise, the database would be significantly more massive and, more important, would likely include too few objects that reach the other critical limit, $V < 18.0$ at brightest.

However, both the MPCOrb table, which is also used by the ALCDEF site, and the oppositions tables are updated about every month, which roughly coincides with the frequency of the release of newly-numbered asteroids. The oppositions database covers the years 2020-2035 and is based on positions computed by Warner. This range allows both historical research and long-term planning.

The family list in Figure 1 is based on those from Nesvorný (2015) and Nesvorný et al. (2015). Also included in the options are the broad orbital groups defined by Warner et al. (2009) in the LCDB. For general searches, choose "Any." You can choose more than one family, except if you also choose "Any." Since "Any" could potentially return the entire database, searches are limited to a specific month and year.

The search is based on combining *all* filter selections (generating a lengthy set of Boolean ANDs for an SQL statement), so make sure that every filter allows finding only those objects you want to find. Proper setting of the filters will allow you to recreate the lists seen in previous papers, or at least very nearly so.



[Home](#)
[CALL](#)
[Observing Guides](#)
[Observation Planning](#)
[ALCDEF](#)
[Minor Planet Bulletin](#)
[Lightcurve Database](#)
[Minor Planet Center](#)
[JPL Small Body DB](#)
[CNEOS](#)
[Lowell MP Services](#)
[Minor Planet Mailing List](#)
[Society for Astronomical Sciences](#)

Acknowledgement
 Development of this web site was made possible by several grants each from NASA and the NSF.



Enter the search parameters for asteroids reaching brightest during the chosen month and year. In most cases, opposition and date of brightest are within a few days of one another. However, for some NEAs, the two dates could be weeks or months apart and the NEA could have up to three oppositions during a given apparition.

To avoid causing a server timeout when selecting all months for a year, make sure to apply one or more filters. "All" with no filters returns a maximum of 200 records.

The filters are applied with Boolean AND, i.e., all conditions must be met.

<input type="button" value="Run Search"/> <input type="button" value="Reset"/>		
Table Filtering Options Results are sorted by order of date of brightest		
Value	Range Low/Qualifier	Range High/Selection
Number	<input type="text" value="0"/>	<input type="text" value="9999999"/>
Name	<input type="text" value="Any"/>	<input type="text" value=""/> Ignored if "Any"
Year/Month	<input type="text" value="2026"/> <input type="text" value="January"/>	Selecting "All" without filters limits the result set to 200 records.
Family/Group	Group numbers precede the colon Any 2041: 1933 VV7 2043: 1981 EY40 2038: 1990 RA3 2039: 1992 DY7 615: 1993 FY12 2037: 1994 UD1 2045: 1995 SU37 006: 1996 RJ 2046: 1997 EM	More than one family can be selected. If "Any" is chosen, any other selected families will be ignored. The family list is based on Nesvorný et al. (2015) with additional families from the AstDys site as well as broad groups that contain objects not in the families. See Section 3 of the LCDB Readme PDF for more information about families and a list of family numbers/names.
Favorable	<input type="text" value="Only Favorable"/>	Favorable is one of the top five brighter apparitions between 1995-2050
CALL Status	<input type="text" value="Ignore"/>	Filter by CALL notifications and/or submission postings
LCDB Status	<input type="text" value="U < 3"/>	Filter by LCDB entries
Period Range	<input type="text" value="0.0002"/> (h)	<input type="text" value="5000"/> (h) One or both blank = No Filter
Mag Range	<input type="text" value="0"/>	<input type="text" value="18.0"/>
Dec Range	<input type="text" value="-90"/>	<input type="text" value="90"/>
PhA Range	<input type="text" value="0.00"/>	<input type="text" value="120.00"/>
Diameter	<input type="text" value="8000"/>	Maximum diameter (km)
<input type="button" value="Run Search"/> <input type="button" value="Reset"/>		

Figure 1. The Observations Target Search page on the *MinorPlanet.info* web site (<https://www.minorplanet.info/php/callopplcdbquery.php>) features a number of filter options to limit search results. It is recommended that "CALL Status" always be set to *Ignore*, since the cross-referencing between the multiple databases is not always in perfect synchronization. "PhA" is solar phase angle, which can be 0 degrees at conjunction *and* opposition. The nature of the databases and search will always return near opposition values, never near conjunction. In other words, solar elongation (great circle distance from the Sun) will be > 90 degrees (with some possible exceptions for NEAs). See the LCDB documentation for more information on family numbering and the LCDB Status (U code) values.

The Ephemeris Start Date and UT are not validated.
Make sure to use YYYY-MM-DD format (e.g., 2021-12-31 for Dec 31, 2021)

Ephemeris Information

Positions

Topocentric

Longitude -116

Latitude +34

Elevation 930

Start Date
(yyyy-mm-dd)

2025-11-07

UT 0

See the [LCDB Readme](#) (section 3) for a listing of family numbers and names.

LCDB	Ephemeris	Reset	LCDB	Eph	CN	CS	Fav	Num	Name	Fam	ODate	OMag	MDate	MDist	BDate	BMag	BDec	PDate	PMin	PDec	PF	Period	AMin	AMax	U	H	pV	Diam
<input checked="" type="radio"/>	<input type="checkbox"/>		N	N	Y			13854	1999 XX104	405	99 99.9	99.9	01 03.4	1.196	01 01.5	17.3	+22	12 31.903	0.7	+22		246.740		0.79	2	15.27	0.28	2.22
<input type="radio"/>	<input type="checkbox"/>		N	N	Y			47127	1999 CJ103	9106	01 01.1	17.1	01 06.1	1.861	01 01.5	17.1	+21	01 01.037	0.6	+21		4.370	0.64	0.71	2	13.50	0.057	11.11
<input type="radio"/>	<input type="checkbox"/>		N	N	Y			98339	2000 SG296	9104	01 02.9	17.6	01 01.5	0.997	01 01.5	17.6	+9	01 01.808	6.8	+09		8.93798		0.12	2	15.63	0.20	2.22
<input type="radio"/>	<input type="checkbox"/>		N	N	Y			5508	Gomyou	9106	01 02.1	15.1	01 02.7	1.232	01 02.0	15.1	+34	01 01.868	4.9	+34		8.802		0.37	2	12.53	0.057	17.36
<input type="radio"/>	<input type="checkbox"/>		N	N	Y			7324	Carret	9104	01 02.1	16.6	01 01.1	0.922	01 02.0	16.6	+39	01 03.315	8.5	+39		11.3005		0.37	2	14.82	0.20	3.23
<input type="radio"/>	<input type="checkbox"/>		N	N	Y			137925	2000 BJ19	9101	01 08.9	18.0	01 01.1	0.881	01 02.0	18.0	-8	01 12.609	14.0	-04		48.		0.17	2	16.07	0.20	1.82

Figure 2. The results table for a search for all objects reaching brightest in 2026 January. The figure does not show the legend on the page that explains individual columns. See the text for more details on some of the results that are displayed.

LCDB Data for (13854) 1999 XX104

[Download the LCDB README.pdf](#) for explanations of field names and data.

[LCDB References](#) with BibCode links to ADS

To shorten some field names, the columns that flag another value have been shortened to one or two characters.

Summary

Number	Name	Desig	Family	CS	Class	DS	DF	Diam	HS	HB	H	GS	G	G1	G2	AS	AF	Albedo	PF	Period	PDesc	AMin	AMax	U	Pole	Bin	Notes
13854	1999 XX104	1999 XX104	405	A	SFC	C		1.85	T		15.66	G		0.075		A		0.28		246.740			0.79	2			

Details

Reference	BibCode	Desig	DateObs	PABL	PABB	Phase	Family	Class	DM	DF	Diam	DErr	HS	HB	H	HErr	GS	G	GErr	G1	G1Err	G2	
Veres 2015	2015icar.261...34V	1999 XX104															G						
Masiero 2012	2012ApJ...759L...8M	1999 XX104									7.21	0.25	A			15.00		A	0.15				
Waszczak 2015	2015AJ...150...75W	1999 XX104	2013-08-08	348.7		1.9	14.6									G	R	15.212	0.013	G			
Nugent 2015	2015ApJ...814...11N	1999 XX104									6.31	1.83	A			15.20		A	0.15				
Nugent 2016	2016AJ...152...63N	1999 XX104									4.36	1.29	A			15.49		A	0.24				
Mainzer 2016	2016PDSS.247....M	1999 XX104	2010-09-14	68.2		0.4	25.6				7.206	0.246	A			15.00		A	0.15				
Erasmus 2020	2020ApJS.247...13E	1999 XX104						9104	C														
Mahlke 2021	2021icar.35414094M	1999 XX104															G	AO	15.13	0.100	G		
Masiero 2021	2021PSJ....2...162M	1999 XX104									4.65	1.37	C			15.20	0.05	A	0.15	0.1			
							24.52														0.019	0.037	0.67

Color Index

Reference	BibCode	DetailsRef	BV	BVErr	VR	VRErr	VI	VIErr	SGR	SGRErr	SRI	SRIErr	SI2	SI2Err	BR	BRErr	RI	RIErr	ATLco	ATLcoErr
Erasmus 2020	2020ApJS.247...13E	651569																	0.19	0.10

Figure 3. The LCDB entries for (13854) 1999 XX104. Not shown is the legend on the page that explains the meaning of each column. The page may not show all results in a single screen, especially the full width of the Details table. Be sure to use *both* scroll bars as needed.

Figure 2 shows a partial list of the results of a search for any objects meeting the default filter settings in 2026 January. There are several columns not seen in the lists from previous papers, including dates of opposition and minimum distance. Some opposition dates will be “99 99.9” and magnitudes “99.9.” This means that the object never reaches opposition during the entire calendar year of the search.

This is not unusual for some NEAs, which never meet the definition of having an ecliptic longitude 180 degrees from the Sun. On the other hand, for a main-belt object, it could simply mean that, for example, the asteroid reaches opposition a few months, or even just days, before or after the calendar year of the search.

The MDate (date of minimum distance) and BDate (date of brightest) may have dates of “01 01.” (no value after the decimal point) if the search is for January. For minimum distance, this

means that the asteroid-Earth distance is constantly increasing, i.e., it was closest in a previous month. The same logic applies to date of brightest, i.e., the asteroid is never brighter than it was on January 1 at 0h UT.

The reverse logic applies for searches in December that show dates of “12 31.” In other words, the asteroid has yet to reach its next minimum distance or is still getting brighter at the end of the year.

You can click the radio button in the “LCDB” column on one and only one object at a time. If you do and then click the “LCDB” button, this displays the full LCDB entry for the asteroid, if any. Figure 3 shows the results when choosing (13854) 1999 XX104. There can be quite a bit of information that’s not seen in a single screen. For example, it’s unlikely you’ll see the full extent of the Details table, so be sure to use *both* scroll bars.

Ephemeris for 5508 Gomyou

- Topocentric positions (J2000) at 7 UT
- Ephemeris interval: 1 day
- Longitude: -116 Latitude: +34 Elevation: 928
- E.D. = Earth Distance in AU
- S.D. = Sun Distance in AU
- Ph = Phase Angle
- E = Solar Elongation
- Az = Azimuth (0 = North, 90 = East, 180 = South, 270 = West)
- PABL = Phase angle bisector longitude
- PABB = Phase angle bisector latitude
- M Ph: Moon phase; 0.0 = New, 1.0 = Full; + = waxing, - = waning
- M E: Elongation from moon
- GL: Galactic longitude
- GB: Galactic latitude

Date	RA	Dec	Mag	E.D.	S.D.	Ph	E	Alt	Az	PABL	PABB	M Ph	ME	GL	GB
2026-12-20	14 23 38.5	-12 46 49.5	18.17	3.277	2.753	15.9	50	-46	71	209.8	1.6	0.888	173	335	44
2026-12-21	14 24 59.6	-12 54 32.2	18.17	3.268	2.756	16.1	51	-46	72	210.1	1.5	0.890	166	336	44
2026-12-22	14 26 20.3	-13 02 10.9	18.17	3.260	2.758	16.2	52	-46	73	210.4	1.5	0.952	152	336	44
2026-12-23	14 27 40.6	-13 09 45.7	18.18	3.251	2.760	16.4	52	-45	73	210.7	1.5	0.990	138	336	43
2026-12-24	14 29 00.5	-13 17 16.4	18.18	3.242	2.763	16.5	53	-45	74	211.0	1.5	-0.998	123	336	43
2026-12-25	14 30 19.9	-13 24 43.1	18.18	3.233	2.765	16.6	54	-44	75	211.2	1.5	-0.975	108	337	43
2026-12-26	14 31 38.9	-13 32 05.9	18.18	3.224	2.767	16.8	54	-44	75	211.5	1.4	-0.924	94	337	43
2027-01-26	15 07 47.2	-16 46 41.5	18.10	2.903	2.839	19.7	77	-28	92	219.3	0.8	-0.810	52	344	35
2027-01-27	15 08 46.0	-16 51 51.8	18.10	2.891	2.842	19.8	77	-27	93	219.6	0.8	-0.716	38	344	35
2027-01-28	15 09 43.9	-16 56 58.0	18.09	2.880	2.844	19.8	78	-27	93	219.8	0.7	-0.616	26	344	35

OscDate: 2461000.5
 Mean Anomaly: 348.0699800
 Perihelion: 70.6797700
 Node: 36.1160200
 Inclination: 6.7668500
 Eccentricity: 0.225136400
 SM Axis: 2.8437580
 T: 2461058.546500

Figure 3. The ephemeris for each object (if more than one is chosen), shows the orbital elements used to generate the *unperturbed* positions. Use the other resources given elsewhere for more accurate positions. This may be particularly important for NEAs coming close to the Earth-Moon system or other planet.

It's also possible to generate topocentric 40-day ephemerides for one or more objects in the list. Set the ephemeris parameters (longitude, latitude, etc.), check one or more boxes in the "Eph" column, and then click the "Eph" button. Figure 3 shows a partial listing of the results for 5508 Gomyou (the full list was more than one page high).

The Lowell Observatory

There are *many* other on-line sites to guide observing programs but one we particularly recommend is the one from Lowell Observatory. You could lose yourself for hours exploring the many features of the site, so we won't go into details here; Figure 4 presents an example.

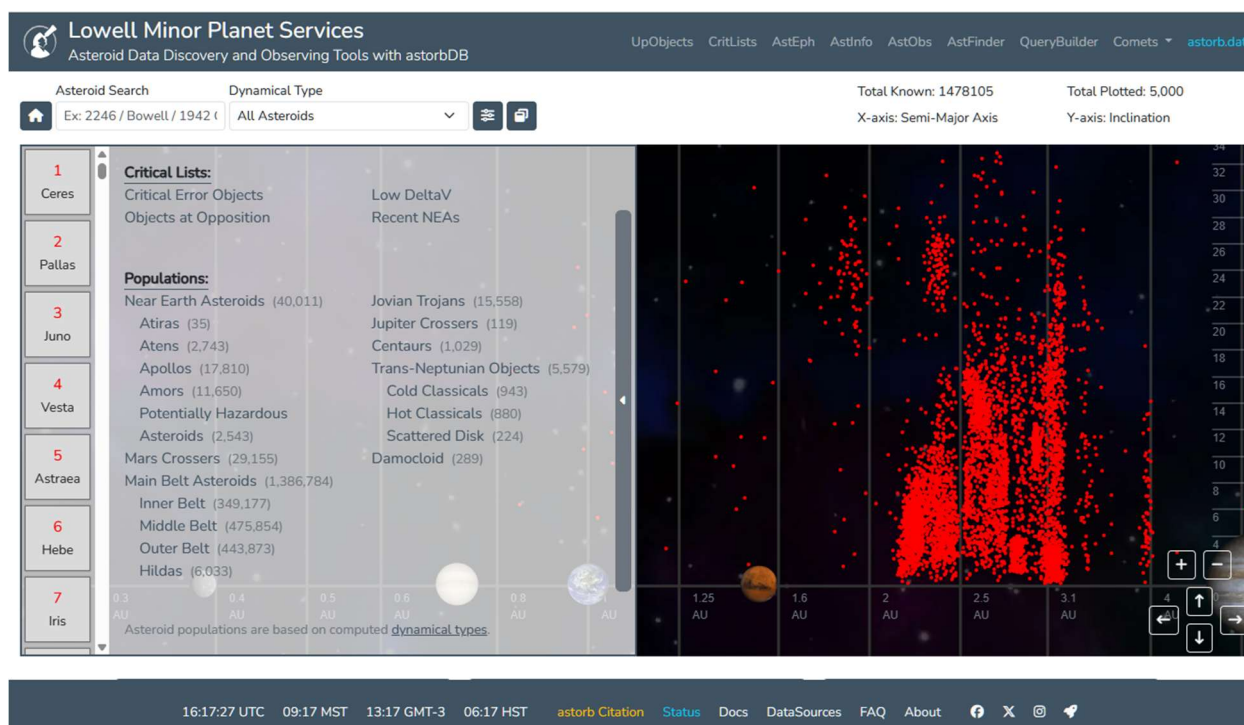


Figure 4. The home page of the highly-recommended Lowell Observatory observing services site (<https://asteroid.lowell.edu/>).

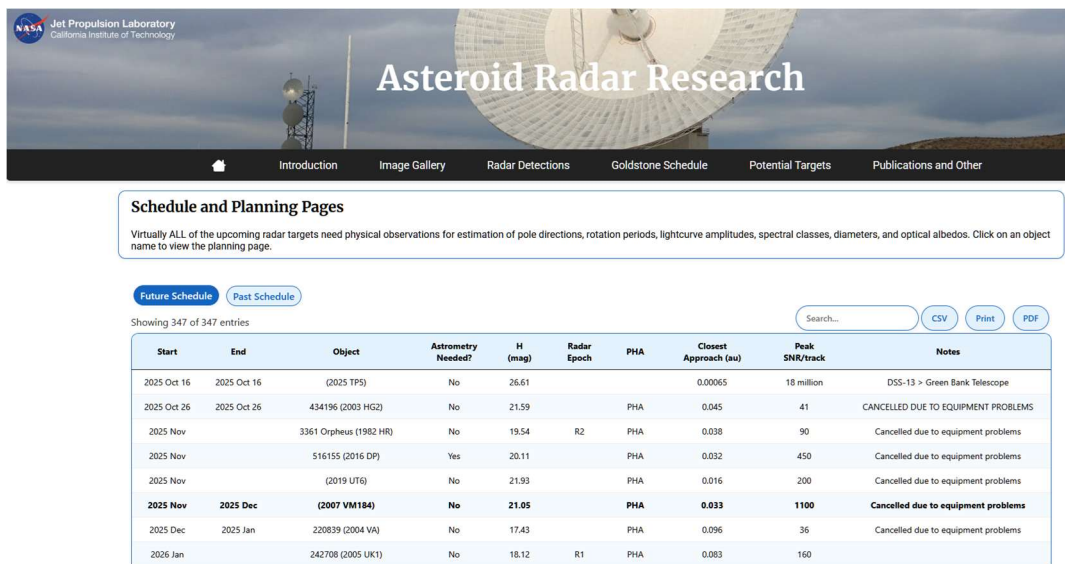


Figure 5. The modernized Asteroid Radar Research page makes it easy to see which targets are “on the team’s radar” (pun fully intended).

	λ	β	P	Files	Comment	More
(1) Ceres				LCref IAUspin IAUspin	albedo effects	
View model	350	81	9.074173	AO.png IAUspin albedo shape.png shape.txt spin.txt shape.obj		***
(2) Pallas				LCref IAUspin IAUspin		
View model	35	-12	7.81323	3D.pdf IAUspin.txt occ_1978-05-29.pdf occ_1983-05-29.pdf occ_1...		***
View model	32	-11	7.81322	AO.png occ.png IAUspin.txt shape.png shape.txt spin.txt shape...		***
View model	42	-15	7.81322	IAUspin shape.png shape.txt spin.txt shape.obj		***
(3) Juno				LCref IAUspin IAUspin		
View model	103	27	7.209531	3D.pdf IAUspin.txt occ_1979-12-11.pdf occ_2000-05-24.pdf shape...		***
View model	105	21	7.20953	IAUspin.txt shape.png shape.txt spin.txt shape.obj	nonconvex model reconstructed from ALMA+AO+LC	***
(4) Vesta				LCref IAUspin IAUspin	albedo effects	
View model	337	56	5.342124	AO.png IAUspin albedo shape.png shape.txt spin.txt shape.obj		***

Figure 6. The browse page of the DAMIT site produced by Josef Durech and colleagues.

Other Important and Useful Web Sites

The dates and values given on the *MinorPlanet.info* site are very good estimates in most cases. NEAs are sometimes an important exception. Use the site for preliminary planning for objects and then confirm those plans using the Minor Planet Center or JPL Horizons web sites.

MPC: <http://www.minorplanetcenter.net/iau/MPEph/MPEph.html>
 JPL: <https://ssd.jpl.nasa.gov/sb/orbits.html>

For near-Earth asteroids in particular, check the list (Figure 5) found on the Goldstone planned targets schedule at:

http://echo.jpl.nasa.gov/asteroids/goldstone_asteroid_schedule.html

and keep in touch with Lance Benner at the email above. For those on social media, the radar team can also be found on the more popular platforms. This is particularly useful for real-time updates during an NEA fly-by. Keep in mind as well that the *MinorPlanet.info* site opposition database includes only numbered objects. Keep a close eye on the MPC NEA pages.

As noted earlier, the information on this *MinorPlanet.info* is not regularly synchronized with the DAMIT web site (Figure 6).

<https://astro.troja.mff.cuni.cz/projects/damit/>

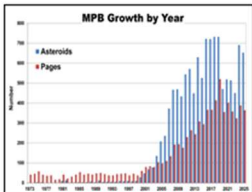
If looking to add lightcurves for objects with existing models, or to confirm if a model does or does not exist, visit the Database of Asteroid Models from Inversion Techniques (DAMIT) web site.

<https://astro.troja.mff.cuni.cz/projects/damit/>

to see what, if any, information it has on a chosen target.

The Minor Planet Bulletin

BULLETIN OF THE MINOR PLANETS SECTION OF THE ASSOCIATION OF LUNAR AND PLANETARY OBSERVERS




Click on image to zoom

The *Minor Planet Bulletin* is the journal for almost all amateurs and even some professionals for publishing asteroid photometry results, including lightcurves, H-G parameters, color indexes, and shape/spin axis models. It is considered to be a refereed journal by the SAO/NASA ADS. All *MPB* papers are indexed in the ADS.

Print subscriptions are no longer available to individuals. Institutions (e.g., college libraries) can still obtain print copies via a special subscription. See details in MPB 37-4 or contact the editor, Richard Binzel.

Annual voluntary contributions of \$5.00 or more in support of the publication are welcome. Please send a check, drawn on a U.S. bank and payable in U.S. funds, to "Minor Planet Bulletin" and send it to:

Minor Planet Bulletin
c/o Melissa Hayes-Gehrke
UMD Astronomy Department
1113 PSC Bldg 415
College Park, MD 20742

[Authors Guide and Word Templates](#) (v.3.0: updated 2024 February 2)
The ZIP file contains the Authors Guide PDF as well as a "starter" paper in Word 2007+ (DOTX). Those using Word 97 (DOC/DOT) are encouraged to download [OpenOffice](#) and convert their files to the most recent Word format (DOCX).
Please read this updated guide since there are a number of changes from previous guides.

Search for

Titles/abstracts ▾

AND ▾

Published between

Issues for the upcoming quarter-year are released on about the 21st of March, June, September, and December. Full issues and individual papers from vol 1 (1973) to present are available via links on this page.

Important: If the ADS bibcode and "Download PDF" links are missing for the latest issue, it is because the ADS has not processed the files. The links will be made available after the ADS processes the files.
If the "Download PDF" link is visible and there is no PDF available, clicking the link will download an arbitrary page. We are working with ADS to make sure all papers are available and, if not, being able to disable the link. The "Download Full Issue" link **does** retrieve the correct file.

Vol 1-7 run Jul-Jun. Vol 8-present run Jan-Dec. Only papers indexed in the ADS are included. Earlier volumes often contain more papers than listed here. It's recommended to download the full issue in vol 1-9.

If downloading several full issues, please wait a minute or two between each download. This will help prevent overloading the hosting site resources, which can take the site down.
Thanks for your cooperation and understanding.

☒ **Volume 52 (2025)**
52-4 (Oct-Dec) pp 279-364
52-3 (Jul-Sep) pp 191-278
52-2 (Apr-Jun) pp 97-190
52-1 (Jan-Apr) pp 1-96

☐ **Volume 51 (2024)**

☐ **Volume 50 (2023)**

Issue 52-4 (2025 Oct-Dec)
[Download Full Issue](#)

☒ Show abstracts


Lightcurves and Rotation Periods of Nearearth Asteroids (137170) 1999 HF1 and 2025 GB
Pages 279-280
Duin, Heiko

Figure 7. The home page of the MPB has downloads for authors and allows searching all past issues.

Once you've obtained and analyzed your data, it's important to publish your results. Papers appearing in the *Minor Planet Bulletin* are indexed in the Astrophysical Data System (ADS) and such that they can be referenced by others in subsequent papers. The MPB web site (Figure 7) is found at

<https://mpbulletin.org>

allows to view the full issue of all past and the most current editions of the *Minor Planet Bulletin*. In addition, you can view all papers in each issue and, optionally, their abstracts. If available in the ADS, a link takes you to the ADS listing to get a complete, accurate reference.



ALCDEF
Asteroid Lightcurve Photometry Database

[What is ALCDEF?](#) [About Asteroid Lightcurves](#) [Acknowledgements](#) [Credits](#) [Data and Privacy Policy](#)

Special Announcements

Download and review the latest [ALCDEF standards PDF](#).

2024 March 4
The site and standard have been updated to distinguish between Pan-STARRS and Sloan *ugriz* filters and magbands. "Px" stands for Pan-STARRS while "Sx" stands for Sloan. Magnitudes based on the ATLAS star catalog (Tonry et al., 2008) are Px

The EPOCH keyword has been deprecated and replaced by EQUINOX. Existing programs that generate EPOCH will still work as will upload files using EPOCH. If using a custom program to read/write ALCDEF files, it should be updated to use EQUINOX.

Avoid Duplicate Submissions

A 2025 August 1 review found almost 24,500 duplicate metadata records, i.e., those for the same object with the same session Date/Time, Filter, and MagBand.

Check the database before you upload.

If you need to submit updated data, please see the ALCDEF documentation, especially the keyword REVISED DATA. Duplicate metadata records and their associated ldata (and compstars, if necessary) will be purged from time-to-time, with the most recent set based on the upload date assumed to be valid.

Statistics and Search

Objects	LC Blocks	Observations
24671	385342	10980067
Last update: 2025-11-10 15:18:30		

Object Search

Required "Opt-in" and File Upload

You must give express permission before your data can be stored and distributed. Without this permission, your data will not be accepted by the ALCDEF site. You must also choose whether or not your data will be automatically made part of a periodic release from the NASA Planetary Data System.

For more information, see the [Data and Privacy Policy](#) statement and the [ALCDEF documentation](#).

Allow sharing Submit to PDS

ALCDEFVerify

ALCDEFVerify is a web-based tool that runs the same verification checks used when uploading files to the ALCDEF database. It was developed for those using programs other than MPO Canopus or scripts to debug and validate their data prior to uploading the files to the ALCDEF database.

Up to three files can be processed during each run. It is *strongly* recommended that each file be < 1 MB.

No file chosen

[Defined Constant Keywords](#)
(see section 3 of ALCDEF standards documentation)

Simple ALCDEF (S-ALCDEF)

S-ALCDEF is for those who have basic text data files, e.g., JD, magnitude[, magerror]. Usually with a minimal amount of editing, these files can be uploaded to the ALCDEF database without

Figure 8. The Asteroid Lightcurve Database Format (ALCDEF) home page.

It's also important to make the data available at least on a personal website or upon request. We urge you to consider submitting your raw data to the ALCDEF database. This can be accessed for uploading and downloading data at (Figure 8).

<http://www.alcdef.org>

The database contains about 10.98 million observations for 24,671 objects (as of 2025 Nov 11), making it one of the more useful sources for *raw* data of *dense* time-series asteroid photometry.

Conclusion

Since the early founding of the *Minor Planet Bulletin*, there has been a paper with a list of specific targets of interest. These served well for a very long time, almost 50 years. In that time, the statistical pools of rotation rates, spin axes, and other physical characteristics have exploded, revealing some of the more import secrets of the minor planets.

More and more, however, undirected observing, at least by smaller observing programs such as backyard astronomers, has mostly just added another data point in the giant blob of the LCDB frequency-diameter plot (Figure 9).

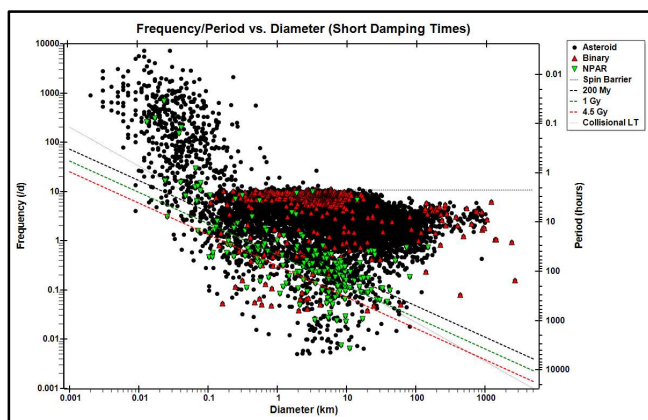


Figure 9. The LCDB frequency-diameter plot showing the “spin barrier”, tumbling damping lines, and tumblers/binaries.

We’ve emphasized in the past the need to search for the outliers, those found by other sources that don’t quite fit into the expected slot on the F-D plot, that have poorly defined lightcurve parameters, that show signs of being a binary or tumbling, or have very long periods – against which there is still a bias despite some of the more recent surveys, especially if space-based.

Even the specific lists we produced in the past introduced some biases, e.g., $V < 15.5$ and were strongly truncated because of printed space limitations. They also presumed a somewhat generic approach and so didn’t, for example, allow developing programs aimed at finding the physical parameters of a limited subset such as a certain family or group.

Part of developing a good observing program is researching what needs or wants to be done and are within the limitations of the individual observers or group of observers. By listing some of the better resources and providing some insight into using the *MinorPlanet.info* pages instead of specific lists, we hope to give the reader a broader experience in program development and to explore opportunities far beyond what were available before.

Except for specific targets coming into view that offer particular science opportunities, this “regular feature” of *The Minor Planet Bulletin* will henceforth focus on presenting (or repeating) information on the resources available to the observer for planning their own programs. We wish you the best of luck and, of course, remain willing and able as much as possible to offer any assistance or guidance in your journey of scientific discovery.

References

- Nesvorný, D. (2015). “Nesvorný HCM Asteroids Families V3.0.” NASA Planetary Data Systems, id. EAR-A-VARGBET-5-NESVORNYFAM-V3.0.
- Nesvorný, D.; Brož, M.; Carruba, V. (2015). “Identification and Dynamical Properties of Asteroid Families.” In *Asteroids IV* (P. Michel, F. DeMeo, W.F. Bottke, R. Binzel, Eds.). Univ. of Arizona Press, Tucson, also available on astro-ph.
- Warner, B.D.; Harris, A.W.; Pravec, P. (2009). “The Asteroid Lightcurve Database.” *Icarus* **202**, 134-146. Updated 2023 Oct. <http://www.minorplanet.info/lightcurvedatabase.html>
- Warner, B.D.; Harris, A.W.; Durech, J.; Benner, L.A.M. (2021a). “Lightcurve Photometry Opportunities: 2021 January-March.” *Minor Planet Bull.* **48**, 89-97.
- Warner, B.D.; Harris, A.W.; Durech, J.; Benner, L.A.M. (2021b). “Lightcurve Photometry Opportunities: 2021 October-December.” *Minor Planet Bull.* **48**, 406-410.
- Warner, B.D.; Harris, A.W.; Durech, J.; Benner, L.A.M. (2023). “Lightcurve Photometry Opportunities: 2023 July-September.” *Minor Planet Bull.* **50**, 240-244.
- Warner, B.D.; Harris, A.W.; Durech, J.; Benner, L.A.M. (2024). “Lightcurve Photometry Opportunities: 2024 October - 2025 January.” *Minor Planet Bull.* **51**, 379-384.

IN THIS ISSUE

This list gives those asteroids in this issue for which physical observations (excluding astrometric only) were made. This includes lightcurves, color index, and H-G determinations, etc. In some cases, no specific results are reported due to a lack of or poor-quality data. The page number is for the first page of the paper mentioning the asteroid. EP is the “go to page” value in the electronic version.

Number	Name	EP	Page	Number	Name	EP	Page
123	Brunhild	59	59	1967	Menzel	32	32
259	Aletheia	3	3	2159	Kukkamaki	59	59
490	Veritas	59	59	2232	Altaj	40	40
665	Sabine	1	1	2359	Debehogne	44	44
689	Zita	59	59	2408	Astapovich	69	69
703	Noemi	44	44	2501	Lohja	59	59
762	Pulcova	63	63	2552	Remek	44	44
845	Naema	40	40	2675	Tolkien	40	40
872	Holda	59	59	2778	Tangshan	35	35
981	Martina	40	40	2778	Tangshan	75	75
1130	Skuld	59	59	2905	Plaskett	40	40
1146	Biarmia	3	3	2949	Kaverznev	32	32
1152	Pawona	59	59	2949	Kaverznev	44	44
1155	Aenna	37	37	2977	Chivilikhin	14	14
1257	Mora	59	59	3024	Hainan	32	32
1276	Uccia	66	66	3066	McFadden	37	37
1326	Losaka	44	44	3066	McFadden	40	40
1365	Henyey	40	40	3507	Vilas	40	40
1588	Descamisada	59	59	3578	Carestia	69	69
1591	Baize	37	37	3792	Trubetskaya	44	44
1648	Shajna	59	59	3846	Hazel	49	49
1688	Wilkins	66	66	3957	Sugie	63	63
1714	Sy	3	3	3967	Shekhtelia	49	49
1714	Sy	7	7	4001	Ptolemaeus	44	44
1714	Sy	44	44	4016	Sambre	37	37
1818	Brahms	63	63	4117	Wilke	63	63
1856	Ruzena	63	63	4620	Bickley	75	75
1858	Lobachevskij	44	44	4671	Drtikol	75	75
1858	Lobachevskij	72	72	4685	Karetnikov	75	75
1892	Lucienne	44	44	4838	Billmclaughlin	40	40
1908	Pobeda	44	44	4997	Ksana	49	49
1913	Sekanina	15	15	5066	Garradd	12	12
1947	Iso-Heikkila	49	49	5132	Maynard	66	66
				5498	Gustafsson	49	49
				5602	1991 VM1	75	75
				5656	Oldfield	66	66
				5676	Voltaire	44	44
				5778	Jurafrance	40	40
				5806	Archieroy	27	27
				6015	Paularego	63	63
				6377	Cagney	66	66
				6394	1990 QM2	72	72
				6422	Akagi	44	44
				6441	Milenajesenska	44	44
				6441	Milenajesenska	59	59
				6690	Messick	11	11
				6735	Madhatter	75	75
				6914	Becquerel	40	40
				6932	Tanigawadake	44	44
				7047	Lundstrom	49	49
				7068	Minowa	75	75
				7747	Michalowski	40	40
				7930	1989 VD	66	66
				8132	Vitginzburg	75	75
				9010	Candelo	75	75
				10022	Zubov	35	35
				11875	Rhone	37	37
				11875	Rhone	49	49
				13007	1984 AU	35	35
				13581	1993 QX4	49	49
				16788	Alyssarose	75	75
				17006	1999 CH63	66	66
				18489	1996 BV2	75	75
				19261	1995 MB	69	69
				24029	1999 RT198	75	75
				25241	1998 UF14	75	75
				29386	1996 JC5	75	75
				31361	1998 VQ29	35	35
				35107	1991 VH	69	69
				45487	2000 AR237	75	75
				49667	1999 OM2	27	27
				63614	2001 QF77	49	49
				69649	1998 FK98	75	75
				98682	2000 WR180	49	49
				137414	1999 TB190	75	75
				138205	2000 EZ148	44	44
				311999	2007 NS2	73	73
					2025 MY89	22	22
					2025 NS1	52	52
					2025 OT4	52	52
					2025 OW	10	10
					2025 OW	52	52
					2025 FE	52	52
					2025 QB21	20	20
					2025 QB21	52	52
					2025 QO7	52	52
					2025 RL2	21	21
					2025 RL2	25	25
					2025 SS5	52	52
					2025 SW	52	52
					2025 SZ4	52	52

THE MINOR PLANET BULLETIN (ISSN 1052-8091) is the quarterly journal of the Minor Planets Section of the Association of Lunar and Planetary Observers (ALPO, <http://www.alpo-astronomy.org>). Current and most recent issues of the *MPB* are available on line, free of charge from:

<https://mpbulletin.org/>

The Minor Planets Section is directed by its Coordinator, Prof. Frederick Pilcher, 4438 Organ Mesa Loop, Las Cruces, NM 88011 USA (fpilcher35@gmail.com). Robert Stephens (rstephens@foxandstephens.com) serves as Associate Coordinator. Dr. Alan W. Harris (MoreData! Inc.; harrisaw@colorado.edu), and Dr. Petr Pravec (Ondrejov Observatory; ppravac@asu.cas.cz) serve as Scientific Advisors. The Asteroid Photometry Coordinator is Brian D. Warner (Center for Solar System Studies), Palmer Divide Observatory, 446 Sycamore Ave., Eaton, CO 80615 USA (brian@MinorPlanetObserver.com).

The *Minor Planet Bulletin* is edited by Professor Richard P. Binzel, MIT 54-410, 77 Massachusetts Ave, Cambridge, MA 02139 USA (rpb@mit.edu). Brian D. Warner (address above) is Associate Editor. Assistant Editors are Dr. David Polishook, Department of Earth and Planetary Sciences, Weizmann Institute of Science (david.polishook@weizmann.ac.il) and Dr. Melissa Hayes-Gehrke,

Department of Astronomy, University of Maryland (mhayesge@umd.edu). The *MPB* is produced by Dr. Pedro A. Valdés Sada (psada2@ix.netcom.com).

Effective with Volume 50, the *Minor Planet Bulletin* is an electronic-only journal; print subscriptions are no longer available. In addition to the free electronic download of the *MPB* as noted above, electronic retrieval of all *Minor Planet Bulletin* articles (back to Volume 1, Issue Number 1) is available through the Astrophysical Data System:

<http://www.adsabs.harvard.edu/>

Authors should submit their manuscripts by electronic mail (rpb@mit.edu). Author instructions and a Microsoft Word template document are available at the web page given above. All materials must arrive by the deadline for each issue. Visual photometry observations, positional observations, any type of observation not covered above, and general information requests should be sent to the Coordinator.

* * * * *

The deadline for the next issue (53-2) is January 15, 2026. The deadline for issue 53-3 is April 15, 2026.

THIS PAGE INTENTIONALLY LEFT BLANK